Characterisation of *XvPrx2*, a type II peroxiredoxin isolated from the resurrection plant *Xerophyta viscosa* (Baker)

Dr Kershini Govender

Thesis submitted in fulfillment of the requirements for the degree of

Doctor of Philosophy

Department of Molecular and Cell Biology

University of Cape Town

Cape Town
February 2006

Ms Kershini Govender presented a thesis titled "Characterisation of *XvPrx2*, a type II peroxiredoxin (Prx) from the resurrection plant, *Xerophyta viscosa* (Baker)." The thesis is well written, with a large number of good quality illustrations. It contains a significant quantity of new, interesting and important data. The objective of the work, which was to undertake a comprehensive physiological and molecular characterisation of *XvPrx2*, with a view to obtaining a deeper understanding of the role of this type II Prx in situations of water deficits in the resurrection plant from which it was identified, has been achieved with commendable success. The study described in this thesis is soundly based on previous studies and identifies *XvPrx2* as important gene involved in desiccation tolerance in *Xerophyta viscosa*. The full characterisation reported in this thesis suggests that the *XvPrx2* gene product and other similar proteins might be attractive targets for future genetic manipulation studies aimed at the improvement of stress tolerance in crop plants.

The thesis is divided into appropriate sections and contains a suitable abstract and appropriate list of references. A number of strategies employing a range of multidisciplinary techniques were successfully employed to characterise the *XvPrx2* gene and its expression patterns and also to unravel the localisation of *XvPrx2* gene product and its importance in stress tolerance. The results of the comprehensive study presented in this thesis not only provide an improved understanding of *XvPrx2* but they also give insights into the complexities of proteins that assist in increasing tolerance to water deficits. Taken together, the data presented here make a significant contribution to the advancement of knowledge in this field of learning.

This thesis and reference list consisting of 153 pages and over 200 references are both highly satisfactory and appropriate. It is to the credit of the candidate that the document was enjoyable and interesting to read and remarkably free from even small errors. In the thesis the candidate reveals a sound knowledge of the background to her work and this general area of plant science, the experimental techniques employed, and the significance of the results. Her enthusiasm for the subject is evident throughout. I recommend that this thesis is generally of a high standard and that it is acceptable for the award of the degree.

Professor Christine H. Foyer
Crop Productivity and Improvement Division
Rothamsted Research, United Kingdom

The thesis titled "Characterisation of *XvPrx2*, a type II peroxiredoxin isolated from the resurrection plant *Xerophyta viscosa* (Baker)" is an excellent piece of research work and the author's thesis writing style is very lucid and scientific. Research work embodied in thesis confirmed that she is fully aware about past and current research literature of plant stresses and practically well up to date with the knowledge of plant science, bioinformatics, enzymology molecular and cell biology.

Her research related to type II *XvPrx2* and Prx genes and their characterisation using comparative DNA sequencing, enzymatic assays, SDS PAGE and 2-D gel electrophoresis, Ramachandran plot, immuno-gold labelling study with the electron microscope work thus demonstrating strong motivation and relevance for developing genetically modified stress tolerant plants for using newly discovered *XvPrx2* gene from *Xerophyta viscosa*. Moreover, author's research work is very important in terms of its significance and commercial applications and she has submitted excellent research data, which should be easily publishable in any top international journal. Therefore, based on her research accomplishments and extraordinary skills in the science, I strongly recommend to the Doctoral Degrees Board Officer for awarding her PhD Degree.

Dr Shashi N. Kumar
University of Central Florida
Plant Gene Expression Centre
Florida, United States of America

The thesis presents results from a study on *in vivo* and *in vitro* characteristics of a peroxiredoxin from *Xerophyta viscosa*. Prxs have been demonstrated to play a major role in the response to stress, as well as in H_2O_2 mediated signalling. Stress tolerance of plants is increasingly receiving attention by the science community because of the extreme practical relevance. It is pivotal to generate crops with an increased stress tolerance within the next decades. Climate change, desertification, salinity, water deficit combined with the ever increasing world population makes this a high priority. Thus, apart from the direct scientific interest, a study such as this is very relevant.

The general approach of this study is good and quite ambitious. It combines an impressive array of techniques and methods. This study adds significant new information to the knowledge of Prxs, particularly in monocots. The abstract sufficiently covers the essence of the study. The literature is quite exhaustive, dealing well with the different relevant elements pertaining to this study. The model presented in 'Chapter 6' of how *XvPrx2* might utilise the second cysteine of Trx is very clever and the author must be complimented with this excellent model. I agree with the recommendation by the author to employ over expression of *XvPrx2* in maize for a functional assessment of the role of *XvPrx2* in stress tolerance, which I think is very essential.

This study adds significant information to our knowledge of the genetics, biochemistry and structure of a higher plant peroxiredoxin. This is a substantial amount of work and of sufficient quality for a PhD degree.

Associate Professor Henk WM. Hilhorst
Wageningen University and Research Centre
Laboratory of Plant Physiology
Wageningen, The Netherlands

Dedication

This thesis is dedicated to my husband, Dr Revel Iyer. You were extremely supportive during this stressful period. There were days during my study when I felt like giving up. You gave me wings and I could believe again. Your love, words of wisdom and faith in me allowed me to believe in myself and provided me the opportunity to reach for my dreams.

To my parents, Mr Thavaraju and Mrs Selvakumarie Govender, thank you for always inspiring and guiding me through life's journey. Mum, your words will always remain with me, "Cross that bridge when you get to it and you will definitely succeed." Dad, your words will always allow me believe in myself, "Just do your best."

To Suvarna, thank you for being a great sister, an accommodating friend and most of all being yourself. You were there to lift my spirits and provide me with a shoulder to lean on during tough times.

Finally, thank you God for always providing me peace of mind, strength and courage to progress and succeed.

Contents

Declaration

I declare that 'Characterisation of XvPrx2, a type II peroxiredoxin isolated from the resurrection plant *Xerophyta viscosa* (Baker)' is my own work, that it has not been submitted before for any degree or examination in any other university, and that all the sources I have used or quoted have been indicated and acknowledged as complete references.

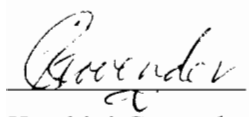

Kershini Govender

14th February 2006

Acknowledgements

I wish to thank the Equity Development Program (EDP), National Research Foundation (NRF), Rockefeller and Maize Trust Fund for financial support during the course of this study.

Thank you to my supervisor, Assoc. Prof. SG Mundree and co-supervisor, Prof. JA Thomson for guidance and support. My thanks to Prof. KJ Dietz (University of Bielefeld) for his input on the biochemical aspect of this project. Dr. U Kahmann for assistance in immuno-gold labeling and Dr. M Jaffer for his assistance with the electron microscopy studies.

I extend my thanks to my lab colleagues at the University of Cape Town. Especially Alice who has been a pillar of strength during those emotional days. Denis, Roger, Betty, Felix, Pule, Marion and Richard for all the humour they provided. Bienyameen for my cup of tea and for his guidance. A special thanks to Livio for his guidance and invaluable assistance with the protein expression studies. To a very special friend, Lemese thank you for your love and support throughout my studies. To my friend Ravathie thank you for your constant support throughout my studies. To a friend in a million, Malini, thank you for your constant phone calls, words of encouragement and wisdom and best of all your loving nature.

A special thank you to my colleagues at the University of Bielefeld. Thorsten for assistance and guidance regarding the confocal microscopy study. Iris for your advice and help with the enzymatic aspect of my studies. Not forgetting the lovable Andrea, Jehad and Sergio for keeping a smile on my face when I was sad.

Dr. S Rafudeen and Dr. MS Sayed for their support and help with the structural biology component of this work. Dr. A Varsani for assistance with editing of the structural models.

Thanks to Di for sequencing my samples and for your motherly support. Not forgetting Pei-Yin for the synthesis of all my oligos.

I wish to thank my extended family for always supporting me when I could not make it to a function and understanding when times were rough: Uncle Sagaran, Aunt Lolly, Amma, Aunt Rogani, Uncle Ronnie, Uncle Dan, Aunt Cookie, Aunt Ambi, Aunt Devi, Uncle Vasi, Uncle Jackson, Uncle Boxer, late Uncle Krish and all my cousins especially Indran, Dinolan, Yashalan, Thaversan, Rumarlin and Leleshya. My thanks to my parents-in-law, Pat and Radha Iyer as well as my sister-in-law, Tercia for their support.

List of figures

List of tables

List of abbreviations

ABA	abscisic acid
amp	ampicillin
BSA	bovine serum albumin
cfu	colony forming units
Cm	chloramphenicol
COOH	cumene hydroperoxide
Cys	cysteine
DTT	dithiothreitol
EtOH	ethanol
GFP	green fluorescent protein
Gpx	glutathione dependent peroxidase
Grx	glutaredoxin
GSH	reduced glutathione
hSrx	human sulphiredoxin
LB	Luria Bertani
LOOH	linoleic acid hydroperoxide
MP	maximum parsimony
pfu	plaque forming units
POOH	phosphatidylcholine dilinoleoyl hydroperoxide
Prx	peroxiredoxin
RNS	reactive nitrogen species
ROS	reactive oxygen species
RSS	reactive sulphur species
RT	room temperature
RWC	relative water content
SDS PAGE	sodium dodecyl sulphate poly acrylamide gel electrophoresis
Ser	serine
Srx	sulphiredoxin
tBOOH	t-butyl hydroperoxide
Trx	thioredoxin
WP	water potential
YFP	yellow fluorescent protein

Abstract

Characterisation of XvPrx2, a type II peroxiredoxin isolated from the resurrection plant *Xerophyta viscosa* (Baker)

Kershini Govender, Department of Molecular and Cell Biology, University of Cape Town

Knowledge of the biochemical and molecular mechanisms by which plants tolerate environmental stresses is necessary for genetic engineering approaches to improve crop performance. A unique feature of resurrection plants, such as *Xerophyta viscosa*, is their ability to cope with severe water loss of greater than 90%. A full-length cDNA library was synthesised from a cold stressed *X. viscosa* plant. Sequencing and BLAST analysis revealed the identity of sixty genes. A type 2 peroxiredoxin (*XvPrx2*) was selected for further analyses as it was observed, by northern analyses, to be stress-inducible. The XvPrx2 protein was confirmed to be involved in the stress response by Western analyses. The *XvPrx2* gene, which displays highest identity to a rice orthologue, has an open reading frame of 162 amino acids, and codes for a hydrophilic polypeptide of 162 residues with a predicted molecular weight of 17.5 kDa. The XvPrx2 polypeptide displays significant identity with other plant type II Prxs, with an absolutely conserved amino acid sequence proposed to constitute the active site of the enzyme (PGAFTPTCS). The XvPrx2 protein has a single catalytic cysteine residue at position 51 similar to Prxs from *Oryza sativa* and *Candida boidinii*. A mutated protein (XvV76C) was generated by converting the valine at position 76 to a cysteine resulting in a conformational change as determined by limited proteolysis. An in vitro DNA protection assay showed that, in the presence of either XvPrx2 or XvV76C, DNA protection occurred. In addition, an in vivo assay showed that increased protection was conferred on cell lines over-expressing either XvPrx2 or XvV76C. Several upstream promoter regions were identified for the *XvPrx2* gene using the splinkerette method. Southern and two dimensional gel analyses revealed that multiple *XvPrx2* homologues exist within the *X. viscosa* genome. These homologues have similar pI values to *Arabidopsis* orthologues. Immuno-cytochemical data revealed that XvPrx2 is localised to the chloroplast, however, this could be attributed to cross reactivity with a chloroplastic homologue. Using YFP technology, the protein was observed to be expressed in the cytosol, and this location is supported by the absence of an upstream targeting signal in the XvPrx2 sequence. The XvPrx2 activity was maximal with DTT as electron donor and H_2O_2 as substrate with t-BOOH being the next preferred. Using $Trx_{E.\ coli}$ a 2-15 fold lower enzyme activity was observed. The XvPrx2 activity with GSH was

significantly lower and Grx had no measurable effect on this reaction. The XvV76C protein displayed significantly lower activity compared to XvPrx2 for all substrates assessed. Enzymatic kinetic parameter values determined for XvPrx2 using DTT as electron donor and H_2O_2 as substrate were: $K_m = 45$ μM, $V_{max} = 278$ μmol $min^{-1}.mg^{-1}$ protein, $k_{cat} = 6.173 \times 10^3$ s^{-1} and $k_{cat}/K_m = 0.136 \times 10^3$ $\mu M^{-1}.s^{-1}$. Based on knowledge-based models of XvPrx2 and XvV76C no structural differences were observed between the two molecules. Furthermore, both proteins displayed a catalytic triad similar to PtPrxII and in the event of homo-dimerisation the formation of a disulphide bond was not supported. In conclusion, XvPrx2 is a cytosol localised, stress-inducible, antioxidant enzyme involved in the protection of nucleic acids by scavenging reactive oxygen species.

14th February 2006

Chapter 1

Literature review

1.1 INTRODUCTION

The last 50 years of agriculture has focussed on meeting the food, feed, and fibre needs of humans. The challenges for the next 50 years however, go far beyond simply addressing the needs of an ever-growing global population. To feed a world population growing by up to 160 people per minute will require a significant increase in food production (Hoisington et al., 1999). In addition to producing more food, agriculture will have to deal with declining resources like water and arable land, the need to enhance nutrient density of crops, and to achieve these and other goals in a way that does not degrade the environment.

Water deficit has a major impact on the area of land available for cultivation and is one of the most commonly experienced environmental stress in southern Africa. In America, soil water deficits are estimated to depress agricultural crop yields by about 70% compared with maximum achievable yields and similar problems are encountered worldwide (Neumann, 1995). Over 35% of the world's land surface is considered to be arid or semi-arid, experiencing precipitation that is inadequate for most horticultural uses.

In recent years, genetic engineering has been used to improve stress tolerance in plants and much work has been done in trying to understand the molecular basis for stress tolerance. A lack of understanding regarding the complexity and interplay of osmotic, desiccation and temperature tolerance mechanisms and their corresponding signalling pathways has generally limited the success of these approaches (Cushman & Bohnert, 2000). Despite this, transgenic approaches have resulted in the development of plants with improved stress tolerance (Chaves & Oliveira, 2004).

With the increase in climate change there is a greater risk that climate extremes will continue and thus impose significant difficulties to the growth of crop plants in many parts of the world. These difficulties will be particularly pronounced in the semi-arid agricultural zones and/or under conditions of irrigation that often exacerbate soil salinisation.The realisation of the urgent need to use rational approaches to develop crop plants with increased abiotic stress tolerance has led to an impressive body of work in the area of plant genetics, plant physiology, plant biochemistry and plant molecular biology (Munns, 2002; Xiong et al., 2002; Ashraf & Harris, 2004; Flowers, 2004).

Despite the significant progress in these fields, to date there are no reports of agriculturally successful applications of biotechnology to increasing drought and salinity tolerance (Denby & Gehring, 2005). Single gene modification approaches have been used to confer significant salt tolerance (Apse et al., 1999; Kasuga et al., 1999; Shi et al., 2003) in transgenic plants. However, such interventions are likely to unbalance the development and physiology of the plant, thus having a significant fitness cost. Previous studies using constitutively expressed promoters to drive stress responsive transcriptional factors have resulted in the transgenic plants being stunted (Kasuga et al., 1999). There is therefore a move to use stress inducible promoters to help reduce gross growth effects but such transgenic lines have not yet been evaluated for fitness parameters such as seed yield.

Speculation on potential impacts in any area of science is difficult; projecting the use of genetic resources in meeting world food requirements is not any different. Crops are being grown on more marginal lands and in harsher and ever-changing environments. Screening programs aimed at identifying new sources of resistance and tolerance should include a wide range of genetic resources, including related and unrelated species. A variety's yield can be considered the final response of a plant's genome to the environment in which it is grown. In this manner, the addition of enhanced stress resistance leads to improved yields. For many developing countries, even slight improvements in stress tolerance would significantly increase yields (Hoisington et al., 1999).

A potential rich source of genes that could confer tolerance to abiotic stresses is a small group of around 200 species of angiosperms known as resurrection plants (Gaff, 1971; Bartels & Salamini, 2001). These plants have developed mechanisms that allow them to withstand severe water deficit and are unique in their ability to tolerate drying of their vegetative tissues. Genes which are postulated to play a role in desiccation tolerance have been isolated from *Craterostigma plantagenium* (Ituriaga et al., 1992; Furini et al., 1997; Bartels & Salamini, 2001), *Tortula ruralis* (Oliver et al., 1998; Chen et al., 2002) and *Xerophyta viscosa* (Mundree et al., 2006). It is hoped that some of these genes could be used to improve the tolerance of crop plants to abiotic stresses and consequently improve their yield.

Antioxidants play a crucial role in the detoxification of toxic compounds that accumulate in cells as a result of plant respiration and photosynthesis. The accumulation of these toxic compounds especially reactive oxygen/nitrogen species can cause cell death which is detrimental to the plant. This study focuses on the isolation and characterisation of a type II

peroxiredoxin, from the resurrection plant *X. viscosa*, which is able to detoxify free radicals generated in plant cells and thus protect cell components.

1.2 THE IMPACT OF WATER DEFICIT ON PLANTS

1.2.1 Water deficit in plants

Plant water deficit occurs when the rate of transpiration exceeds the rate of water uptake (Bray, 1997). Desiccation can result in considerable damage at the cellular level such as changes in cell volume and membrane shape, concentration of solutes, disruption of water potential gradients, loss of turgor, disruption of membrane integrity and denaturation of proteins (Bray, 1997). Plants generally respond to water loss by closing their stomata. This results in the transfer of high-energy electrons to oxygen resulting in the formation of highly reactive oxide radicals that are particularly damaging (Sherwin & Farrant, 1998).

An understanding of the biochemical and molecular mechanisms by which plants tolerate environmental stresses is necessary for genetic engineering approaches to improving crop performance under stress. To this end, Shinozaki & Yamaguchi-Shinozaki (1996) pointed out that it is essential to understand how:

(i) plants survive desiccation;
(ii) plants sense water loss;
(iii) stress signals are transduced into cellular signals and transmitted to the nucleus;
(iv) gene transcription is affected by these signals; and
(v) gene products function in stress tolerance.

Environmental stresses come in many forms, yet the most prevalent stresses have in common their effect on plant water status. The availability of water for its biological roles as solvent and transport medium, as electron donors in the Hill reaction, and as evaporative coolants is often impaired by environmental conditions. Although plant species vary in their sensitivity and response to the decrease in water potential caused by drought, high salinity, or low temperature, it may be assumed that all plants have encoded capability for stress perception, signalling, and response (Bohnert et al., 1995).

For a plant to survive it must be able to respond and adapt to the stress condition (Shinozaki & Yamaguchi-Shinozaki, 1997). Some higher plant species are well adapted to arid environments through mechanisms that mitigate drought stress, including both physiological and biochemical adaptations. Physiological adaptations take many forms ranging from partial senescence of tissues, to structural adaptations such as water storage organs and restrictions in surface area of aerial tissues as seen in *Cactaceae* and

Euphorbiaceae (Scott, 2000). Biochemical adaptations range from damage limitation mechanisms to additions to photosynthetic pathways such as crassulacean acid metabolism (Smith & Bryce, 1992). All of these mechanisms are very effective and they allow plants to inhabit a wide range of arid environments, but when subjected to prolonged lack of water these plants will dehydrate and die.

1.2.2 Water stress in plants

Drought, salinity and freeze-induced dehydration constitute direct osmotic stresses; chilling and hypoxia can indirectly cause osmotic stress via effects on water uptake and loss. Soil salinity alone affects some 340 million hectares of cultivated land (Jain & Selvaraj, 1997). The early events of plant adaptation to environmental stress are the sensing and subsequent signal transduction to activate various physiological and metabolic responses, including stress responsive gene expression. The complete loss of free water results in desiccation or dehydration of plants. The ability of the whole plant to respond and survive cellular water deficit depends on whole-plant mechanisms that can integrate the cellular responses. Responses to water deficit may occur within a few seconds (such as change in phosphorylation status of the protein) or within minutes and hours (such as change in gene expression). Whole plant responses to water deficit are controlled by an array of genes with numerous functions (Fig. 1.1).

Genes induced under water stress conditions are thought to function not only in protecting cells from water deficit by the production of important metabolic proteins but also in the regulation of genes for signal transduction in the water stress response (Shinozaki & Yamaguchi-Shinozaki, 1997). Thus the gene products can be divided into two groups (Fig. 1.2). The first group of proteins involved in stress tolerance are water channel proteins involved in the movement of water through membranes, the enzymes required for the biosynthesis of various osmoprotectants (sugars, proline, glycine-betaine), proteins that may protect macromolecules and membranes (LEA proteins, osmotin, antifreeze protein, chaperon, and mRNA binding proteins), proteases for protein turnover (thiolproteases, Clp protease and ubiquitin) and detoxification enzymes (glutathione S-transferase, catalase, superoxide dismutase and ascorbate peroxidase). The second group of proteins are involved in further regulation of signal transduction and gene expression. These include protein kinases, transcription factors, phospholipase C and 14-3-3 proteins.

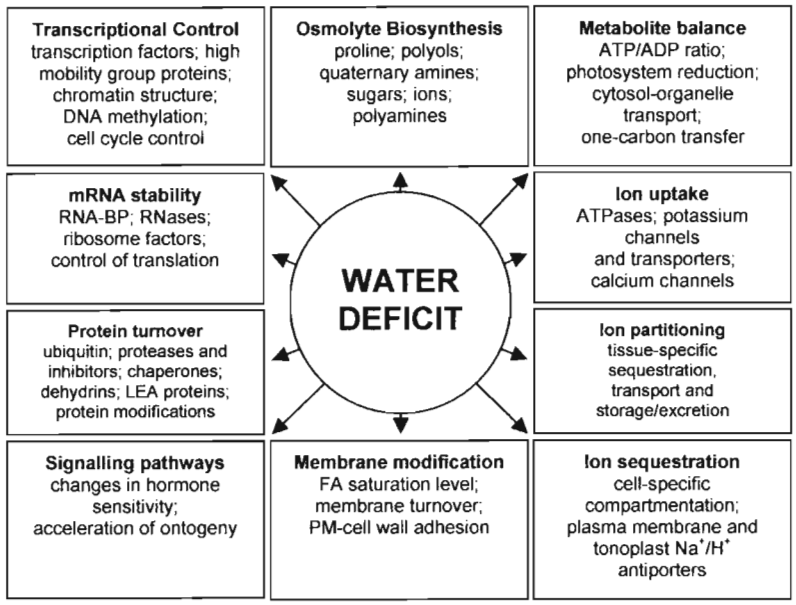

Figure 1.1 Plant responses to water deficit (Bohnert et al., 1995).

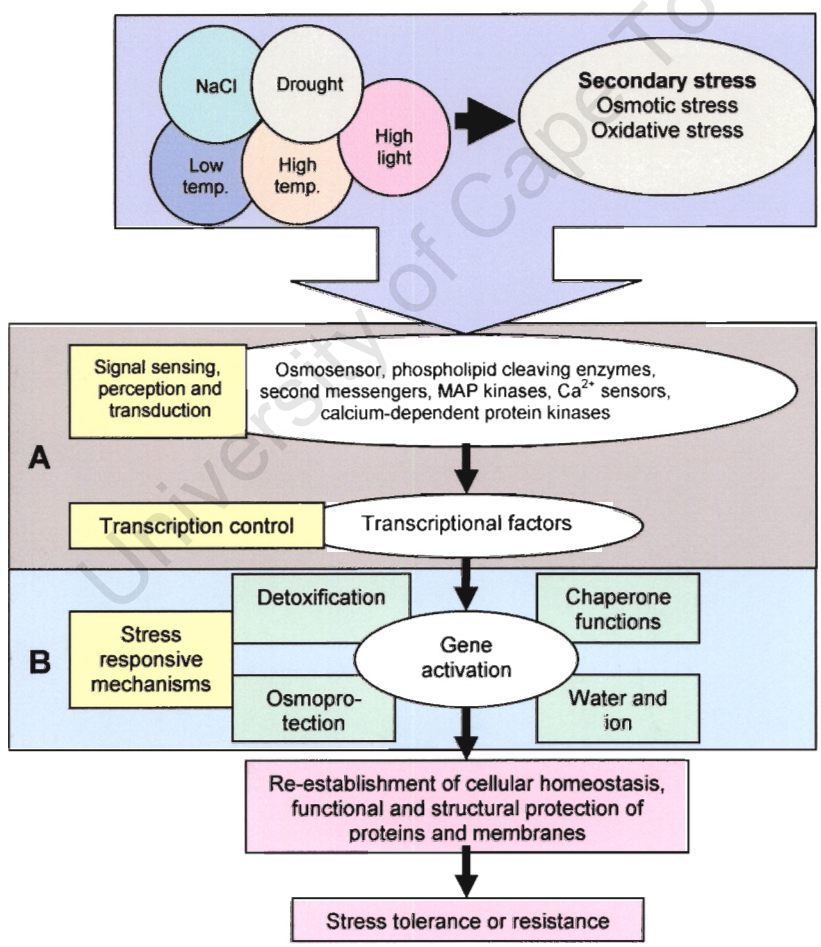

Figure 1.2 Abiotic stresses are often interconnected. They result in cellular damage and secondary stresses. Two groups of gene products are involved in the plant stress response: (A) regulatory proteins (signalling and transcriptional controls); and (B) functional proteins (adapted from Wang et al., 2003).

Expression patterns of dehydration inducible genes are complex. Some genes respond to water stress very rapidly, whereas others are induced slowly after the accumulation of abscisic acid (ABA). It appears that dehydration triggers the production of ABA, which in turn induces various genes. Most of the genes that respond to drought, salt and low temperature stress are also induced by exogenous application of ABA (Shinozaki & Yamaguchi-Shinozaki, 1997). Several genes that are induced by water stress are not responsive to exogenous ABA treatment. These findings suggest the existence of both ABA independent and ABA dependent signal transduction cascades between the initial signal of drought or low temperature stress and the expression of specific genes (Bray, 1997). Analysis of the expression of these dehydration inducible genes in *Arabidopsis* have indicated that multiple independent signal pathways (Fig. 1.3) function in the induction of these stress inducible genes in response to abiotic stress (Ramanjulu & Bartels, 2002).

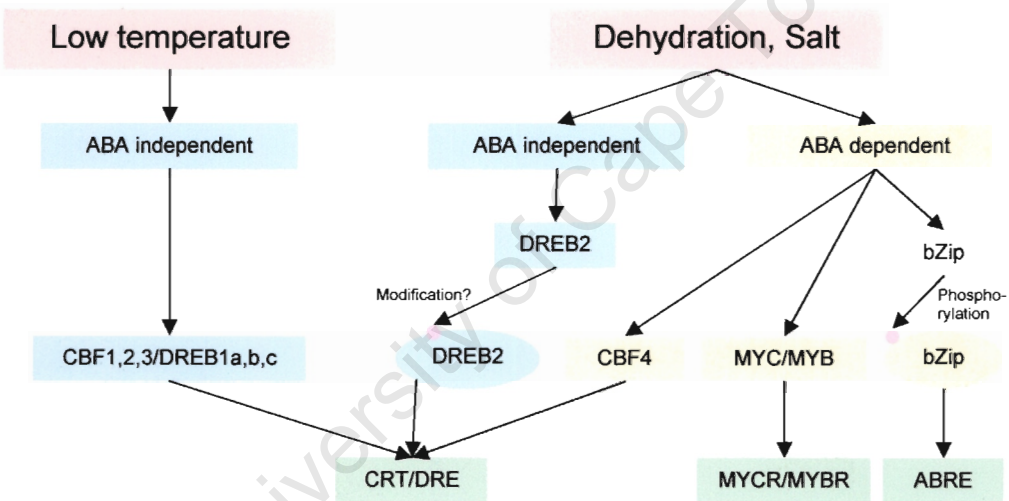

Figure 1.3 ABA independent and ABA dependent signal transduction pathways between the perception of a water stress signal and gene expression (adapted from Ramanjulu & Bartels, 2002).

1.2.3 Genetic engineering for improved plant response to water deficit

In the past decade most of the successful genetic engineering work in agricultural terms was directed towards crop resistance, to biotic stress, or to technological properties (Sonnewald, 2003). Studies addressing plant resistance to abiotic stress have been confined to experimental work and to single gene approaches (Ramanjulu & Bartels, 2002). However, recent advances suggest that rapid progress may be possible in the near future, with large economical impact (Table 1.1; Dunwell, 2000; Garg et al., 2002; Wang et al., 2003).

Table 1.1 Recent achievements in improving drought tolerance in crops through genetic engineering (Chaves & Oliveira, 2004)

Gene/enzyme	Origin	Target	Effect	Author
Functional proteins				
Superoxide dismutase (MnSOD)	*Nicotiana plumbaginifolia*	Alfalfa	Improved performance in the field under drought	McKersie et al. (1996)
HVA1 (group 3 *lea* gene)	Barley	Rice	Constitutive expression leads to protein accumulation in leaves and roots and improved recovery after drought and salt stress	Xu et al. (1996)
Myo-inositol O-methyltranferase (*IMT1*)	*Mesembryanthemum crystallinum*	Tobacco	Enhanced photosynthesis protection and increased recovery under drought, through the accumulation of D-ononitol	Sheveleva et al. (1997)
Trehalose-6-P synthase, Trehalose-6-P phosphatase	Bacteria	Tobacco	Better phosynthetic efficiency and higher dry weight under drought stress	Pilon-Smiths et al. (1998)
HVA1 (group 3 *lea* gene)	Barley	Wheat	Constitutive expression (*ubiP*) improved biomass productivity and water use efficiency under water stress	Sivamani et al. (2000)
Aldose/aldehyde reductase (*MsALR*)	Alfalfa	Tobacco	Detoxification effect (reduced amounts of reactive aldehydes) leading to tolerance to multiple stresses	Oberschall et al. (2000)
NADP malic enzyme	Maize	Tobacco	Drought avoidance through decreased stomatal conductance and increased fresh weight per unit water consumed	Laporte et al. (2002)
Fusion gene, Trehalose-6-P synthase and Trehalose-6-P phosphatase (*TPSP*), regulated by ABA inducible promoter or rbcS promoter	*E. coli*	Rice	Sustained plant growth and reduced photo-oxidative damage under abiotic stresses. Improved photosynthetic activity under non-stress conditions	Garg et al. (2002)
Mannitol-1-phosphate dehydrogenase (*mtlD*)	*E. coli*	Wheat	Improved drought tolerance with mannitol accumulation at a concentration insufficient for osmotic adjustment	Abebe et al. (2003)
Aquaporin NtAQP1	Tobacco	Tobacco	Increased membrane permeability for CO_2 and water, and increased leaf growth	Uehlein et al. (2003)
Regulatory proteins				
Calcium dependent protein kinase (*OsCDPK7*)	Rice	Rice	Induced expression of a glycine rich protein (*salT*) and LEA proteins (*rab16A*, *wsi18*) under stress. Increased salt and drought tolerance	Saijo et al. (2000)
CBF1 (DREB1B) driven by P35SCaMV	*Arabidopsis*	Tomato	Increased resistance to water stress, but dwarf phenotype. Higher levels of proline, and faster closure of stomata under water stress	Hsieh et al. (2002)

According to Chaves & Oliveira (2004) even modest improvements in crop resistance to water deficit and in water use efficiency will increase yield and save water. A major challenge of this technology is to develop plants that are both able to survive stress and grow under adverse conditions with reasonable biomass production, overcoming the negative correlation between drought resistant traits and productivity, which was often present in past breeding programs (Mitra, 2001). Such a compromise requires improved efficiency in maintaining homoeostasis, detoxifying cells from harmful elements, and recovering growth that is arrested upon acute osmotic stress (Xiong & Zhu, 2002). This therefore requires the introduction of sets of genes that govern quantitative traits, as demonstrated in the case of transgenic rice with introduced provitamin A (Ye et al., 2000).

The increasing knowledge of stress adaptation processes and the identification of key pathways and interactions involved in the plant response to the stress conditions are being exploited to engineer plants with higher tissue tolerance to dehydration or with drought avoidance characteristics (Laporte et al., 2002). The latter is more difficult to achieve, because it is linked to whole plant morphological and physiological characteristics (Altman, 2003).

Recent progress in gene discovery and knowledge of signal transduction pathways raises the possibility of engineering important traits by manipulation of a single gene, downstream of signalling cascades, with putative impact on more than one stress type. Moreover in genetic engineering it is important to mimic nature and activate at the correct time only the genes that are necessary to protect the plants against stress effects. Chaves & Oliveira (2004) indicate that this may be achieved using appropriate stress inducible promoters and consequently would minimise effects on growth under non-stressing conditions that is essential for agricultural crops. Furthermore, to ensure that negative effects do not arise, the desired tissue/cellular location should be targeted, the intensity and time of expression should be controlled, and availability of all metabolic intermediates should be ensured (Holmberg & Bülow, 1998). A final requirement to prove that a transgenic plant is more resistant to water stress requires a rigorous evaluation of the physiological performance as well as the water status of transformed plants (Chaves & Oliveira, 2004). The result is that the impact of the introduced genes is separated in their direct versus indirect effects (e.g. increased resistance of the photosynthetic apparatus versus effects on plant or leaf size, phenology, etc.).

1.3 RESURRECTION PLANTS

1.3.1 General characteristics of resurrection plants

Resurrection plants are unique among angiosperms in that they possess a uniquely effective mechanism for coping with drought stress by being desiccation tolerant. These plants can tolerate severe water loss of greater than 90%. Resurrection plants have very little water retaining characteristics, morphological or physical, and hence their internal water content rapidly equilibrates with the water potential of the environment. These plants survive the loss of their tissue water content until a quiescent stage is reached. Upon watering they rapidly revive and are restored to their former state. Tissue damage due to this drying and rehydration process appears to be minimal to non-existent. Unlike other plant responses to drought stress, resurrection plants prevent growth and reproduction over the dehydrated period (Scott, 2000) and promote growth when conditions become favourable, whereas non-resurrection plants die upon drying.

Resurrection plant species are represented in most taxonomic groups ranging from pteridophytes to dicotyledons. Terrestrial species include the monocotyledonous plant, *Xerophyta viscosa* and the dicotyledonous shrub *Myrothamnus fabellifolia*, and an aquatic species *Chamaegigas intrepidus*. Most species are native to arid climates in the world such as southern Africa, southern America, and Western Australia (Gaff, 1987). These plants grow in shallow, sandy soils in rocky outcrops and inhabit ecological niches uninhabitable by most higher plants, which are subjected to lengthy periods of drought with periods of rain during the year (Scott, 2000). The growth and reproduction of the plant occurs in these wet seasons, but upon drying the plants can remain dormant for considerable periods, for example *Craterostigma* species can last up to two years without water. Mechanisms that protect plants from water stress are frequently effective against other environmental stresses. Some resurrection grass species were found to be salt tolerant and it has been postulated that some may be resistant to large fluctuations in temperature (Hartung et al., 1998).

1.3.2 Physiology of resurrection plants

One of the most remarkable features of the resurrection plant *C. plantagineum* is its ability to shrink during dehydration. The leaves of *C. plantagineum* shrink to around 15% of their original area (Scott, 2000). Evidence on how leaves achieve this reduction suggests that the plasmalemma and the cell wall form a concertina that minimises damage within and between cells. In woody species, such as *M. flabellifolia*, such shrinkage is not observed, however the water content on desiccated state is similar to *Craterostigma.* In higher plants the

formation of air bubbles is a well known cause of xylem blockage during desiccation. To overcome this problem *M. flabellifolia* has produced narrow reticule xylem vessels that cavitate on desiccation but refill from capillary and root pressure on resurrection. Another remarkable feature of resurrection plants is their ability to rehydrate rapidly, for example *C. plantagineum* revives in less than 24 hours (Scott, 2000).

In contrast to what is known to be occurring in the leaves, very little research has been performed on the roots of resurrection plants. In such tissues the response to drought stress is probably more rapid than in the leaves since it is the root that first senses soil water deficit (Scott, 2000). Roots are also very much more restricted in their ability to shrink during dehydration since they are embedded in a soil matrix. Thus shrinkage of roots beyond that of the soil could result in major root network damage.

Resurrection plants can be divided into two groups:

(i) homoiochlorophyllous plants, which retain their chlorophyll during drying, e.g. *M. flabellifolia*; and

(ii) poikilochlorophyllus plants, which lose chlorophyll on drying, e.g. *X. viscosa*.

1.3.3 Significance of resurrection plants

Resurrection plants can be regarded as extremophiles, as they can survive severe temperature, salinity, high light and desiccation environments. Resurrection plants are studied in attempts to understand the mechanisms of desiccation tolerance, often with the ultimate aim of identifying genes that can be used to bioengineer crops for improved tolerance to water stress. The occurrence of different mechanisms of protection to a given stress has implications for bioengineering work, in that the genetic pathways needed for successful transformation to drought tolerance are likely to differ among crops. An understanding of the different mechanisms of tolerance that does exist might allow for more informed decisions as to which ones might be more effective in a particular crop (Farrant, 2000). Consequently resurrection plants, such as *X. viscosa*, are potentially valuable sources of stress tolerance genes.

1.3.4 Metabolic changes during dehydration and rehydration in resurrection plants

Numerous metabolic changes occur in resurrection plants as they dehydrate and rehydrate. The most thoroughly investigated is carbohydrate accumulation, of which sucrose is the dominant carbohydrate in all resurrection plants. Almost three-times more sucrose is accumulated by *C. plantagineum* than the highest of the other plant species. Sucrose accumulation has been proposed to maintain cell integrity during dehydration (Ingram &

Bartels, 1996). These sugars could act to stabilise membranes and proteins in the dry state by maintaining hydrogen bonding within and between macromolecules (Allison et al., 1999). Sugars could also vitrify the cell contents and stabilise internal cell structure (Crowe et al., 1996). In *X. viscosa,* as leaves dry, fructose and glucose are metabolised allowing for sucrose to accumulate as the dominant carbohydrate in the dehydrated plant. Experiments in which isolated enzymes have been dried in the presence of sucrose display evidence that the enzymes remain stable in the dried state (Bustos & Romo, 1996; Suzuki et al., 1997). Parallel work on isolated membrane vesicles also supports the view that sucrose preserves the integrity of the lipid bilayer during dehydration (Crowe et al., 1998). Trehalose and raffinose were also shown to help stabilise cell membranes, particularly the phospholipid bilayer and membrane proteins during cellular dehydration and freezing (Turner et al., 2001). This is important as cell membranes have been regarded for a long time as the site of desiccation injury, mainly because the earliest symptom of injury is enhanced leakage of cytoplasmic solutes during rehydration (Simon, 1974). Another feature to be noted is that sucrose and trehalose measurements in identical plant species by different laboratories are very variable. Additionally, trehalose has been reported to accumulate to a great extent in only *M. flabellifolia.* Data such as these have fuelled a great deal of interest in the use of sugars as a mechanism for protection of other living tissues (Pilon-Smits et al., 1998; Zentella et al., 1999).

1.3.5 Gene expression in resurrection plants

In response to drought, protein expression changes with many genes being induced upon dehydration whereas others are down regulated. Through the use of inhibitors such as actinomycin D (inhibits transcription) and cyclohexamide (inhibits translation) it was observed that most of the mRNA needed for rehydration was synthesised during dehydration (Bartels et al., 1990). Six cDNA clones displayed increased expression in leaves of the resurrection grass *Sporobolus stapfianus* during drought stress (Blomstedt et al., 1998). Some of these genes bear homology to genes such as dehydrins and thiol proteases of other plant species thought to be involved in the maintenance of cell integrity during water stress (Scott, 2000). Most proteins that increase during desiccation are inducible with ABA, suggesting that ABA forms the initial signal for metabolic events that are necessary for desiccation. Bartels et al. (1990) isolated a large number of cDNA clones from *C. plantagineum*, which were induced upon rehydration. Several of these clones possessed homology with late

embryogenesis abundant (LEA) proteins which are associated with the later stages of embryo development in seeds.

Studies of *C. plantagineum* have revealed that transcripts encoding proteins relevant to photosynthesis are down regulated during the dehydration process and thus possibly reduce photo-oxidative stress (Ingram & Bartels, 1996). Jiang et al. (1995) demonstrated that the promoter regions of storage protein genes contain the information for their down regulation during seed desiccation.

1.3.6 Significance of *Xerophyta viscosa* (Baker)

The *X. viscosa* (Velloziaceae, Fig. 1.4) plant species, is endemic to southern Africa and grows in mountain top habitats such as Cathedral Peak in the Drakensberg mountains. These plants grow on rocky outcrops and are exposed on a daily basis to extremes of temperature. The *X. viscosa* plant can survive extremes of dehydration, as low as 5% relative water content (RWC; Jin et al., 2000), and upon rehydration reach full turgor and regain all physiological activities within 80 hours of re-watering (Sherwin & Farrant, 1996). The Plant Stress Lab (University of Cape Town) is focused on developing transgenic maize that is able to withstand drought. Consequently, *X. viscosa* is being studied as a source of genes that are involved in abiotic stress tolerance.

Mechanical stress is the consequence of the considerable reduction of cell volume upon desiccation (Iljin, 1957). This results in the plasmalemma tearing away and collapse of the cell walls in leaf cells. This is avoided in *X. viscosa* by the subdivision of the large central vacuole present in hydrated leaves into a number of smaller ones, which become progressively filled with non-aqueous material as water is lost from them (Mundree & Farrant, 2000). This phenomenon has also been observed in desiccation tolerant seeds (Bewley & Black, 1994; Farrant et al., 1997) and in other resurrection plants (Farrant & Sherwin, 1997; Farrant et al., 1999), which minimises cell volume reduction and thus mechanical stress.

Photosynthesis and respiration can result in the production of reactive oxygen species, which if not detoxified by antioxidants can cause severe subcellular damage and loss of viability. The *X. viscosa* plant appears to use mechanisms for both the prevention of free radical formation and quenching of their activity (Sgherri et al., 1994a, b; Sherwin & Farrant, 1998). The presence of chlorophyll is detrimental to cells during drying and the chlorophyll is degraded and the thylakoid membranes are dismantled into small vesicles during desiccation in *X. viscosa* and this minimises free radical formation (Tuba et al., 1996; Farrant et al.,

1999). The levels of other pigments like carotenoids and anthrocyanins increase on drying in *X. viscosa* and this together with the process of dismantling the photosynthetic apparatus is thought to be a means of protecting the plant against UV-light and from damage as a result of oxygen free radical generation during desiccation (Sherwin & Farrant, 1995; Sherwin & Farrant, 1998). Respiratory activity continues at high levels, dropping only below a RWC of 30% and ceases below 15% RWC.

Figure 1.4 The *X. viscosa* plant in its ecological niche at Cathedral Peak Nature Reserve. The fully hydrated (blue arrow), dehydrated (yellow arrow) and blooming (red arrow) *X. viscosa* plants growing on a rocky outcrop in the Drakensberg mountains are displayed.

Resurrection plants possess a suite of genes that are expressed co-ordinately under stress and functioning together are able to facilitate certain cellular mechanisms that allow the plant to tolerate environmental extremes. A number of interesting genes have been identified in *X. viscosa* as upregulated in response to various stresses.

A 1-Cys peroxiredoxin, *XvPer1*, is a stress-inducible antioxidant enzyme (Mowla et al., 2002). Other 1-Cys Prxs have been reported in plants, but only in seeds and immature embryos (Mundree et al., 2002). The *XvPer1* gene is unique in that it is upregulated in vegetative tissues exposed to abiotic stresses (Mowla et al., 2002).

The XvGrp94 (a glucose regulated protein localised to the endoplamic reticulum and homologous to *Hsp90*) protein is upregulated under conditions of stress and is the first report of such upregulation in response to desiccation stress. The XvGrp94 protein was observed to be decreased during rehydration but continued to increase throughout heat stress treatment (Walford et al., 2004). This increase in response to heat shock was only observed in two other plants (viz. maize and barley; Schroder et al., 1993).

The *XvGolS* gene isolated from a dehydration stressed *X. viscosa* leaves encodes a galactinol synthase and may be an important component in compatible solute biosynthesis. It was found to be up-regulated in the leaves of *X. viscosa* during drought stress (Peters, 2005).

The *XvIno1* gene encodes a myo-inositol-1-phosphate synthase, which catalyses the conversion of glucose-6-phosphate to myo-inositol-1-phosphate, which is subsequently dephosphorylated to myo-inositol. Myo-inositol is a precursor for a number of important metabolites, which include membrane components, storage molecules, phytohormones and a variety of osmoprotectants. The *XvIno1* gene has been shown to be up-regulated during various abiotic stresses (Chopera, 2006).

An *ERD15* (Kiyosue et al., 1994) orthologue has been observed to be upregulated during early stages of dehydration (Lee, 2005). No function has been currently attributed to this protein. Molecular characterisation has led to observation that XvERD15 is hydrophobic, acidic and lacks cysteine residues.

The *XvVHA-c``1* gene codes for the subunit c`` protein of V-ATPase. Transcripts were observed to increase in response to NaCl, dehydration and low temperature stress (Marais et al., 2004). It is postulated that XvVHA-c``1 plays a role in creating a proton translocating pore and assisting in adapting to osmotic pressure fluctuations as well having a housekeeping role to maintain luminal acidification.

The *XvCaM* gene was isolated from dehydration stressed *X. viscosa* leaves and codes for a classic calmodulin with 4 EF-hands (Conrad, 2005). Northern blot analyses indicate that transcript levels fluctuate only under dehydration stress. Western blot analyses show that the protein accumulates at low relative water content and is present during the rehydration of the plant.

The XvSap1 protein is highly hydrophobic and possesses two membrane lipoprotein lipid attachment sites (Garwe et al., 2003). It displays high sequence similarity with G-protein coupled receptors and consequently is postulated to play a signalling role during abiotic stress.

The *XvAld1* gene codes for an aldose reductase, which catalyses the reduction of sugars to their analogous alcohol (Mundree et al., 2000). Oberschall et al. (2000) demonstrated that plant aldose reductase can detoxify cytotoxic aldehydes, such as 4-hydroxynon-2-enal that is a product of ROS-induced lipid peroxidation. Transcript and protein levels of XvAld1 have been shown to increase within leaves in response to water deficit (Mundree et al., 2000).

1.4 OXIDATIVE STRESS IN PLANT CELLS

Survival during periods of environmental stress is vital for agricultural crops. Protective responses at the leaf level must be triggered quickly to prevent the photosynthetic machinery from being irreversibly damaged. Damage is a result of reactive oxygen species generated via the Mehler reaction, such as superoxide, hydrogen peroxide (H_2O_2) and the hydroxyl radical that may lead to photo-oxidation if the plant is not efficient in scavenging these molecules (Chaves & Oliveira, 2004).

Redox signals are early warnings, exerting control over the energy balance of a leaf. Alterations in the redox state of the redox-active compounds regulate the expression of several genes linked to photosynthesis (both in the chloroplast and in the nucleus), thus providing the basis for the feedback response of photosynthesis to the environment, or in other words, the adjustment of energy production to consumption. Redox signalling molecules include some key electron carriers, such as plastoquinone pool, or electron acceptors (e.g. ferredoxin/thioredoxin system) as well as reactive oxygen species (ROS; Chaves & Oliveira, 2004).

1.4.1 Reactive oxygen species

Reactive oxygen species (ROS) can be produced when an organism is exposed to a variety of abiotic stresses or during the course of normal aerobic metabolism. Widespread damage to biological macromolecules may occur due to ROS (Apel & Hirt, 2004). In plant metabolism the major sources of ROS are the photosynthetic electron transport, photorespiration, respiration, and also many other enzymatic and non-enzymatic reactions (Fig. 1.5; Foyer & Noctor, 2000). Examples include:

(i) in the chloroplast, superoxide is produced by reduction of oxygen at the electron acceptor site of photosystem I;

(ii) in photorespiration, molecular oxygen is reduced by glycollate oxidase in the peroxisome under formation of H_2O_2, which is disproportionated by catalase; and

(iii) NAD(P)H dehydrogenases and the cytochrome bc_1 complex are the basic sites of superoxide production in the mitochondria. While superoxide is rapidly dismutated to H_2O_2 by a mitochondrial manganese superoxide dismutase, the metabolism of H_2O_2 is not yet clear (Foyer & Noctor, 2000).

These examples show that each cellular compartment must cope with ROS to avoid oxidative stress within cells. These reactive oxygen species can also act as signals modulating gene expression, enzyme activities or defence reactions.

The intracellular concentration of ROS is controlled by the plant detoxifying system, which includes ascorbate and glutathione pools. Accumulating evidence suggests that these compounds are implicated in redox signal transduction, acting as secondary messengers in hormonal-mediated events (Foyer & Noctor, 2003), namely stomatal movements (Pei et al., 2000).

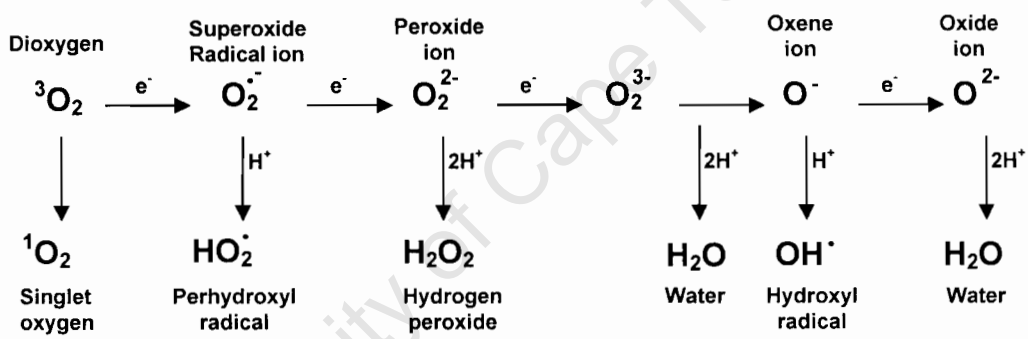

Figure 1.5 Generation of different ROS by energy transfer or sequential univalent reduction of ground state triplet oxygen (Apel & Hirt, 2004).

1.4.2 Reactive nitrogen species

Peroxinitrite produced in the mitochondrial electron-transfer chain results in the formation of reactive nitrogen species (RNS). Nitric oxide, a RNS, acts as a signalling molecule, in particular by mediating the effects of hormones and other primary signalling molecules in response to environmental stimuli. It may act by increasing cell sensitivity to these molecules (Neill et al., 2003). Recently, nitric oxide was shown to play a role as an intermediate of ABA effects on guard cells (Hetherington, 2001; Neill et al., 2003). Like H_2O_2, nitric oxide may be also involved in stress perception by the apoplast, since this compartment can be a major site of its synthesis. It is also likely that both nitric oxide and H_2O_2 are synthesised in parallel and act in a concerted way in a number of physiological

responses, including stomatal responses to environmental stresses. Although the links between dehydration and nitric oxide are not yet fully resolved, it seems that some of signalling components down-stream of nitric oxide and H_2O_2 in the ABA induced stomatal closure are calcium, protein kinases, and cyclic GMP (Desikan et al., 2004). Nitric oxide also serves as an antioxidant by interacting with ROS produced under different stresses, such as superoxide, and by inhibiting lipid peroxidation. However, if nitric oxide is produced in excess it may result in nitrosative stress (Neill et al., 2003). The balance between nitric oxide and H_2O_2 also seems to play a role in some critical cellular responses, including programmed cell death (Chaves & Oliveira, 2004).

1.4.3 Hydrogen peroxide as a signalling molecule

Hydrogen peroxide acts as a local or systemic signal for leaf stomata closure, leaf acclimation to high irradiance and the induction of heat shock proteins (Karpinska et al., 2000; Pastori & Foyer, 2002). The effects of H_2O_2 on guard cells were first reported in *Vicia faba* by McAinsh et al. (1996), who found that exogenous applications of H_2O_2 induced an increase in cytosolic calcium as well as stomatal closure. On the other hand, ABA applied to guard cells of *Arabidopsis* was shown to induce a burst of H_2O_2 that resulted in stomatal closure (Pei et al., 2000; Desikan et al., 2004). However, when H_2O_2 production exceeds a threshold, programmed cell death might follow.

Hydrogen peroxide and other redox compounds play an important role in the stress perception of the apoplast, which acts as a bridge between the environment and the symplast. Pastori & Foyer (2002) observed that H_2O_2 is transported from the apoplast to the cytosol through aquaporins, suggesting that the regulation of signal transduction can also occur via the modulation of transport systems. The interplay between the signalling oxidants and their antioxidants counterparts, in particular ascorbic acid, the most important buffer of the redox state in the apoplast, are key factors of the regulation in plant growth and defence in relation to biotic and abiotic stresses (Pignocchi & Foyer, 2003).

1.5 PEROXIREDOXINS

1.5.1 Functional significance of peroxiredoxins

Peroxiredoxins (Prxs) are abundant low efficiency peroxidases located in distinct cell compartments including the chloroplast and mitochondria (Dietz, 2003). The first Prx was isolated from yeast by identifying a protein fraction that protected DNA from oxidative damage and protected sensitive enzymes from oxidative inactivation in vitro (Finkemeier et

al., 2005). In these studies, the authors employed a mixed function oxidation system containing Fe^{2+}, O_2 and dithiothreitol (DTT) used to initiate oxidative damage to macromolecules. Addition of a Prx suppressed damage development (Finkemeier et al., 2005). These antioxidant enzymes are characterised as peroxidases with broad substrate specificity, reducing diverse peroxides such as H_2O_2, alkyl hydrogen peroxides and peroxinitrite to water and the corresponding alcohol, and water and nitrite, respectively (Bryke et al., 2000). Peroxiredoxins have been shown to detoxify ROS (Brehelin et al., 2003), RNS (Peng et al., 2004) and reactive sulphur species (RSS; Chae et al., 1994a). Peroxiredoxins function in antioxidant defence in photosynthesis, respiration, stress response and redox signalling.

1.5.2 Four types of plant peroxiredoxins

A genome wide search in *A. thaliana* led to the identification of members of all four Prx subfamilies with a total of 10 genes (Table 1.2; Horling et al., 2002; Dietz, 2003). Prxs have one or two essential cysteines in conserved sequences and can be divided into four subgroups: 1-Cys Prx, 2-Cys Prx, PrxQ, and type II Prx (Horling et al., 2003).

This family of peroxidases reduces H_2O_2 and alkyl hydroperoxides to water and alcohol, respectively, with the use of reducing equivalents provided by thiol containing proteins (Rhee et al., 2001; Hofmann et al., 2002). Unlike other peroxidases such as ascorbate peroxidase, Prx does not depend on a prosthetic group like heme (Horling et al., 2002). The four Prx subgroups can be distinguished by their reaction mechanisms. The reaction mechanism comprises three steps: oxidation, derivatisation, and regeneration of ground state (Hofmann et al., 2002). All Prx enzymes contain a conserved catalytic cysteine residue at the amino terminal and exist as homodimers.

1.5.2.1 1-Cys Prx

The 1-Cys peroxiredoxin was the first Prx type identified in plants and was characterised as a dormancy related protein. The 1-Cys Prx is localised to the nucleus as well as the cytosol and is suggested to protect macromolecules from oxidative damage (Stacy et al., 1996, 1999). Rouhier & Jacquot (2005) report that all plant Prxs, except 1-Cys Prx, have been shown to reduce a broad range of hydroperoxides, from the most simple compound (H_2O_2), to alkyl hydroperoxides such as t-butyl hydroperoxide or cumene hydroperoxide, and to more complex phospholipid hydroperoxides such as linoleic acid, phophatidylcholine, or phophatidylcholine dilinoleylhydroperoxides (Brehelin et al., 2003; Rouhier et al., 2004a, b).

Table 1.2 Characterisation of peroxiredoxins identified in *A. thaliana*. The third column displays the amino acid length of the pre-protein (AA) and the predicted targeting address (tp), respectively; the fifth column displays isoelectric point (IEP); the sixth column displays the position of conserved Cys residues in the mature protein (adapted from Dietz, 2003)

	MIPS[‡] accession numbers	AA/tp	kDa	IEP	Position of Cys-residues	Subcellular location
1-Cys Prx	At1g48130	216/-	24.1	6.14	46	Nucleus
2-Cys Prx						
A	At3g11630	266/83	29.1	4.91*	36, 158	Chloroplast
B	At5g06290	271/88	29.6	4.71*	36, 158	Chloroplast
PrxQ	At3g26060	216/57	23.7	5.53*	54, 59	Chloroplast
Type II Prx						
A	At1g65990	553	62.7	6.04	51, 76	Pseudogene
B	At1g65980	162	17.4	5.17	51, 76	Cytosol
C	At1g65970	162	17.4	5.33	51, 76	Cytosol
D	At1g60740	174	19.2	6.1	51, 76	Cytosol
E	At3g52960	234/70	24.7	5.03*	51, 76	Chloroplast
F	At3g06050	199/28	21.2	6.29*	59, 84	Mitochondrion

[‡]MIPS refers to Munich information centre for protein sequences

*IEP calculated without transit sequence

A 1-Cys peroxiredoxin (*XvPer1*) isolated from *X. viscosa* showed that the protein is highly abundant under stress conditions. The XvPer1 protein is localised to the nucleus of *X. viscosa* leaf cells under conditions of dehydration stress and upon treatment with ABA (Mowla et al., 2002; Mowla, 2005). The XvPer1 protein was also found to be localised to the cytosol as has also been observed for the Barley orthologue (Per1; Stacy et al., 1999). Stacy et al. (1999) postulated that during active protein translation, Per1 is present in the cytosol, but is thereafter translocated to the nucleus. Alternatively, or additionally, Per1 might be performing different tasks in the cytosol and nucleus, which is specific to the tissue type. Tobacco seeds in which the rice 1-Cys Prx was over-expressed were less susceptible to H_2O_2-mediated oxidative damage. This supports the hypothesis that 1-Cys Prx protects the embryo and the aleurone layer from oxidative damage during desiccation of the seed. The protein is nuclear localised, which means that it might protect DNA and the nuclear machinery of transcription

(Stacy et al., 1999). The yeast and the barley 1-Cys Prx were found to protect DNA from nicking in a mixed function oxidation DNA protection assay (Dietz, 2003). A rice orthologue has been identified in dormant seeds with the *1-Cys Prx* transcript rapidly decreasing to low levels as germination proceeded (Lee et al., 2000).

Very little is known about the reaction mechanism of 1-Cys Prxs (Fig. 1.6). These Prxs lack the C terminal cysteine and the N terminal cysteine is oxidised during the catalytic cycle but the resulting Cys-SOH cannot form a disulphide because no other Cys-SH is available. Although the physiological reductant of the 1-Cys Prx remains to be identified it may possibly be a reductase or another thiol whose cysteine residue reacts with the sulphenic acid residue first and liberates H_2O. Subsequently, a second Cys residue attacks the intermolecular disulphide bridge to form an intra-molecular disulphide bridge, thereby regenerating the functional Cys-residue of the Prx. In vitro studies show that DTT is able to support the regeneration of these Prxs (Rhee et al., 2005). Whether reduced glutathione (GSH) also can serve as an electron donor is controversial (Kang et al., 1998a; Peshenko et al., 1998; Fisher et al., 1999).

The 1-Cys Prx possesses a nuclear bipartite signal, which targets the protein to the nucleus of barley embryos and aleurone cells (Stacy et al., 1999), but GFP experiments also localised the protein to the cytosol (Haslekas et al., 2003a). Previously, 1-Cys Prxs were only detected in seed tissues and the protein was proposed to play a role in the maintenance of dormancy and in the protection of seed tissues against oxidative injury (Haslekas et al., 1998; Lee et al., 2000) but recent reports indicate that it is also expressed in vegetative tissues (Mowla et al., 2002) and that the germination process is not influenced in plants devoid of 1-Cys Prx or possessing a constitutive expression (Lee et al., 2000; Haslekas et al., 2003a). Seeds over expressing 1-Cys Prx and submitted to oxidative stress have a reduced capacity to germinate (Haslekas et al., 2003a). This protein could therefore play a role in the regulation of germination by preventing it under unfavourable conditions. The over-expression of *A. thaliana* 1-Cys Prx was also found to be under the control of antioxidant and abscisic acid promoter responsive elements (Haslekas et al., 2003b). In *X. viscosa*, Mowla et al. (2002) showed that a 1-Cys Prx was induced in vegetative tissues in response to abiotic stresses.

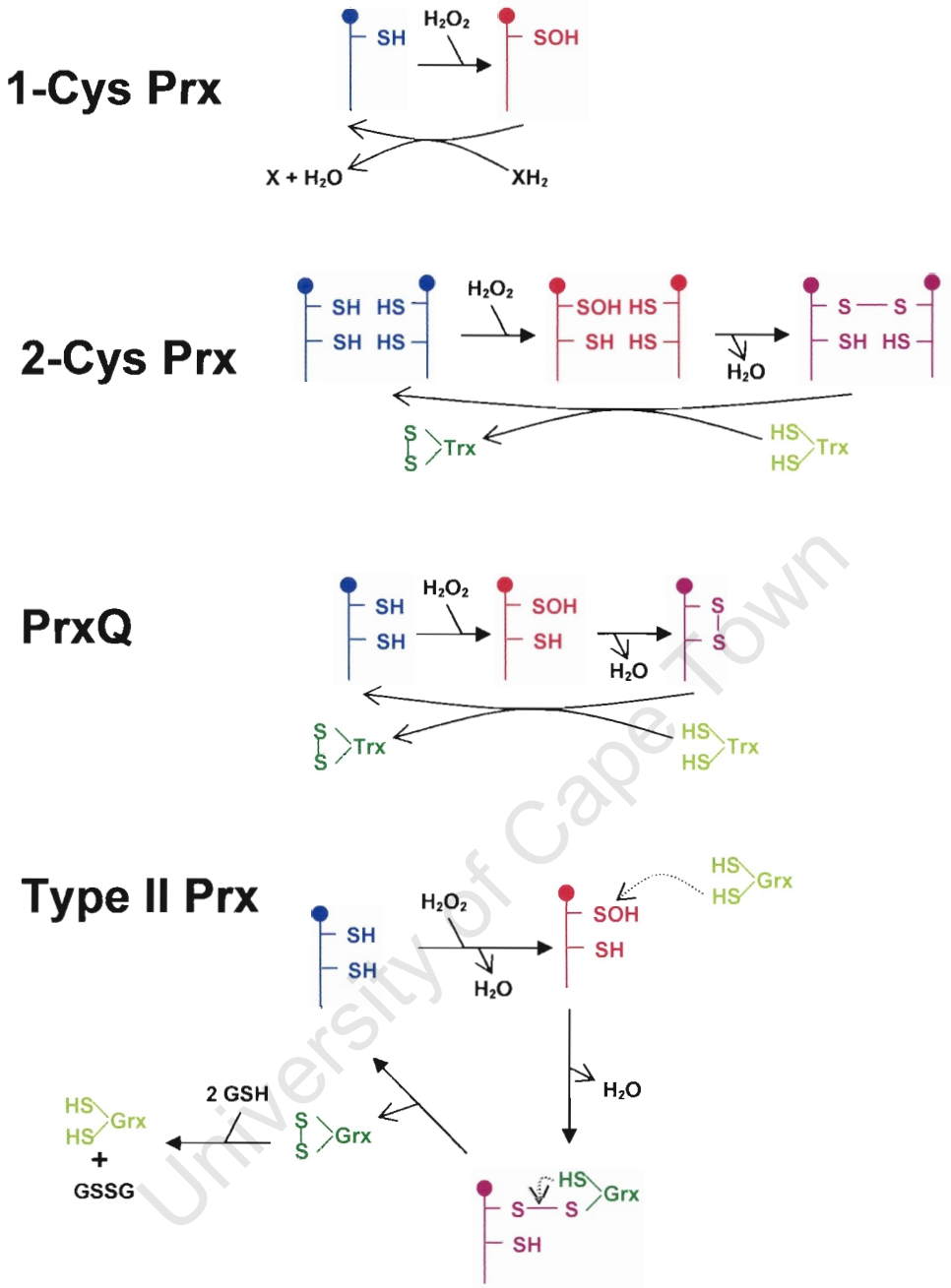

Figure 1.6 Illustration of the proposed catalytic mechanisms of H_2O_2 reduction and Prx regeneration for the four Prx groups. The proteins are represented by pins with the knob being the N-terminus (adapted from Rouhier & Jacquot, 2002).

1.5.2.2 2-Cys Prx

The second member of the Prx family to be identified was the 2-Cys Prx. These proteins are nuclear encoded and targeted to the chloroplast where they protect the photosynthetic membrane from oxidative damage (Baier & Dietz, 1997; Baier & Dietz, 1999). The 2-Cys Prx functions as a homodimer with a head-to-tail arrangement. The barley 2-Cys Prx complemented peroxide sensitivity of AhpC-deficient *E. coli* (Baier & Dietz, 1997). Heterologously expressed 2-Cys Prx reduced H_2O_2, cumene hydroperoxide, tert-butylhydroperoxide (Choi et al., 1999; König et al., 2002) and other hydroperoxides (König et al., 2002; König et al., 2003).

The catalytic unit of the 2-Cys Prx is the homodimer (Fig. 1.6). For the 2-Cys it was found that two catalytic cysteines at positions 36 and 158 are crucial for peroxide reduction (Horling et al., 2002). The first step involves the reduction of the peroxide by the N terminal cysteine residue of one subunit resulting in a sulphenic acid intermediate (Cys-SOH), which then interacts with the C terminal cysteine of the other subgroup forming an intermolecular disulphide bond in the homodimer. By mutating both cysteine residues with a serine no Prx activity was observed (König et al., 2002). Crystal structures of animal homologues of 2-Cys Prx show large conformational changes during the catalytic cycle including partial unwinding of the active site helix in the vicinity of the N terminal cysteine (Hirotsu et al., 1999; Schröder et al., 2000). These Prxs are regenerated by thioredoxins.

The 2-Cys Prx are thylakoid bound chloroplastic enzymes (König et al., 2002) found in nearly all plant tissues except roots (Cheong et al., 1999; Broin et al., 2002). The expression of 2-Cys Prx was observed to decrease with leaf age, even if the protein content was maintained at a high level in old leaves (Horling et al., 2002). Its regulation was also observed to be regulated under salt stress or ascorbate treatments or by changes in illumination and in oxygen concentration (Horling et al., 2001; Goyer et al., 2002; Horling et al., 2002, 2003) whereas it is not or only slightly modified in response to oxidative treatments with diamide or H_2O_2 (Kandlbinder et al., 2004). Some chloroplast proteins were damaged and photosynthesis was impaired in antisense *A. thaliana* plants suggesting a protective function of the photosynthetic apparatus for 2-Cys Prx. In co-suppressed CDSP32 potato mutants (Broin & Rey, 2003), drought or methyl viologen treatments led to an increase in lipid peroxidation in thylakoids, concomitant with over oxidation of 2-Cys Prx. This suggests that the absence of CDSP32 prevents the reduction of 2-Cys Prx under these stress conditions and thus its action against lipid peroxidation of the photosynthetic membranes.

1.5.2.3 Type II Prx

Verdoucq et al. (1999) isolated a target protein of cytoplasmic thioredoxin h with antioxidant activity in *A. thaliana*. This Prx was demonstrated to be a new member of the peroxiredoxin family (type II Prx). Type II Prxs were simultaneously identified in yeast (Jeong et al., 1999) and Chinese cabbage (Choi et al., 1999). The latter is a small protein (17.5 kDa) and has two Cys residues (positions 51 and 76). This type II protein protected glutamine synthetase from oxidative inactivation and possessed H_2O_2 reduction activity with yeast thioredoxin as the electron donor (Choi et al., 1999). This activity was also shown for the *Arabidopsis* type II C Prx (Horling et al., 2002). A type II Prx was identified in the xylem/phloem library of *Populus trichocarpa*, and was observed to be preferentially expressed in the sieve tubes (Rouhier et al., 2001). In vitro, PtPrxII was regenerated by both glutaredoxin and thioredoxin h with similar efficiency and reduced H_2O_2, tBOOH and COOH. Rouhier et al. (2001) stated that natural fusions of Prx and glutaredoxin (Grx) motifs are found in some prokaryotes such as *Vibrio cholerae*.

Type II Prx forms an intramolecular disulphide bond during the catalytic cycle (Fig. 1.6). A 25 amino acid intervening sequence separates the two cysteines unlike PrxQ. Analysis of the human orthologue suggests that the sulphhydryl group corresponding to Cys 51 in *Arabidopsis* is the site of initial oxidation by the peroxide substrate and that the oxidised cysteine reacts with the C terminal sulphhydryl group and forms an intramolecular disulphide bridge (Seo et al., 2000). Rouhier et al. (2001) showed that PtPrxII can be regenerated by both thioredoxins and glutaredoxins with similar efficiencies in vitro whereas *A. thaliana* PrxIIB is only reduced by Grxs but not by Trxs (Brehelin et al., 2003). In *Arabidopsis*, the in vivo interaction of a type II Prx with cytosolic thioredoxin h was demonstrated by Verdoucq et al. (1999). The crystal structure of the human orthologue reveals a distance of 13.8 Å between both cysteine residues, indicating that a major conformational change is necessary to form the disulphide bridge between the catalytic cysteine residues upon oxidation (Declercq et al., 2001). Echalier et al. (2005) showed for the first time that the combination of the crystal structure and the solution NMR dynamics provides evidence of a conserved homodimeric state of the reduced Prx in the crystal and in solution. It was also reported that the Prx-Prx interface involves a surface perpendicular to the β sheet with conserved interfacial residues, which suggests that all type II (D) Prxs could homo-dimerise.

Type II Prxs are ubiquitous in that they are expressed in all plant organs (Choi et al., 1999; Rouhier et al., 2001; Brehelin et al., 2003). The *A. thaliana* PrxIIB, C and D are cytosolic, PrxIIE chloroplastic and PrxIIF mitochondrial (Kruft et al., 2001; Brehelin et al.,

2003). PrxIIF is constitutively expressed in all tissues tested and its expression is not or very slightly modified whatever the treatments applied, suggesting a housekeeping function for this homologue in mitochondria (Baier et al., 2000; Horling et al., 2002; Brehelin et al., 2003; Horling et al., 2003). In *A. thaliana* PrxIIE is expressed mostly in reproductive tissues and variation of its expression is in general comparable to other chloroplastic nuclear encoded Prxs, i.e., 2-Cys Prx A and B (two types of 2 Cys Prxs are found in *A. thaliana* named Prx A and Prx B) and PrxQ. Its expression is thus modified following changes in illumination, decreased in response to ascorbate or NaCl treatments but unaltered following oxidative conditions (Horling et al., 2002, 2003).

The *PrxIIB* and *PtPrxII* genes from *A. thaliana* and poplar, respectively are expressed in all tissues tested (Rouhier et al., 2001; Brehelin et al., 2003), whereas the expression of *PrxIIC* and *D* is almost restricted to pollen (Brehelin et al., 2003). Surprisingly, poplar PtPrxII was detected by immuno-localisation in plastid-like structures of phloem sieve tubes (Rouhier et al., 2001). This localisation could be explained as cross-hybridisation of the antibody between different Poplar homologues as there was no signal peptide in the native protein (Dietz, 2003). Horling et al. (2002) reported that in *Arabidopsis,* PrxIIE (chloroplastic) as well as PrxIIB (cytosolic) was able to be recognised by an antibody raised against PrxIIC (cytosolic). Changes in expression for *PrxIID* were not always described, since it was only recently found to be expressed (Brehelin et al., 2003). Nevertheless, the transcript amount is strongly increased in leaves of phosphorus-deprived plants (Kandlbinder et al., 2004). In *A. thaliana*, the expression of *PrxIIB* is increased upon salt or t-BOOH exposure, but is largely unaffected by ascorbate and light changes (Horling et al., 2002, 2003). The *PrxIIC* expression is low under steady-state conditions, but is in general strongly affected by salt, ascorbate, and oxidative treatments or by plant phosphorus deprivation (Horling et al., 2002, 2003; Kandlbinder et al., 2004). Finally, the PtPrxII protein content is modified in response to a pathogenic attack of poplar by the rust fungus *Melampsora larici-populina* (Rouhier et al., 2004a). The PtPrxII amount increases during an incompatible reaction and decreases during a compatible reaction, indicating that the regulation of its expression and of plant peroxide levels varies as a function of the infection.

1.5.2.4 PrxQ

The fourth group of Prx was initially identified in *Sedum lineare* (Kong et al., 2000) as a homologue of *E. coli* bacterioferritin co-migratory protein (Bcp). In *Arabidopsis*, a single *PrxQ* gene has been identified (Dietz et al., 2002). The active PrxQ is a monomer and reduces

H_2O_2, tBOOH, and COOH and is regenerated by thioredoxin (Fig. 1.6). In the absence of the *bcp* gene *E. coli* is highly sensitive to tBOOH and COOH. The mutant phenotype reverted upon heterologous expression of the *S. lineare* Prx, proving the function of PrxQ as an antioxidant in vivo (Kong et al., 2000).

PrxQ also contains two cysteine residues in its amino acid sequence with both essential for its catalytic activity. The amino terminal cysteine is located in the same position as in the 2-Cys Prxs but the second cysteine is situated only 5 amino acid residues away from the first. The thioredoxin dependent peroxidase activity was abolished by mutating either of the two cysteines (Kong et al., 2000). This indicates that both cysteines are catalytic and form the intramolecular disulphide bond upon oxidation.

In Poplar, PrxQ (targeted to the chloroplast) is only expressed at detectable levels in leaves but not in stems or roots (Rouhier et al., 2004a). Its expression pattern during *Melampsora larici-populina* infection is similar to PtPrxII, both in compatible or incompatible reactions (Rouhier et al., 2004a). Levels of PrxQ also decrease with leaf age, upon salt stress or ascorbate addition, and after transfer from adequate light to low light (Horling et al., 2002, 2003). An increase in PrxQ is observed under conditions of high light and in response to oxidative stress conditions (Horling et al., 2003).

1.5.4 Electron donors involved in the reduction of peroxiredoxins

1.5.4.1 Glutaredoxins and thioredoxins

The thiol redox status of the cytosol is maintained by the thioredoxin (Trx) and the glutathione/glutaredoxin (GSH/Grx) systems. Both Trx and Grx are small heat stable disulphide oxidoreductases with the conserved active site, CXXC, which is required for their redox properties. The Grxs are maintained reduced with the help of NADPH, glutathione reductase and GSH, whereas cytosolic and mitochondrial Trx are reduced by NADPH and NADPH thioredoxin reductase. A characteristic of Grxs is their efficiency in reducing protein and GSH, using only the first catalytic cysteine of the active site (Starke et al., 2003). Qin et al. (2000) reported that Grxs can reduce disulphides with a dithiol mechanism using both their active site cysteines and that Grxs can utilise a mono-thiol mechanism for the reduction of mixed disulphides between proteins and GSH. Both Trx and Grx are able to reduce Prxs and non-heme peroxidases that catalyse the reduction of hydroperoxides (Chae et al., 1994a; Rouhier et al., 2002). In *A. thaliana* and presumably in all higher plants there are at least 26 Trx homologues and 31 Grx homologues predicted to be located in various cellular compartments and this is excluding the significant set of Trx and Grx like proteins (Meyer et

al., 2002; Rouhier et al., 2004c). Currently, very few plant Grxs have been characterised in terms of expression, localisation, or biochemical and structural data (Rouhier et al., 2004c), whereas the function of most Trx homologues has been characterised in various plant subcellular compartments (Schürmann & Jacquot, 2001).

1.5.4.2 Sulphiredoxin

The ability of the yeast protein sulphiredoxin (Srx1) to repair or reduce the over-oxidised state of a yeast 2-Cys Prx called Tsa1 (Biteau et al., 2003) was unexpected, as Cys sulphinic and sulphonic acid generation was considered to be biologically irreversible (Claiborne et al., 1999; Hamann et al., 2002). Purified Srx1 was able to reduce over-oxidised Tsa1 in the presence of ATP and Mg^{2+} or Mn^{2+} (Biteau et al., 2003). A reductant, either DTT or Trx, was also required for the reduction of Tsa1-SO_2^- to the Tsa1-SH form. Given the requirement for ATP hydrolysis, generation of a sulphinic phosphoryl ester (Cys-$S_pO_2PO_3^{2-}$) intermediate was proposed. The inactivity of the Cys84Ser mutant also led Biteau et al. (2003) to further hypothesise the nucleophilic attack of Cys84-SH of Srx1 on the phosphorylated intermediate, resulting in formation of a thiosulphinate bond. Resolution of this complex with a reductant (e.g. Trx or GSH) in this proposed mechanism would then return both enzymes to their reduced states through putative Prx-Cys-S_pOH and Srx1-S-S-R intermediates. The structure of the human Srx (hSrx) crystal structure was determined to discern the molecular basis for the novel sulphur chemistry of Srx and its interactions with Prxs. The structures reveal a new protein fold and a novel nucleotide binding motif. Biochemical analysis has also confirmed the site of ATP cleavage during the first of the catalytic reaction. The overall concave shape of the hSrx active site surface suggests that hSrx is ideally suited to interacting with the over-oxidised, doughnut like Prx decamer (Jönsson et al., 2005).

1.6 SIGNIFICANCE OF THIS STUDY

Water has become a major limiting factor in South Africa's agriculture. Environmental stresses have been the scourge of agriculture over the ages, bringing with them poor harvests and the threat of famine. In general, most crop plants are highly sensitive to even a mild dehydration stress. Today, the importance of crop resistance to water stress, extremes of salinity, and harsh temperature is likely to increase further as the range of environments in which crops are cultivated expands and the incidence of extreme weather conditions increases with the spectre of global warming. Many stress inducible genes have been identified over the

past decade and their functional roles in stress tolerance have recently been elucidated. The improvement of crop stress tolerance by targeting stress-related genes for genetic manipulation is therefore now feasible. Resurrection plants, such as *X. viscosa,* which can tolerate extreme water loss (greater than 90%) or desiccation makes them ideal systems to study desiccation stress tolerance. The isolation of stress inducible promoters and the driving of stress inducible genes in transgenic crops can lead to striking improvements in plant tolerance to abiotic stresses such as low temperature, salt and mainly dehydration/drought stress. Genes isolated from such plants can be used to improve drought tolerance of essential crops such as maize, wheat and rice. To ensure that the responses of the transformed plants to desiccation and water stress treatments are agronomically relevant, plants must be subjected to the drought regimes that crops experience in the fields. This will greatly benefit the agricultural sector in South Africa. This would also provide developing countries within sub-Saharan Africa with the potential to produce crops that would be able to withstand the harsh dessert conditions and possibly provide greater yields. This should impact favourably on the levels of starvation and malnutrition that occurs in this geographical region.

The aim of this study was to characterise a type II peroxiredoxin (*XvPrx2*) isolated from the resurrection plant *X. viscosa* on a molecular and biochemical basis. The following objectives were pursued in order to achieve this goal:

(i) Synthesis of a full-length cDNA library from low temperature stressed *X. viscosa*;

(ii) Molecular characterisation of a type II peroxiredoxin (*XvPrx2*);
   (a) Southern blot analysis to estimate the copy number of the gene in the *X. viscosa* genome;
   (b) Northern blot analyses to determine the expression patterns of *XvPrx2* in response to abiotic stresses such as dehydration, low temperature, salt, abscisic acid, high temperature and high light stress;
   (c) 2-D gel electrophoresis to identify homologues and to determine the pI.

(iii) Localisation of XvPrx2;
   (a) Large scale protein expression and purification for antibody generation;
   (b) Sub-cellular localisation of XvPrx2;

(iv) Biochemical characterisation of a type II peroxiredoxin (XvPrx2);
   (a) Assessing the antioxidant activity of XvPrx2 in vitro as well as in vivo;
   (b) Generation of a point mutation in XvPrx2;
   (c) Enzyme assays assessing various electron donors as well as substrates; and
   (d) Determining conformational change of XvPrx2 using limited proteolysis.

Chapter 2

Molecular characterisation of *XvPrx2*

2.1 INTRODUCTION

Environmental stresses such as drought, low/high temperature and salinity impact negatively on the quality and quantity of crop yield. Resurrection plants, such as *X. viscosa*, possess effective mechanisms for coping with drought stress by being able to survive severe water loss in excess of 90% and therefore potentially represent a rich source of regulatory mechanisms that confer tolerance to abiotic stresses.

Due to the ability of *X. viscosa* to withstand severe desiccation stress, genes upregulated during abiotic stress and specifically those that are involved in oxidative processes were sought. The following objectives were pursued to achieve this goal:

(i) synthesis of a cDNA library of *X. viscosa* from cold temperature stressed *X. viscosa*;

(ii) initial characterisation of selected genes; and

(iii) further characterisation of a single gene potentially involved in oxidative processes.

2.2 MATERIALS AND METHODS

2.2.1 Collection of plant material and stress treatment

The *X. viscosa* plants were collected from Cathedral Peak Nature Reserve in the Drakensberg mountains (KwaZulu-Natal, South Africa). Plants were grown under green-house conditions as described by Sherwin & Farrant (1996). A single plant was used for a low temperature stress analysis. Two leaves were initially excised from the plant prior to the plant being exposed to low temperature (non-stressed sample). The plant was incubated for 60 h at 4°C; thereafter two leaves were excised (stressed sample). Leaves were dissected into minute pieces and flash frozen in liquid nitrogen.

2.2.2 RNA extraction

All plastic and glassware used were double autoclaved; all solutions were prepared using DEPC water. Plant material was ground in liquid nitrogen using a mortar and pestle. The ground material was maintained at low temperature (4°C) to prevent RNA degradation. Seven hundred and fifty microlitres of Trizol (Invitrogen Life Technologies, USA) was added to Eppendorf tubes containing ground plant material. The mixture was vortexed for 5 min and thereafter incubated for 5 min at RT. Two hundred microlitres of chloroform was added to the homogenised sample. Samples were mixed gently by inversion (ca. 1 min). Tubes were incubated for 3 min at RT followed by centrifugation for 15 min at 12000 x g at 4°C. The aqueous phase was transferred into a fresh Eppendorf tube using a pipette. The organic phase was discarded. Five hundred microlitres of isopropanol was added to the aqueous phase. Tubes were incubated for 10 min at RT to allow for precipitation of DNA. The RNA was pelleted by centrifugation for 10 min at 12000 x g at 4°C. The supernatant was discarded. The RNA pellet was washed in 1 ml of cold 75% ethanol (EtOH). RNA samples were centrifuged for 5 min at 6000 x g at 4°C and the EtOH was discarded. RNA samples were briefly centrifuged and the remaining EtOH removed with a pipette. The RNA pellet was air-dried for ca. 10 min. Fifty microlitres of DEPC water was added to the RNA pellet. Tubes were incubated for 5 min at 55°C to assist in resuspension of RNA pellets.

2.2.3 Generation of a full-length *Xerophyta viscosa* cDNA library

A full-length *X. viscosa* cDNA library was synthesised using the Creator SMART cDNA library synthesis kit (Clontech, USA). All procedures were carried out according to the manufacturer's instructions.

2.2.3.1 First strand cDNA synthesis

An RNA-oligonucleotide mix (*X. viscosa* RNA, Smart IV, CDSIII) was prepared in a volume of 5 µl (Table 2.1). The mix was combined in a sterile Eppendorf tube, mixed gently, briefly centrifuged and thereafter incubated for 2 min at 72°C. Samples were subsequently incubated for 2 min on ice. The final components (buffer, DTT, dNTPs and reverse transcriptase) required for the reverse transcription reaction were added to the RNA-oligonucleotide mix (Table 2.1). The reaction components were mixed gently, briefly centrifuged and thereafter incubated for 1 h at 42°C. First strand cDNA synthesis was terminated by placing the samples on ice. Samples were stored at -20°C.

Table 2.1 Components of the first strand cDNA synthesis reaction

Component	Volume (µl)
RNA (1 µg)	χ (1-3)
Smart IV (10 µM; Appendix B)	1
CDSIII (10 µM; Appendix B)	1
Deionised H_2O	make up volume to 5 µl
First strand buffer (5X)	2
DTT (20 mM)	1
dNTPs (10 mM)	1
Powerscript Reverse Transcriptase (100 $U.\mu l^{-1}$)	1

2.2.3.2 cDNA amplification by long distance PCR

Amplification of cDNA by long distance PCR was performed using the Advantage 2 PCR system (Clontech, USA). The long distance PCR reaction was prepared in a total volume of 100 µl (Table 2.2). Reaction components were mixed by gentle flicking of the tube, followed by brief centrifugation to collect the contents at the bottom of the tube. Tubes were placed in a preheated (95°C) thermal cycler (Gene Amp 9700; Perkin Elmer Applied Biosystems, USA). Cycling conditions were as follows: 95°C for 20 s; 20 cycles of 95°C for 5 s and 68°C for 6 min. A 5 µl aliquot of the PCR product was analysed on a 1% agarose/ethidium bromide (EtBr) gel. Samples were stored at -20°C.

Table 2.2 Components of the second strand cDNA synthesis reaction

Component	Volume (µl)
First strand cDNA	2
Advantage 2 PCR buffer (10X)	10
dNTPs (50X)	2
5' PCR primer (10 µM; Appendix B)	2
CDS III (10 µM)	2
Advantage 2 Polymerase mix (50X)	2
Deionised H_2O	make up volume to 100 µl

2.2.3.3 Proteinase K digestion

Two micrograms of amplified double stranded (ds) cDNA was pipetted into a sterile Eppendorf tube, containing 40 µg proteinase K. The reaction components were mixed gently, briefly centrifuged and thereafter incubated for 20 min at 45°C. Fifty microlitres of deionised water was added to the sample. A further 100 µl of phenol:chloroform:isoamyl alcohol (25:24:1) was added and mixed by gentle inversion (ca. 1 min). The sample was centrifuged for 5 min at 12000 x g to separate the organic and aqueous phases. The upper aqueous layer was carefully transferred to a sterile Eppendorf tube using a pipette (the interface and lower layer were discarded). One hundred microlitres of chloroform:isoamyl alcohol (24:1) was added and mixed by gentle inversion (ca. 1 min). The sample was centrifuged for 5 min at 12000 x g to separate the organic and aqueous phases. The upper aqueous layer was carefully transferred to a sterile Eppendorf tube using a pipette (the interface and lower layer were discarded). Ten microlitres sodium acetate (3 M), 1.3 µl of glycogen (20 $\mu g.\mu l^{-1}$) and 260 µl of RT 95% EtOH were added to the aqueous layer. Samples were centrifuged for 20 min at 12000 x g at RT. The supernatant was carefully removed and discarded using a pipette ensuring that the pellet was not disturbed. The DNA pellet was washed with 100 µl of cold 80% EtOH. The pellet was air-dried for ca. 10 min to allow for evaporation of residual EtOH. The DNA pellet was resuspended in 79 µl deionised water.

2.2.3.4 *Sfi*I digestion of ds cDNA

Digestion of the ds cDNA amplimers was set up in a sterile 0.5 ml tube in a total volume of 100 µl. The reaction mix included 79 µl ds cDNA, 10 µl *Sfi*I buffer (10X), 10 µl *Sfi*I (20U.µl^{-1}) and 1 µl BSA (100X). The reaction components were mixed well by gentle flicking of the tube and incubated for 2 h at 50°C. At the end of the incubation period 2 µl of 1% xylene cyanol dye was added to the sample and mixed well by gentle flicking of the tube.

2.2.3.5 Size fractionation of ds cDNA

Sixteen Eppendorf tubes were labelled and arranged in a rack. The Chroma Spin-400 Column (Clontech, USA) for drip procedure was prepared according to the manufacturer's instructions. The column was inverted several times to completely resuspend the gel matrix. A pipette was used to resuspend the matrix gently thus avoiding air bubbles. The bottom cap was removed and the column fluid was allowed to drip naturally while the column was attached to a ring stand. The storage buffer was allowed to drain through the column by gravity flow until the surface of the gel beads in the column matrix (optimal volume ca. 1 ml) was visible. An optimal flow rate of ca. 1 drop per 40-60 s was obtained with a volume of 1 drop being approximately 40 µl. Once the flow of storage buffer had ended, 700 µl of column buffer was carefully added along the inner wall of the column and allowed to drain out (ca. 15-20 min). Samples (100 µl mixture of *Sfi*I digested cDNA and xylene cyanol dye) were carefully applied to the top centre surface of the matrix and allowed to be fully absorbed into the surface of the matrix. The tube that previously contained the cDNA was washed with 100 µl of column buffer and this material was then carefully applied to the surface of the matrix. The buffer was allowed to drain out of the column until no liquid was left above the resin. Once dripping ceased with the dye layer several millimetres into the column the rack containing the collection tubes were placed under the column so that the first tube was aligned under the column outlet. Six hundred microlitres of column buffer was added and immediately single drop fractions were collected (approximately 35 µl per tube) in tubes 1-16. The column was recapped after the last fraction was collected. To assess the profiles of the fractions, 3 µl of each fraction was electrophoresed for 10 min at 150 V on a 1.1% agarose/EtBr gel separately but in adjacent wells. The peak fractions were visualised by observing the intensity of the bands under UV light. Fractions containing DNA in the desired size range were pooled in a sterile Eppendorf. The following reagents were added to the tube with 3-4 pooled fractions containing the cDNA: 1/10 volume sodium acetate (3M, pH 4.8),

1.3 µl glycogen (20 mg.ml^{-1}l) and 2.5 volumes ice cold 95% EtOH. Samples were mixed by gentle inversion (ca. 1 min), incubated overnight at -20°C and thereafter centrifuged for 20 min at 12000 x g at RT. The supernatant was carefully removed with a pipette leaving the pellet undisturbed. The tube was briefly centrifuged to bring all residual liquid to the bottom. Excess liquid was removed and the pellet was air dried for ca. 10 min. The DNA pellet was resuspended in 7 µl deionised water and mixed well by gentle flicking of the tube.

2.2.3.6 Ligation of ds cDNA to pDNR-Lib

Pure ds cDNA was ligated to *Sfi*I digested, dephosphorylated pDNR-Lib vector (Clontech, USA; Appendix C). Three ds cDNA to vector ratios were utilised to ensure maximal ligation (Table 2.3). Ligation reactions were mixed well by gentle flicking of the tube (being careful to avoid the production of air bubbles), briefly centrifuged and incubated overnight at 16°C. Ninety five microlitres of sterile DEPC-treated H_2O and 1.5 µl of glycogen were added to each of the ligation reactions and mixed well with a pipette. Two hundred and eighty microlitres of ice cold 95% EtOH was added. Samples were mixed well by gentle inversion (ca. 1 min), incubated for 1 h at -70°C and thereafter centrifuged for 20 min at 12000 x g at RT. The EtOH was carefully removed without disturbing the pellet. The pellet was air-dried and subsequently resuspended in 5 µl sterile DEPC-treated H_2O.

Table 2.3 Ligation of ds cDNA using three different insert to vector ratios

Component	Ligation A (µl)	Ligation B (µl)	Ligation C (µl)
cDNA	0.5	1.0	1.5
pDNR-Lib (0.1 µg.µl^{-1})	1.0	1.0	1.0
Ligation buffer (10X)	0.5	0.5	0.5
ATP (10 mM)	0.5	0.5	0.5
T4 DNA ligase (400U.µl^{-1})	0.5	0.5	0.5
Deionised H_2O	2.0	1.5	1.0

2.2.3.7 Preparation of electrocompetent cells

Cells were maintained at 4°C throughout the procedure. A pre-chilled rotor (JA-14; Beckman, USA) and centrifuge (J2-21M; Beckman, USA) were used for all centrifugation steps. Cells were streaked onto fresh Luria Bertani (LB) agar plates and incubated overnight at 37°C. A single colony was selected from the overnight culture and streaked onto a fresh LB agar plate, which was incubated overnight at 37°C. A single colony was selected from the

overnight culture and inoculated into 25 ml LB broth. The culture was incubated overnight at 37°C with shaking. A 1 litre flask of LB broth was inoculated with 10 ml of overnight culture. The cells were cultured with vigorous shaking (225-250 rpm) at 37°C to an OD_{600} of between 0.5-0.7. The flask was incubated for 1 h on ice. The culture was transferred to sterile centrifuge bottles and centrifuged for 15 min at 2800 x g at 4°C. The supernatant was transferred to a sterile, centrifuge bottle and maintained on ice. The pellet was gently resuspended in 1 litre of ice cold 10% glycerol. Cells were centrifuged for 15 min at 2800 x g at 4°C. The pellet was gently resuspended in 0.5 litres of ice cold 10% glycerol. Cells were centrifuged for 15 min at 2800 x g at 4°C. The pellet was gently resuspended in 25 ml of ice cold 10% glycerol. Cells were centrifuged for 15 min at 2800 x g at 4°C. The pellet was gently resuspended in 3.5 ml of ice cold 10% glycerol. One hundred microlitre aliquots were prepared and immediately flash frozen in liquid nitrogen and stored at -80°C. The efficiency of the competent cells was assessed by transforming with pBSK (Stratagene, USA).

2.2.3.8 Transformation of recombinant plasmids into electrocompetent cells

Electrocompetent cells were thawed on ice and used immediately upon thawing to obtain maximum efficiency in electroporation. Nine hundred and seventy microlitres of LB broth was added to five Eppendorf tubes labelled A, B, C, '+' (pBSK; positive control) and '-' (no DNA; negative control). Twenty five microlitres of thawed cells was added to each ligation reaction mix (see section 2.2.3.6) and to the positive and negative controls. Each transformation mix was transferred to a chilled 0.1 cm electroporation cuvette. Electroporation conditions were as follows: voltage 1.8 kV, capacitance 25 μF and resistance 200 ohms. Cells were electroporated by electrical discharge and the cuvette immediately removed from the chamber. The entire transformation volume was immediately transferred to pre-labelled Eppendorf tubes containing 970 μl LB broth. Tubes were incubated for 1 h with shaking (225 rpm) at 37°C. Eppendorf tubes labelled A, B, C, '+' and '-' each containing 50 ml LB broth were prepared during the incubation period. At the end of the 1 h incubation, 1 μl of each transformation mixture was transferred to the respective tube containing 50 μl LB broth and mixed gently by swirling. The remaining transformation mix was stored at 4°C. The cells in LB broth were spread on pre-warmed 90 mm LB agar plates supplemented with 30 μg $.ml^{-1}$ chloramphenicol (LB-Cm plate). The inoculum was allowed to soak into the plate for 10 min prior to being inverted and incubated overnight at 37°C.

2.2.3.9 Pooling and amplification of transformants

Three confluent plates (containing several thousand colonies) were selected. Such plates were estimated to produce a library of approximately 1 x 10^6 clones. The percentage of recombinant clones in each transformation was determined. DNA from fifteen independent clones were analysed from each transformation. Inserts were screened by digestion of miniprep DNA with *Sfi*I to excise inserts. The library was pooled on confirmation that 10 out of 15 transformants had positive inserts, thus generating an unamplified library.

The LB-Cm plates were pre-warmed for 2 h at 37°C. An aliquot of the library was thawed and placed on ice. One microlitre of the library was transferred to 1 ml of LB broth in an Eppendorf tube (Dilution A; 1:10^3) and mixed by gently vortexing. A 1 µl aliquot of Dilution A was transferred to 1 ml of LB broth in an Eppendorf tube (Dilution B; 1:10^6) and mixed by gently vortexing. A second 1 µl aliquot of Dilution A was transferred to 50 µl of LB broth in an Eppendorf tube, mixed by gentle vortexing and the entire volume spread onto a pre-warmed LB-Cm plate. Fifty and one hundred microlitre aliquots were removed from Dilution B and spread onto separate LB-Cm plates. Plates were incubated for 20 min at RT to allow the inoculum to soak into the agar prior to being inverted and incubated overnight at 37°C. Colony numbers were determined to estimate the titre (cfu.ml^{-1}):

(cfu in Dilution A) x 10^3 x 10^3 = titre of Dilution A

(cfu in Dilution B) / plating volume x 10^3 x 10^3 x 10^3 = titre of Dilution B

(titre of Dilution A) + (titre of Dilution B) / 2 = average library titre

The library was plated directly on selective medium (LB-Cm plates) at a high enough density so that the resulting colonies were nearly confluent (ca. 20 000 cfu per 150 mm plate). Sufficient cfus were plated to obtain at least 3 times the number of independent clones in the library. The number of plates to be used was determined:

(# of independent clones) x 3 = # of clones

The number of independent clones is the number of independent clones present in the library prior to amplification.

(# of clones) / (20 000 cfu) = # of plates

The amount of library stock to spread on each plate was determined:

(# of clones) / (library titre) = microlitres of library to plate

The volume of media needed to plate 150 µl of the library on each plate was calculated:

(# of plates) x 150 µl = χ µl

Ten microlitres of the library was added to χ µl of LB-Cm broth. One hundred and fifty microlitres of this culture was spread onto each pre-warmed (3 h at 30°C) LB-Cm plate and incubated for 18-20 h at 37°C. Five millilitres of LB broth and 25% glycerol were added to each plate and colonies were scraped into liquid. All the resuspended colonies were pooled in a single 50 ml Sterilin tube and mixed thoroughly. Five 1 ml aliquots of the library culture were set aside (stored at -80°C) in the event that it was necessary to re-amplify the library at a later time. The remainder of the library culture was divided into 50 µl aliquots and thereafter stored at -80°C.

After the library had been titered and amplified a 50 µl aliquot was screened for insert sizes larger than 500 bp. Plasmid DNA was isolated from 60 cDNA clones using the High Pure Plasmid Extraction kit (Roche, Germany) according to the manufacturer's instruction. Ten microlitres of purified recombinant plasmid was digested with *Sfi*I. The ds cDNA insert within the pDNR-Lib vector is flanked by two *Sfi*I sites hence digestion produced two DNA fragments corresponding to the insert and the pDNR-Lib vector backbone. Plasmid DNA was incubated with 8 units of *Sfi*I per 1 µg plasmid DNA for 3 h at 50°C. Digested samples were analysed on a 0.8% agarose/EtBr mini-gel.

2.2.4 Sequencing and BLAST analysis of cDNA clones

The nucleotide sequences of fifty cloned cDNAs were determined on both strands using the MegaBACE 500 (Molecular Dynamics, USA). Sequencing reactions were carried out using the DYEnamic ET Dye terminator sequencing kit (Molecular Dynamics, USA) according to the manufacturer's instructions. The BLAST program of the National Centre for Biotechnology Information (Altschul et al., 1990) was used to search the Genbank database for sequence similarities.

2.2.5 Bioinformatic analysis of *XvPrx2*

The inferred amino acid sequence of *XvPrx2* was obtained by translation of the cDNA sequence using DNAMAN software (vers. 5.2.10; Lynnon Biosoft, Canada). The Bioinformatics and Biological Computing Unit (Weizmann Institute of Science, Israel) was used to plot the hydrophilicity/hydrophobicity of XvPrx2. The ScanProsite tool provided by ExPASy (us.expasy.org) was used to scan XvPrx2 for conserved motifs. Phylogenetic and molecular evolutionary analyses were conducted using MEGA (vers. 3.0; Kumar et al., 2004). A strict consensus maximum parsimony (MP) trees was inferred using the close-neighbour-

interchange heuristic search. The initial tree was generated by randomly selecting a sequence and adding it to the growing tree on a randomly selected branch (random addition tree option). The reliability of the inferred phylogenetic trees was assessed using the bootstrap test (Felsenstein, 1985). A thousand replicates were tested with a random starting seed. A homology tree was constructed using DNAMAN. This tree was setup with the distance matrix using the UPGMA method (Sneath & Sokal, 1973). The homology tree shows related homologies between two sequences or groups. Sequences used in the phylogenetic and homology analyses are displayed in Appendix B.

2.2.6 Southern blot analysis

The Southern protocol was adapted from Sambrook et al. (1989). Genomic DNA was extracted from leaves of fully hydrated *X. viscosa* plants according to the procedure described by Dellaporta et al. (1983). Leaf tissue (ca. 1 g) was ground to a fine powder in liquid nitrogen prior to extraction. The DNA was precipitated using isopropanol, resuspended in TE buffer (10 mM Tris, pH 7.6; 1 mM EDTA) and quantitated spectrophotometrically. Aliquots of genomic DNA (15 µg) were digested in separate tubes using the following restriction enzymes: *Bgl*II, *Eco*RI, *Eco*RV, *Hin*dIII, *Xba*I, *Eco*RI + *Eco*RV, *Eco*RI + *Pvu*I and *Eco*RI + *Xba*I. Digested DNA was electrophoresed overnight at 20V on a 0.8% agarose/EtBr gel in separate but adjacent wells. On completion of electrophoresis the DNA was transferred by capillary transfer (Sambrook et al., 1989) onto a nylon membrane (Hybond-XL; Amersham Biosciences, USA) and UV cross-linked (UV Crosslinker; Amersham Biosciences, USA) onto the membrane.

A radio-labelled probe was prepared by PCR amplification of pDNR-Lib::*XvPrx2*. Primers used in the amplification procedure were XvPrx2-F (10 µM; Appendix B) and XvPrx2-R (10 µM; Appendix B). The reaction contained [α-^{32}P] dCTP at a concentration of 50 uCi. The PCR reaction was conducted using a Gene Amp 9700 thermal cycler with the following parameters: 95°C for 5 min; 15 cycles of 95°C for 30 s, 58°C for 1 min and 72°C for 10 min; and a final extension step at 72°C for 10 min. A longer extension time of 10 min was used to ensure that the 'heavier' radio-labelled dCTP would incorporate during amplification. Unincorporated nucleotides were removed by passing the PCR product through a sephadex-G50 column. The specific activity of the labelled probe was determined in a scintillation counter by counting 1 µl of probe in 2 ml of scintillation fluid. The membrane was pre-hybridised in buffer (0.5 M NaH_2PO_4; 1 mM EDTA; 7% SDS; 1% BSA) for a

minimum of 2 h at 65°C. Following pre-hybridisation, the radio-labelled probe was denatured by incubation for 10 min in a boiling water bath and immediately thereafter placed on ice. The denatured probe was added to the pre-hybridisation buffer and hybridisation was carried out for 18 h at 65°C with gentle shaking. The membrane was washed once for 12 min at 65°C in Wash Buffer A (0.5% SDS; 2X SSC), followed by a second wash for 10 min at 65°C in Wash Buffer B (0.1% SDS; 0.5X SSC). The membrane was autoradiographed at -70°C onto Hyperfilm MP (Amersham Biosciences, USA). Following 5 days exposure, the film was developed manually using developer and fixer reagents (Amersham Biosciences, UK) according to the manufacturer's instructions.

2.2.7 Generation of an *XvPrx2* point mutation

A point mutation was generated in *XvPrx2* to allow for a second cysteine residue to be substituted at codon 76 for the existing valine (Fig. 2.1). The resulting protein with two cysteine residues was named XvV76C.

A gene specific forward primer (F4 HisTOPO-S; Appendix B) and reverse primer (F4 Point Mut-S; Appendix B) incorporating the required base changes at codon 76 were used to generate a fragment of the gene (amplimer A; codons 1-76). Similarly, a gene specific reverse primer (F4 HisTOPO-A; Appendix B) and forward primer (F4 Point Mut-A; Appendix B) incorporating the required base changes at codon 76 were used to generate the second fragment of the gene (amplimer B; codons 76-162). Sixty nanograms each of amplimer A and B were used as template with gene specific forward and reverse primers (F4 HisTOPO-S, F4 HisTOPO-A) to generate the point mutated *XvPrx2* gene. The Expand High Fidelity PCR system (Roche, Germany) was utilised in all PCR reactions (Table 2.4). Due to the polymerase's inherent 3' – 5' exonuclease or proofreading activity, a 3 fold increase in the fidelity of the DNA synthesis reaction is observed compared to standard Taq DNA polymerase. PCR reaction volumes were made up to 25 µl and run on a GeneAmp 9700 thermal cycler with the following cycling conditions: 94°C for 3 min; 35 cycles of 94°C for 30 s, 58°C for 45 s and 72°C for 1.5 min; and a final extension step at 72°C for 5 min.

Table 2.4 PCR reagents and final concentrations used to generate *XvV76C*

Components	Final concentration
Deoxynucleotide mix	200 µM of each dNTP
Forward primer	300 nM
Reverse primer	300 nM
Template DNA	10 - 60 ng
Expand High Fidelity Buffer	1X (1.5 mM $MgCl_2$)
Expand High Fidelity Enzyme mix	2.6 U

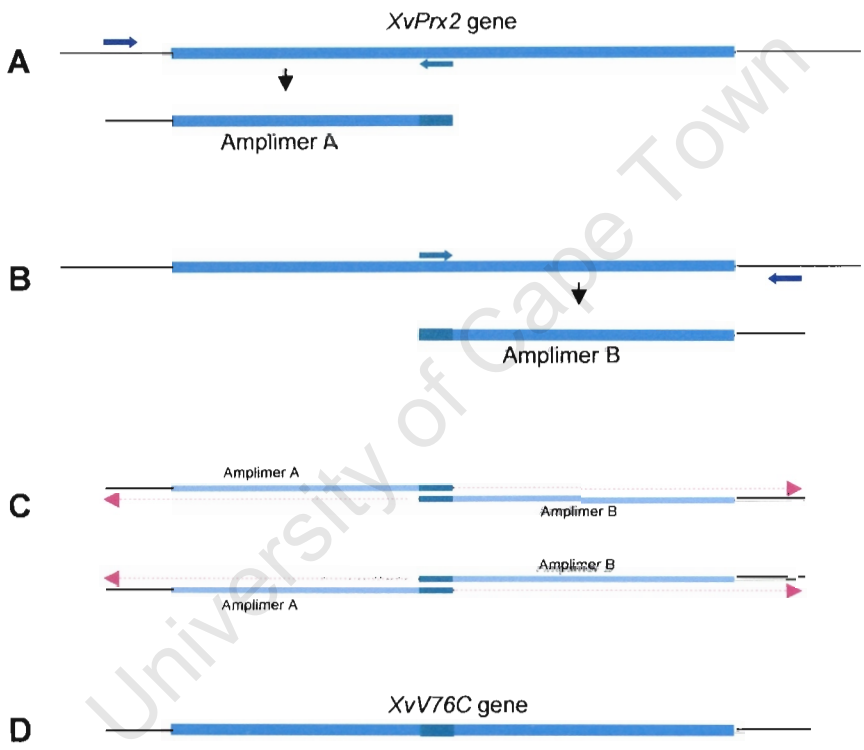

Figure 2.1 Schematic diagram displaying the generation of a point mutation in *XvPrx2*. Amplimer A was generated using a gene specific reverse primer including the necessary base changes (A). Similarly, Amplimer B was generated using a gene specific forward primer including the necessary base changes (B). Aliquots of Amplimer A and B were used as template to generate the point mutated *XvPrx2* gene (C). The resulting point mutated *XvV76C* gene includes the necessary nucleotide substitutions in codon 76 (D).

2.2.8 Analysis of *XvPrx2* promoter regions

The splinkerette protocol was employed to obtain the upstream genomic sequence of *XvPrx2*. This protocol was modified from Devon et al. (1995). Restriction endonucleases used were *Bam*HI, *Dra*I, *Eco*RI, and *Nde*I.

Adaptors were prepared by the addition of splnktop (Appendix B; 150 $\mu g.ml^{-1}$) separately to 4 oligonucleotides (splnkBamHI, splnkDraI, splnkEcoRI, splnkNdeI; Appendix B; 150 $\mu g.ml^{-1}$) in 20 µl of splnk buffer (20 mM Tris, pH 7.4; 10 mM $MgCl_2$). The 4 oligonucleotide mixes were heated to 90°C and cooled (ca. 15 min) on the bench top to allow the adaptors to anneal. Four aliquots of *X. viscosa* genomic DNA (3 µg) were digested with 20 U of the respective restriction endonuclease in a 20 µl reaction volume. The restriction endonucleases were heat inactivated for 10 min at 65°C. Annealed adaptors were ligated to the digested genomic DNA (Table 2.5). The ligation reaction volume was made up to 20 µl with sterile water and incubated overnight at RT.

Table 2.5 Components of ligation reaction of adaptors to digested genomic DNA

Component	Volume (µl)
Annealed splinker (adaptor)	6
Digested DNA	2
pGemT Easy ligase buffer (2X)	10
pGemT Easy T4 DNA ligase (50 $ng.\mu l^{-1}$)	1
H_2O	1

Two gene specific primers (Prom-R2, Prom-R1; Appendix B) were used in the first step PCR reaction (Table 2.6). PCR reaction volumes were made up to 25 µl (standard PCR reaction; Appendix A) and run with the following cycling conditions: 94°C for 2 min; 7 cycles of 94°C for 1 min, 65°C for 1 min and 72°C for 5 min. The amplification protocol was repeated using splnkB forward primer (Appendix B) and internal reverse primer Prom-R1 (Appendix B). One microlitre of diluted template (1:50) was used in the second round of PCR. The PCR reagents and conditions were unchanged except for the cycles that were increased to thirty. PCR products were electrophoresed on a 1% agarose/EtBr gel.

Table 2.6 PCR reagents used in the Splinkerette protocol

Component	Volume (µl)
Ligated adaptors to digested genomic DNA	1
$MgCl_2$ (25 mM)	3
Buffer (10X)	5
dNTP mix (2.5 mM)	4
Supertherm Taq (0.2 $U.\mu l^{-1}$)	1
splnkA (5 µM; Appendix B)	1.5
PromR2 (10 µM)	1.5

The band of interest was excised and purified using the High Pure PCR Product Purification Kit (Roche, Germany) according to the manufacturer's instruction. A third PCR was performed using reagents and conditions as described for the second PCR, the only change being primers splnk B and Prom-R1 were used in the amplification of the purified excised band. A single band product was again purified following the procedure described previously. Ligation of the purified amplimer to TOPO vector (Invitrogen, USA) was carried out according to the manufacturer's instruction (Table 2.7).

Table 2.7 Ligation of *XvPrx2* upstream region into TOPO cloning vector

Component	Volume (µl)
Purified PCR product	2
TOPO vector	0.5
Salt solution*	0.5

*No ligase was required in the ligation reaction

The reagents were added to an Eppendorf tube and incubated for 30 min at RT. Three microlitres of the ligation mix was transformed in TOP10F' *E. coli* cells (standard transformation condition; Appendix A). Colony PCR was performed using T7 TOPO-F primer (Appendix B) and Prom-R1 reverse primer to select for positive clones.

2.3 RESULTS

2.3.1 Collection of plant material and stress treatment

Plants that were bagged and transported to University of Cape Town from Cathedral Peak appeared healthy (Fig. 2.2). After a few months under greenhouse conditions *X. viscosa* plants were observed to be flourishing with green healthy leaves and new shoots. Plants had to be divided and repotted as the pots had become too small for the existing plants. The *X. viscosa* plants produced flowers in Spring, which is an indication that the conditions under which they were cultured were well suited to the physiological and reproductive functions of these plants. Once plants were acclimatised to the new habitat whole plants or excised leaves were used in stress treatments.

Figure 2.2 The *X. viscosa* plants in their natural habitat and under greenhouse conditions. The *X. viscosa* plant in its natural habitat in the Drakensberg mountains (A); potting of *X. viscosa* immediately after collection (B); a healthy *X. viscosa* plant in the greenhouse (C); and *X. viscosa* plants in bloom in the greenhouse (D).

2.3.2 RNA extraction

Good quality RNA (Fig. 2.3) was isolated from an unstressed and low temperature stressed *X. viscosa* plant. The RNA was not degraded and was of high concentration (ca. 1 $\mu g.\mu l^{-1}$). One microgram of this RNA was used for the generation of cDNA, which was subsequently utilised in the construction of the library.

2.3.3 Generation of a full-length *Xerophyta viscosa* cDNA library

RNA obtained from a plant stressed at low temperature for 12 h was utilised for the generation of the library (Fig. 2.3). A DNA size range of 0.5-4 kb was observed for ds cDNA generated from long distance PCR utilising 2 µl of the first strand synthesis cDNA. Bands were visible and not too faint indicating that the cycling parameters used was correct. The bright bands observed corresponded to abundant mRNA specific to *X. viscosa*.

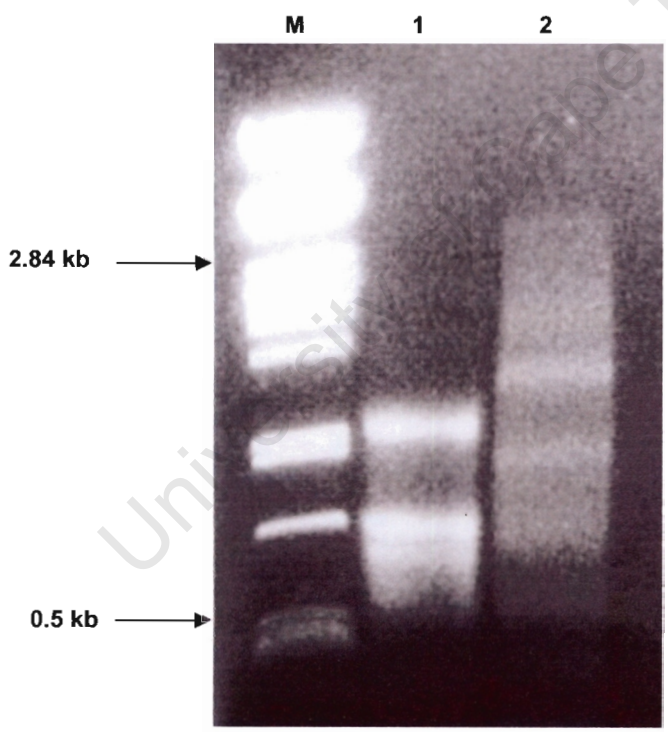

Figure 2.3 Gel electrophoresis of *X. viscosa* total RNA (lane 1) and ds cDNA (lane 2). M, λ DNA digested with *Pst*I.

Fifteen fractions were collected with only four containing ds DNA of the required size. The ds cDNA was eluted in fractions 6, 7, 8 and 9 (Fig. 2.4). DNA sizes were observed to range from 0.5 - 4 kb within these fractions (Fig. 2.4). This particular size range was chosen to obtain full-length cDNAs of a large range of gene sizes. Fragment sizes were observed to decrease in subsequent fractions (that is the larger fragments were eluted first). Since elution 9 was the last elute containing fragment sizes greater than 0.5, the remaining fractions together with the first five (containing no DNA) were discarded.

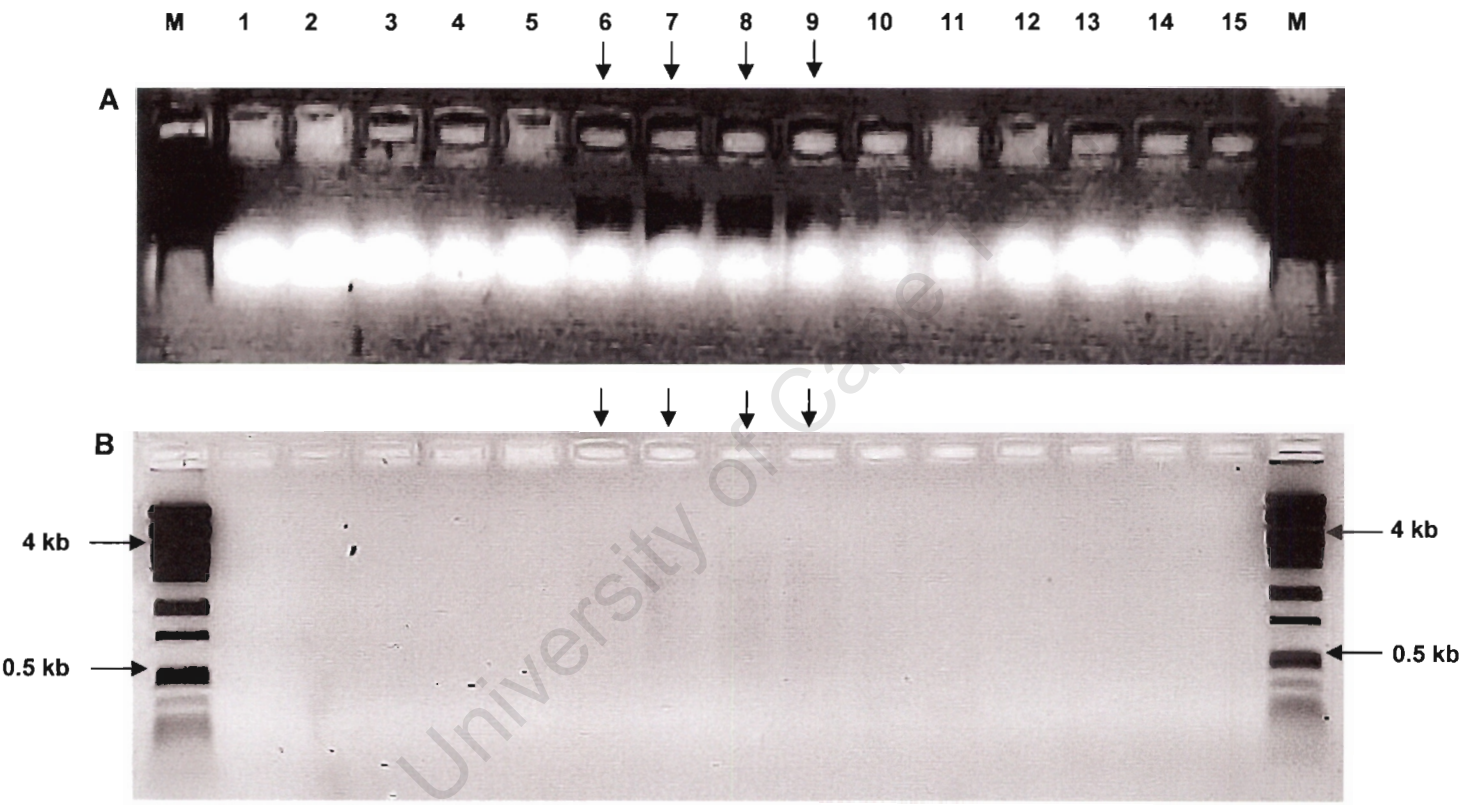

Figure 2.4 Gel electrophoresis of 15 DNA fractions following digestion with proteinase K, ammonium acetate precipitation and *Sfi*I digestion. Arrows indicate fractions that were pooled and utilised for library construction. Electrophoresis was conducted for 30 min initially (A) and then for a further 3 h (B) to view the size range of fractions isolated.

Of the 75 colonies selected, 50 were sequenced. Insert sizes were observed to range from 0.5 - 1.7 kb in size following plasmid digestion with *Sfi*I (Fig. 2.5). A common band of 4.2 kb was observed in all lanes. This band corresponds to the linearised vector after excision of the insert.

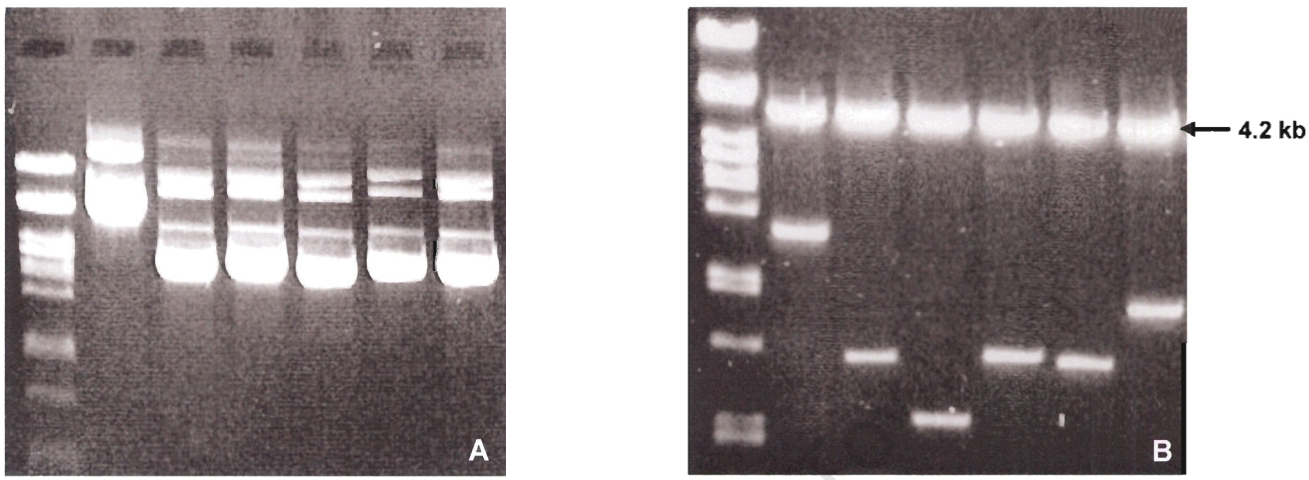

Figure 2.5 Six plasmids isolated from randomly selected clones (A). Insert sizes ranged from 0.5 - 1.7 kb for the 6 randomly chosen as observed after *Sfi*I digestion (B). The arrow indicates the 4.2 kb linearised pDNR-Lib vector.

2.3.4 Sequencing and BLAST analysis of cDNA clones

Fifty clones were isolated from the cDNA library. BLAST searches were performed on the sequences obtained for the 50 clones to determine their identities to known genes (Table 2.8). A majority of the genes (94%) displayed identity with genes in the Genbank database. Three genes lacked identity to any currently described gene. A large number of genes (22%) were similar to genes in the database that had not been ascribed a function as yet (cryptic expressed protein). One clone (E18) was determined to be a partial cDNA (i.e. not full-length), which would be due to a *Sfi*I recognition site within the cDNA sequence. Table 2.8 displays the fifty genes isolated and their identity to genes in the Genbank database. A peroxiredoxin type II (*XvPrx2*) was selected for further analysis (Table 2.8, in bold). The type II peroxiredoxin was demonstrated to be stress inducible (Chapter 4) and was analysed further at both a molecular and biochemical level in this study.

Table 2.8 cDNAs isolated from a low temperature stressed library and their identity to characterised genes in Genbank

Clone	Homology	Identity
A8	e-31	Cryptic expressed protein
B1	e-70	Cinnamyl alcohol dehydrogenase
B2	e-44	Seed maturation protein DNAJ protein
B6	e-63	Cysteine proteinase precursor
B9	e-24	Cryptic expressed protein
B19	e-14	Galactinol synthase
B21	e-54	Cryptic expressed protein
C5	e-37	ATP dependent Clp protease proteolytic subunit
C10	e-105	RAB1C (GTP binding protein)
C15	e-54	RuBisCo (large subunit)
E16	e-84	Cryptic expressed protein
E17	e-51	Apospory associated protein ankyrin-repeat protein HBP
E18	e-12	Glutamate synthase
E19	e-49	60S ribosomal protein L24
E20	e-77	PS1 type III chlorophyll a/b binding protein
F1	e-39	Photosystem II 10 kDa polypeptide
F2	e-30	Cryptic expressed protein (probable Sin3)
F4	**e-66**	**Peroxiredoxin (Type II)**
F10	e-11	Potassium-dependent sodium-calcium exchanger-like protein
F13	e-8	Carbonic anhydrase
F14	e-33	Phosphatidylinositol transfer protein (Sec14)
F17	0	No identity
G4	e-20	S-like ribonuclease RNS2
G6	0	No identity
G11	e-39	Ripening-related protein (putative sugar starvation induced protein)
G17	e-39	Ferredoxin-NADP reductase
H3	e-33	Cryptic expressed protein (*A. thaliana*)
H5	e-22	Cryptic expressed protein (*Chlorobium tepidum*)
H7	0	No identity
H12	e-76	Ubiquitin precursor polyubiquitin
H14	e-22	Intracellular pathogenesis-related protein
H16	e-59	Calmodulin
I2	e-7	Photosystem II 5 kDa polypeptide
I13	e-16	Cryptic expressed protein (*Oenothera elata*)
I17	e-20	Adenine nucleotide translocator
I18	e-26	Protein phosphatase 2C

Table 2.8 continued

Clone	Homology	Identity
J1	e-32	Cryptic expressed protein (*A. thaliana*)
J3	e-56	Oxygen-evolving enhancer protein 2 (part of photosystem II)
J4	e-32	Cryptic expressed protein (similar to DNAJ-2/molecular chaperone)
J12	e-61	Cysteine proteinase precursor (stress induced)
J13	e-23	15.9 kDa subunit of RNA polymerase II
J14	e-39	Polyubiquitin
J15	e-17	Ubiquitin carrier protein
J17	e-41	Cryptic expressed protein (*A. thaliana*)
K1	e-68	S18 ribosomal protein (40S ribosomal protein)
K2	e-31	Photosystem II 10 kDa phosphoprotein
K6	e-56	Carbonic anhydrase (carbonate dehydratase) NPCA1
K8	e-37	Photosystem II 10 kDa polypeptide
K13	e-10	Photosystem I assembly protein (ycf-4)
K15	e-17	Dehydration induced protein (ERD15)

2.3.5 Bioinformatic analysis of *XvPrx2*

The nucleotide sequence of the *XvPrx2* cDNA was determined to be 715 bp long with an open reading frame of 489 bp (Fig. 2.6). The deduced amino acid sequence was observed to encode a protein of 162 amino acids with a molecular weight of 17.5 kDa and a predicted pI of 5.3 at pH 7. The 5' and 3' untranslated regions consisted of 29 bp and 197 bp, respectively. A prosite database of protein families and domains suggests five possible casein kinase II phosphorylation sites (9-12, 58-61, 78-81, 91-94 and 153-156), as well as one possible amidation site (34-37), two N-myristoylation sites at position (42-47 and 147-152), and three possible protein kinase C phosphorylation sites (105-107, 119-121 and 127-129).

The XvPrx2 protein contains the highly conserved PGAFTPTCS amino acid sequence common to the active site of type II Prxs. The catalytic centre of Prxs contains a cysteine residue (Fig. 2.6, codon 51) that can reduce diverse peroxides. The valine at codon 76 (Fig. 2.6) is the amino acid that was modified to generate a point mutant referred to as XvV76C (i.e. the valine residue was substituted with a cysteine residue).

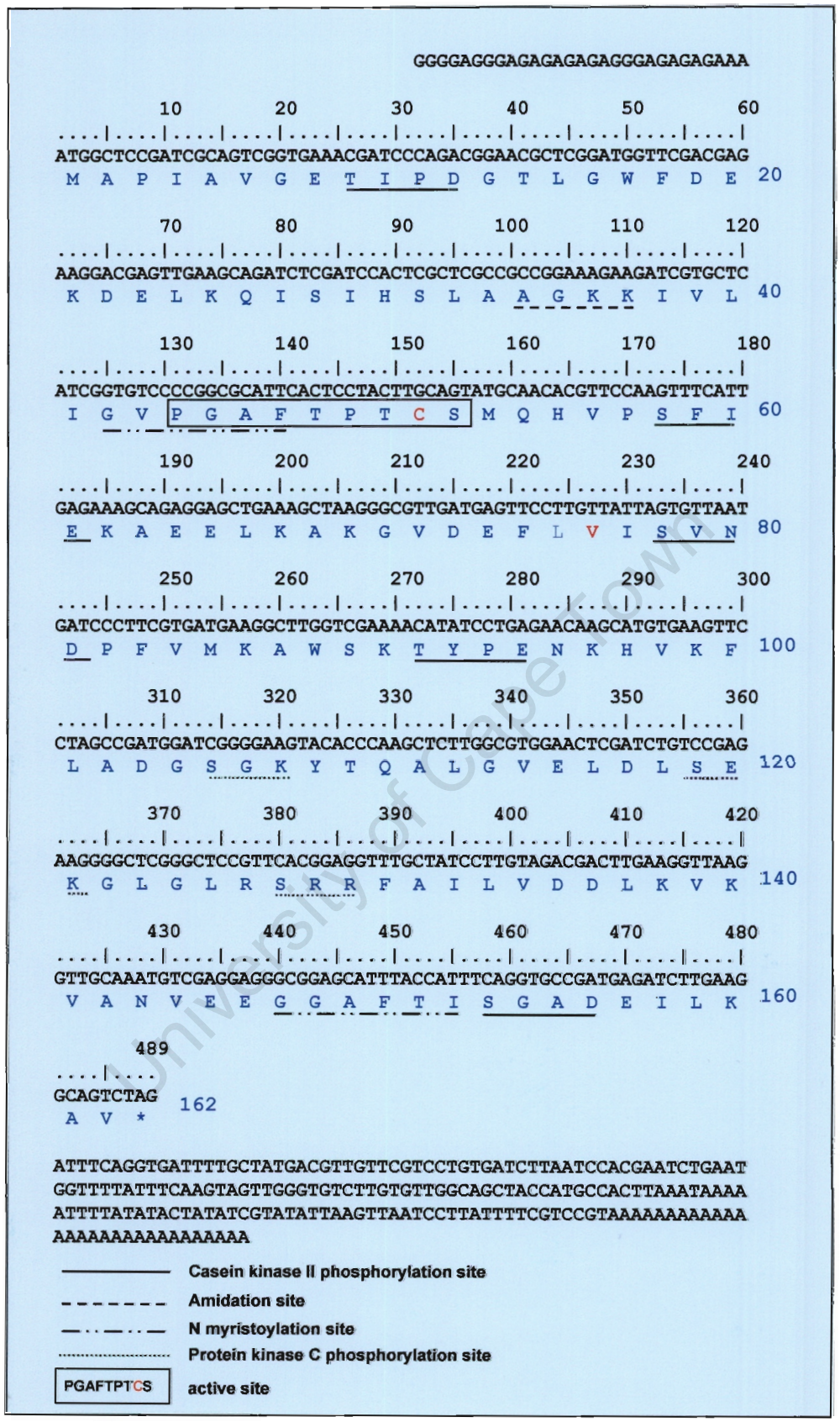

Figure 2.6 Nucleotide sequence of *XvPrx2* (black), displaying the inferred amino acid sequence of the XvPrx2 polypeptide (blue). The conserved catalytic sequence is blocked. The catalytic cysteine (C51) as well as a valine that was substituted with a cysteine residue in XvV76C is displayed in red.

A hydropathy plot (Kyte & Doolittle, 1982; window size 7) revealed that the protein is mostly hydrophilic as no hydrophobic domain is apparent (Fig. 2.7). Since it is a cytosolic protein one would expect the protein to be hydrophilic. Based on analyses of the Recombinant Protein Solubility Prediction Software (www.biotech.ou.edu), XvPrx2 displays a 50.5% chance of solubility when over-expressed in *E. coli*.

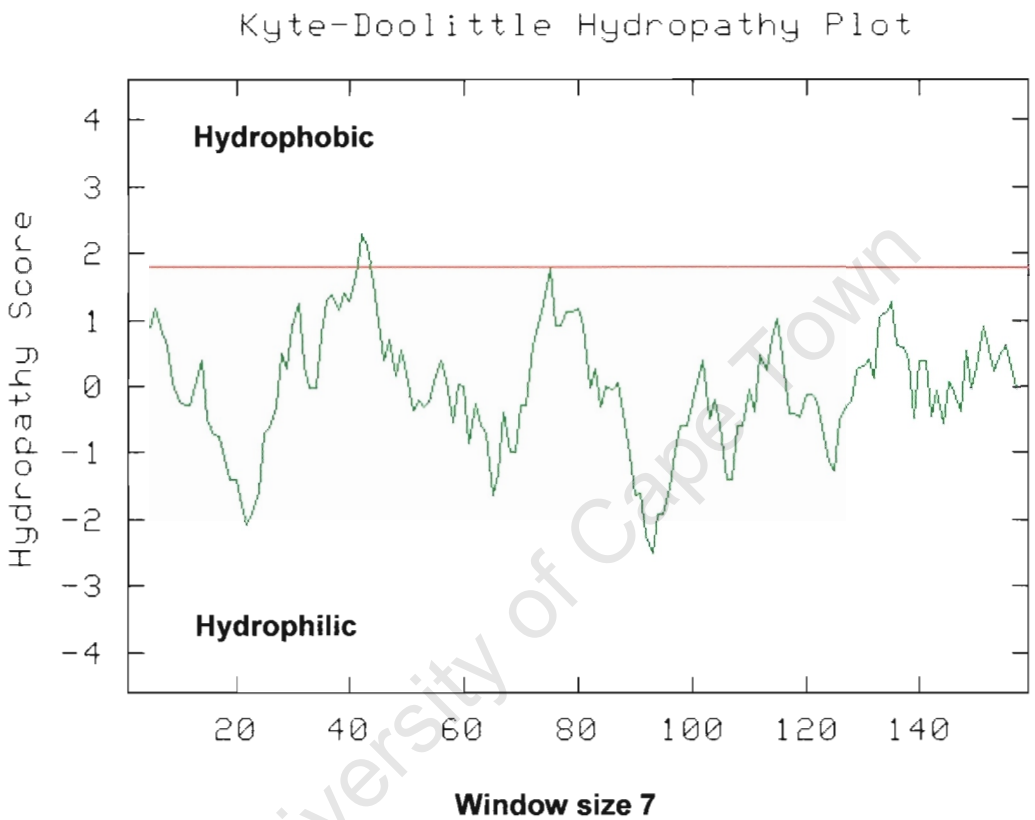

Figure 2.7 A hydropathy plot of XvPrx2 as determined by the method of Kyte & Doolittle (1982) indicating that the protein is soluble.

The XvPrx2 protein has 9 potential phosphorylation sites as predicted by in silico analysis (Fig. 2.8). There are six serine residues (amino acid position 58, 78, 105 119, 127 and 153), two threonine residues (amino acid positions 14 and 48) and one tyrosine residue (amino acid position 108) with phosphorylation potentials above the threshold value of 0.5 (Fig. 2.8). Similar in silico analysis to predict glycosylation sites points to XvPrx2 lacking O-glycosylation sites.

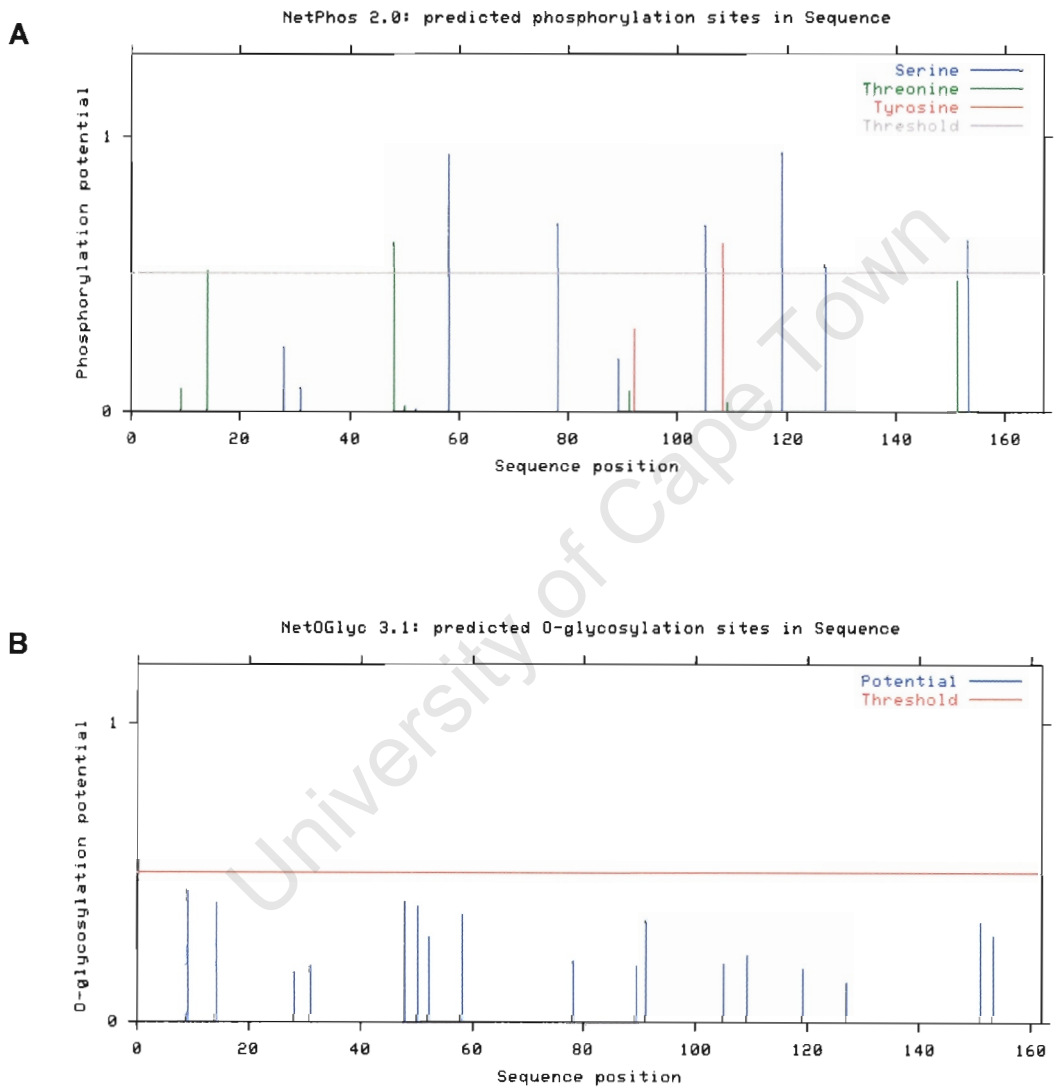

Figure 2.8 In silico based prediction of phosphorylation potential (A) and O-glycosylation potential (B) of XvPrx2.

At the amino acid level XvPrx2 is similar to the *Oryza sativa* and *Candida boidinii* orthologues in that it only possesses a single catalytic cysteine residue at position 51 (Fig. 2.9). Other orthologues possess a second cysteine residue at position 76. However, XvPrx2 possesses a valine at position 76 in place of the second cysteine residue (Fig. 2.9).

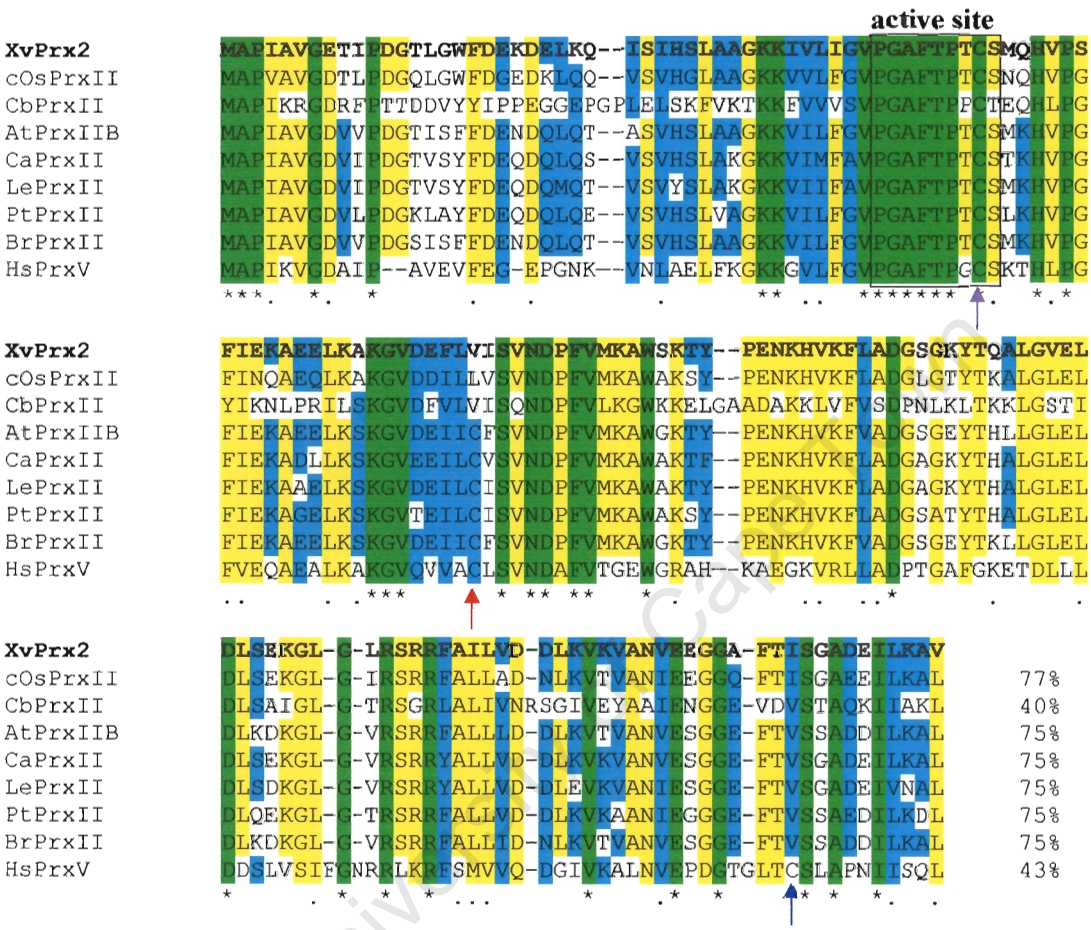

Figure 2.9 Multiple sequence alignment of type II Prx orthologues (accession numbers in Appendix B). The proteins aligned include: cOsPrxII (*Oryza sativa*), CbPrxII (*Candida boidinii*), AtPrxIIB (*A. thaliana*), CaPrxII (*Capsicum annuum*), LePrxII (*Lycopersicon esculentum*), PtPrxII (*Populus tremula* x *Populus tremuloides*), BrPrxII (*Brassica rapa* subsp. *pekinensis*), HsPrxV (*Homo sapiens*), and XvPrx2 (*X. viscosa*). Asterisks (*) denote identities and dots (.) denote similarities. The highly conserved active site in plants (PGAFTPTCS) is boxed. Purple arrow indicates the catalytic cysteine in all species, red arrow indicates the second cysteine residue observed in most type II species and the third arrow (blue) indicates the third cysteine residue found in human HsPrxV.

The deduced amino acid sequence of XvPrx2 exhibited considerable similarity to other plant type II Prx orthologues (Fig. 2.9). The XvPrx2 protein displays greatest homology with the *O. sativa* (77%) and *A. thaliana*, *Populus* sp., *B. rapa* and *C. annuum* (75%) Prx orthologues (Fig. 2.10). From the homology tree it can be observed that the *Homo sapien* PrxV (HsPrxV) shares 43% homology with XvPrx2 and the least homologous is *C. boidinii* (40%).

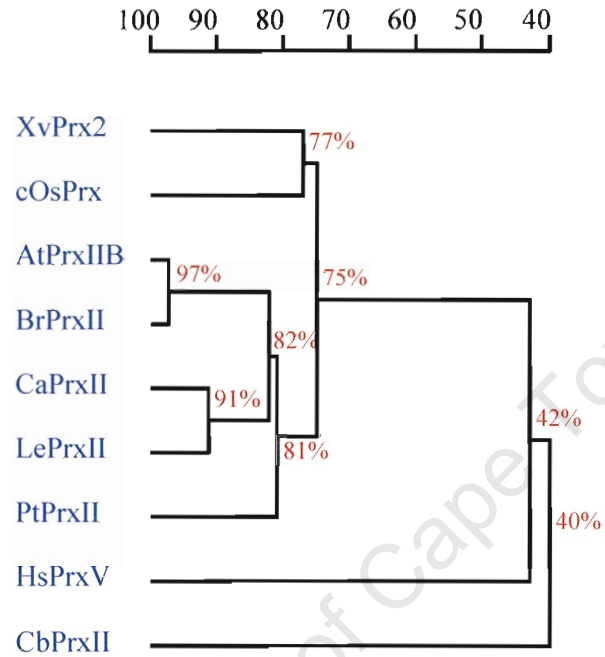

Figure 2.10 Homology tree of XvPrx2 and related orthologues. Values on branches display percentage homology.

A maximum parsimony tree was generated in an attempt to determine the evolutionary relationships between type II peroxiredoxin family members. The parsimony tree revealed that XvPrx2 is most closely related to a rice orthologue (Fig. 2.11). Six distinct clades were delineated within the parsimony tree. Plant Prxs clustered within two clades (Clades 1 and 5). The XvPrx2 protein clustered in the larger plant clade (Clade 1). Within Clade 2, AtPrxII from *Agrobacterium tumefaciens* (bacteria) and PwPrxII from *Prototheca wickerhamii* (algae) appear to be closely related. For Clade 3 it can be observed that this group comprises a mixed assemblage of Prxs from bacteria, insects and animals. Clade 6 shows that fungal Prxs are closely related to each other and are probably of a separate lineage to other Prxs from other taxonomic groups.

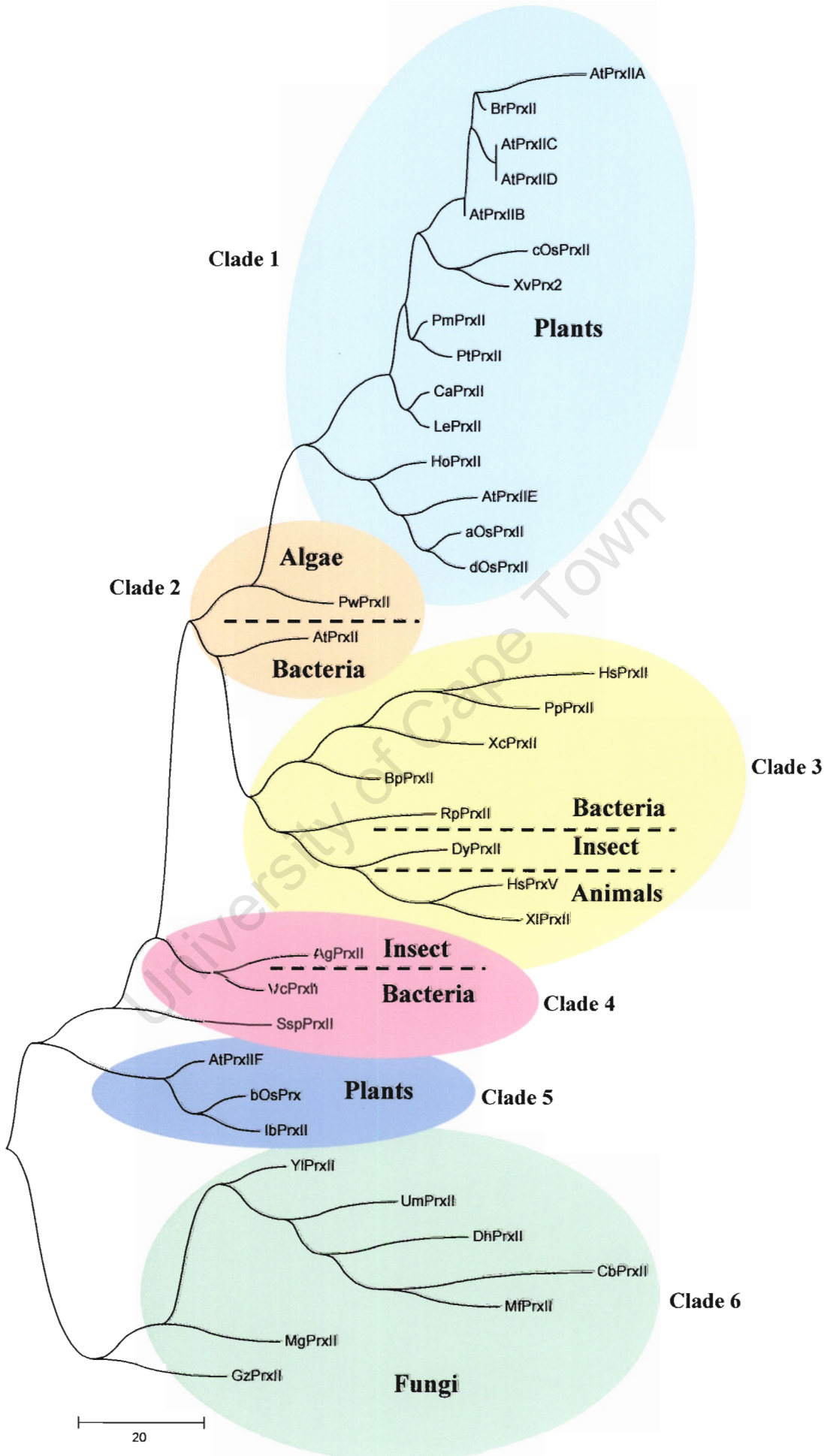

Figure 2.11 Maximum parsimony tree inferred from protein sequence data of type II Prxs.

Type II Prxs appear to be very divergent when compared to the other Prxs (Fig. 2.12). Of the ten existing Prxs from *A. thaliana*, 6 homologues belong to the type II Prx group. From the Prx II clade it is evident that CbPrxII and HsPrxV as well as the mitochondrial forms (AtPrxIIF and bOsPrxII) are more distantly related to the other type II Prxs. Sequence identities range from 4-98% between Prxs and from 51-80% between Gpxs.

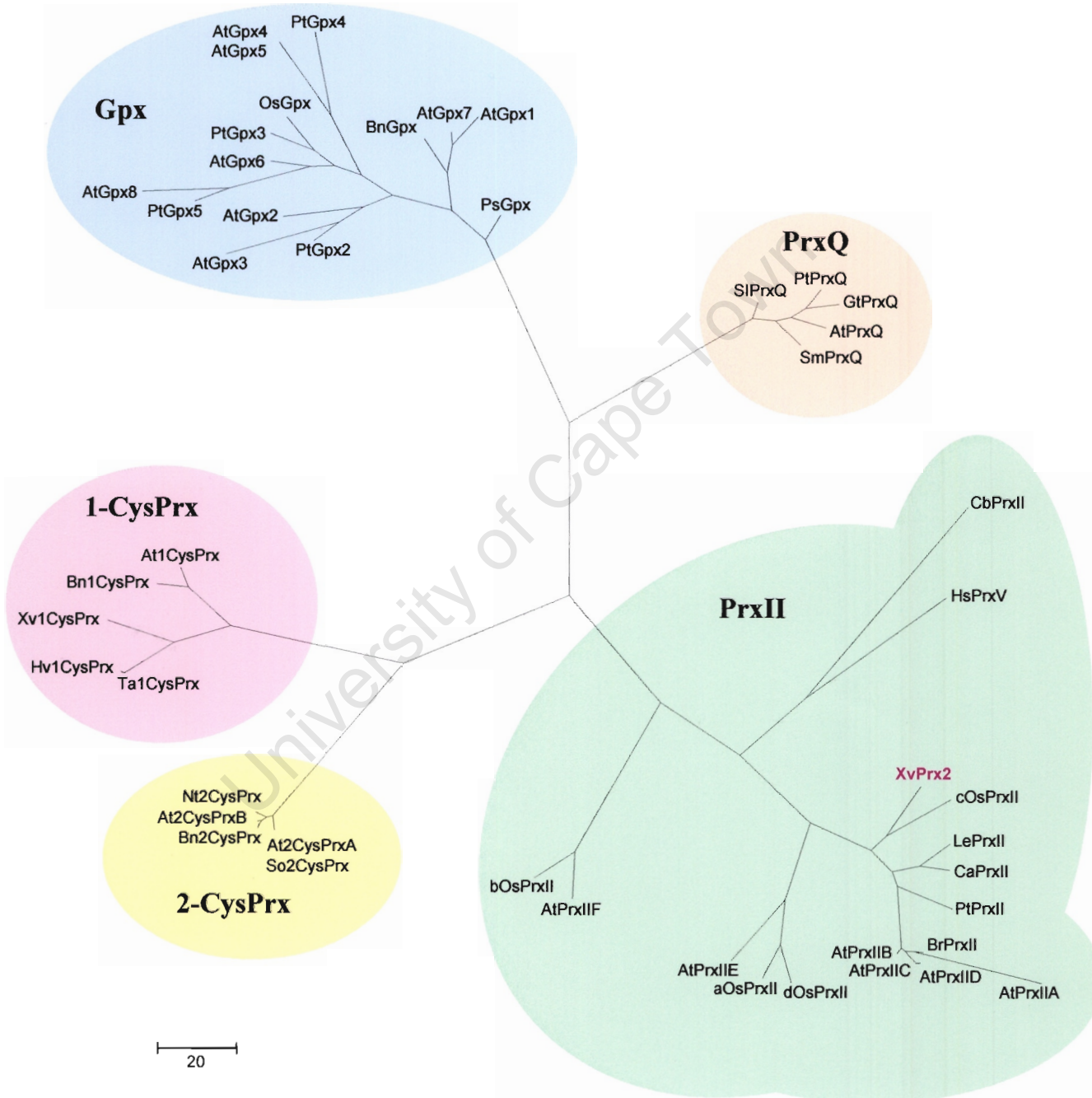

Figure 2.12 Maximum parsimony tree of thioredoxin peroxidases.

2.3.6 Southern blot analysis

Southern blot analysis of *X. viscosa* genomic DNA (Fig. 2.13A) probed with *XvPrx2* cDNA was carried out to confirm that *XvPrx2* was present in the *X. viscosa* genome and also to estimate the gene copy number. The following restriction enzymes were successfully used in the digestion of *X. viscosa* genomic DNA: *Bgl*II, *Eco*RI, *Eco*RV, *Hin*dIII, *Xba*I and *Pvu*I (Fig. 2.13B). Successful labelling of *XvPrx2* with [α-^{32}P] dCTP was confirmed by viewing the PCR product after removal of unlabelled probe and by Geiger counts. Of the restriction enzymes used, *Bgl*II has two and *Pvu*I has one predicted restriction site/s within *XvPrx2*. All other endonucleases utilised in this experiment do not possess recognition sites within the cDNA sequence. Multiple bands were observed when using all of these enzymes (Fig. 2.13C). Double digestions with *Eco*RI/*Eco*RV, *Eco*RI/*Pvu*I and *Eco*RI/*Xba*I, each resulted in two to four hybridisation bands of varying intensities.

2.3.7 Generation of an *XvPrx2* point mutant

A point mutation of XvPrx2 was generated for comparative enzyme assays (Chapter 5). This was carried out to mimic the other type II Prxs that generally possess two cysteine residues one at codon 51 and the other at codon 76. Modification of the valine to a cysteine would allow for determining whether the second cysteine residue had any effect on enzyme activity when compared to the wild type protein. The mutant protein was successfully generated and named XvV76C due to the change in the amino acid sequence.

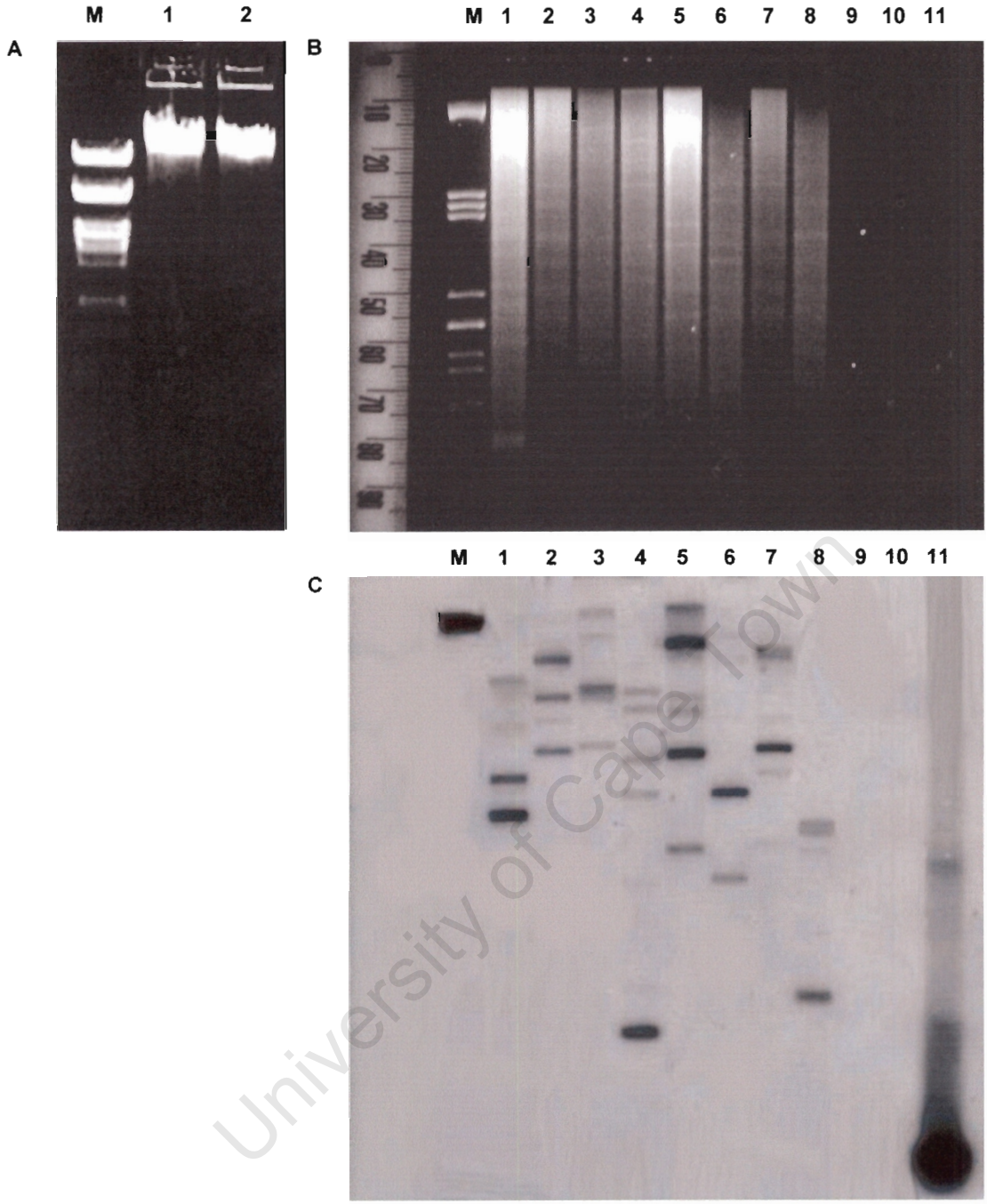

Figure 2.13 Gel electrophoresis of undigested genomic DNA isolated from *X. viscosa* (A, lanes 1 and 2). Twenty micrograms of *X. viscosa* genomic DNA was digested with a number of restriction endonucleases either as single or double digests (B). Autoradiograph following 2 day exposure to membrane probed with radiolabelled *XvPrx2* (C). M, lambda DNA digested with *Pst*I. Genomic DNA was digested with *Bgl*II (lane 1), *Eco*RI (lane 2), *Eco*RV (lane 3), *Hin*dIII (lane 4), *Xba*I (lane 5), *Eco*RI/*Eco*RV (lane 6), *Eco*RI/*Pvu*I (lane 7), *Eco*RI/*Xba*I (lane 8), no DNA (lane 9), negative control (100 pg of genomic DNA from seaweed; lane 10) and positive control (100 pg of 489 bp *XvPrx2* PCR fragment; lane 11).

2.3.8 Analysis of *XvPrx2* promoter regions

Although reverse primers were designed to a specific region of *XvPrx2* numerous cloned upstream regions were obtained. Of the six upstream regions (Fig. 2.14) obtained none contained the 5' untranslated region occurring in the *XvPrx2* cDNA, although the first 40 bp of the *XvPrx2* gene was in some cases identical to, or differed by a few base pairs from, *XvPrx2* in the 5' coding region. A BLAST search using the last 100 bp of the cloned sequences, which included the ATG region displayed identity to type II Prxs. The upstream regions isolated are possibly of promoter regions of XvPrx2 homologues present in the *X. viscosa* genome. This result provides further evidence that there may be many *XvPrx2* homologues in *X. viscosa* as occurs in *A. thaliana*. The Prom B3 and Prom B8 clones were very similar in sequence and shared 98% identity with each other. These clones were sequenced twice and on both strands, however, the same result was obtained thus discounting the possibility of errors occurring. The 6 upstream regions do not possess antioxidant response elements [core sequence (GTGACNNNGC)] as shown for mammal and plant Prxs. Mammalian antioxidant response elements usually have an activating protein-1-binding site [AP-1, sequence (TGACTCA)]. A highly homologous 3' region with high variability at the 5' end for the upstream regions was observed for the cloned sequences.

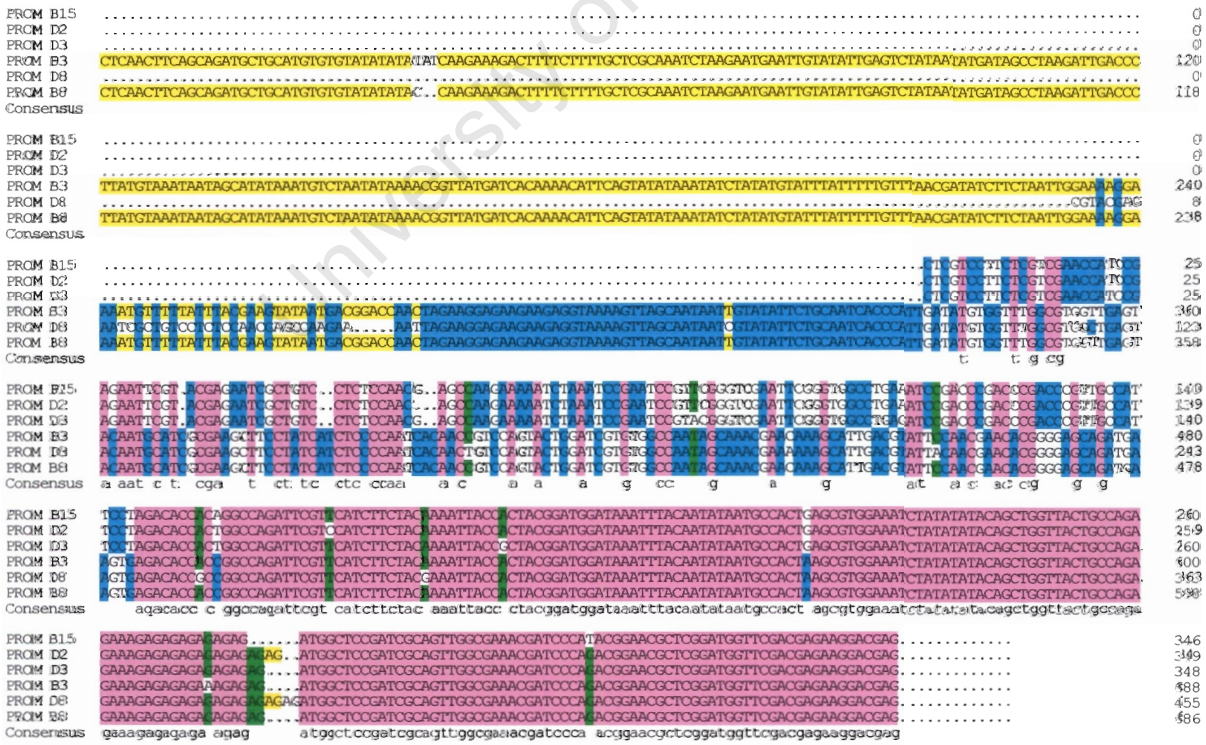

Figure 2.14 Multiple sequence alignment of 6 upstream promoter regions obtained using the Splinkerette method (Devon et al., 1995). The *XvPrx2* upstream region was omitted from the alignment as only 29 bp of the 5' upstream region was known from the cDNA clone.

2.4 DISCUSSION

A complete set of full-length cDNA, containing the entire sequence of the mRNA, is the ultimate goal for cDNA cloning. Unfortunately, cDNA libraries constructed by conventional methods have a large number of partial length cDNAs. The first strand cDNA is usually synthesised from an oligo d(T) primer, which hybridises to the polyA tail resulting in the selective synthesis of mRNA from the 3' end. In some cases, reverse transciptase terminates before transcribing the complete mRNA sequence. This is particularly true for long mRNAs, especially if the first strand is primed with oligo d(T) primers only, or if the mRNA contains abundant secondary structures. As a result, the largest part of the cDNA library is occupied by cDNA which lack the 5' end of the mRNA.

The Creator SMART cDNA Library Construction Kit for full-length cDNA enrichment was employed in this study. The protocol is relatively simple and can be performed with small amounts of starting material (0.025–1 μg mRNA). SMART cDNA amplification technology is a PCR-based method for cDNA library construction. Completely reverse transcribed cDNAs are 5'-tagged via the SMART oligo and selectively amplified after cDNA synthesis. In the current study it was observed that greater than 90% of cDNAs screened were full-length highlighting the advantage of this technique.

The ds cDNA size fractionation prior to library amplification allows for amplification and cloning of cDNAs within defined size ranges. In the current study, fragments in the size range 0.5-4 kb were pooled. The advantage of the fractionation process is apparent as no cDNAs smaller than 450 bp were obtained. However, there is a natural size bias against large fragments during cloning (ligation and bacterial transformation). Therefore, clones with very large insert sizes are difficult to obtain in full-length cDNA libraries. Consequently, clones in the size range 0.5-1.7 kb were observed for those screened, with the majority being smaller than 1 kb. Optimally each fraction should have been ligated and transformed separately for the different size fractions, a size bias due to out-competition by small fragments would have been minimised. Sub-libraries made from fractions containing larger fragments would possess larger average insert sizes. Such insert sizes are strongly under represented when all cDNAs are ligated and transformed at once as was done in this study. However, for the purposes of this study the synthesised full-length cDNA library was well suited.

A large percentage of the cDNA clones were shown to display identity to chloroplast genes. This bias is due to the larger number of chloroplastic mRNA transcripts present within the plant cell relative to nuclear transcripts. These mRNAs are not necessarily upregulated

during stress but are merely enriched because of their natural abundance. It is possible to minimise such an effect by either:

(i) performing subtractive hybridisation; or

(ii) using nuclei as starting material.

Subtractive hybridisation methods are valuable tools for identifying differentially regulated genes in a given tissue. These methods avoid redundant sequencing of clones representing the same expressed genes, maximise detection of low abundant transcripts and thus, positively affect the efficiency and cost effectiveness of small scale cDNA sequencing projects aimed to the specific identification of genes upregulated during abiotic stress.

The location of the bulk of cellular mRNA is in the cytosol since cytoplasmic degradation mechanisms are an important factor regulating mRNA half-lives. Using nuclei as starting material has the advantage that it reflects the state of gene transcription at any given moment since only nuclei mRNAs are analysed. An obvious disadvantage to this method is that many interesting genes would be omitted due to the time-dependent dynamics of mRNA synthesis and translocation.

A stress inducible gene designated *XvPrx2* (Clone F4) was chosen for further analyses due to its apparent role in oxidative stress as a type II Prx. The Prx family was first described as alkyl hydroperoxide reductase C (Jacobson et al., 1989) and later as thiol-specific antioxidant in *Saccharomyces cerevisiae* and *E. coli* (Chae et al., 1994a, b). In contrast to other peroxidases, Prx enzymes do not have redox cofactors such as metal or prosthetic groups. Prxs reduce hydrogen peroxides and alkyl peroxides to water and alcohols, respectively, by using reducing equivalents. These reducers are derived specifically from thiol-containing donor molecules. Members of the Prx family have now been identified in a wide variety of organisms ranging from prokaryotes to eukaryotes.

The data presented in this study indicate that *XvPrx2* encodes a type II Prx. The full-length cDNA sequence constitutes 715 bp with an open reading frame of 489 bp. The amino acid sequence deduced from the full-length cDNA indicates that *XvPrx2* encodes a polypeptide of 162 amino acid residues with a predicted molecular mass of 17.5 kDa and a predicted pI of 5.3 at pH 7. These primary characteristics points to XvPrx2 being a typical type II Prx with no extraordinary features.

A hydropathy plot of the deduced amino acid sequence of XvPrx2 revealed no major hydrophobic domains, which indicates that XvPrx2 is hydrophilic and unlikely to be associated with membranes. The protein once isolated for expression studies (Chapter 3) has

been shown to be highly soluble reinforcing its solubility index. Furthermore, it would appear logical for the protein to be soluble as its functional role precludes attachment to membranes.

Immenschuh & Baumgart-Vogt (2005) reported that Prx activity is modified not only by the regulation of gene expression, but also by post-translational mechanisms. These mechanisms comprise protein phosphorylation, redox dependent oligomerisation, proteolysis and modification by ligand binding. It was demonstrated that PrxI, II, III and IV are phosphorylated at a threonine residue of a specific phosphorylation recognition sequence via the cyclin dependent kinase Cdc2 (Chang et al., 2002). This Cdc2 mediated phosphorylation was shown to inhibit peroxidase activity of Prxs. The potential mechanism(s) of how phosphorylation decreases peroxidase activity could be the introduction of a negatively charged phosphate group that may modulate the peroxidatic active site via an unfavourable electrostatic effect. It was also reported by Immenschuh & Baumgart-Vogt (2005) that phosphorylated PrxI was demonstrated to occur during mitosis, but not during the interphase. Therefore, it was proposed that the phosphorylation of Prx could be an important switch for the upregulation of cellular levels of hydrogen peroxide, resulting in a progression of the cell cycle.

Two possible N-myristoylation sites exist in the protein as well as five possible casein kinase II phosphorylation sites and three possible protein kinase C phosphorylation sites. Protein N-myristoylation refers to the covalent attachment of myristic acid by an amide bond to the N-terminal glycine residue of a nascent polypeptide (Johnson et al., 1994). This co-translational modification occurs on many proteins involved in signal transduction, including serine/threonine kinases, tyrosine kinases, calcium binding proteins, etc. In most cases, this modification is essential for protein function to mediate membrane association or protein–protein interaction (Ishitani et al., 2000). In some cases however, no functional significance can be associated with myristoylation. Protein phosphorylation is probably the most important regulatory event and many enzymes are switched 'on' or 'off' by phosphorylation and dephosphorylation. The presence of three putative phosphorylation sites may indicate possible means of regulation of the XvPrx2 protein.

Since the discovery of type II Prxs in 1999, a large number of sequences have become available and multiple sequence alignment with type II Prxs from diverse groups such as plants, bacteria, fungi and vertebrates is possible. Type II Prxs appear to be the most diverse of the four Prx groups. This observation is highlighted by the existence of 10 *A. thaliana* Prxs, of which six are type II Prxs. The XvPrx2 protein displays greater than 70% homology with other plant type II Prxs. This homology decreases when comparisons are made with type II

Prxs from non-plant groups. The XvPrx2 protein is strongly homologous to other plant Prxs of its class (77%, 75%, 75% amino acid identity with *O. sativa*, *A. thaliana* and *B. rapa*, respectively) and also to the well characterised CbPmp20 protein from *C. boidinii* and to the human Prx V (42% and 40% amino acid identity, respectively).

The conservation of amino acid sequence among type II Prx proteins identified from widely divergent species emphasise its importance in function (Fig. 2.15). The XvPrx2 protein contains a highly conserved active site consisting of the following amino acid sequence PGAFTPTCS (44-52) where the residue at position 51 is either the catalytic residue or the peroxidatic residue involved in the detoxification process of reactive oxygen species. This catalytic residue is conserved among all type II Prx proteins isolated. All other type II Prxs except for XvPrx2, cOsPrxII and CbPrxII possess a second cysteine residue at position 76. An important difference occurring in type II Prxs is the presence of an additional cysteine (i.e. 3 cysteine residues) in the human Prx (HsPrxV) at position 152 of the amino acid sequence. The *X. viscosa* and all other characterised non-mammalian sequences do not possess this third cysteine residue. This cysteine participates in the formation of an intermolecular disulphide bridge in the human enzyme (Rouhier et al., 2002) and is conspicuous by its absence in plant proteins.

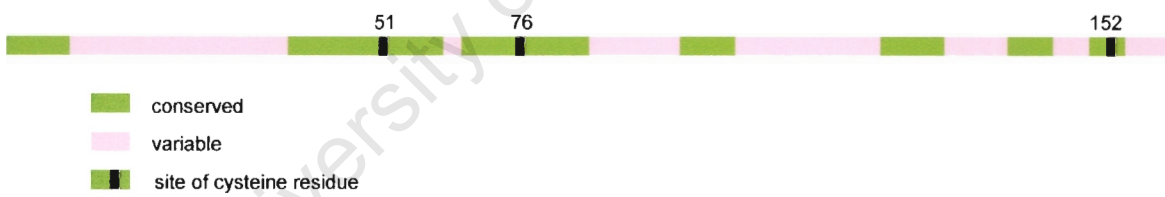

Figure 2.15 Schematic representation of type II Prx genes (not to scale). Regions showing conserved and variable tendencies are displayed. Position of known cysteine residues are shown (cysteine 152 is found only in HsPrxV).

Phylogenetic and biochemical analyses indicate that *A. thaliana* and presumably all photosynthetic organisms possess five distinct classes of thioredoxin-dependent peroxidases. Four classes represent Prxs sensu stricto with a strictly conserved catalytic cysteine, and the fifth contains Gpxs, which also display conserved cysteines, but in consensus sequences and positions different from those previously described for Prxs (Rouhier & Jacquot 2002; Dietz, 2003; Rouhier & Jacquot, 2005). From the phylogenetic analyses it is evident that type II Prxs are more divergent than the other thiol classes. Since *X. viscosa* and *O. sativa* are both monocots it is not surprising that these two are the most closely related based on the

phylogenetic analyses as these orthologues probably share a common ancestor. Furthermore, these proteins possess a single cysteine residue only, which distinguishes them from other plant type II Prxs. Other known cytosolic plant type II Prxs are from dicots and possess two cysteines. Interestingly, in *O. sativa* two chloroplastic type II Prx orthologues (aOsPrxII and dOsPrxII) as well as one mitochondrial type II orthologue (bOsPrxII) contains 2 cysteine residues as occurs in dicot species. Based on the rarity of plant type II Prxs possessing a single cysteine and on their specific occurrence in monocots it can be hypothesised that these proteins represent a relatively recent evolutionary development. If this is indeed the case, questions arise regarding differences in functionality and efficiency when compared to typical type II Prxs.

Based on several lines of evidence, cysteine 51 is proposed to be the catalytic cysteine. First, it is in a conserved position with respect to all other Prx types where it has been shown to be the peroxidatic cysteine. Second, studies performed by Rouhier et al. (2002) using poplar type II Prx, show that site directed mutagenesis of the N terminal cysteine residue (position 51) clearly indicates that Cys-51 of Prx is the catalytic cysteine. Mutation of Cys-76, however, does reduce the catalytic efficiency but the protein still remains active with Grx as a proton donor. Third, this residue is also absent in *O. sativa* and *C. boidinii* gene sequences. Since *X. viscosa* only has a single cysteine residue, which is also the catalytic one, substituting this cysteine would not be practical. Therefore in this study a second cysteine was substituted for a valine in order to mimic the other type II Prxs that contain a second cyteinyl residue at codon 76. The biochemical characteristics of this protein have been analysed in this study (Chapter 5).

Isolating the promoter region of the *XvPrx2* gene is significant in that it is required for an understanding of regulation of *XvPrx2*. Since this enzyme plays a role in detoxification and possibly signalling (Wood et al., 2003) it would be important and beneficial in isolating the promoter region. Stress inducible promoters provide a better approach when driving transgenic crops as opposed to constitutively expressed promoters. Six potential upstream regions of possible type II Prx homologues have been isolated in this study. All six upstream regions are 99% similar at their 3' ends. A BLAST search of the conserved region points to high level of identity to type II Prxs. It is likely that these are potential upstream regions of other Prx homologues present in the *X. viscosa* genome. These homologues were not isolated and therefore not characterised further in this study.

An examination of the upstream regions of *XvPrx2* homologues show no antioxidant response elements, although current literature (Haslekas et al., 2003b) have shown antioxidant

response elements in the upstream region of 1-Cys peroxiredoxins. This regulatory element is present in promoters of genes coding for proteins involved in cellular response to agents evoking oxidative stress and can be recognised by protein complexes exerting either inhibitory or, upon cell activation, stimulatory effect on promoter activity leading to elevated expression of many genes.

An analysis of the genomic organisation of *XvPrx2* by Southern blotting confirmed the presence of the gene in the *X. viscosa* genome. Although the hybridisation and the washing of the membranes were performed under high stringency conditions, several hybridisation signals were detected from Southern analysis of the *X. viscosa* genome. This result indicates a multiplicity of putative type II Prxs, although the exact number of *XvPrx2* genes in the *X. viscosa* genome remains to be determined. Since there are many homologues of type II Prxs in *Arabidopsis* one may infer that there is more than one homologue of *XvPrx2* in the *X. viscosa* genome suggesting that *XvPrx2* belongs to a small multigene family. It is not clear whether the weakly hybridising bands represent additional divergent homologues, low copy number homologues, or other closely related genes in *X. viscosa*. Considering the variety of Prxs in yeast and mammalian cells (Kang et al., 1998b), the bands observed may also represent other closely related Prx proteins (i.e. either 1 Cys, 2 Cys or PrxQ). The reason why numerous homologues are required by the plant is significant. It is possible that different homologues, although they may have many conserved properties, specialise in individual functions on the basis of their diversity, distinct cell-specific and/or developmentally regulated expression, and differential responses to environmental stimuli.

Chapter 3

Expression and localisation of XvPrx2

3.1 INTRODUCTION

Recombinant proteins synthesised in heterologous hosts may accumulate in one of three 'compartments': the cytoplasm, the periplasm or the extracellular medium (Tan et al., 2002). Many over-expressed proteins from various origins have been purified from each of these locations. Whenever possible, secretion is the preferred strategy since it permits easy and efficient purification from the extracellular medium. However, each expression system needs specific tailoring to meet the stringent requirements for each protein product to ensure correct folding, activity and desired yield. Furthermore, the flexibility of a common secretion signal sequence with which to secrete a wide variety of heterologous fusion proteins from various hosts into the extracellular medium is not available.

In vivo engineering of proteins in transgenic plants is a technique that has gained increasing importance for biotechnological applications. A powerful technique to monitor compartmentation and subcellular targeting is the use of GFP technology. According to Haseloff et al. (1999) GFP technology provides numerous advantages due to its functionality in living organisms:

(i) eliminates the need for fixation and dehydration and their associated artefacts;
(ii) allows each stage of development to be studied in a single intact embryo; and
(iii) GFP functions in all cell types and is able to reveal their morphology, thus making it simpler to identify different cells without compromising their viability.

In this chapter the expression and localisation of XvPrx2 is described employing various molecular techniques. For protein expression three different methods were used:

(i) TOPO based expression;
(ii) baculovirus-mediated expression; and
(iii) pProEx expression.

Two separate localisation studies were employed in this study:

(i) immuno-cytochemical localisation; and
(ii) YFP localisation studies.

3.2 MATERIALS AND METHODS

3.2.1 TOPO expression of XvPrx2 and XvV76C

The pCR-T7-TOPO TA Expression Kit (Invitrogen, USA) was used according to the manufacturer's instructions for the cloning of *XvPrx2* and *XvV76C* into pCR-T7-TOPO expression vector (Appendix C; Invitrogen, USA). The enzyme, *Taq* polymerase, has a non-template-dependent terminal transferase activity that adds a single deoxy-adenosine (A) to the 3′ ends of PCR products. Linearised pCR-T7-TOPO has single, overhanging 3′ deoxy-thymidine (T) residues. This allows PCR inserts to ligate efficiently with the vector. The recombinant vector was initially stably maintained in TOP10F' cells (Invitrogen, USA) and subsequently transferred to Bl21 DE3 Lys-S cells for protein expression (Invitrogen, USA).

3.2.1.1 Cloning of *XvPrx2* and *XvV76C* into pCR-T7-TOPO

Both *XvPrx2* and *XvV76C* were amplified using gene specific primers, F4 HisTOPO-S (Appendix B) and F4 HisTOPO-A (Appendix B). PCR reaction volumes were made up to 25 µl (standard PCR reaction; Appendix A) and run with the following cycling conditions: 94°C for 3 min; 35 cycles of 94°C for 30 s, 58°C for 45 s and 72°C for 90 s; and a final extension step of 5 min. The PCR products were electrophoresed on a 1% agarose/EtBr gel. The band of interest was excised and purified using the High Pure PCR Product Purification Kit according to the manufacturer's instruction (Appendix A). Ligation of the purified amplimer to TOPO vector was carried out according to the manufacturer's instruction (Table 3.1).

Table 3.1 Ligation reaction of TOPO vector to purified PCR products

Components	Volume (µl)
Purified amplimer	2.0
TOPO vector (Invitrogen, USA)	0.5
Salt solution*	0.5

*No ligase was required in the ligation reaction

The reagents were added to an Eppendorf tube and incubated for 30 min at RT. Three microlitres of the ligation mix was transformed in TOP10F' *E. coli* cells (standard transformation condition; Appendix A). Colony PCR was performed using primers, T7 TOPO-F and Prom-R1 (Appendix B) to select for positive clones. The TOP10F' cells containing either pTOPO::*XvPrx2* or pTOPO::*XvV76C* were inoculated in LB broth supplemented with 100 µg.ml^{-1} ampicillin (LB-amp). Plasmid DNA was isolated from the

respective clones using the High Pure Plasmid Extraction Kit according to the manufacturer's instruction (Appendix A). Samples were sequenced to confirm that errors were not incorporated during the PCR amplification procedure.

Prior to protein expression pTOPO::*XvPrx2* and pTOPO::*XvV76C* were transformed into BL21 DE3 Lys-S *E. coli* cells. Colony PCR was performed using primers, T7 TOPO-F and F4 HisTOPO-A (Appendix B) to select for positive clones. Positive *XvPrx2* and *XvV76C* clones were used in the expression studies.

3.2.1.2 Protein expression

For small scale induction, 1 ml of an overnight LB-amp broth culture (either pTOPO::*XvPrx2* or pTOPO::*XvV76C*) was inoculated in 100 ml LB-amp broth and incubated with vigorous shaking at 37°C until an OD_{600} of between 0.6-0.8 was obtained. A 1 ml aliquot was removed from the broth culture (un-induced sample) at this point. The 100 ml culture was induced by addition of isopropyl-β-D-thiogalactoside (IPTG; 1 mM final concentration). A 1 ml aliquot was collected every hour for 5 h (induced samples). The 1 ml samples were centrifuged for 1 min at 8000 x g and the supernatant discarded. Eighty microlitres of water was added to the pelleted cells and gently resuspended by pipetting. Twenty microlitres of 5X SDS loading buffer (0.225 M Tris, pH 6.8; 50% glycerol; 5% SDS; 0.05% bromophenol blue; 0.25 M DTT) was added to the resuspended cells. Samples were electrophoresed on a 12% polyacrylamide gel (standard PAGE conditions; Appendix A).

For large scale induction, 20 ml of an overnight LB-amp broth culture (either pTOPO::*XvPrx2* or pTOPO::*XvV76C*) was inoculated in one litre LB-amp broth and incubated with vigorous shaking at 37°C until an OD_{600} of between 0.6-0.8 was obtained. A 1 ml aliquot was removed from the broth culture (un-induced sample) at this point. The one litre culture was induced by addition of IPTG (1 mM final concentration) and incubated for an additional 5 h with vigorous shaking at 37°C. A 1 ml aliquot was collected after 5 h (induced sample). The 1 ml samples (induced and un-induced) were treated as described for small scale induction. The remaining one litre induced culture was cooled for 10 min on ice. The culture was distributed into 6 GSA centrifuge tubes and centrifuged for 30 min at 4000 x g at 4°C. The supernatant was discarded. Pelleted cells from all 6 centrifuge tubes were pooled following resuspension in 50 ml LB broth. Cells were again pelleted by centrifugation for 10 min at 5600 x g at 4°C. The supernatant was discarded. Pelleted cells were stored overnight at -20°C or for longer periods at -80°C.

The frozen cells were thawed for 45 min on ice. The pellet was initially resuspended in a small volume (ca. 1-2 ml) of lysis buffer [50 mM NaH_2PO_4; 300 mM NaCl; 10 mM imidazole; 10 mM ascorbic acid (added fresh); pH 8] by gentle pipetting. Further small amounts of lysis buffer were added at short intervals to allow the cells to slowly dissolve. This facilitated the homogenisation of the cell solution. The final volume of lysis buffer added to the cell solution was between 20-40 ml depending on the size of the pellet and the viscosity of the solution. Lysozyme (0.01 g in 1 ml lysis buffer; Sigma, Germany) was added to the cell solution, which was incubated for 1 h with gentle shaking at 4°C to allow cell lysis to occur. Five millitre aliquots of the infected cells were sonicated in 6 bursts of 10 s interrupted by five intervals of 10 s to prevent overheating of the sample. The lysate was centrifuged for 30 min at 10000 x g at 4°C. The supernatant containing the crude protein extract was purified through a Ni-NTA column.

3.2.1.3 Protein purification

To prepare a resin column the bottom of a 20 ml syringe was plugged with glass wool. Homogenised Ni-NTA resin (Qiagen, Germany) was loaded in the syringe over the glass wool. Ten millilitres of wash buffer I (50 mM NaH_2PO_4; 300 mM NaCl; 10 mM imidazole; pH 8) was applied to the top of the resin column and allowed to pass through by gravitational flow. The supernatant containing the crude protein extract was loaded onto the column. The recombinant protein was allowed to bind to the column due to the interaction of the protein's His-Tag and nickel ions on the Ni-NTA column. A 100 µl aliquot of the flow-through was removed (pre-wash sample). The resin bound protein was washed with 20 ml wash buffer I and a second 100 µl aliquot of the flow-through was removed (first wash sample). The resin bound protein was washed with 20 ml wash buffer II (50 mM NaH_2PO_4; 300 mM NaCl; 10 mM imidazole; 20% glycerol; pH 8) and a third 100 µl aliquot of the flow-through was removed (second wash sample). The washed protein in the column was treated with 10-20 ml elution buffer (50 mM NaH_2PO_4; 300 mM NaCl; 250 mM imidazole; pH 8) and the elutes collected in 1.5 ml Eppendorf tubes as 1 ml fractions. A fourth 100 µl aliquot of the flow-through was removed at the end of the elution process (post elution sample). The OD_{280} of each fraction was determined in a spectrophotometer (Beckman, USA) using quartz cuvettes. From these absorbance readings the samples with the highest OD_{280} values (greater than 0.5) were pooled and a 100 µl aliquot removed (eluted sample).

The concentration of the protein was determined using the following formula:

Protein concentration = E/ε.d

where,

E = absorbance at 280 nm

ε = extinction coefficient (using protparam tool page in expasy) = 15220.1

d = cuvette diameter = 1 cm

The pooled protein sample was dialysed overnight in 40 mM phosphate buffer (KPi buffer; Appendix D). Fresh 40 mM KPi buffer was added to the sample and dialysis was allowed to continue for a further 5 h. Following dialysis the sample was transferred to a 50 ml Sterilin tube. The OD_{280} of the dialysed sample was determined in a spectrophotometer, which was blanked with 40 mM KPi buffer. Five hundred microlitre aliquots of the purified protein sample were prepared and stored at -70°C. A 10 µl aliquot (dialysed sample) was removed for gel electrophoresis.

Sample aliquots (pre-wash, first wash, second wash, eluted, post elution and lysed) prepared during the protein purification procedure were prepared for electrophoresis. Samples were electrophoresed on a 12% SDS PAGE gel (standard PAGE conditions; Appendix A).

3.2.2 Baculovirus expression of XvPrx2

Recombinant baculoviruses have become widely used as vectors to express heterologous genes in cultured insect cells and insect larvae. In most cases, the recombinant proteins are processed, modified, and targeted to their appropriate cellular locations, where they are functionally similar to their authentic counterparts.

Bac-to-Bac (Invitrogen Life Technologies, USA) protocol relies on the generation of recombinant baculovirus by site-specific transposition in *E. coli* rather than homologous recombination in insect cells. The gene of interest is cloned into a pFastBac1 vector and transformed into DH10Bac competent *E. coli* cells. DH10Bac cells contain a parent bacmid with a *lacZ*-mini-*att*Tn7 fusion. Transposition occurs between the elements of the pFastBac1 vector and the parent bacmid in the presence of transposition proteins provided by a helper plasmid. When the transposition is successful, the expression cassette disrupts the *lacZ* gene. The new expression bacmid is visualised as white bacterial colonies. High molecular weight DNA is isolated and transfected into Sf21 cells using Cellfectin transfection reagent (Invitrogen Life Technologies, USA). After two days high-titre recombinant baculovirus can be isolated for amplification and expression. Cells are infected using the viral stock and protein expression can be detected within 2 days.

3.2.2.1 Cloning of *XvTrx2* into pFastBac1

The *XvPrx2* gene was amplified using gene specific primers, EcoR1CAT-F (incorporating an *Eco*RI site; Appendix B) and XvPrx2-R (Appendix B). PCR reaction volumes were made up to 25 µl (standard PCR reaction; Appendix A) and run with the following cycling conditions: 94ºC for 3 min; 35 cycles of 94ºC for 30 s, 58ºC for 45 s and 72ºC for 90 s; and a final extension step of 5 min. The PCR products were electrophoresed on a 1% agarose/EtBr gel. The band of interest was excised and purified using the High Pure PCR Product Purification Kit according to the manufacturer's instruction (Appendix A).

The purified *XvPrx2* amplimer was digested using *Eco*RI and *Xba*I with overnight incubation at 37°C. The digested fragment was purified using the High Pure PCR Product Purification Kit according to the manufacturer's instruction (Appendix A). Similarly, pFastBac1 was digested using *Eco*RI and *Xba*I, electrophoresed on a 1% agarose/EtBr gel, excised and purified. The digested *XvPrx2* amplimer and pFastBac1 were ligated (standard ligation conditions; Appendix A).

The recombinant plasmid was transformed into *E. coli* XLI-blue cells (standard transformation conditions; Appendix A). Colony PCR was performed using primers, EcoR1CAT-F and XvPrx2-R to select for positive clones. The XLI-blue cells containing pFastBac1::*XvPrx2* were inoculated in LB broth supplemented with 100 µg.ml^{-1} ampicillin. Plasmid DNA was isolated from the respective clones using the High Pure Plasmid Extraction Kit according to the manufacturer's instruction (Appendix A). Samples were sequenced to confirm that errors were not incorporated during the PCR procedure.

Plasmid DNA was isolated from two positive clones and re-transformed into *E. coli* DH10Bac cells. Ten nanograms of pFastBac1::*XvPrx2* DNA was added to competent *E. coli* DH10Bac cells and gently mixed. The transformation mix was incubated for 45 min on ice. The cells were heat shocked by incubation for 45 s at 42ºC and immediately thereafter on ice for 2 min. Nine hundred microlitres of SOC broth (Appendix D) was added to the transformed cells and incubated for 4 h at 37ºC with shaking. Fifty microlitres of the transformation mix was plated on LB agar plates (supplemented with 50 µg.ml^{-1} kanamycin, 7 µg.ml^{-1} gentamycin, 10 µg.ml^{-1} tetracycline, 40 µg.ml^{-1} X-gal and 40 µg.ml^{-1} IPTG) and incubated overnight at 37°C. Clones were observed as large white colonies.

3.2.2.2 Generation of recombinant bacmid DNA

A single bacterial colony was selected and inoculated in 2 ml LB (supplemented with 50 $\mu g.ml^{-1}$ kanamycin, 7 $\mu g.ml^{-1}$ gentamycin and 10 $\mu g.ml^{-1}$ tetracycline) and incubated for 16 h at 37°C with shaking. The bacterial culture was transferred to a 2 ml Eppendorf tube and centrifuged for 1 min at 12000 x g at RT. The supernatant was discarded. The pellet was resuspended in 0.3 ml solution I (15 mM Tris, pH 8; 10 mM EDTA; 100 $\mu g.ml^{-1}$ RNase A) by gently pipetting. To this 0.3 ml solution II (0.2 N NaOH; 1% SDS) was added, mixed gently by inversion (ca. 25 times) and incubated for 5 min at RT. The appearance of the cell suspension was observed to change from very turbid to almost translucent as the cells lysed. A volume of 0.3 ml solution III (3 M potassium acetate, pH 5.5) was added and mixed gently by inversion (ca. 25 times). Protein and genomic DNA precipitated out of solution at this point resulting in a white precipitate. The tube containing the lysed cells was incubated for 10 min on ice and thereafter centrifuged for 10 min at 12000 x g at RT. The bacmid containing supernatant was transferred to a 2 ml Eppendorf tube containing 0.8 ml isopropanol, mixed gently by inversion (ca. 50 times) and incubated for 10 min on ice. The precipitated bacmid DNA was centrifuged for 15 min at 12000 x g at RT. The supernatant was discarded. The DNA pellet was washed in 0.5 ml of cold 75% EtOH. DNA samples were centrifuged for 5 min at 6000 x g at RT and the EtOH was discarded. DNA samples were briefly centrifuged and the remaining EtOH removed with a pipette. The DNA pellet was air-dried for ca. 10 min. The bacmid DNA pellet was resuspended in 50 µl TE buffer (10 mM Tris, pH 8; 1 mM EDTA) and stored at -20°C. Repeated freeze/thaw cycles of the bacmid DNA were avoided as this reduced transfection efficiency.

A 35 mm perspex dish with 2 ml of complete media (10% FCS (Sigma, Germany); 50 $\mu g.ml^{-1}$ neomycin; 62.9 $\mu g.ml^{-1}$ penicillin G; 100 $\mu g.ml^{-1}$ streptomycin, made up in 100% TC100] was seeded with 1 x 10^6 Sf21 cells (Invitrogen Life Technologies, USA). The cells were allowed to settle (forming a monolayer) by overnight incubation at 27°C. Excess liquid was removed from the monolayer cells, which were washed twice with 2 ml TC100 (Sigma, Germany). Solution A (5 µl bacmid mini prep DNA; 100 µl TC100) and B (6 µl Cellfectin; 100 µl TC100) were mixed and incubated for 45 min at RT. This mixture comprised the lipid-DNA complexes. Eight microlitres of TC100 was added to the lipid-DNA complexes and mixed gently. The remaining media was removed from the monolayer cells and overlaid with 1 ml lipid-DNA mix. The overlaid monolayer cells were incubated for 5 h at 27°C prior to the addition of 1 ml complete media. The overlaid monolayer cells were incubated for a further

72 h at 27°C. Infected insect cells in the supernatant were harvested. The supernatant was clarified by centrifugation for 5 min at 5000 x g at RT. The supernatant containing infected insect cells (First Supernatant; expected titre of 1 x 10^7 pfu.ml^{-1}) was incubated in the dark at 4°C. Two millilitres of complete media was added to the infected insect cells and incubated for a further 72 h at 27°C to allow for amplification of the virus. Infected insect cells in the supernatant were again harvested. The supernatant was clarified by centrifugation for 5 min at 5000 x g at RT (second supernatant; expected titre of 1 x 10^9 pfu.ml^{-1}). An aliquot of the infected insect cells was analysed for protein expression by lysis in 400 µl protein disruption buffer (62.5 mM Tris, pH 6.8; 2% SDS). Samples were electrophoresed on a 12% SDS PAGE gel (standard PAGE conditions; Appendix A).

The supernatant containing infected insect cells was clarified by centrifugation for 5 min at 500 x g at RT. Infected insect cells were transferred to sterile capped cryotubes (Nunc, USA). Tubes were stored in the dark with half at 4°C and the remainder at -70°.

3.2.2.3 Confirmation of viral infection of insect cells

The infection of insect cells with virus particles was confirmed by both PCR and electron microscopy.

PCR was performed on DNA isolated from infected insect cells. The *XvPrx2* gene was amplified using gene specific primers, XvPrx2-F (Appendix B) and XvPrx2-R (Appendix B). PCR reaction volumes were made up to 25 µl (standard PCR reaction; Appendix A) and run with the following cycling conditions: 94ºC for 3 min; 35 cycles of 94ºC for 30 s, 58ºC for 45 s and 72ºC for 90 s; and a final extension step of 5 min. The PCR products were electrophoresed on a 1% agarose/EtBr gel.

Five day post-infection insect cells (intact and lysed) were prepared for electron microscopy. For the lysed sample, 5 ml aliquots of infected cells were sonicated in 3 bursts of 10 s interrupted by two intervals of 10 s to prevent overheating of the sample. Following sonication the disrupted cells were centrifuged for 10 min at 4250 x g at RT. The supernatant was transferred to a fresh tube. The supernatant was coated on the matt side of copper grids by floating grids for 10 min in 20 µl of supernatant on parafilm. For the intact sample, cells were coated on the matt side of copper grids by floating grids for 10 min in 20 µl of infected cells on parafilm.

For both intact and lysed samples 20 µl of sterile dH_2O was spotted on a separate piece of parafilm. Grids were gently transferred (matt side down), with a sterile forceps, onto the 20

µl sterile dH_2O spots and allowed to wash for 1 min. Excess water from the grids were removed by blotting with strips of Whatmann filter paper (Merck, Germany). A second wash was performed for 1 min with fresh sterile dH_2O on parafilm and the excess water was again removed by blotting. Uryl acetate was used to fix cells onto grids. The uryl acetate was centrifuged for 2 min at 12000 x g at RT. Twenty microlitres of uryl acetate was placed on a piece of parafilm and the grids were placed (matt side down) on the solution for 2 min. The excess solution was removed by blotting and the grids were stored in a grid box. Grids were viewed using a JEM 200 electron microscope (JEOL, Tokyo, Japan) at 120 kV to confirm the presence of virus particles.

3.2.2.4 Purification of XvPrx2 from baculovirus infected insect cells

Infected insect cells were washed with phosphate buffered saline [PBS (50 mM potassium phosphate; 150 mM NaCl; pH 7.2)] and collected by centrifugation for 5 min at 5000 x g at RT. Lysis buffer (50 mM NaH_2PO_4; 300 mM NaCl; 10 mM imidazole; pH 8) was prepared fresh in a total volume of 25 ml and was supplemented with a single protease inhibitor tablet (EDTA free; Roche, Germany). The washed cells were lysed by briefly vortexing in 10 ml lysis buffer supplemented with 1% Nonidet R40 (Roche, Germany) per 1 x 10^7 cells. The lysed cells were incubated for 10 min on ice and thereafter centrifuged for 10 min at 5000 x g at RT to pellet cellular debris and DNA. The supernatant (cleared lysate) containing His-tagged XvPrx2 was treated with RNaseA (10 $\mu g.ml^{-1}$; Sigma, Germany) and DNaseI (1 $\mu g.ml^{-1}$; Sigma, Germany) according to the manufacturer's instructions. Two hundred microlitres of 50% Ni-NTA (Qiagen, Germany) slurry per 4 ml cleared lysate was added and incubated for 2 h at 4°C with shaking. The resin was equilibrated by first adding it to the slurry and incubating for a few min on ice. The column was washed with lysis buffer and thereafter the lysate Ni-NTA mixture was loaded onto the column (outlet capped). The outlet cap was removed and the flow-through collected (pre-wash sample). The column was washed twice with 800 µl wash buffer (50 mM NaH_2PO_4; 300 mM NaCl; 20 mM imidazole; pH 8) and the flow-through collected (first and second wash samples). Proteins (His-tagged) were eluted in 100 µl elution buffer (50 mM NaH_2PO_4; 300 mM NaCl; 250 mM imidazole; pH 8). The elute was collected in four fractions. A 1 µl aliquot was removed from each of the eluted fractions (eluted samples). Purified protein was dialysed overnight in either Tris (pH 7.5) or phosphate buffer. This final dialysis step was necessary to ensure the protein was free of any residual salt or imidazole. Sample aliquots (pre-wash, first wash, second wash and

eluted) prepared during the protein purification procedure were prepared for electrophoresis. Samples were electrophoresed on a 12% polyacrylamide gel (standard PAGE conditions; Appendix A).

3.2.3 Expression of XvPrx2 in pProEx

The pProEx-HT prokaryotic expression system (Invitrogen Life Technologies, USA) was used to express recombinant XvPrx2 in *E. coli*. The gene of interest is cloned into the multiple cloning site of either pProExA, B or C. The histidine sequence at the amino terminus has a strong affinity to the Ni-NTA resin matrix making it simple to purify the desired protein. Protein purification using the Ni-NTA resin is based on the principles of immobilised metal chelate affinity chromatography. The pProEx-HT vector (Invitrogen Life Technologies, USA) also contains the TEV protease recognition site for cleavage of the 6X histidine from the protein. The *trc* promoter and *lacI*^{q} gene enable inducible expression of the cloned gene with IPTG.

3.2.3.1 Cloning of *XvPrx2* into pProEx

The *loxP* cassette (Clontech, USA) was amplified using gene specific primers, LoxPEcoRI-F (incorporating an *Eco*RI site; Appendix B) and LoxPXbaI-R (incorporating a *Xba*I site; Appendix B). PCR reaction volumes were made up to 25 µl (standard PCR reaction; Appendix A) and run with the following cycling conditions: 94°C for 1 min; 16 cycles of 94°C for 30 s and 60°C for 2 min; and a final extension step of 60°C for 5 min. The PCR products were electrophoresed on a 1% agarose/EtBr gel. The band of interest was excised and purified using the High Pure PCR Product Purification Kit according to the manufacturer's instruction (Appendix A).

The purified *loxP* cassette was digested using *Eco*RI and *Xba*I with overnight incubation at 37°C. The digested fragment was purified using the High Pure PCR Product Purification Kit according to the manufacturer's instruction (Appendix A). Similarly, pProExA, B, C (Appendix C; Invitrogen, USA) were digested using *Eco*RI and *Xba*I, electrophoresed on a 1% agarose/EtBr gel, excised and purified. The digested *loxP* cassette and pProExA, B, C were ligated (standard ligation conditions; Appendix A).

The recombinant plasmids were transformed into *E. coli* XL1-blue cells (standard transformation conditions; Appendix A). Colony PCR was performed using primers, LoxPEcoRI-F and LoxPEcoRI-R to select for positive pProEx::LoxP clones. The XL1-blue cells containing either pProExA::*loxP*, pProExB::*loxP* or pProExC::*loxP* were inoculated in

LB broth supplemented with ampicillin (100 μg.ml^{-1}). Plasmid DNA was isolated from the respective clones using the High Pure Plasmid Extraction Kit according to the manufacturer's instruction (Appendix A). Samples were sequenced to confirm that errors were not incorporated during the PCR procedure.

The pDNR-Lib::*XvPrx2* plasmid (see section 2.3.4) was digested with *Eco*RI resulting in the excision of a fragment (ca. 70 bp) upstream of the gene flanked by two *Eco*RI sites. The digested pDNR-Lib::*XvPrx2* plasmid was re-ligated and transformed into *E. coli* XL1-blue cells (standard ligation and transformation conditions; Appendix A).

The *XvPrx2* gene was transferred from pDNR-Lib into pProExA::*loxP*, pProExB::*loxP* and pProExC::*loxP* using Cre recombinase (Clontech, USA). Reaction mixtures were prepared in a 20 μl volume (Table 3.2).

Table 3.2 Reaction mixture for the transfer of *XvPrx2* from the donor vector, pProEx (A, B, C) to the acceptor vector, pDNR-Lib using Cre recombinase

Component	Concentrations/volumes
Donor vector	200 ng
Acceptor vector	200 ng
10X Cre reaction buffer	2 μl
10X BSA (1 mg.ml^{-1})	2 μl
Cre recombinase (100 ng.μl^{-1})	1 μl
dH_2O	make up to 20 μl

The contents were mixed well by gently tapping the tube and briefly centrifuging the contents. The reaction mix was incubated for 15 min at RT. The incubation period was not extended beyond 15 min as competing recombination reactions, which do not generate desired recombinants can reduce the yield of the desired recombinants. The reaction was terminated by heat inactivation for 5 min at 70°C.

The recombinant plasmid was transformed into *E. coli* XL1-blue cells (standard transformation conditions; Appendix A). Transformed cells were plated on LB agar plates supplemented with 30 μg.ml^{-1} chloramphenicol and 7% sucrose. All clones containing pDNR-Lib::*XvPrx2* would die due to the presence of a *sacB* gene in pDNR-Lib. All clones containing pProExA::*loxP*, pProExB::*loxP* or pProExC::*loxP* would die due to the absence of a chloramphenicol resistance gene. Only clones with pProExA::*XvPrx2*, pProExB::*XvPrx2* or

pProExC::*XvPrx2* would survive due to the co-transfer of *XvPrx2* and a chloramphenicol resistance gene from pDNR-Lib.

The XL1-blue cells containing either pProExA::*XvPrx2*, pProExB::*XvPrx2* or pProExC::*XvPrx2* were inoculated in LB broth supplemented with 34 $\mu g.ml^{-1}$ chloramphenicol. Plasmid DNA was isolated from the respective clones using the High Pure Plasmid Extraction Kit according to the manufacturer's instruction (Appendix A). Samples were sequenced to confirm that the gene was cloned in frame with the histidine tag.

3.2.3.2 Protein expression and purification

Proteins were expressed and purified as described in sections 3.2.1.2 and 3.2.1.3, respectively.

3.2.4 Antibody generation, western blotting and immuno-detection

3.2.4.1 Antibody generation

Purified protein was concentrated using an Electro-eluter (model 422; Bio-Rad, USA.) according to the manufacturer's instructions. The purified XvPrx2 protein at a concentration of 1 $mg.ml^{-1}$ was used for antibody generation. An antiserum against XvPrx2 heterologously expressed in *E. coli* was generated in rabbit by Pineda (Germany). Pre-immune sera from 3 separate rabbits were tested for cross reactivity against total protein extracted from *A. thaliana* and *X. viscosa* as well as against purified XvPrx2 protein. The rabbit that produced pre-immune serum displaying the least cross reactivity was selected for generation of XvPrx2 antibodies. Other antibodies used in this study included:

(i) AtPrxIIB antibody (provided by Finkemeier, University of Bielefeld, Germany);
(ii) PtPrxII antibody (provided by Rouhier, Université Henri Poincaré, France); and
(iii) anti-His antibody (Sigma, Germany).

3.2.4.2 Western blotting

Gels were placed in transfer buffer (25 mM Tris; 192 mM Glycine; 0.1% SDS; 20% methanol added fresh) following SDS electrophoreses. The Hoefer miniVE vertical electrophoresis system (Amersham Biosciences, USA) was used for the blotting procedure. The transfer stack was assembled on the cathode module whilst submerged in transfer buffer in the following order:

(i) two packing sponges (dampened in transfer buffer) centred on the cathode module;
(ii) two pieces of filter paper (moistened in transfer buffer) placed on the packing sponge;

(iii) the gel (equilibrated in transfer buffer) positioned on the filter paper;
(iv) Osmonics nitrocellulose membrane (Osmonics, USA), with pore size 0.45 μm, immersed for 5 min in transfer solution and thereafter placed on the gel;
(v) two pieces of filter paper (moistened in transfer buffer) placed on the membrane; and
(vi) two packing sponges (moistened in transfer buffer) placed on the filter paper.

The module was sealed and placed in the module holder, which was placed into the electrophoresis tank. The tank was filled with transfer buffer and the lid closed. Electrophoretic transfer was conducted for 3 h at 300 mA.

3.2.4.3 Chromogenic detection

The membrane was removed from the blotting apparatus and placed in TBS/Tween/Triton buffer [TBSTT (50 mM Tris; 150 mM NaCl; 0.05% Tween 20; 0.2 % Triton X100, prepared fresh)]. The membrane was stained in Ponceau S stain [0.1% Ponceau S (BioBasic, USA); 5% acetic acid] to verify transfer and equal loading of proteins as Ponceau S reversibly stains proteins red. Stained protein bands were photographed and immediately thereafter TBSTT was added to the membrane to remove the stain. The membrane was washed thrice for 10 min in TBSTT at RT with shaking. The membrane was incubated for 1 h in blocking solution (1% milkpowder in TBSTT) at RT with shaking and thereafter washed thrice for 10 min in TBSTT at RT with shaking. The membrane was incubated for 3 h in primary antibody [1:1000 dilution of tetra-His BSA free mouse monoclonal IgG (Qiagen, Germany)] in blocking buffer at RT and thereafter washed thrice for 10 min in TBSTT buffer at RT with shaking. The membrane was incubated for 1 h in secondary antibody [1:5000 dilution of goat anti-mouse IgG alkaline phosphatase conjugate (Sigma, Germany)] in blocking buffer at RT and thereafter washed thrice for 10 min in TBSTT buffer at RT with shaking. The membrane was stained with alkaline phosphatase solution [one tablet of NBT/BCIP ready to use tablets (Roche, Germany)] until the signal was clearly visible (ca. 5-15 min). The chromogenic reaction was terminated by rinsing the membrane twice in water. The membrane was air-dried and photographed immediately.

3.2.4.4 Chemiluminescent detection

The membrane was removed from the blotting apparatus and placed in TBSTT. The membrane was stained in Ponceau S stain to verify transfer and equal loading of proteins as Ponceau S reversibly stains proteins red. Stained protein bands were photographed and immediately thereafter TBSTT was added to the membrane to remove the stain. The membrane was washed thrice for 10 min in TBSTT at RT with shaking. The membrane was incubated for 1 h in blocking solution (1% milkpowder in TBSTT) at RT with shaking and thereafter washed thrice for 10 min in TBSTT at RT with shaking. The membrane was incubated for 3 h in primary antibody (1:5000 dilution of XvPrx2 antibodies) in blocking buffer at RT and thereafter washed thrice for 10 min in TBSTT buffer at RT with shaking. The membrane was incubated for 1 h in secondary antibody [1:20000 dilution of goat anti-rabbit IgG horseradish peroxidase conjugate (Sigma-Aldrich, UK)] in blocking buffer at RT and thereafter washed thrice for 10 min in TBSTT buffer at RT with shaking. Detection was carried out using the SuperSignal West Pico Chemiluminescent Substrate Detection System (Pierce, USA) according to the manufacturer's instructions. Fluorescence was captured on CL-XPosure Film (Pierce, USA).

3.2.5 Immuno-cytochemical localisation of XvPrx2

Immuno-cytochemical analyses were performed according to the protocol of König et al. (2002). Mature leaves and roots of non-stressed and stressed (100 µM ABA) *X. viscosa* were dissected in 1 mm^2 sections and immediately fixed for 45 min in 2.5% glutaraldehyde (w/v) in EM buffer (50 mM KH_2PO_4; Na_2HPO_4, pH 7.0). Similarly, *A. thaliana* leaves (4 week old) were prepared in the same manner. Following dehydration in acetone gradients, the samples were embedded step-wise in Transmit EM resin (TAAB Laboratories Equipment, UK). Ultra thin sections of 60-70 nm were generated using an Ultracut microtome (Reichert Ultracut E, Germany) and placed onto 400 mesh gold grids. Samples were either immuno-labelled with rabbit anti-XvPrx2 antiserum (1:100; see section 3.2.4.1) or with rabbit anti-AtPrxIIC antiserum for 1 h and diluted in 3% BSA [made up in Tris buffered saline (10 mM Tris, pH 7; 150 mM NaCl)] supplemented with 0.05% NaN_3 (w/v). Grids were rinsed in 5X Tris buffered saline and incubated for 1 h with gold conjugated (15 nm) anti-rabbit IgG (1:30; Sigma, Germany) in 3% BSA (made up in Tris buffered saline). Samples were stained for 5 s with 0.1% uranyl acetate (w/v) followed by a further 5 s with 2% lead citrate (w/v). Samples were examined with an electron microscope (Hitachi H500, Japan) at 75 kV.

3.2.6 YFP localisation of XvPrx2 in *Arabidopsis thaliana* protoplasts

The plasmid, pEYFP (Appendix C) encodes an enhanced yellow-green variant of the *Aequorea victoria* green fluorescent protein (GFP). The fluorescence excitation maximum of EYFP is 513 nm, and the emission spectrum has a peak at 527 nm (in the yellow-green region). When excited at 513 nm, the E_m of EYFP is 36500 $cm^{-1}.M^{-1}$ and the fluorescent quantum yield is 0.63, resulting in a bright fluorescent signal. The upstream sequences flanking EYFP have been converted to a Kozak consensus translation initiation site. These changes increase the translational efficiency of the EYFP mRNA and consequently the expression of EYFP in mammalian and plant cells.

A vector with a strong promoter and a terminator was required for localisation studies. Due to problems with restriction sites to clone the *XvPrx2*::YFP into the p35S-GFP vector a multiple cloning strategy was employed (Fig. 3.1). To determine the in vivo subcellular localisation of XvPrx2, *A. thaliana* protoplasts were stably transformed with

(i) an expression construct encoding a XvPrx2::YFP fusion protein;
(ii) pEYFP encoding for YFP (YFP control); and
(iii) an expression construct encoding an ABI5::YFP fusion protein, known to be localised to the nucleus (known control).

3.2.6.1 Cloning of *XvPrx2* into pEYFP

The *XvPrx2* gene was amplified using gene specific primers, XvPrx2HindIIIXbaI-F (incorporating a *Hin*dIII site; Appendix B) and XvPrx2NcoI-R (incorporating a *Nco*I site; Appendix B). PCR reaction volumes were made up to 25 µl (standard PCR reaction; Appendix A) and run with the following cycling conditions: 94°C for 3 min; 35 cycles of 94°C for 30 s, 58°C for 45 s and 72°C for 90 s; and a final extension step of 5 min. The PCR products were electrophoresed on a 1% agarose/EtBr gel. The band of interest was excised and purified using the High Pure PCR Product Purification Kit according to the manufacturer's instruction (Appendix A).

The purified *XvPrx2* amplimer was digested using *Hin*dIII and *Nco*I with overnight incubation at 37°C. The digested fragment was purified using the High Pure PCR Product Purification Kit according to the manufacturer's instruction (Appendix A). Similarly, pEYFP was digested using *Hin*dIII and *Nco*I, electrophoresed on a 1% agarose/EtBr gel, excised and purified. The digested *XvPrx2* amplimer and pEYFP were ligated (standard ligation conditions; Appendix A).

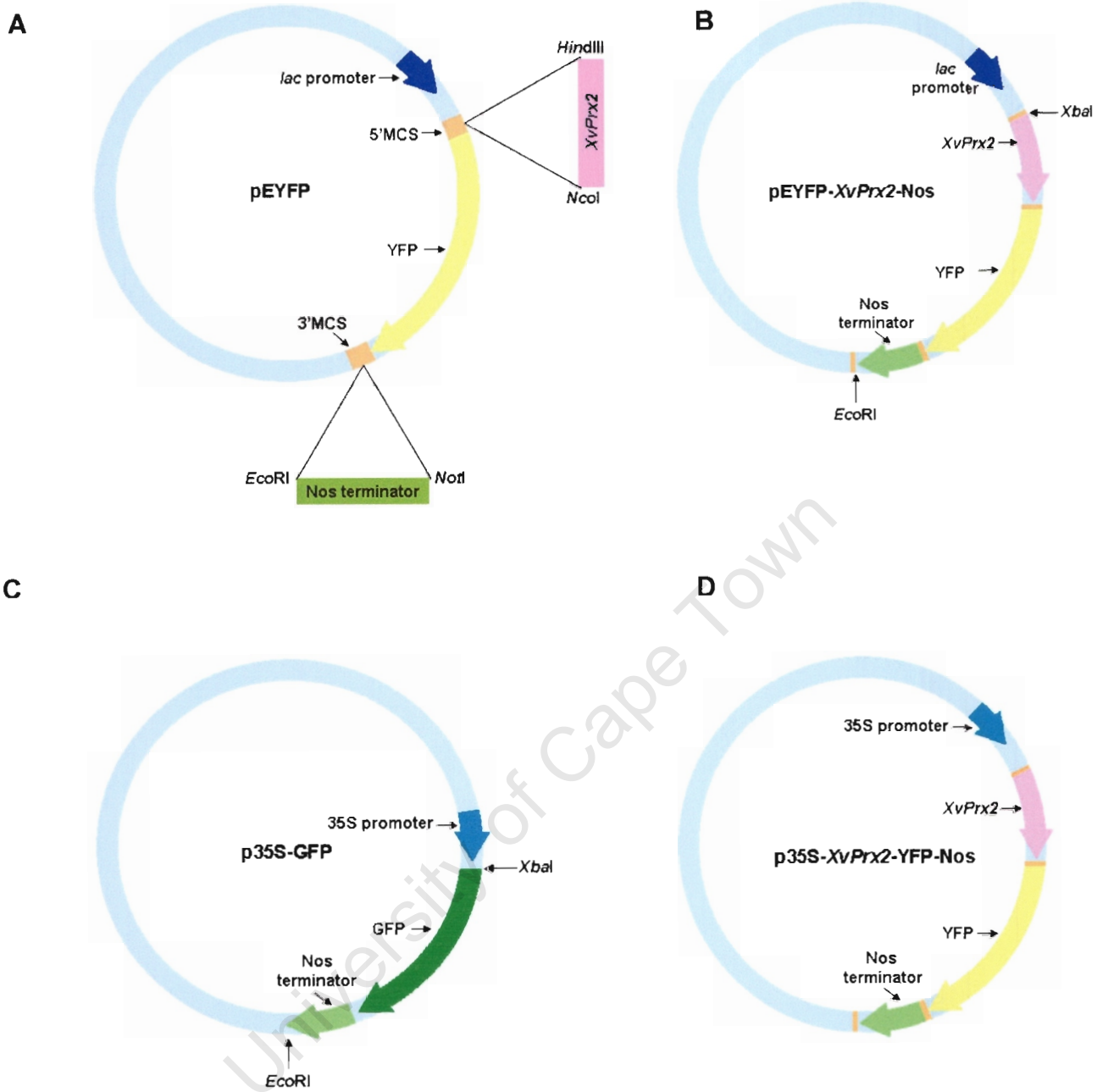

Figure 3.1 Schematic illustration of the synthesis of a YFP construct for the localisation of XvPrx2. The *XvPrx2* gene was amplified and digested with *Hin*dIII and *Nco*I and cloned into the 5' MCS of pEYFP vector (A). Similarly, nos_{term} was amplified and digested with *Not*I and *Eco*RI and thereafter cloned into the 3' MCS of pEYFP (A). The *XvPrx2*::YFP::nos_{term} construct was excised with *Xba*I and *Eco*RI from plasmid pEYFP::*XvPrx2*::nos_{term} (B). At the same time p35S-GFP was digested with *Xba*I and *Eco*RI (C). The *XvPrx2*::YFP::nos_{term} construct was cloned into *Xba*I and *Eco*RI sites generated in the p35S-GFP vector and named p35S::*XvPrx2*::YFP::nos_{term} (D).

The recombinant plasmid was transformed into *E. coli* XL1-blue cells (standard transformation conditions; Appendix A). Colony PCR was performed using primers, XvPrx2HindIIIXbaI-F and XvPrx2NcoI-R to select for positive clones. The XL1-blue cells containing pEYFP::*XvPrx2* were inoculated in LB broth supplemented with 100 $\mu g.ml^{-1}$ ampicillin. Plasmid DNA was isolated from the respective clones using the High Pure Plasmid Extraction Kit according to the manufacturer's instruction (Appendix A). Samples were sequenced to confirm that errors were not incorporated during the PCR procedure.

The *nos* terminator was amplified from the p35S-GFP vector (Clontech, USA) using gene specific primers, p35SGFPNosTerm-F (incorporating an *Eco*RI site; Appendix B) and p35SGFPNosTerm-R (incorporating a *Not*I site; Appendix B). PCR reaction volumes were made up to 25 µl (standard PCR reaction; Appendix A) and run with the following cycling conditions: 94°C for 3 min; 35 cycles of 94°C for 30 s, 58°C for 45 s and 72°C for 90 s; and a final extension step of 5 min. The PCR products were electrophoresed on a 1% agarose/EtBr gel. The band of interest was excised and purified using the High Pure PCR Product Purification Kit according to the manufacturer's instruction (Appendix A).

The purified *nos* terminator was digested using *Eco*RI and *Not*I with overnight incubation at 37°C. The digested fragment was purified using the High Pure PCR Product Purification Kit according to the manufacturer's instruction (Appendix A). Similarly, pEYFP::*XvPrx2* was digested using *Eco*RI and *Not*I, electrophoresed on a 1% agarose/EtBr gel, excised and purified. The digested *nos* terminator and pEYFP::*XvPrx2* were ligated (standard ligation conditions; Appendix A).

The recombinant plasmid was transformed into *E. coli* XL1-blue cells (standard transformation conditions; Appendix A). Colony PCR was performed using primers, p35SGFPNosTerm-F and p35SGFPNosTerm-R to select for positive clones. The XL1-blue cells containing pEYFP::*XvPrx2*::nos_{term} were inoculated in LB broth supplemented with 100 $\mu g.ml^{-1}$ ampicillin. Plasmid DNA was isolated from the respective clones using the High Pure Plasmid Extraction Kit according to the manufacturer's instruction (Appendix A). Samples were sequenced to confirm that errors were not incorporated during the PCR procedure.

The pEYFP::*XvPrx2*::nos_{term} construct in pEYFP was digested using *Xba*I and *Eco*RI, electrophoresed on a 1% agarose/EtBr gel, excised and purified. Similarly, p35S-GFP was digested using *Xba*I and *Eco*RI, electrophoresed on a 1% agarose/EtBr gel, excised and purified. The digested *XvPrx2*::YFP::nos_{term} construct and p35S (with the *GFP* gene and nos_{term} removed) were ligated (standard ligation conditions; Appendix A).

The recombinant plasmid was transformed into *E. coli* XL1-blue cells (standard transformation conditions; Appendix A). Colony PCR was performed using primers, XvPrx2int-F and XvPrx2int-R to select for positive *XvPrx2* clones. The XL1-blue cells containing p35S::*XvPrx2*::YFP::nos_{term} were inoculated in LB broth supplemented with 100 $\mu g.ml^{-1}$ ampicillin. Plasmid DNA was isolated from the respective clones using the High Pure Plasmid Extraction Kit according to the manufacturer's instruction (Appendix A).

3.2.6.2 Large scale preparation of plasmid DNA

Large scale plasmid DNA extraction of two fusion constructs [p35S::*XvPrx2*::YFP::nos_{term} and ABI5::YFP (supplied by Peter Hare, Rockefeller Institute, USA)] as well as the pEYFP vector was performed.

A 15 ml LB-amp culture containing the respective plasmid was incubated for 16 h at 37°C with shaking. The culture was inoculated into fresh LB-amp broth and incubated for a further 16 h at 37°C with shaking. The culture was centrifuged for 5 min at 4250 x g and the pellet resuspended in 18 ml solution I (50 mM glucose; 25 mM Tris; 10 mM EDTA). Two millilitres of lysozyme (10 $mg.ml^{-1}$; prepared one night before in 10 mM Tris, pH 8) was added to the resuspended cells. Forty millilitres of freshly prepared solution II (0.2 M NaOH; 1% SDS) was added, mixed gently (ca. 25 times) and incubated for 10 min at RT to allow the cells to lyse. A volume of 20 ml solution III (3 M sodium acetate, pH 5.2) was added to the lysed cells and mixed gently by inversion (ca. 25 times). The tube containing the lysate was incubated for 10 min on ice and thereafter centrifuged for 15 min at 3500 x g at 4°C. The supernatant was filtered through 4 layers of Miracloth (Calbiochem, Germany). Isopropanol (0.6 volume of the supernatant) was added to the filtered supernatant and mixed gently by inversion (ca. 50 times). The tube was incubated for 10 min at RT and thereafter centrifuged for 20 min at 3000 x g at RT. The supernatant was discarded. The pellet was resuspended in 3 ml TE (10 mM Tris, pH 7.6; 1 mM EDTA). Three millilitres of pre-chilled 5 M LiCl was added to the resuspended DNA. The tube was centrifuged for 30 min at 3500 x g at 4°C. The pellet was discarded and the supernatant transferred to a fresh 2 ml Eppendorf tube. An equal volume of isopropanol was added to the supernatant and mixed well by inversion (ca. 25 times). The tube was centrifuged for 30 min at 3500 x g at RT. The supernatant was discarded. The DNA pellet was washed with 70% EtOH, air-dried (ca. 10 min) and thereafter resuspended in 600 µl TE supplemented with RNaseA (20 $\mu g.ml^{-1}$) by incubation for 2 h at 37°C. Four hundred microlitres of PEG 8000 (BDH, UK) was added and mixed gently by

inversion. The tube was incubated for 10 min on ice and thereafter centrifuged for 5 min at 12000 x g at 4°C. The DNA pellet was resuspended in 400 µl TE buffer.

Two hundred microlitres of phenol/chloroform (1:1) was added to the plasmid DNA. The tube was vortexed for 30 s and thereafter centrifuged for 5 min at 11000 x g at RT. The upper aqueous phase was removed and transferred to a fresh Eppendorf tube containing 200 µl chloroform. The tube was mixed gently by inversion (ca. 50 times) and thereafter centrifuged for 5 min at 11000 x g at RT. The upper aqueous phase was removed and transferred to a fresh Eppendorf tube. Ammonium acetate (0.25 volumes; 10 M, pH 7.5) and 100% EtOH (2 volumes) were added to the aqueous solution. The contents were mixed gently by inversion and incubated for 10 min at RT to allow the DNA to precipitate. The DNA was pelleted by centrifugation for 5 min at 12000 x g at 4°C. The DNA pellet was washed with 70% EtOH, air dried (ca. 10 min) and thereafter resuspended in 50 µl Tris (pH 7.5).

3.2.6.3 Protoplast generation and transformation

The *A. thaliana* plants were grown in soil culture according to the procedure of Horling et al. (2003). Growth conditions included light at 120 µmol quanta $m^{-2}.s^{-1}$, 60% relative humidity, temperature at 20°C, and a daily photoperiod of 12 h duration. Rosette leaves from 3-5 week old *A. thaliana* plants were used for protoplast transformation. Protoplasts were isolated from *A. thaliana* and transformed with 60 µg of plasmid DNA according to the procedure described by Kluge et al. (2004).

3.2.6.4 Confocal microscopy of YFP fusion protein

Transformed *A. thaliana* protoplasts were observed using confocal microscopy as described by Kluge et al. (2004).

3.3 RESULTS

3.3.1 TOPO expression of XvPrx2 and XvV76C

The XvPrx2 and XvV76C genes were successfully cloned into pCR-T7-TOPO. For protein expression of XvPrx2 and XvV76C from *E. coli* BL21pLysS cells, good expression yields were obtained. The proteins XvPrx2 and XvV76C were observed to be induced 5 h post-IPTG addition. Expression yield was higher for XvV76C than XvPrx2 (Fig. 3.2) and was observed in three independent experiments. A protein band of ca. 22 kDa was observed for both XvPrx2 and XvV76C expressed cells. Both 22-kDa bands were accompanied by second fainter bands with the latter appearing at ca. 24 kDa. Another ca. 14-kDa protein band was observed in both samples but only in the lysed supernatant (Fig. 3.2).

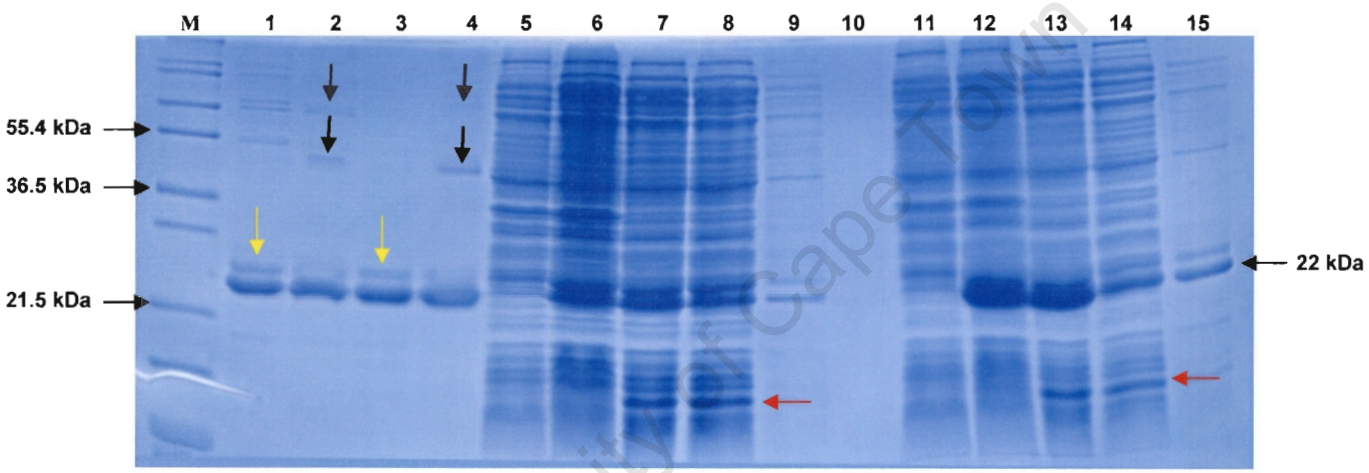

Figure 3.2 Purified protein (lanes 1-4) and expression samples (5-15) of XvPrx2 (1, 2, 5-10) and XvV76C (3, 4, 11-15). Arrows: (black) dimer and trimer forms of the protein; (yellow) 24-kDa protein band; and (red) 14-kDa protein band evident in lysed cells. Lanes: (M) M12 marker; (1) XvPrx2 pure protein + 10mM DTT; (2) XvPrx2 pure protein; (3) XvV76C pure protein + 10 mM DTT; (4) XvV76C pure protein; (5) un-induced sample; (6) induced sample; (7) lysate sample; (8) pre-wash sample; (9) wash one sample; (10) wash two sample; (11) un-induced sample; (12) induced sample; (13) lysate sample; (14) pre-wash sample; and (15) wash one sample.

The concentration of the purified XvPrx2 and XvV76C proteins were 0.85 and 1.2 $mg.ml^{-1}$, respectively. Following purification the 14-kDa band present in the lysed supernatant was no longer visible in the purified extract. Two protein bands of ca. 44 kDa and 66 kDa were visible in the purified extract. Few contaminating protein bands were also visible on the SDS PAGE gel. This was especially evident for the XvPrx2 preparation in which a few high molecular weight bands were observed. In the presence of 10 mM DTT, the 44- and 66-kDa bands were no longer visible, however, the ca. 24-kDa band was more evident. The same observations were made for the XvV76C purified protein.

3.3.2 Baculovirus expression of XvPrx2

The *XvPrx2* gene was successfully cloned into pFastBac1. Purification of XvPrx2 protein was successful with ca. 0.25 $mg.ml^{-1}$ protein obtained. For the XvPrx2 purified protein, a distinct band was observed at ca. 22 kDa (Fig. 3.3A), which is the expected size of this protein. Additionally, a lighter band was observed at ca. 44 kDa, which would correspond to the dimeric protein size. When DTT was added to the purified protein (XvPrx2) the 44-kDa band was no longer visible (Fig. 3.3B). The pure protein was obtained with few faint high molecular weight bands, which could be due to either the dimer not being fully reduced or the presence of contaminating bands.

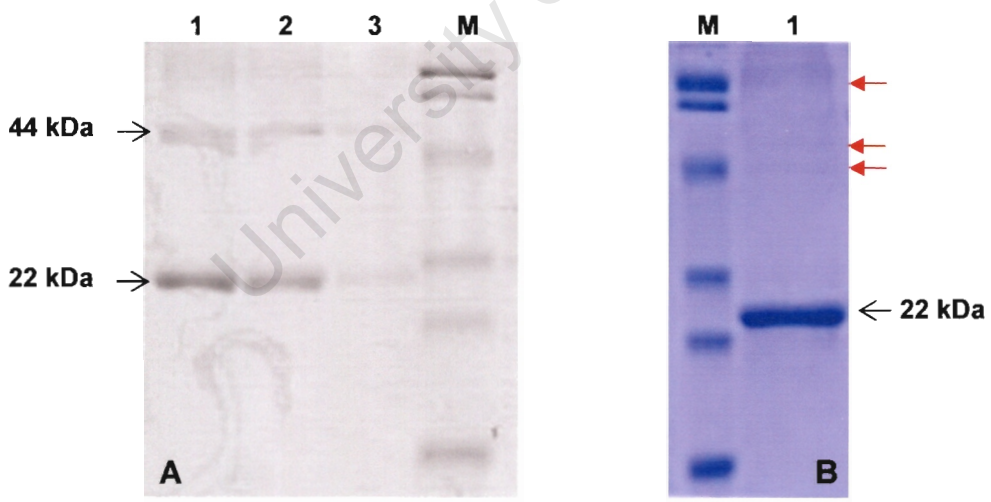

Figure 3.3 SDS-PAGE electrophoresis of purified XvPrx2 expressed from baculovirus infected insect cells. For untreated purified protein (A) both the monomeric (22 kDa) and the dimeric (44 kDa) forms were observed (lanes 1-3). When purified protein was treated with DTT (B), a single 22-kDa monomer was observed (lane 1). Red arrows indicate additional faint bands. (M) represents the Biorad marker.

Prior to concentrating the XvPrx2 protein a lower yield of protein was observed compared to the yield obtained for XvV76C. Attempts to concentrate the purified XvPrx2 protein from baculovirus were not successful with a low protein concentration obtained. It was assumed that protein was lost during the concentration process. Therefore, this expression system was not pursued further.

3.3.3 Expression of XvPrx2 using the pProEx system

The cloning of the *XvPrx2* gene into pProExA, B, C using the LoxP recombination system was successful. Sequencing showed that the gene was in frame in pProExB, consequently the other two constructs were used as negative controls.

Low expression yields were obtained for XvPrx2 (Fig. 3.4). Protein bands were not discernible on a SDS PAGE gel but were observed following western blot analysis (section 3.3.4.2). This expression system was not pursued further.

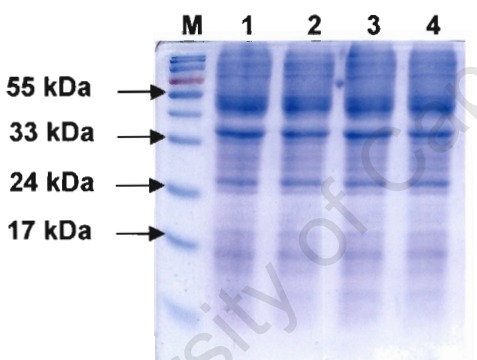

Figure 3.4 SDS PAGE electrophoresis of total protein from *E. coli* using pProExB::XvPrx2. Lanes: (M) Fermentas Page Ruler pre-stained protein ladder; (1) un-induced sample; (2) 1 h post induction sample; (3) 2 h post induction sample; and (4) 4 h post induction sample.

3.3.4 Antibody generation, western blotting and immuno-detection

3.3.4.1 Antibody generation

One hundred and fifty millilitres of XvPrx2 antibody as well as 5 ml pre-immune serum were obtained from rabbit bleeds. Minimal cross reactivity was observed using the latter. The XvPrx2 antibody cross reacted strongly with purified XvPrx2 proteins. The XvPrx2 antibody displayed minimal cross reactivity with other proteins, indicating that the XvPrx2 antibody was specific to purified XvPrx2 protein. However, when testing cross reactivity against similar type II Prx proteins, XvPrx2 antibodies did cross react with these homologues to a lesser extent (see Chapter 4).

3.3.4.2 Western blotting

Western blot analysis of purified proteins from the TOPO and baculovirus system revealed two bands at ca. 22 kDa and 44 kDa. No non-specific banding was observed indicating that the antibody was quite specific and that the protein isolated was quite pure.

The probing of XvPrx2 antibody against lysed bacterial cells using pProEx expression pointed to the presence of numerous contaminating proteins (Fig. 3.5). Using anti-His antibodies both the monomeric as well as the dimeric forms of XvPrx2 were observed. Since anti-His antibodies recognise multiple histidine sequences, non-specific cross reactivity was expected. The multiple bands observed could also be attributed to using a less sensitive detection method (chromogenic detection). Although expression was observed, quality and quantity of protein were low and consequently the pProEx expression system was not pursued further.

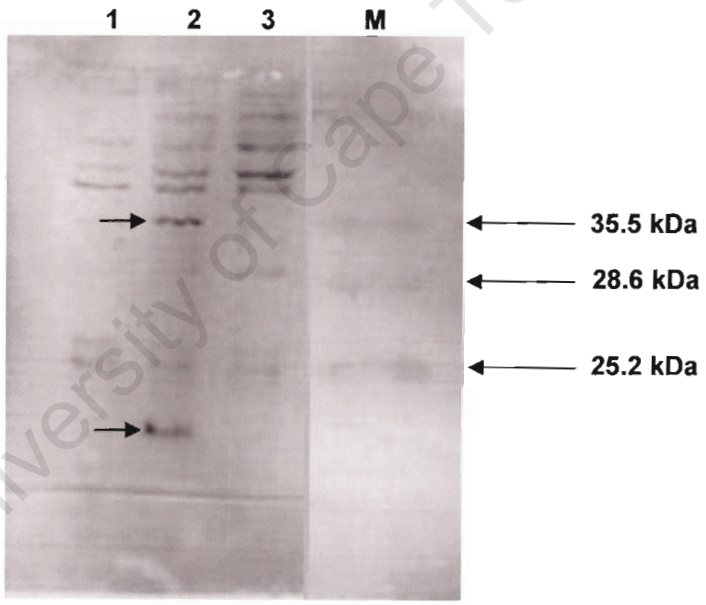

Figure 3.5 Western blot analysis of *E. coli* total protein following pProEx induction of XvPrx2. Lanes: (M) Biorad marker; (1) pProExA; (2) pProExB; and (3) pProEx C induction of XvPrx2 in *E. coli* cells.

Western analysis was also performed on total protein isolated from *X. viscosa* and *A. thaliana* plants. The XvPrx2 antibodies bound strongly to type II Prx in *X. viscosa* as well as *A. thaliana*. The XvPrx2 antibodies cross reacted with a 17.5-kDa protein from both *X. viscosa* and *A. thaliana* total protein (Fig. 3.6A) the size of which corresponds to the XvPrx2 native protein. A dimer of ca. 35 kDa was also visible for both samples. A second less intense band was also evident slightly higher than the 35-kDa protein. This band was more pronounced in the *A. thaliana* sample. The cross reactivity of XvPrx2 antibodies was more intense against the *X. viscosa* 17.5- and 35-kDa protein bands when compared to the *A. thaliana* proteins probably due to the higher specificity of the antibody to the *X. viscosa* protein.

Cross reactivity analysis was also performed using two other purified proteins from *X. viscosa* (viz. XvAld1 and XvPer1). The XvPrx2 antibodies did not display any cross reactivity with either XvAld1 or XvPer1 (Fig. 3.6B).

Figure 3.6 Autoradiograph of total protein from *X. viscosa* (lane 1) and *A. thaliana* (lane 2) probed with XvPrx2 antibodies (A). Western analysis of various protein extracts using PtPrxII antibodies (B). Lanes: (M) Biorad Marker; (1, 2) blank; (3) elution 2 (1st purification from baculovirus expression system); (4) Aldose reductase (XvAld1); (5) 1-Cys Peroxiredoxin (XvPer1); (6) Pure XvPrx2 protein from baculovirus expression system before concentrating; (7) pure XvPrx2 protein from baculovirus expression system after concentrating; and (8) blank.

3.3.5 Immuno-cytochemical localisation of XvPrx2

For immuno-cytochemical studies using both XvPrx2 and AtPrxIIC antibodies, signals were observed only in the stromal region of the chloroplast. When cross sections of *X. viscosa* leaves were probed with pre-immune serum, no labelling was observed (Fig. 3.7A). High amounts of immuno-gold labelling were observed localised to the stromal region of the chloroplast when cross sections of *X. viscosa* leaves were probed with XvPrx2 antibodies (Fig. 3.7B). High amounts of immuno-gold labelling were observed localised to the stromal region of the chloroplast when cross sections of ABA treated *X. viscosa* leaves were probed with PtPrxII antibodies (data not shown).

Minimal immuno-gold labelling was observed in the chloroplast when cross sections of *A. thaliana* leaves were probed with pre-immune serum (Fig. 3.7C). For XvPrx2 antibodies probed against *A. thaliana* leaf sections increased labelling was observed localised to the chloroplast (Fig. 3.7D). The labelled particles visible in the chloroplast however, were fewer when compared to XvPrx2 antibodies probed against *X. viscosa* leaf material.

No immuno-gold labelling was observed when cross sections of *X. viscosa* leaves were probed with pre-immune serum (Fig. 3.7E). For AtPrxIIC antibodies probed against *X. viscosa* leaf cross sections low levels of immuno-gold labelling was observed localised to the chloroplast (Fig. 3.7F).

No immuno-gold labelling was observed in any subcellular compartment when cross sections of *X. viscosa* roots were probed with XvPrx2 antibodies (data not shown).

For all immuno-gold analyses XvPrx2 antibodies cross reacted highly with protein in the chloroplast of *X. viscosa* and to a lesser extent with the protein in the chloroplast of *A. thaliana* leaf sections. Similarly AtPrxIIC reacted to a lesser extent (i.e. lower amount of gold labelling) to the protein in the chloroplast of *X. viscosa* leaf sections. No labelling was observed in the cytosol or any other cell compartment.

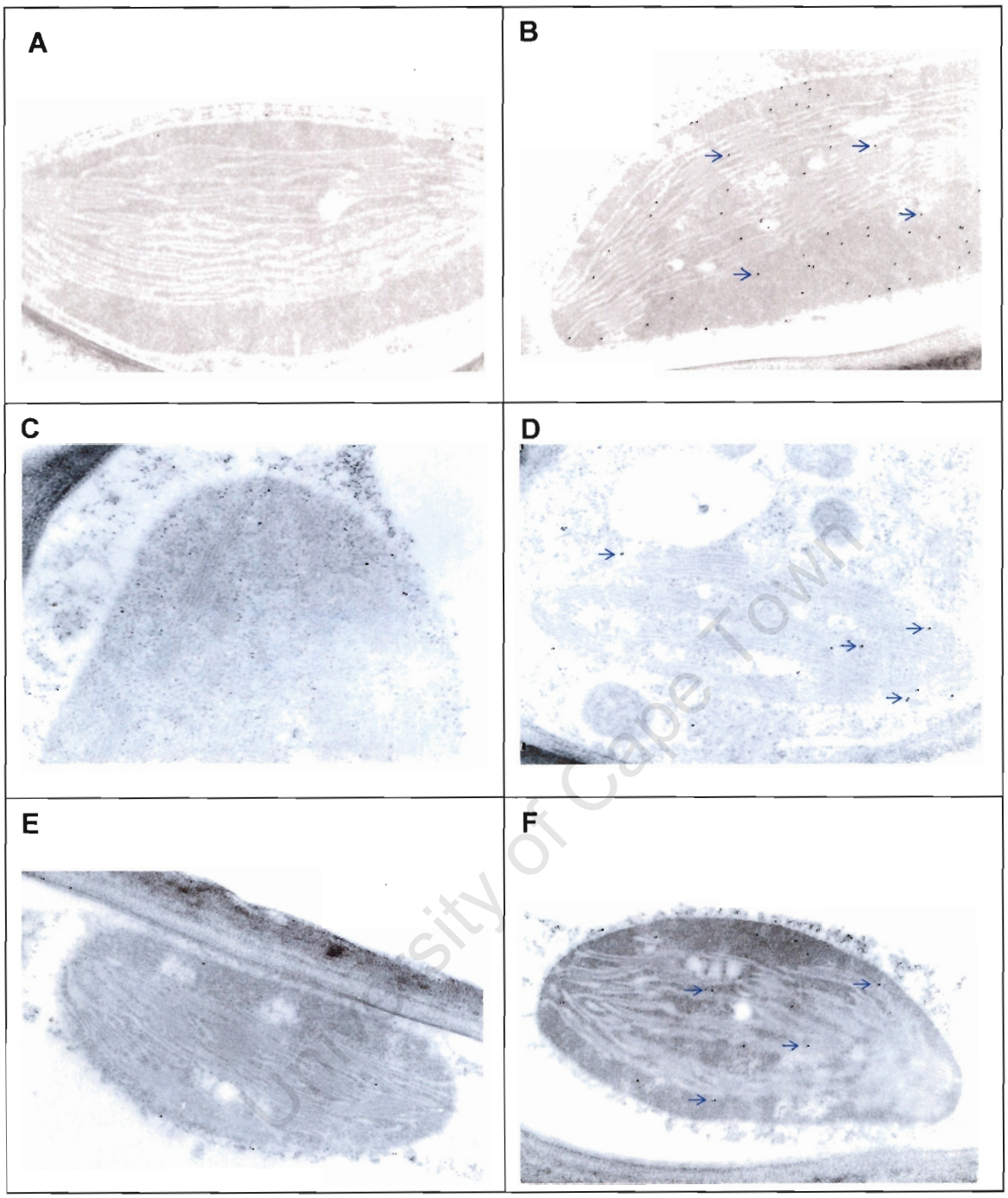

Figure 3.7 Electron micrographs of non-stressed *X. viscosa* leaf sections displaying immuno-gold localisation of XvPrx2 using antibodies generated against XvPrx2 and AtPrxIIC. Only the chloroplasts are shown. Pre-immune sera (A, C) and XvPrx2 antibody (B, D) probed against *X. viscosa* (A, B) and *A. thaliana* (C, D) leaf sections. Pre-immune sera (E) and AtPrxIIC antibody (F) probed against *X. viscosa* leaf sections.

3.3.6 YFP localisation of XvPrx2 using *Arabidopsis thaliana* protoplasts

PCR amplification of the 35S promoter, *XvPrx2* gene and nos_{term} was successful. No non-specific amplification was observed and all three were cloned into the new pEYFP construct. Colony PCR revealed that 2 out of 10 colonies screened contained the 35S promoter, *XvPrx2* gene and nos_{term} inserts of the appropriate sizes (ca. 680, 490 and 300 bp, respectively).

Large scale plasmid DNA extraction of the 35S::*XvPrx2*::YFP::nos_{term} construct, ABI5::YFP construct and pEYFP vector produced purified plasmids of high purity and concentration. The $A_{260/280}$ ratios were 1.85, 1.88 and 1.89 and the concentrations 55, 28 and 45 $\mu g.\mu l^{-1}$, respectively.

Once isolated, protoplasts were viewed under the light microscope and most were intact, indicating successful preparation. Both fluorescent and confocal microscopy were performed to determine the subcellular localisation of XvPrx2 (Fig. 3.8). Confocal microscopy appeared to provide a sharper image than fluorescent microscopy. The control ABI5-YFP fusion construct was observed to produce fluorescence in the nucleus only (Fig. 3.8A, B). In contrast, cells transformed with the construct encoding the XvPrx2-YFP fusion protein exhibited fluorescence exclusively to the cytosol (Fig. 3.8C, D). Protoplasts prepared from cells transformed with the pEYFP vector displayed YFP fluorescence (green colour) through the entire cell (in the nucleus as well as cytosol; Fig. 3.8E, F). The chloroplasts were also observed to display fluorescence due to auto-fluorescence of chloroplast pigments and was observed as red fluorescence (Fig. 3.8). Untransformed protoplasts were observed as red circular structures.

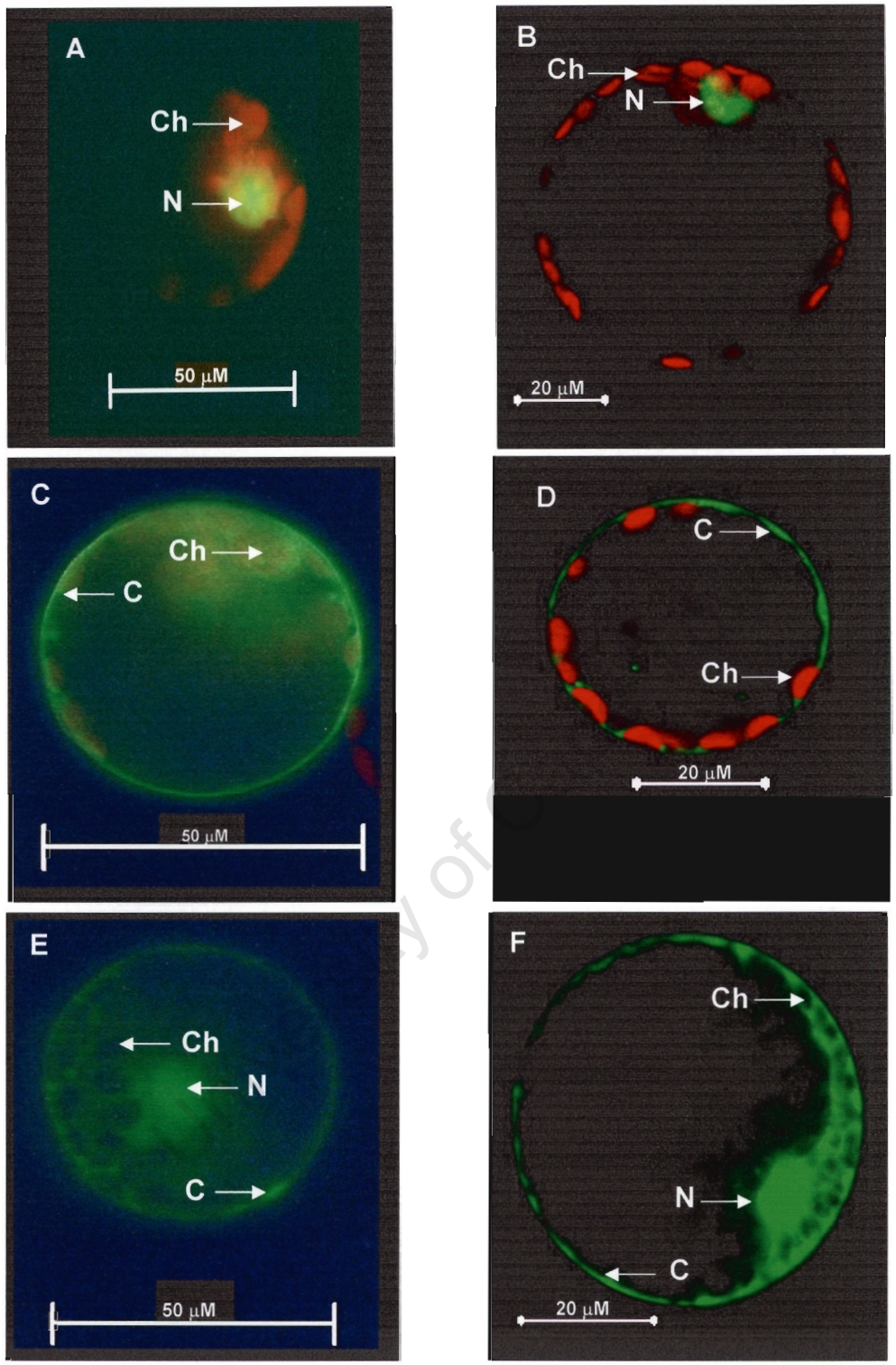

Figure 3.8 Microscopy images of *A. thaliana* protoplasts. Both fluorescent (A, C, E) and confocal (B, D, F) microscopy were used to determine the subcellular localisation of XvPrx2 in *A. thaliana* protoplasts. Images: (A, B) ABI5::YFP fusion protein; (C, D) XvPrx2::YFP fusion protein; and (E, F) YFP protein. Ch, chloroplast; N, nucleus; and C, cytosol. The excitation of YFP in a protoplast at 514 nm and emission at 520-570 nm is depicted by green signals. Autofluorescence of the chloroplast is represented by red signals.

3.4 DISCUSSION

Three different methods of XvPrx2 expression were employed in this study with only the TOPO system providing suitable results. Expression and purification of XvPrx2 from a litre of media yielded a very high protein concentration (ca. 1.2 $mg.ml^{-1}$), suitable for the generation of antibodies, for biochemical analyses and structural biology studies (Chapter 5).

Expression and affinity-tagged purification of proteins is one of the primary means of obtaining large quantities of recombinant proteins in a purified form. Commonly used affinity tags include poly-histidine (His-tag), glutathione-s-transferase, maltose binding protein and calmodulin. Among these tags, the His-tag is the most widely used and has several advantages including:

(i) it is small in size thus less immunogenically active, and often it does not need to be removed from the purified protein for downstream applications;

(ii) the availability of a large number of commercial vectors for expressing His-tagged proteins;

(iii) the tag may be placed at either the N or C terminus; and

(iv) the interaction of the His-tag does not depend on the tag structure making it possible to purify otherwise insoluble proteins using denaturing conditions.

The affinity interaction that serves as the basis for His-tag purification is believed to be a result of the co-ordination of nitrogen on the imidazole moiety of poly-histidine with a vacant co-ordination site on the metal. The metal, in most cases nickel, is immobilised to a support through complex formation with a chelate that is covalently attached to the support.

Proteins expressed using all 3 systems were purified using the His-tag system. For the TOPO system, which produced the highest yield, a high concentration (>1 $mg.ml^{-1}$) was obtained following purification. The His-tag fused to XvPrx2 was not cleaved following purification and was used successfully in this form for antibody synthesis, biochemical analyses and structural work. For western analyses (Chapters 3 and 4) non-specific binding to unrelated proteins was not observed indicating that the antibodies produced were not immunologically active against the His-tag. For the biochemical analyses (Chapter 5) it could be speculated that the His-tag would not affect the protein's activity due to its very small size.

For SDS gel electrophoresis the purified XvPrx2 protein was initially boiled and then electrophoresed on a denaturing gel. Under these conditions the purified protein was considered to be denatured. Denaturation of proteins involves the disruption and possible destruction of both the secondary and tertiary structures. Since denaturation reactions are not strong enough to break the peptide bonds, the primary structure remains the same after a

denaturation process. Denaturation disrupts the alpha-helices and beta sheets in a protein and uncoils it into a random shape. Denaturation occurs because the bonding interactions responsible for the secondary structure (hydrogen bonds to amides) and tertiary structure are disrupted. Within tertiary structures there are four types of bonding interactions between "side chains" including: hydrogen bonding, salt bridges, disulphide bonds, and non-polar hydrophobic interactions, which may be disrupted. Consequently, the formation of XvPrx2 homodimers were not expected. However, the formation of these dimers could be due to high thermostable properties, which would ensure that the tertiary structures remain intact after boiling.

For the XvPrx2 and XvV76C purified proteins, a distinct band was observed at the expected size of ca. 22 kDa. The recombinant protein was larger than the native protein (17.5 kDa) due to the His-tag fusion. Additionally, a lighter band was observed at ca. 44 kDa, which probably corresponds to the dimeric protein size (Fig. 3.9). The high molecular bands namely, 44-, 66- and 88-kDa bands, were observed during western analyses using XvPrx2 antiserum. However, these high molecular weight proteins were omitted from the study due to them being non reproducible. The formation of the dimer though unexpected has been reported previously (Brehelin et al., 2003) and is possibly due to very strong tertiary interaction. When DTT was added to the purified protein (XvPrx2 and XvV76C) the faint band at 44 kDa was no longer visible. Furthermore, a faint band at ca. 24 kDa became visible in these DTT treated samples.

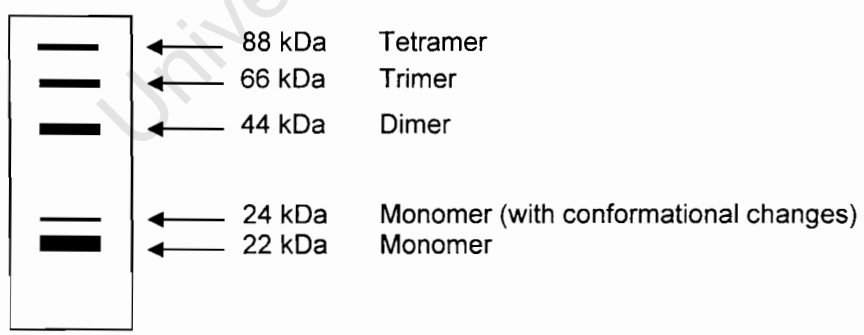

Figure 3.9 Illustration of banding pattern observed for XvPrx2 and XvV76C purified protein.

A strong reducing agent like β-mercaptoethanol has been shown to reduce the dimer to the monomeric form. Such treatments do not depend on the proteins thermostability but rather on specific chemical interaction. For purified XvPrx2 and XvV76C reducing equivalents such as β-mercaptoethanol and DTT were shown to reduce the amount of dimer (44 kDa) with an

increase in the amount of the 24-kDa protein. In other studies the doublet protein band (i.e. 24 kDa) in the region of the monomer (i.e. 22 kDa) are considered to be the reduced and oxidised forms of the protein, respectively. In the current study, the effect of the reductant was not always apparent as the dimer was observed in most stress treatments even in the presence of the reductant (Chapter 4). This points to the protein being resistant to chemical denaturation to a certain extent. Obviously this resistance to chemically induced denaturation would be related to the actual reductant used. For some stress treatments the trimer and tetramer forms were also evident. For these studies, the dimer, trimer and tetramer bands were excluded from western analyses as the expression of the monomeric protein only was considered.

Previously Horling et al. (2002) reported that AtPrxIIB and C were only detected in the monomeric form irrespective of the reduction state of the protein. However, in comparison with the reduced form, the oxidised type II revealed a slightly increased electrophoretic mobility, which is likely to reflect the intramolecular formation of the disulphide bridge with an accompanying change in conformation. Substrate dependent dithiol-disulphide transition involving the cysteine group in the active site of Prx induces major conformational changes with concomitant modification of quaternary structure and an electrophoretic mobility shift (Horling et al., 2002; König et al., 2003). Finkemeier et al. (2005) reported that for type II Prx, the formation of an intramolecular disulphide bond could be observed, while 2-Cys Prx form intermolecular dimers. For a recombinant AtPrxIIF both forms were observed, similar to results obtained by Brehelin et al. (2003). Finkemeier et al. (2005) also report that oxidation with H_2O_2 produced a band shift after loading recombinant AtPrxIIF on a SDS PAGE gel. At lower H_2O_2 concentrations the formation of the intramolecular disulphide bridge was predominantly observed, which could be distinguished from the reduced form by its slightly increased electrophoretic mobility. At higher H_2O_2 concentration the presence of the dimeric form increased.

Antibodies targeted to XvPrx2 were successfully generated in this study. Antibodies targeted to a specific protein are useful in localisation studies and in western expression analyses. The antibodies generated in this study were relatively specific for XvPrx2. However, it appears that type II Prx homologues display similar immunological properties. Hence the antibody was observed to bind to XvPrx2 and its homologues in both *X. viscosa* and *A. thaliana*. These proteins of 17.5 kDa and of 35 kDa correspond to the native type II Prx monomer and dimer. This is in contrast to Brehelin et al. (2003) who reported that type II dimers were not detected in crude plant extracts under non-reducing conditions by western blot using sera raised against AtPrxIIB or AtPrxIIE.

The XvPrx2 antibodies did not cross react with a 1-Cys Prx (XvPer1) nor to an unrelated protein (XvAld1). They did, however, cross react with the type II Prx orthologues from *A. thaliana* total protein as well. This is probably due to the fact that XvPrx2 shares 75% homology at the amino acid level with certain *A. thaliana* type II Prxs. It can be deduced that XvPrx2 is not immunologically related to 1-Cys Prxs, however, common immunological properties between type II homologues and orthologues appears to be the norm. This could be due to the antigenic site/s occurring within conserved regions, which would be the most probable scenario.

Sequence alignment and homology analyses of XvPrx2 point to the protein being closely related to AtPrxIIB, which is localised to the cytosol (Brehelin et al., 2003). Furthermore, analysis of the amino acid sequence of XvPrx2 revealed that it has no upstream signal peptide. The assumption that a protein lacking a transit sequence is localised to the cytosol is not always absolutely safe since an immuno-localisation study on a type II Prx from poplar (with identity to a cytosolic type II Prx from *A. thaliana*) was found to be localised in plastid-like structures contained in phloem sieve tubes (Rouhier et al., 2001). Two different localisation studies were carried out to elucidate the subcellular localisation of XvPrx2. The first involved performing immuno-gold labelling on ultrathin *X. viscosa* leaf sections using XvPrx2 antibodies. The second method involved the use of a reporter gene, *yfp* fused to *XvPrx2*.

Immuno-gold labelling studies point to XvPrx2 being localised to the chloroplasts of *X. viscosa* cells. The labelling was strongest in the stroma of the chloroplast in both non-stressed and ABA stressed leaf material, which is contrary to the expected cytosolic localisation. However, it has been demonstrated that XvPrx2 antibodies are able to cross react with type II homologues. Therefore, it is plausible to argue that the antibodies cross reacted with the most abundant type II Prx homologue, which would probably be present in the chloroplast. The type II Prx homologue in the chloroplast may be expressed to a greater extent due to the continuous generation of ROS in this organelle, especially during abiotic stress. Cross reactivity between AtPrxIIC (localised to the cytosol) and AtPrxIIE (localised to the chloroplast) has been observed in immuno-gold labelling of cross sections of *A. thaliana* leaf material (Dietz, 2003). However, studies performed by Brehelin et al. (2003) indicate that serum raised against AtPrxIIB can recognise at least 5 ng of recombinant AtPrxIIB but does not show any signal with up to 80 ng of AtPrxIIE (the recombinant protein of AtPrxIIE was generated omitting the 5' signal peptide). It was concluded that AtPrxIIB serum does not recognise AtPrxIIE but it was assumed that it would detect AtPrxIIC and D as well as

AtPrxIIB because of the high similarity between the proteins. Horling et al. (2002) showed that serum raised against recombinant AtPrxIIC recognised recombinant AtPrxIIC and B. The antibodies generated against AtPrxIIE antibodies (Brehelin et al., 2003), however, cross reacted with 20 ng of AtPrxIIB purified proteins. The XvPrx2 antibody does not seem to be sufficiently specific to distinguish between XvPrx2 homologues in *X. viscosa* and hence was not suitable for the localisation of XvPrx2 using the immuno-gold method.

The cloning of *XvPrx2* into a suitable vector containing both a 35S promoter as well as a *nos* terminator was complicated. However, successful cloning was achieved. The resultant construct was transformed into *E. coli* cells and large scale plasmid preparation performed to obtain high plasmid yield since protoplast transformation requires at least 20 µg of purified plasmid DNA. Intact protoplasts were transformed and used for YFP localisation experiments.

To the best of our knowledge, this is the first report of the use of YFP technology on intact protoplasts for the localisation of a type II Prx from *X. viscosa*. These studies were carried out to prove that XvPrx2 is localised to the cytosol and not the chloroplast. This would represent a more specific method in that XvPrx2 is directly expressed from the YFP vector and localised to a specific compartment within the protoplast. The only negative aspect of this type of localisation is that it is studied in *A. thaliana* and not *X. viscosa* protoplasts.

Haslekas et al. (2003a) reported that in the onion epidermis transient expression assay, GFP::AtPER1 fusion protein was localised to the cytosol and nucleus. The signal distribution of the fusion protein was similar to that of GFP, which does not contain a nuclear localisation signal. The partial nuclear localisation of GFP is caused by bi-directional diffusion through the nuclear pore complex (von Arnim et al., 1998). Haslekas et al. (2003a) therefore used a known nuclear localised protein, Heterochromatin Protein 1 (HP1) from *Drosophila melanogaster*. In this study a similar result was obtained with YFP in which the expressed protein was found in the cytosol and in the nucleus. Therefore YFP-ABI5, an *A. thaliana* transcriptional factor known to be localised to the nucleus (Lopez-Molina et al., 2003), was used as a control. Results obtained for the YFP::*XvPrx2* construct confirmed that XvPrx2 is localised to the cytosol of transformed protoplasts.

The YFP localisation conform with the expected result and appear to be a more appropriate method to determine localisation of type II Prxs (Fig. 3.10), which generally possess many homologues (as can be seen in *Arabidopsis* the percentage identity between the three cytosolic type II Prxs is 97.7%). The Southern blot (Chapter 2) and 2-D gel analyses (Chapter 4) confirm that there are potentially multiple type II Prx homologues present in *X. viscosa*.

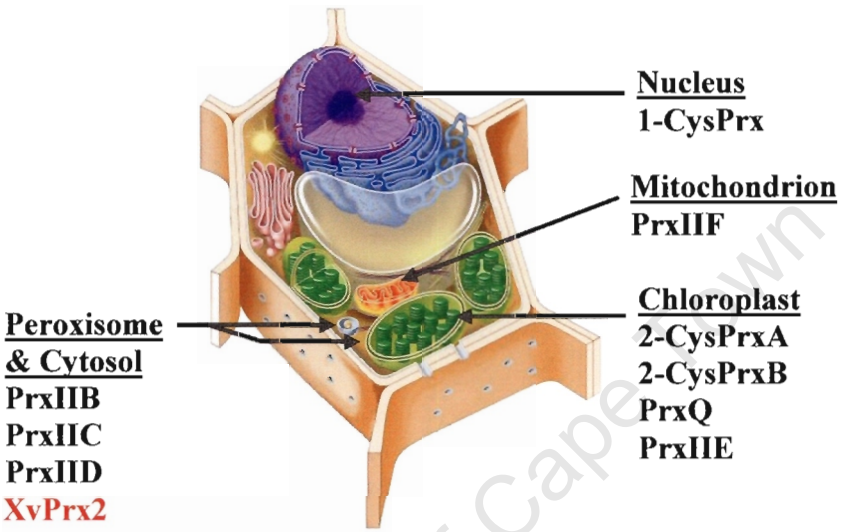

Figure 3.10 Illustration of a plant cell showing the subcellular localisation of the various *A. thaliana* Prxs and XvPrx2.

The proposed subcellular localisation of XvPrx2 (Fig. 3.10), a type II Prx, in the cytoplasm indicates a role for scavenging ROS that are produced in the cytosol due to enzymatic and non-enzymatic processes or the detoxification of ROS that leaches out from other organelles such as the photosynthetic apparatus or the nucleus. It would be important to know whether XvPrx2 is tissue specific, that is whether the protein is expressed in flowers, leaves, seeds and roots or if it is expressed in all tissues of *X. viscosa*. If this can be determined then one can speculate on the protein's function based on tissue specificity. This knowledge would be beneficial in providing a broader picture as to how resurrection plants cope with oxidative stress.

Chapter 4

Gene and protein expression analyses of XvPrx2

4.1 INTRODUCTION

According to Ramanjulu & Bartels (2002) there is increasing evidence indicating that genes responding to water stress can be categorised in two classes based on the time of their response. Some genes may respond immediately, within seconds or minutes, whilst others may respond later, in hours, days or even weeks. It appears that the early responsive genes may provide initial protection and amplification of signals while the genes that respond later may be involved in adaptation to stress conditions.

Transcripts of all *A. thaliana* Prx homologues have been detected in green tissues. Horling et al. (2002) noted that transcript abundance varied with the developmental stage of the tissue. Under normal conditions transcript levels differ considerably between the various Prx genes, and under stress conditions these differences become even more evident. The Horling et al. study highlighted these variations in transcript levels. The mRNA transcript levels of *AtPrxIIE* (chloroplastic) dropped to a low level within 2 h of transfer to a salt stress regime with no further decrease upon longer incubation. The expression of *AtPrxIIF* (mitochondrial) was not altered significantly upon salt stress treatment. In contrast, the amount of *AtPrxIIB* (cytosolic) increased slightly after 6-8 h of salinity stress with a drastic change in expression for *AtPrxIIC* (cytosolic). The *AtPrxIIC* mRNA level increased within 2 h with maximum transcript level being observed 6 h after start of the treatment.

In this chapter, the expression of an *X. viscosa* type II Prx (XvPrx2) is described at both the mRNA and protein levels under various artificially imposed abiotic stress conditions.

4.2 MATERIALS AND METHODS

4.2.1 Plant stress treatments

Plant treatments were performed in a phytotron at 25°C, 50% humidity, a photon flux density of 300 μmol.m^{-2}.s^{-1} and a day-night cycle of 16-8 h, unless otherwise stated. All plants except those that were dehydrated were kept well hydrated. Dehydration-rehydration, high light and temperature treatments were performed on whole plants, while salt and abscisic acid treatments were performed on excised leaves from healthy plants and on tissue culture plantlets. Leaf samples were prepared by cutting off 3-5 leaves from the treated plant and removing dried areas. The excised leaves were dissected into smaller pieces, wrapped in aluminium foil, flash-frozen in liquid nitrogen and subsequently stored at -70°C until RNA extractions were performed. Each treatment was performed in triplicate.

For the salt and abscisic acid treatments, the leaves of whole plants were placed under water and excised to prevent the intake of air-bubbles into the xylem. Immediately thereafter leaves were immersed in either 150 mM NaCl, 100 μM ABA or distilled water (control). For the NaCl and distilled water treatments, samples were harvested at 0, 6, 12, 24, 48, 72, 96 and 120 h. For the ABA treatment, samples were harvested at 0, 6, 12, 24, 48 and 72 h.

The NaCl and ABA treatments were also performed on tissue culture plantlets since the water control on excised leaves showed increased expression over time. Plantlets were placed in either hydroponic NaCl (150 mM), ABA (100 μM) or Murashige and Skoog medium (MS control; Highveld Biological, South Africa). The plantlets were acclimatised in a plant growth room with a day-night cycle of 16-8 h at 25°C, 50% relative humidity and a photon flux density of 150 μmol.m^{-2}.s^{-1}. For all 3 treatments, samples were harvested at 0, 12, 24 and 48 h.

Dehydration treatment was performed by withholding water from the plant over a period of 28 days, at the end of which the leaf RWC (relative water content) was ca. 5%. Leaf samples were harvested at RWCs of ca. 94, 74, 50, 35, 14, 7 and 5%. The dehydrated plant was watered daily once the RWC had reached ca. 5%. For the rehydration treatment, samples were harvested at ca. 34, 79 and 93% RWC. A second dehydration treatment was performed by withholding water from the plant over a period of 16 days. Root samples were harvested after 0, 10 and 16 days of dehydration.

High temperature treatment was performed by increasing the temperature in the phytotron to 42°C and maintaining all other parameters constant. Samples were harvested at 0, 6, 12, 24, 48, 72, 96 and 120 h. Low temperature treatment was performed in a 4°C chamber

with a photon flux density of 250 μmol.m^{-2}.s^{-1}. Samples were harvested at 0, 6, 12, 24, 48 and 72 h.

High light treatment was performed by increasing the photon flux density to ca. 1500 μmol.m^{-2}.s^{-1} and maintaining all other parameters constant. Samples were harvested at 0, 6, 12, 24, 48, 72, 96, 120, 144 and 168 h.

4.2.2 Relative water content and water potential measurements

The RWC and water potential (WP) were determined for leaf samples at each sampling time point for all treatments. The initial weight (W_{ini}) of each sample was determined prior to immersion in sterile distilled water. The weight at full turgor (W_{ft}) was determined following 24 h incubation in water. Leaf samples were dried for 2 days at 70°C prior to the dry weight (W_d) being determined. The formula described by Jin et al. (2000) was used to calculate the RWC:

$RWC = (W_{ini} - W_d) / (W_{ft} - W_d) \times 100.$

A thermocouple psychrometer (Aqualab 1.5; Decagon, USA) was used according to the manufacturer's instructions to estimate the WP of leaf samples for each sampling time point.

4.2.3 Northern blot analyses

Total RNA was extracted from treated leaf material according to the protocol described previously (section 2.2.2). The organic layer (crude protein extract) obtained after phase separation of Trizol treated leaf material was stored at -70°C for protein extraction. For each treatment, 10 μg of RNA obtained for each time point was electrophoresed on a 1.2% agarose/EtBr gel in separate but adjacent wells. On completion of electrophoresis the RNA was transferred by capillary transfer onto a nylon membrane and UV cross-linked onto the membrane.

A radio-labelled probe was prepared by PCR amplification of pDNR-Lib::*XvPrx2*. Primers used in the amplification procedure were XvPrx2-F (10 μM; Appendix B) and XvPrx2-R (10 μM; Appendix B). The reaction contained [α-^{32}P] dCTP at a concentration of 50 μCi. The PCR reaction was conducted using a Gene Amp 9700 thermal cycler with the following parameters: 95°C for 5 min; 15 cycles of 95°C for 30 s, 58°C for 1 min and 72°C for 10 min; and a final extension step at 72°C for 10 min. A longer extension time of 10 min was used to ensure that the 'heavier' radio-labelled dCTP would incorporate during amplification. Unincorporated nucleotides were removed by passing the PCR product through

a sephadex-G50 column. The specific activity of the labelled probe was determined in a scintillation counter by counting 1 µl of probe in 2 ml of scintillation fluid. The membrane was pre-hybridised in buffer (0.5 M NaH_2PO_4; 1 mM EDTA; 7% SDS; 1% BSA) for a minimum of 2 h at 65°C. Following pre-hybridisation, the radio-labelled probe was denatured by incubation for 10 min in a boiling water bath and immediately thereafter placed on ice. The denatured probe was added to pre-hybridisation buffer and hybridisation was carried out for 18 h at 65°C with gentle shaking. The membrane was washed once for 12 min at 65°C in Wash Buffer A (0.5% SDS; 2X SSC), followed by a second wash for 10 min at 65°C in Wash Buffer B (0.1% SDS; 0.5X SSC). The membrane was autoradiographed at -70°C onto Hyperfilm MP (Amersham Biosciences, USA). Following 3 days exposure, the film was developed manually using developer and fixer reagents (Amersham Biosciences, UK) according to the manufacturer's instructions.

4.2.4 Western blot analyses

For all leaf samples, the organic phase, containing total protein, retained during RNA extraction (see section 4.2.3) was used for protein extraction. Three hundred microlitres of cold 100% EtOH was added to the protein extract. The tube was inverted ca. 25 times, incubated for 5 min at RT and thereafter centrifuged for 10 min at 2500 x g. The supernatant containing soluble proteins was transferred to a fresh 2 ml Eppendorf tube containing 1.5 ml isopropanol. The soluble protein extract was incubated for 10 min at RT and thereafter centrifuged for 10 min at 10250 x g at 4°C. The protein pellet was washed thrice with 2 ml of 0.1 M ammonium acetate (prepared in 100% methanol), washed once with 2 ml cold acetone and thereafter air-dried for ca. 10 min. The pellet was resuspended in 5X SDS PAGE loading buffer (0.225 M Tris, pH 6.8; 50% glycerol; 5% SDS; 0.05% bromophenol blue; 0.25 M DTT).

For root material, total protein was isolated according to the protocol of Swidzinski et al. (2004) with a few modifications. Root material (ca. 0.1 g) was ground in liquid nitrogen using a mortar and pestle. The ground material was resuspended with agitation in 1 ml chilled extraction buffer (0.5 M Tris-HCl, pH 7.5; 10 mM EDTA; 1% Triton X-100; 2% β-mercaptoethanol). The sample was vortexed for 10 min and centrifuged for 5 min at 12000 x g. The supernatant was transferred to a fresh Eppendorf tube and centrifuged for 5 min at 12000 x g. The supernatant was transferred to a fresh Eppendorf tube and an equal volume of phenol (pH 8) was added to the tube. The sample was centrifuged for 1 min at 12000 x g. The upper aqueous layer was discarded. Extraction buffer (up to 1 ml) was added to the protein

sample (organic layer). An equal volume of phenol (pH 8) was added to the tube. The tube was centrifuged for 1 min at 12000 x g. The upper aqueous layer was discarded. Two and a half volumes of 0.1 M ammonium acetate (made up in methanol) was added to the protein solution (organic layer) and incubated for 16 h at -20°C. The pellet was washed once with 0.1 M ammonium acetate (prepared in methanol) and once with cold 80% acetone. The protein pellet was air-dried for 30 min, resuspended in Laemmli buffer (0.625 M Tris, pH 6.8; 2% SDS; 10% glycerol; 5% β-mercaptoethanol added fresh) and stored at -20°C.

Proteins isolated from *X. viscosa* leaf and root material were used for western blot analyses. The protein samples were quantified using Bradford Reagent (Biorad, Germany). For each treatment, 10 µg of total protein obtained for each sampling point was electrophoresed in separate but adjacent wells on a 12% polyacrylamide gel (standard PAGE conditions, Appendix A). Western blotting was performed according to the protocol described previously (section 3.2.4.2). Chemiluminescent detection was performed using XvPrx2 antiserum according to the protocol described previously (section 3.2.4.4).

4.2.5 Protein analysis by 2-D gel electrophoresis

Three *X. viscosa* leaves were excised from a healthy plant, ground in liquid nitrogen using a mortar and pestle and transferred equally into 4 Eppendorf tubes each containing 1 ml of 25 mM Tris (pH 7.5). The tubes were centrifuged for 10 min at 12000 x g at 4°C. The supernatants were removed and pooled in a fresh 10 ml Sterilin tube. Total protein was precipitated by the addition of 3 volumes cold 100% acetone. The sample was incubated for 16 h at -20°C and thereafter centrifuged for 10 min at 12000 x g at 4°C. The supernatant was discarded. The pellet was washed with 1 ml cold 100% acetone and thereafter centrifuged for 10 min at 12000 x g at 4°C. The supernatant was discarded. The protein pellet was air-dried for 5 min and thereafter stored at -20°C.

Two protein pellets were resuspended and pooled using 270 µl lysis buffer (8 M urea; 2% CHAPS; 40 mM Tris, pH 7.5). The protein sample was purified using the 2-D Clean-Up Kit (Amersham Biosciences, USA) according to the manufacturer's instruction. An aliquot was removed for quantification. Seventy microlitres of 1 M DTT and 17.5 µl IPG 4-7 (Amersham Bioscience, USA) were added to a 1 ml aliquot of rehydration buffer (8 M urea; 2% CHAPS; 0.05% bromophenol blue). One hundred microlitres of this mix was added to the protein sample in lysis buffer.

The IPGphor Isoelectric Focussing System (Amersham Biosciences, USA) was used for 2-D gel electrophoresis. The protein concentration was determined using the 2-D Quant Kit (Amersham Biosciences, USA) according to the manufacturer's instruction. The protein concentration was determined from the standard curve generated using the kit. Seven hundred micrograms of total protein was loaded into the porcelain chamber. The 1-D Immobiline Dry Strip (pH 4-7, 18 cm; Amersham Biosciences, USA) was placed over the protein sample and this was in turn overlaid with a thin layer of mineral oil to prevent drying. Isoelectric focusing was performed via step wise voltage increments from 50-8000 V until the total volt hours reached 35 kV.

The 1-D strip was placed in 10 ml equilibration buffer (6 M urea; 30% glycerol; 50 mM Tris, pH 6.8; 2% SDS; 0.05% bromophenol blue) containing 650 µl 1 M DTT (prepared fresh) and incubated for 10 min with shaking. A 12 % acrylamide gel was prepared (standard PAGE conditions, Appendix A). The strip was placed between the glass plates at the surface of the SDS PAGE gel. A marker lane was also prepared. Agarose (0.8%) containing bromophenol blue was poured over the strip and allowed to solidify for 30 min. The prestained SeeBlue marker (Biorad, Germany) was loaded into the marker lane using a Hamilton syringe. Protein samples were electrophoresed at 50 mA and thereafter blotted onto a nitrocellulose membrane (Osmonics, USA) according to the protocol described previously (section 3.2.4.2). The membrane was probed with XvPrx2 antiserum. Chemiluminescent detection was performed according to the protocol described previously (section 3.2.4.4).

4.3 RESULTS

4.3.1 Relative water content and water potential measurements

The RWC and WP of leaf tissue for all treatments performed on whole plants remained fairly constant in the 80-100% and 0 to -5 MPa range, respectively (Fig. 4.1). A notable exception was the dehydration treated material. For dehydration-rehydration treatment the RWC decreased from 94 to 5% and increased after watering to 93%. The water potential dropped from ca. -20 to -110 MPa and increased after watering to 0 MPa.

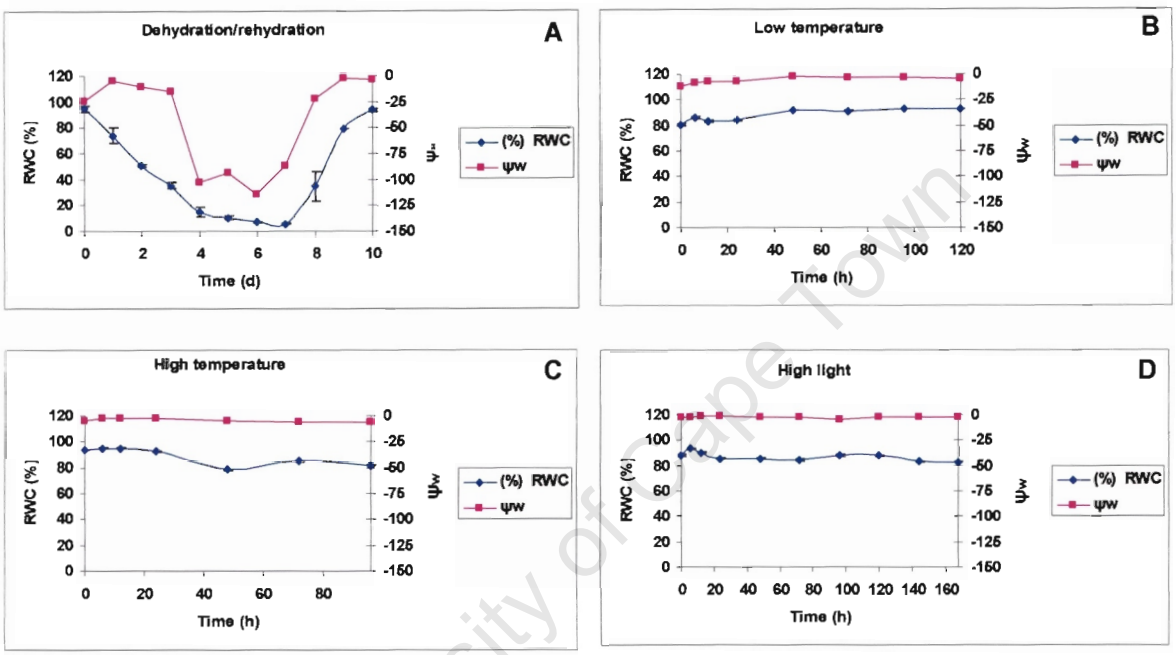

Figure 4.1 Relative water content and water potential data for abiotic stress treatments on whole plants (A-D). Treatments included: (A) dehydration-rehydration; (B) low temperature (4°C); (C) high temperature (42°C); and (D) high light (1500 $\mu mol.m^{-2}.s^{-1}$). Treatments were performed in triplicate. In most cases, the error bars (± standard error) are wholly contained within the symbol.

The RWC and WP data of leaf tissue for all treatments performed on excised leaves were observed to remain fairly constant in the 80-100% and 0 to -5 MPa range, respectively (Fig 4.2). For the tissue culture plantlets, the RWC and WP were observed to be lower compared to excised leaves (Fig. 4.2). For the NaCl treatment, there was no significant change in RWC, which remained in the 75-85% range. The WP, however, decreased to ca. -50 MPa following 24 h of NaCl treatment from a WP of ca. -20 MPa. For the ABA treatment, a significant shift in the RWC was observed with a decrease from 80% (0 h) to 42% (12 h) and a subsequent increase to above 95% (24-48 h). The WP remained unchanged at ca. -20 to -25 MPa.

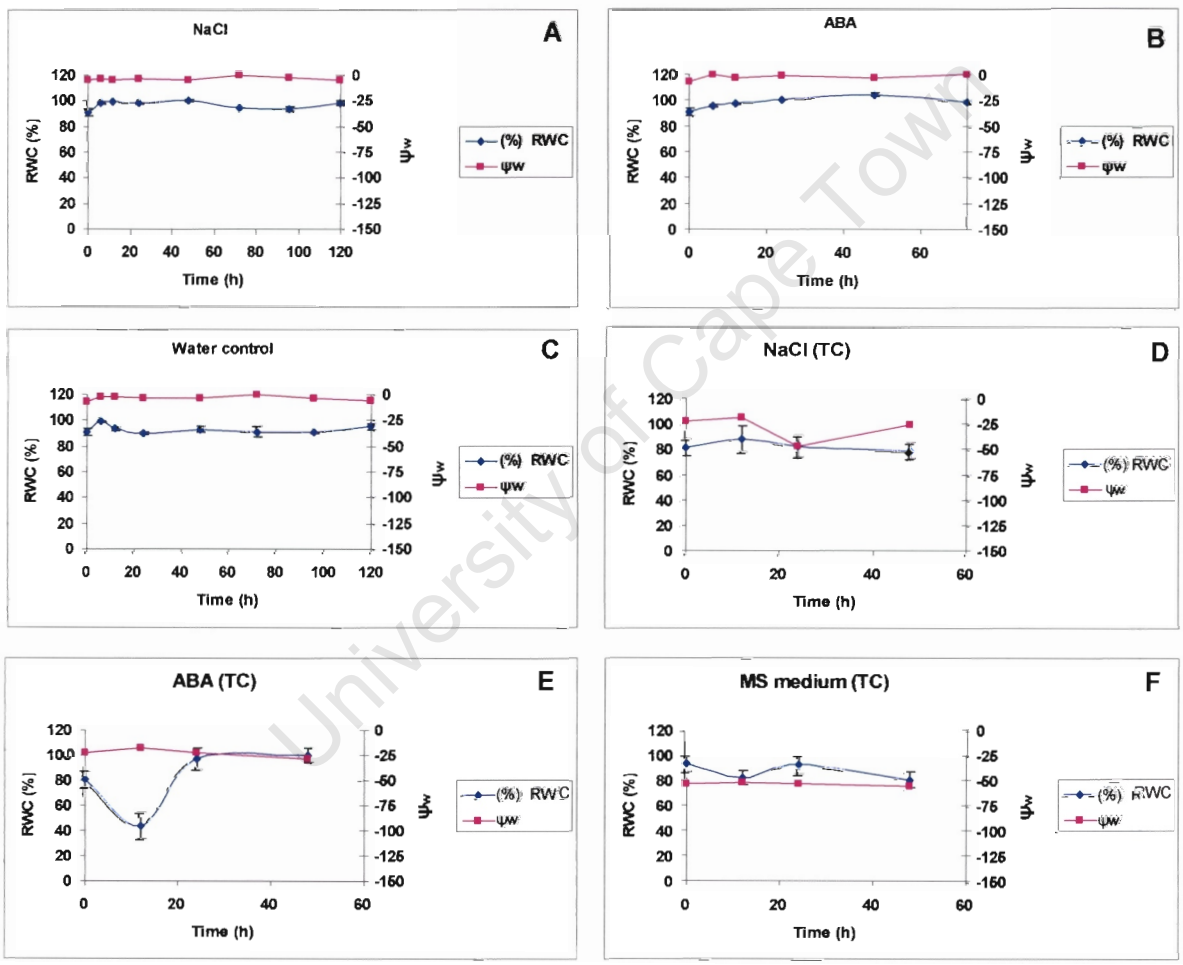

Figure 4.2 Relative water content and water potential data for abiotic stress treatments on both *X. viscosa* excised leaves (A-C) and tissue culture plantlets (D-F). Treatments included: (A, D) NaCl (150 mM); (B, E) ABA (100 µM); (C) water control; and (F) MS medium (control). Treatments were performed in triplicate. In most cases, the error bars (± standard error) are wholly contained within the symbol.

4.3.2 Northern blot analyses

An initial small scale northern blot analysis was performed to determine whether *XvPrx2* is stress inducible. During low temperature stress, the *XvPrx2* transcript remained constant during the first 48 h of stress, however, a significant increase in transcript level was evident after 120 h (Fig. 4.3). During the dehydration treatment, quantification of RNA was difficult as a difference in loading was observed. Even though no RNA was observed in the unstressed sample (0 h) following gel electrophoreses, a faint hybridisation signal was visible following autoradiography. The *XvPrx2* transcript was observed at 8 days dehydration whereas almost no transcript was visible from days 15-30. During the NaCl treatment, the *XvPrx2* transcript level increased after 12-48 h of salt stress with a maximum level observed at 24 h. These results point to *XvPrx2* being stress inducible.

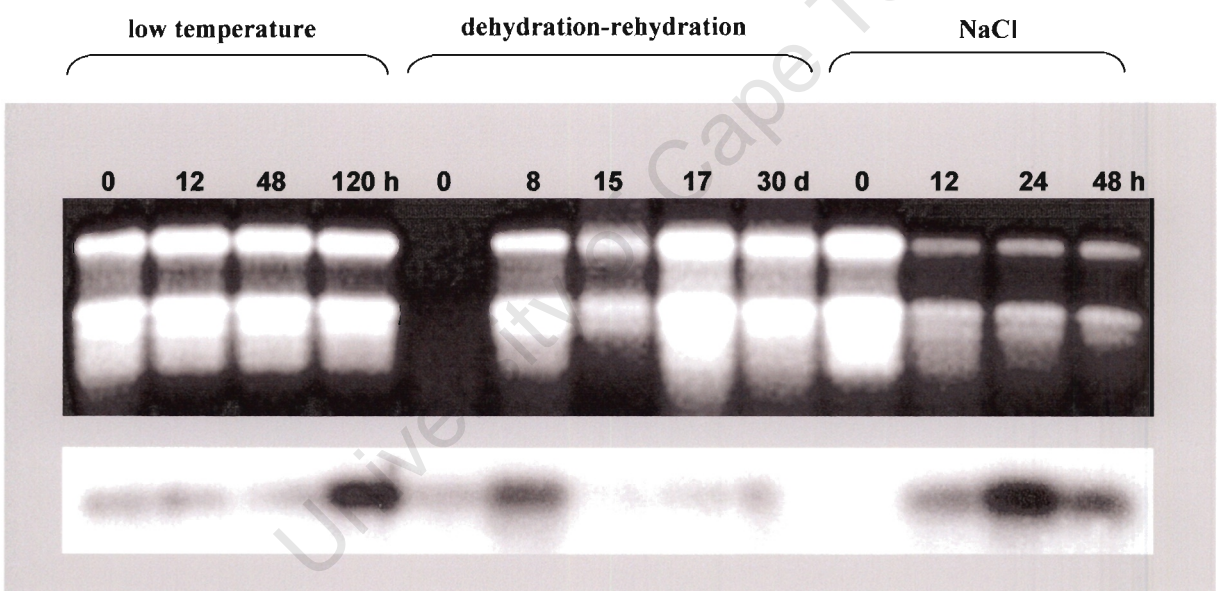

Figure 4.3 Northern blot analyses of *XvPrx2* using *X. viscosa* whole plants and excised leaves exposed to abiotic stresses. Treatments included: low temperature (4°C), dehydration-rehydration and NaCl (150 mM). Upper panels display ribosomal RNA bands on an agarose/EtBr gel (loading control). Lower panels display *XvPrx2* hybridisation signals on an autoradiograph.

A second, broader analysis incorporating more treatments and increased time-points of *XvPrx2* expression was performed (Figs. 4.4 and 4.5). During dehydration-rehydration upregulation was only observed at 74% RWC (8 d dehydration) and upon rehydration at ca. 93% RWC (Fig. 4.4A). For the low temperature treatment the transcript level remained constant until 120 h of stress, at which point a significant increase was observed (Fig. 4.4B). During high temperature treatment the transcript remained at a basal level during the first 48 h with a slight decrease at 6 h (Fig. 4.4C). There was a marked increase in transcript level between 72-120 h. For the high light treatment, a basal transcript level was observed at 0 and 6 h. Increased transcript levels were observed for 12-168 h with slight variation. Maximal induction was observed at 24 and 120 h (Fig. 4.4D).

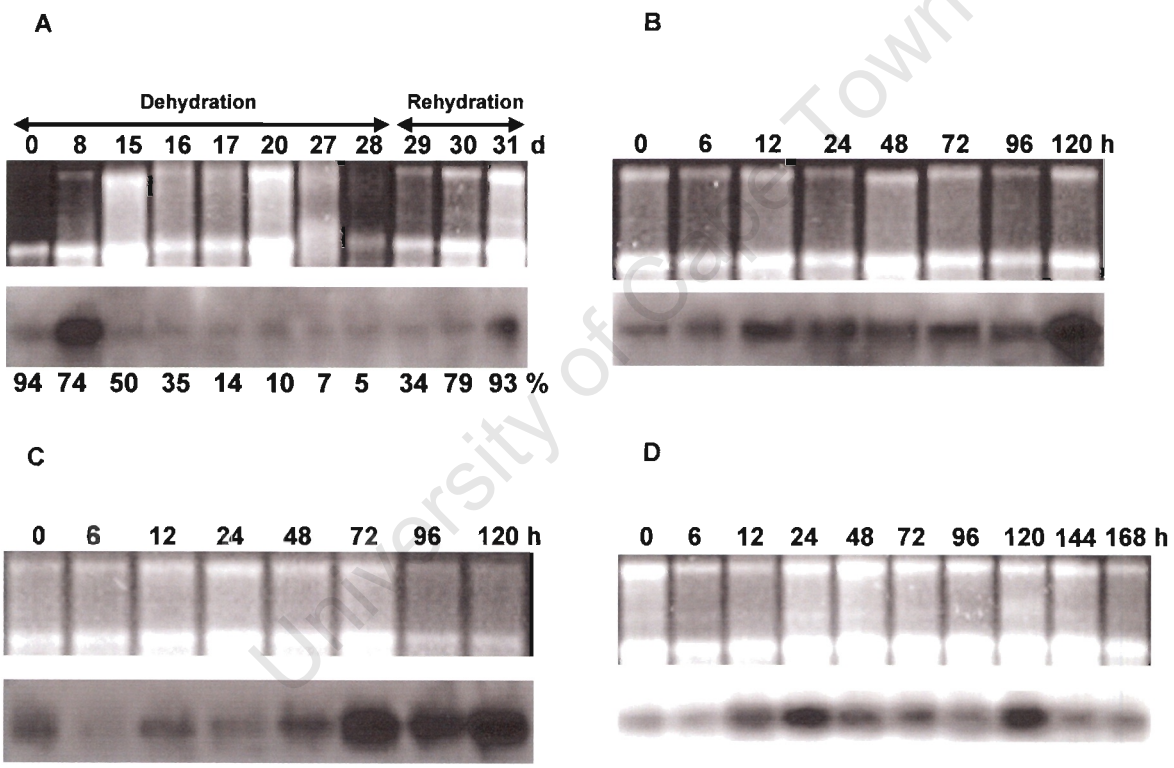

Figure 4.4 Northern blot analyses of *XvPrx2* using whole plants exposed to abiotic stresses. Upper panels display ribosomal RNA bands on an agarose/EtBr gel (loading control). Lower panels display *XvPrx2* hybridisation signals on autoradiographs. Treatments included: (A) dehydration-rehydration; (B) low temperature (4°C); (C) high temperature (42°C); and (D) high light (1500 $\mu mol.m^{-2}.s^{-1}$). For all treatments the time after onset of the treatment is displayed in hours or days. For the dehydration-rehydration treatment (A) the percentage RWC is displayed below the panel.

For the NaCl treatment, a basal expression level was observed at most time points. Increased expression was observed at 24 h and again at 96 and 120 h of stress (Fig. 4.5A). For the ABA treatment, a general increase in transcript level was observed when compared to the non-stressed sample (0 h). Maximal induction was observed at 48 and 72 h (Fig. 4.5B). A distilled water treatment (wounding control) was also analysed since excised leaves were used for NaCl and ABA stress treatments. A gradual increase in transcript level was observed in this analysis (Fig. 4.5C), it can therefore be concluded that in some cases gene expression is suppressed.

For the NaCl treatment on tissue culture plantlets, slight variation was observed between the expression of two separate plantlets. The *XvPrx2* transcript level was observed to remain constant in plant 1 during the first 12 h after onset of treatment. A decrease in expression at 24 h and an increase at 48 h was also evident (Fig. 4.5D). For plant 2, a similar expression was observed, except for a slight increase in expression that was evident at 12 h. For the ABA treatment, a marked increase was observed at 12 h, with a decrease at 24 h and an increase at 48 h up to the basal level (Fig. 4.5E). For plant 2, a similar trend was observed, however, the transcript level was lower at most time points. For the MS control, the *XvPrx2* transcript remained constant for both plant 1 and 2 (Fig. 4.5F).

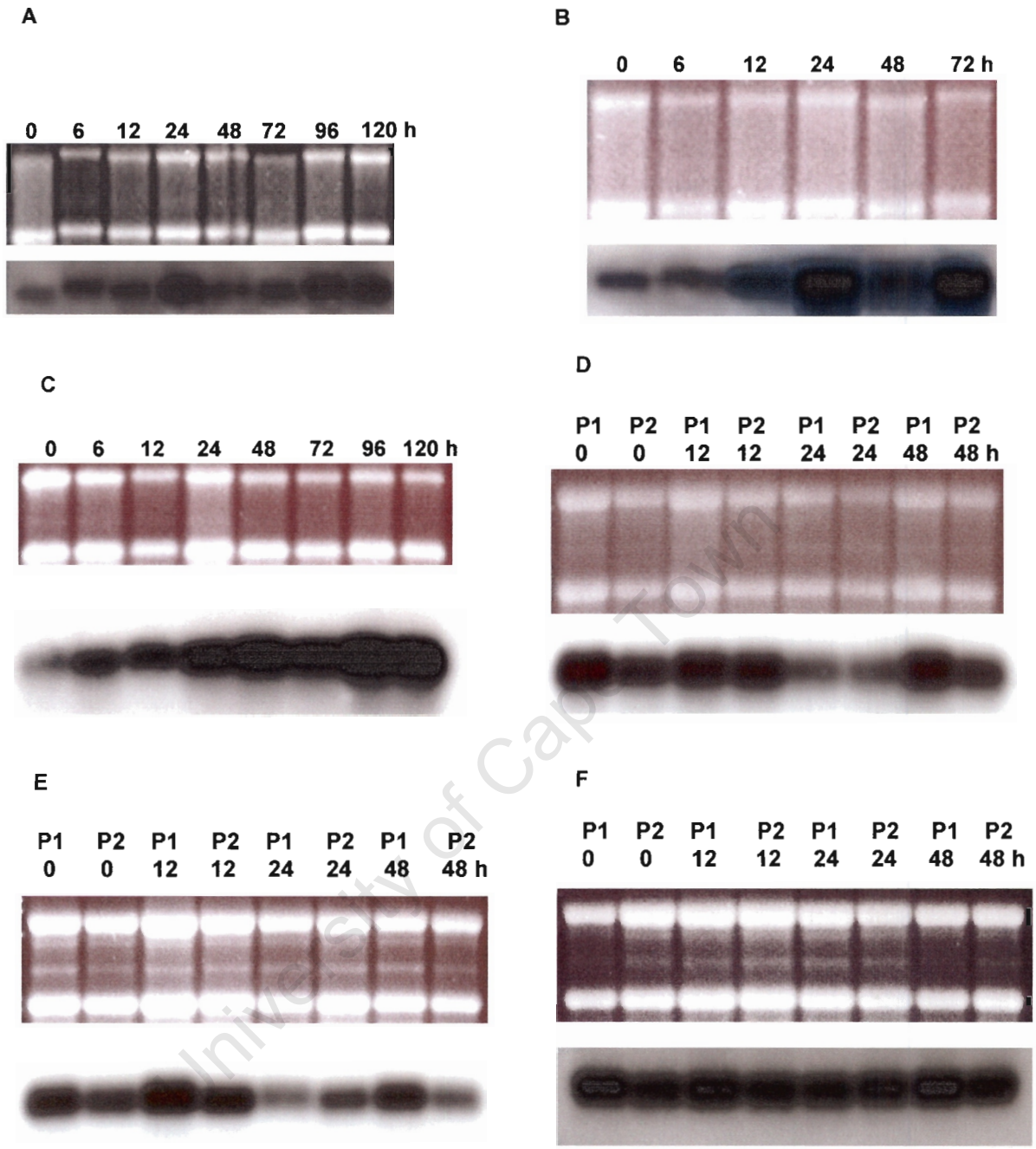

Figure 4.5 Northern blot analyses of *XvPrx2* using excised leaves (A-C) and tissue culture plantlets (D-F) exposed to abiotic stresses. Upper panels display ribosomal RNA bands on an agarose/EtBr gel (loading control). Lower panels display *XvPrx2* hybridisation signals on autoradiographs. Treatments included: (A, D) NaCl (150 mM); (B, E) ABA (100 µM); (C) H_2O control; and (F) MS medium (control). P1 and P2 refer to plant 1 and plant 2, respectively. For all treatments the time after onset of the treatment is displayed in hours.

4.3.3 Western blot analyses

For all treatments the loading controls were observed to be at similar levels indicating that transfer onto the membrane was optimal (Figs. 4.6 and 4.7). A protein of ca. 17.5 kDa was detected for all treatments. Additionally, for some treatments a second hybridisation signal at ca. 19 kDa was observed, a size slightly larger than the predicted mass of the polypeptide (17.5 kDa). This upper protein band was not visible in all lanes. For the water control and dehydration treatments the second band of 19 kDa was not observed, however, a band of ca. 17 kDa could be detected. Interestingly, only a single 17.5-kDa band was observed for the root tissue sample.

Due to the loading of the 0 h dehydration sample being lower than the other time points very little or no protein was observed for 0 h (Fig. 4.6A). Protein levels were high and relatively constant at RWCs of 74 to 10% (8 to 20 d). A very low signal was observed at 5% RWC (28 d). Protein levels were observed to be high and relatively constant for the rehydration samples at RWCs of 34 to 93% (29 to 31 d). The XvPrx2 protein levels were observed to be high in the roots of *X. viscosa* plants at full turgor and decreased significantly upon dehydration (Fig. 4.6B). Very little protein was observed after 10 d dehydration with no protein being visible after 16 d of dehydration.

For low temperature stress, the XvPrx2 protein level decreased significantly until no protein was observed at 12 h stress (Fig. 4.6C). From 24 to 120 h a gradual but significant increase was visible. For the high temperature treatment, a basal level of the protein was observed for all samples throughout the treatment (Fig. 4.6D). A slight increase was evident at 72 and 96 h. For the high light treatment the XvPrx2 level decreased gradually from 0 to 24 h. The protein level increased at 48 h and was at very low levels (below basal) for samples obtained at 96 to 144 h (Fig. 4.6E).

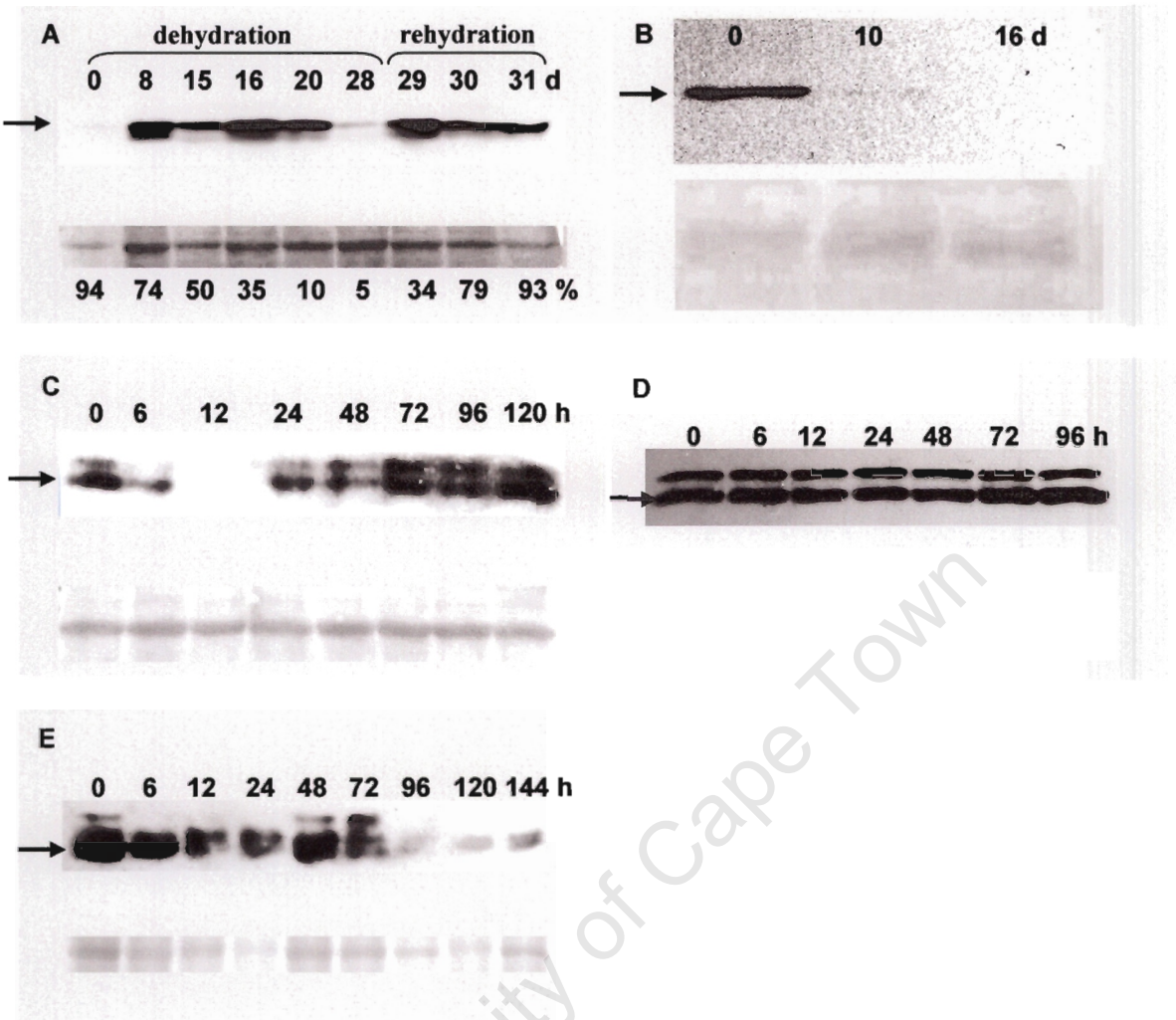

Figure 4.6 Western blot analyses of XvPrx2 using whole plants (A, C-E) and root tissue (B) exposed to abiotic stresses. Upper panels display XvPrx2 antiserum hybridisation signals on autoradiographs. Lower panels display Ponceau S stained Rubisco protein bands on nitrocellulose membranes (loading control). Treatments included: (A) dehydration-rehydration (leaf material); (B) dehydration (roots); (C) low temperature (4°C); (D) high temperature (42°C); and (E) high light (1500 $\mu mol.m^{-2}.s^{-1}$). Arrows indicate the 17.5-kDa XvPrx2 protein band.

Protein levels of XvPrx2 were observed to fluctuate in the NaCl treatment of excised leaves. A gradual decrease was observed from 6 to 24 h with a marked increase at 48 h and a gradual decrease again from 48 to 120 h (Fig. 4.7A). For the ABA treatment, the XvPrx2 level was highest after 0 and 12 h of stress (Fig. 4.7B). All other time points produced XvPrx2 levels lower than the basal level (0 h). The water control displayed a constant protein level from 0 to 48 h. However, no protein was visible at 72 and 96 h (Fig. 4.7C).

For the NaCl treatment on tissue culture plantlets, the XvPrx2 level was observed to decrease gradually until 24 h stress and increased slightly at 48 h (Fig. 4.7D; only taking into account the lower 17.5-kDa band). This result differs from that observed for excised leaves where a greater increase was observed at 48 h stress. Furthermore, the doublet was more apparent when compared to samples from excised leaves. For the ABA treatment a gradual decrease was observed until 24 h with a significant increase at 48 h (Fig. 4.7E). For samples from this treatment the doublet was of equal intensity. Using MS as a control medium appears to have influenced the protein level. Although the loading was lower initially and increased gradually the actual protein signal decreased with time (Fig. 4.7F). For all time points the upper band (ca. 19 kDa) was visible.

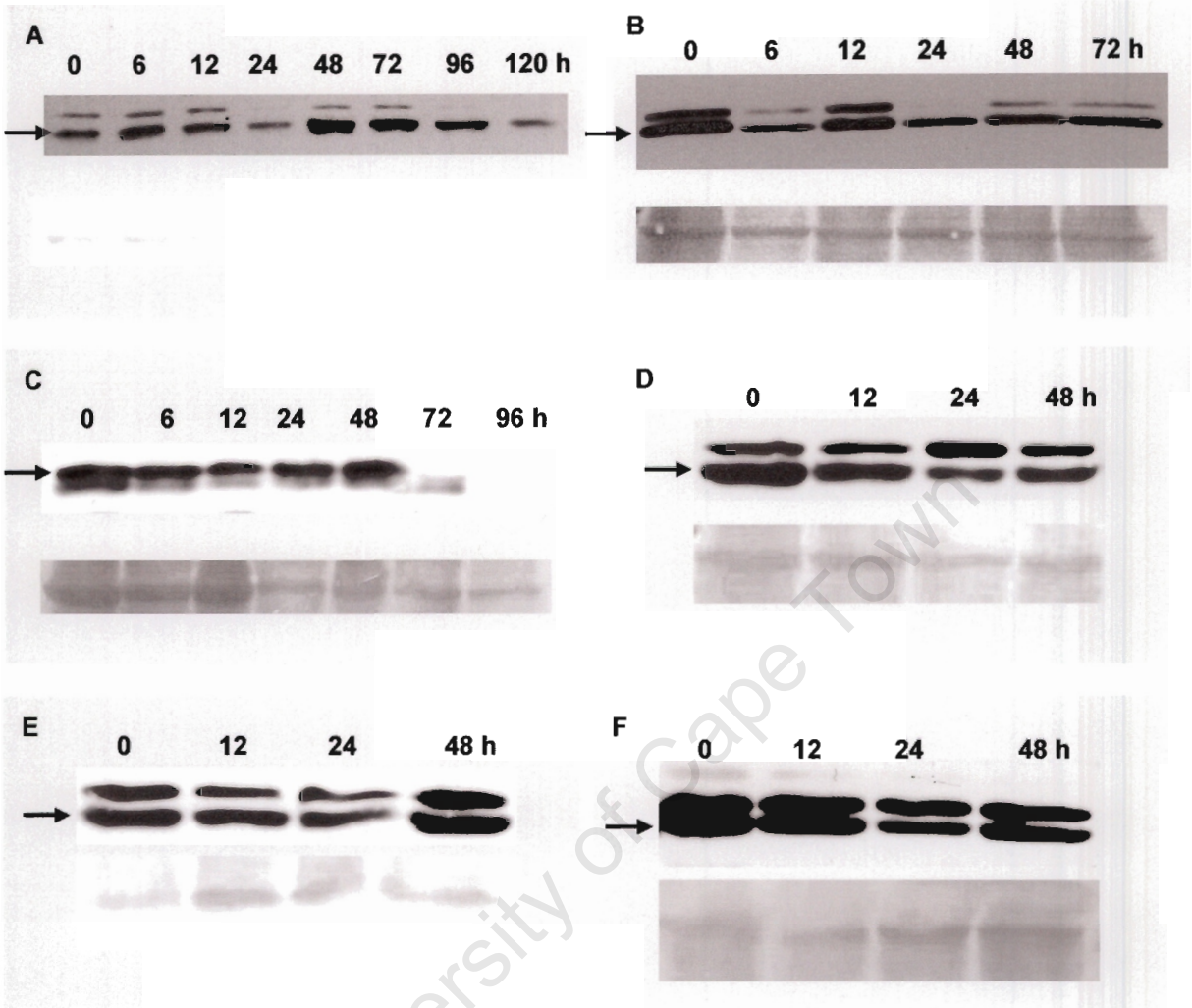

Figure 4.7 Western blot analyses of XvPrx2 using excised leaves (A-C) and tissue culture plantlets (D-F) exposed to abiotic stresses. Upper panels display XvPrx2 antiserum hybridisation signals on autoradiographs. Lower panels display Ponceau S stained Rubisco protein bands on nitrocellulose membranes (loading control). Treatments included: (A, D) NaCl (150 mM); (B, E) ABA (100 μM); (C) H_2O control; and (F) MS medium (control). Arrows indicate the 17.5-kDa XvPrx2 protein band.

4.3.4 Two dimensional gel electrophoresis analysis of XvPrx2

The two dimensional gel electrophoresis data point to there being potentially many homologues of XvPrx2. Approximately 8 spots of varying intensities were observed on the autoradiograph ranging from a pI of 4.75-5.46 (Fig. 4.8). The size of these spots was in the region of ca. 17.5 kDa. There also appeared to be a mobility shift for these spots. For the spots at lower pI especially, the proteins appear to cover a larger size range of ca. 17.5-20 kDa. In addition, it appears that the XvPrx2 antibody cross-reacted with a further two proteins, which are ca. 36.5 kDa. This size is slightly larger than the dimeric size of ca. 35 kDa.

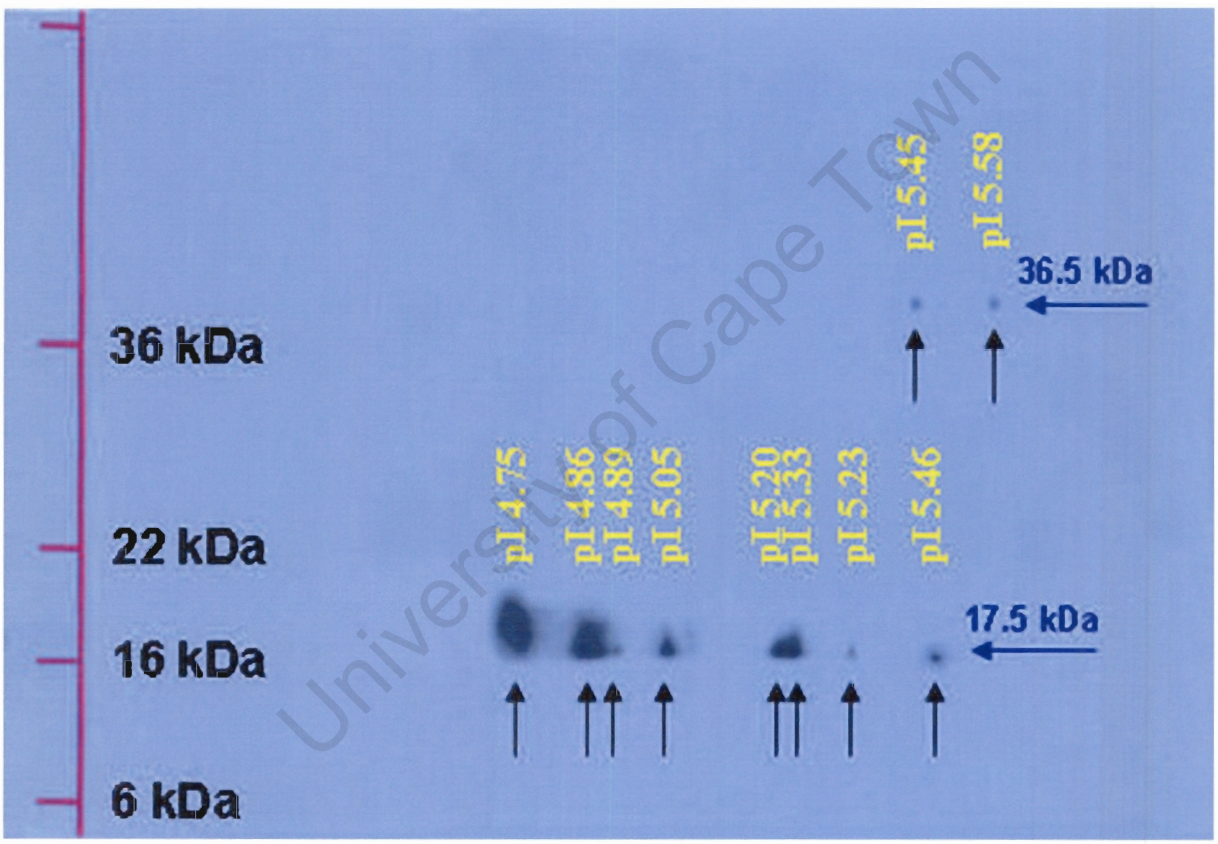

Figure 4.8 Two dimensional gel electrophoresis of *X. viscosa* total protein probed with XvPrx2 antiserum. Vertical arrows indicate potential type II Prx homologues ranging from pI 4.75-5.6. The Y-axis corresponds with molecular weight, whereas the X-axis corresponds with pI.

4.4 DISCUSSION

Since Prxs represents a fairly new field of interest, the *XvPrx2* gene was selected as a suitable candidate for analysis. Due to the protein's antioxidant capacity and its potential stress inducible nature this gene was further characterised with specific interest to its expression at the mRNA and protein levels. An initial objective in determining *XvPrx2* expression involved treating *X. viscosa* plants such that harsh abiotic stress conditions were imposed. The stresses included salinity (150 mM NaCl), abscisic acid (100 μM ABA), dehydration-rehydration, low temperature (4°C), high temperature (42°C) and high light stress (1500 $\mu mol.m^{-2}.s^{-1}$). Interestingly, all plants treated survived the stresses imposed. This tolerance to the extreme conditions imposed highlights the hardiness of this plant species. It may be postulated that *X. viscosa* has adapted to tolerate severe environmental abiotic conditions due to its constant exposure to such conditions. This in turn reinforces the notion that *X. viscosa* is a suitable candidate for sourcing stress tolerant genes.

To ensure that the changes in the levels of the *XvPrx2* transcript and protein were a consequence of the stress imposed, the RWC and WP of the leaf tissues subjected to the stresses were monitored at each sampling point. These remained more or less constant throughout the treatment. The exception was the dehydration-rehydration treatment where the RWC and WP decreased upon dehydration and increased upon rehydration. This, however, would be the normal scenario as the plant loses water initially and regains water once rewatered.

Dimerisation of type II Prxs has been reported previously (Brehelin et al., 2003; Rouhier & Jacquot, 2005). A strong reducing agent like β-mercaptoethanol has been shown to reduce the dimer to the monomeric form. For the purified XvPrx2 protein, reducing equivalents such as β-mercaptoethanol and DTT were shown to reduce the dimer. However, this was not the case for protein expression studies as the dimer was present in almost all stress treatments. In addition, in some cases trimers and tetramers were observed after treatment with β-mercaptoethanol or DTT. The oligomers were excluded from the protein expression analyses since these were not always produced, hence the monomeric protein was only considered.

Most of the stresses performed were on whole plants. However, due to the large number of treatments performed in this study, sufficient plants were not available. Consequently, for two treatments (ABA and NaCl) together with non-stressed controls, excised leaves and tissue culture plantlets were used.

In the analyses (ABA and NaCl) involving excised leaves a general increase in *XvPrx2* transcript was observed with an initial increase followed by a decrease and an increase thereafter. An increase in transcript was anticipated for the NaCl treatment as applications of high exogenous salt concentrations cause an imbalance in the ions in the plant cells leading to ion toxicity, osmotic stress and production of ROS (Hasegawa et al., 2000). Therefore, the XvPrx2 protein may be involved in the scavenging of ROS and in maintaining membrane integrity during NaCl stress. However, even though the transcript and protein levels were observed to fluctuate throughout the stress treatment there appeared to be no apparent correlation between their abundance. These contrasts in mRNA and protein levels could not be explained.

An increase in transcript was also anticipated for the ABA treatment as this hormone is involved in the generation of many stress-inducible genes and is required for changes in gene expression in response to water deficit stress (Bray, 1997). A general increase in transcript above the basal level was observed. However, protein levels were below basal levels at all times after initiation of the treatment.

The non-stressed control displayed a gradual increase in transcript level possibly due to a wounding response, which probably occurred during leaf excision. This could be attributed to the pathogen defence mechanism, which is initiated when a plant is invaded by pathogens. When a pathogen attacks a plant the future of the infection depends on the capacity of the plant to attack and destroy the pathogen. A hypersensitive response occurs via an oxidative burst with the production of large amounts of H_2O_2 and nitric oxide in the infected tissues (Levine et al., 1994). Rouhier et al. (2004a) showed that a high over-expression of PrxQ and type II Prx was observed in response to an incompatible pathogen attack and reported that this may be due to the need to maintain the low peroxide concentrations outside the sites of infection and spare the uninfected cells. The non-stressed control displayed a constant protein level for the first 48 h of the treatment. However, little or no protein was visible thereafter. Again, this does not correlate with the transcript level observed were a general increase was recorded.

To compensate for this apparent wounding response obtained with excised leaves, tissue culture plantlets were also used for the ABA and NaCl treatments. As these plants did not require pre-treatment (such as leaf excision) it was envisaged that these plants would provide more significant results. For the MS control, the *XvPrx2* transcript remained constant during the entire treatment. However, using MS as a control medium appears to have

influenced the protein level. The protein signal was observed to decrease slightly during the course of the treatment.

For the NaCl and ABA treatments on tissue culture plantlets, similar results were obtained. The *XvPrx2* transcript level was observed to increase minimally after the onset of the treatments. A decrease in expression at 24 h and an increase thereafter at 48 h were also evident for both treatments. The XvPrx2 protein level was observed to decrease gradually until 24 h and increased at 48 h. The tissue culture plantlets used were very young compared to the older potted plants from which leaves were excised, hence these younger leaves probably possessed higher quantities of high quality RNA. The accumulation of *XvPrx2* transcripts was observed to be higher in the tissue culture plantlets than in the excised leaves. The accumulation of XvPrx2 protein levels in tissue culture plantlets were also higher than in excised leaves. It appears that the tissue culture plantlets, being fairly young, possibly produce larger amounts of antioxidants to protect the young plant against free radical attack as a prerequisite for its survival. Future work should involve gene and protein expression profiling over a time course on young and old *X. viscosa* plants to explore this theory further.

The XvPrx2 protein is postulated to be involved in the scavenging of ROS and is therefore expected to be induced under high light stress. However, the formation of ROS by photo-oxidation is not only linked to high light stress but also to other environmental stresses including water deficit (Sherwin & Farrant, 1998; Loggini et al., 1999). Poikilochlorophyllous plants (including *X. viscosa*) lose their chlorophyll and dismantle their photosynthetic system while in a dehydrated state (Sherwin & Farrant, 1997). Analysis of dehydration treated leaves point to the *XvPrx2* transcript being expressed at basal levels between 74 and 5% RWC. Increased transcript levels were only observed at the onset of dehydration (74% RWC) and upon rehydration at ca. 93% RWC. Protein levels were high and relatively constant during dehydration although a very low signal was observed at 5% RWC. Protein levels were observed to be high and relatively constant during rehydration (RWCs of 34 to 93%). The XvPrx2 protein levels were observed to be high in the roots of *X. viscosa* plants at full turgor and decreased significantly upon dehydration. This difference between the roots and leaves can be explained by the probability that the leaves require more of the protein during stress than the root tissues due to greater ROS being generated in these organs.

A dehydration treatment performed on *X. viscosa* by Ekmekci et al. (2005) demonstrated that the plant acclimated to water deficit within the first 8-10 d. This resulted in a reduction in photosynthesis and an increase in superoxide dismutase levels, with no ultimate apparent damage. It was also reported that there was an absence in the increase of peroxidase

activity suggesting that there was no peroxidative damage to its membrane. Similarly in this study, during dehydration the transcript levels of *XvPrx2* decreased initially and a very low level was observed. This could be due to the gradual cessation of photosynthesis during dehydration as the chlorophyll is being degraded with the consequence that less ROS is produced and hence less enzyme required for scavenging.

In its natural environment, which is often at very high altitudes, the *X. viscosa* plant is often exposed to very low temperatures, even below freezing. Therefore, it is possible that an imposed low temperature stress of 4°C may not constitute an extreme condition for the *X. viscosa* plant. For the low temperature treatment, *XvPrx2* transcript levels were observed to remain constant until 120 h of stress, at which point a significant increase was observed. The XvPrx2 protein level decreased significantly until no protein was observed at 12 h stress. From 24 to 120 h a gradual but significant increase was visible. The *X. viscosa* plant is considered an extremophile in that it can thrive in harsh environmental conditions. Therefore it is not surprising that the plant responds quite late to a temperature stress of 4°C. It is possible that the mRNA transcript might be accumulating in anticipation of a further decrease in temperature, in which case a rapid production of the protein might be required. Future work should involve freezing conditions to assess how *X. viscosa* responds to such a stress.

Heat stress affects most cellular processes as it leads to the denaturation of proteins, the inactivation of biological enzymes and damage to lipid membranes brought on by the production of ROS (Munro & Pelham, 1985). To tolerate and survive heat stress, the plant requires the ability to repair the damages incurred by heat or the prevention thereof. It is expected therefore that *XvPrx2* would have a role to play in either the detoxification of ROS, or the protection of the lipid membrane. During high temperature treatment the *XvPrx2* transcript remained at basal levels through the initial part of the stress with a marked increase in transcript level after 72 h. A basal level of the protein was observed throughout the treatment with a slight increase evident at 72 and 96 h. These results suggest that the XvPrx2 protein is not involved in the initial stages of the plant's response to heat stress.

For the high light treatment, basal transcript levels were observed initially, but, increased during 12-168 h with slight variations. The XvPrx2 protein level decreased gradually from 0 to 24 h. The protein level increased at 48 h and was at very low levels (below basal) for samples obtained at 96 to 144 h. Again, this could be due to the fact that *X. viscosa* is an extremophile and is regularly exposed to high light intensities in its natural habitat. The *XvPrx2* transcript might have accumulated in anticipation of a more severe high light intensity stress, in which case the protein will also accumulate and provide protection to

the plant. High light can be very damaging to plants as it is frequently associated with damage to the photosynthetic reaction centre (Strid et al., 1994). Photosystem II is a major target for photo-inhibition of photosynthesis, which occurs when the amount of light available exceeds that necessary for photosynthetic processes. Consequently, there is excessive production of ROS. If the free radicals are not quenched, DNA damage and lipid peroxidation occurs. At earlier stages of high light stress, *X. viscosa* probably has other mechanisms in place for protection against cellular damage such as the more 'conventional' antioxidant enzymes like superoxide dismutase, catalase and peroxidases. The type II peroxiredoxin enzyme probably only comes into play during the later stages of the stress.

The possibility that the XvPrx2 probes used in the northern and western hybridisation analyses could also be binding to other homologues in the crude RNA or protein extract cannot be overlooked. Consequently, mRNA and protein expression profiles observed could be for a combination of homologues. Future work would therefore involve the isolation of the various type II homologues from *X. viscosa* and the generation of probes to the 3' untranslated region thereof, as it appears to be a highly variable region in *A. thaliana* transcripts. This is required to verify the expression patterns observed under the various abiotic stresses performed in this study.

From the current study it is evident that analyses of the expression of *XvPrx2* mRNA does not provide an indication of whether the protein is produced as well (Fig. 4.9). Much of the regulation of the synthesis of proteins occurs through regulation of transcription of the mRNA encoding those proteins. Post-transcriptional regulation does occur though at varying levels for each transcript therefore there is no guarantee that the presence of the mRNA transcript will lead to translation immediately into a functional protein. Performing western blot analyses thus provides a clearer indication of whether the XvPrx2 protein is present as a functional protein under the various stress conditions.

Analysing the combined mRNA-protein expression data provides an idea of how regulation occurs for a particular protein. For the XvPrx2 protein, there appears to be a significant level of post-transcriptional regulation as the protein and mRNA levels do not correlate in most cases (Fig. 4.9). This points to a complex regulation of the antioxidant protein, which is probably a requirement by the plant to prevent a metabolic burden due to possible over supply of the protein. Consequently, the protein is only produced when it is required. It may be postulated that XvPrx2 and other *X. viscosa* antioxidant enzymes act in a co-ordinated manner to prevent the build-up of ROS.

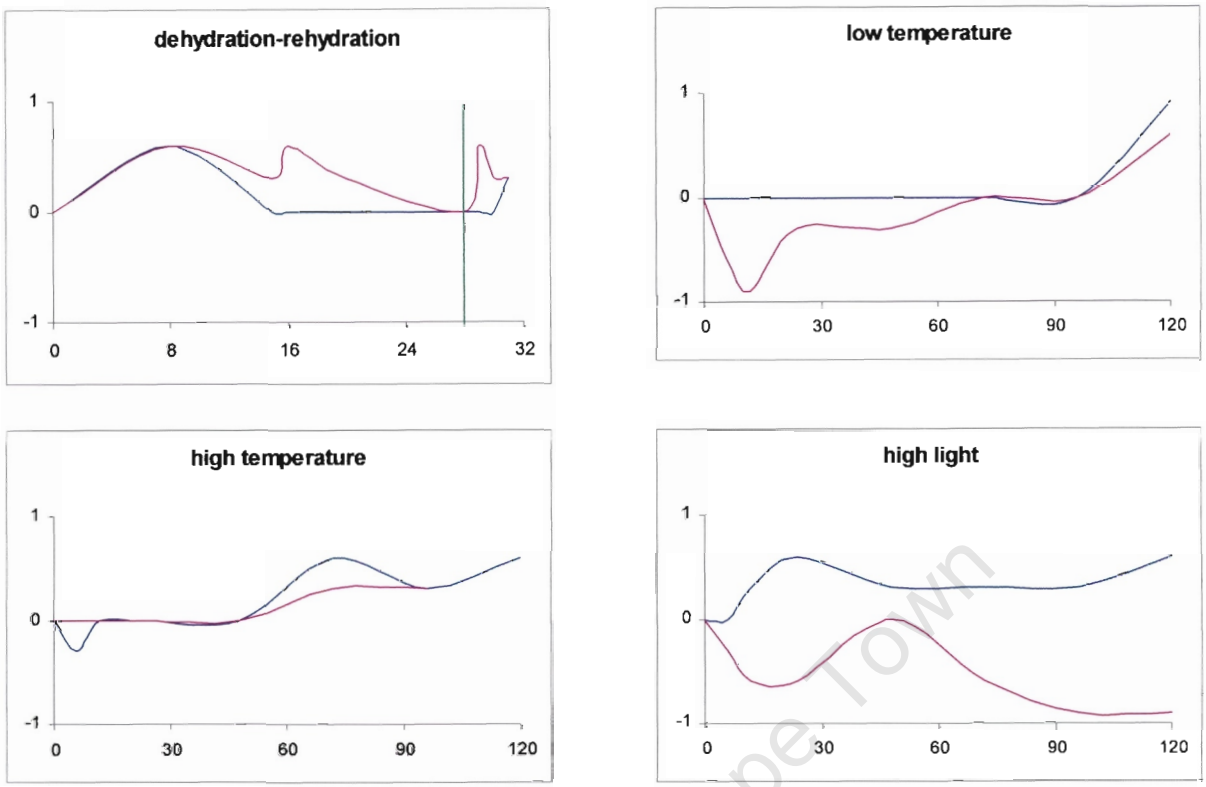

Figure 4.9 Expression profile curves of *XvPrx2* at both the transcript and protein level as a ratio of basal expression. The *XvPrx2* expression curve is presented in blue and the protein curve in purple. The green line shows the change from dehydration to rehydration conditions.

From the accumulated expression data in the northern and western analyses, it is clear that the *X. viscosa* type II Prx is a stress-inducible enzyme. It appears that the *XvPrx2* transcript is present in the plant cell most of the time either at basal levels under non-stress conditions or differentially expressed at specific time-points during the various stresses. Another Prx from *X. viscosa*, *XvPer1* (Mowla et al., 2002) is not expressed in non-stressed plants, but is transcribed as soon as the plant is exposed to abiotic stresses. At the protein level XvPer1 was not detectable during low temperature stress and in the control plant. It was observed from these two antioxidants that protection measures of each vary regarding the stress imposed. These proteins are transcribed or translated according to the requirements of the plant during abiotic stresses as other antioxidants can also play a crucial role depending on the period during the stress.

The *A. thaliana* peroxiredoxins AtPrxIIB, C and D differ only by 0.06 kDa from one another. Therefore, Brehelin et al. (2003) used two dimensional electrophoresis to distinguish AtPrxIIB from C and D proteins using their predicted pI difference of 0.15. The mature

AtPrxIIE predicted by PSORT is about 0.15 kDa smaller than the three cytosolic PrxIIs and can also be distinguished by its size as well as by its pI which is 0.15 more acidic than AtPrxIIB and 0.30 point from AtPrxIIC and D.

In the current study, 2-D PAGE analyses point to the potential existence of many homologues of XvPrx2. Eight spots of varying intensities were observed in a pI range of 4.75-5.46. The estimated molecular mass of these protein spots was ca. 17.5 kDa. In addition, the XvPrx2 antibody cross-reacted with an additional two proteins of ca. 36 kDa. This size correlates with the dimeric size of ca. 35 kDa, although the observed spots are slightly larger in size. There also appears to be a mobility shift in the lower size range (i.e. the 17.5-kDa proteins) when compared to the dimers in terms of pI. It may be concluded that the 2-D PAGE data provides further evidence for the existence of multiple XvPrx2 homologues.

Chapter 5

Biochemical and structural characterisation of XvPrx2

5.1 INTRODUCTION

The Prxs play a crucial role in the detoxification of ROS. These enzymes catalyse the reduction of either hydrogen peroxide (H_2O_2) or various alkyl hydroperoxides to water and the corresponding alcohol in the presence of a hydrogen donor, which is in turn converted to the oxidised form. During catalysis, Prxs utilise a very conserved cysteine defined as the peroxidatic cysteine to reduce hydroperoxides and peroxinitrites (Chae et al., 1994b; Bryk et al., 2000). The reaction below defines the Prx catalysed reduction of H_2O_2:

$$2RSH + H_2O_2 \xrightarrow{Prx} RSSR + H_2O$$

After a nucleophilic attack, the sulphydryl (SH) moiety on this cysteine is transformed into sulphenic acid (SOH), which is regenerated either by direct reduction or by intra- or intermolecular disulphide bond formation (Wood et al., 2003). Finally, the disulphide is reduced with the help of various reducing systems, the thioredoxin (Trx) or glutaredoxin (Grx) systems or cyclophilin in eukaryotic organisms (Lee et al., 2001; Bryk et al., 2002; Rouhier et al., 2002). The generation of a sulphenic acid moiety during Prx catalysis leads sometimes to over-oxidation of this species into sulphinic acid (SOOH). However, this sulphinic acid is partly reversible in an ATP-dependent process involving a sulphiredoxin (Biteau et al., 2003; Woo et al., 2003).

The classical assay of plasmid DNA protection against ROS generated by the Fenton reaction induced by a metal catalysed system is frequently used to test the protection of DNA in the presence of a Prx. Brehelen et al. (2003) using an in vitro assay reported that DNA was protected in the presence of AtPrxIIB and Δ70AtPrxIIE but not in the absence of either protein. At the cellular level, in vivo assays have shown that the over-expression of a Prx in *E. coli* cells offer protection to the cells against free radical attack allowing for an increased survival rate (Baier & Dietz., 1997; Horiguchi et al., 2001; Haslekas et al. 2003a).

In order to characterise the XvPrx2 protein at a biochemical level the following objectives were pursued:

(i) assessing the ability of XvPrx2 to protect DNA against ROS using an in vitro DNA protection assay;

(ii) assessing the ability of XvPrx2 to protect *E. coli* cells from the toxic effects of ROS using an in vivo protection assay; and

(iii) assessing the catalytic efficiency of XvPrx2 to utilise various substrates in the presence of various electron donors.

Limited proteolysis has been used as a sensitive method for detecting conformational changes in proteins (Kampranis & Maxwell, 1998). It is a method that has been widely used to obtain information about domain structure in proteins and conformational changes that occur upon ligand binding (Kampranis et al., 1999). Application of this method can provide useful information about conformational changes resulting from the interaction of the protein with a substrate or an effector molecule.

The traditional technique for determining protein structure has been single crystal X-ray crystallography. However, multiple problems are associated with this technique.

(i) growing single crystals of proteins is time consuming, experimentally difficult, and requires milligrams of isolated, pure protein; and

(ii) protein diffraction patterns are often difficult to solve for the 3-D co-ordinates of the protein.

Structural information can still be obtained from protein sequence using knowledge-based modelling. This involves the sequence of a protein of unknown structure and comparison of this information to a database of proteins for which structural and sequence information is available. Proteins in the database, which are homologous are retrieved and used as the basis for a structural model. Once the topology of the folding pattern has been determined from the structures of two or more members of a family it can be assumed to exist in a similar form in all homologous proteins (Overington et al., 1990).

In order to characterise the XvPrx2 protein at a structural level the following objectives were pursued:

(i) comparison of proteolytic profiles of the reduced and oxidised forms of XvPrx2 to that of XvV76C to determine whether conformational differences exist between these proteins;

(ii) elucidation of the crystal structure of XvPrx2; and

(iii) development of knowledge-based models of XvPrx2 and XvV76C by structural bioinformatics.

5.2 MATERIALS AND METHODS

5.2.1 In vitro DNA protection assay

The in vitro DNA protection assay employed in this study involved a combination of the methods of Klimowski et al. (1997) and Brehelin et al. (2003). Individual reactions were set up in a total volume of 50 µl in an Eppendorf tube (Table 5.1). A $FeCl_3$-DTT mix was prepared by the addition of 10 µl of 0.5 M $FeCl_3$ and 10 µl of 50 mM DTT to 60 µl H_2O. The mix was incubated for 30 min at RT to generate ROS. Eight microlitres of the $FeCl_3$-DTT mix was added to tubes 4-8 (Table 5.1). The final concentrations of DTT and $FeCl_3$ used in each reaction were 1 mM and 10 µM, respectively. Reaction mixes were incubated for 5 h at RT and thereafter electrophoresed on a 1% agarose/EtBr gel.

Table 5.1 Eight reactions were prepared for the in vitro DNA protection assay. Volumes are displayed in microlitres. The final concentration of protein (XvPrx2 and XvV76C) used was 20 µM with χ referring to the volume

Component	1	2	3	4	5	6	7	8
DTT (50 mM)		1						
$FeCl_3$ (0.5 mM)			1					
$FeCl_3$-DTT mix				8	8	8	8	8
XvPrx2				χ				
XvV76C					χ			
Plasmid DNA (pBSK)	2.5	2.5	2.5	2.5	2.5	2.5	2.5	2.5
BSA (2 µg/ml)							8	16
H_2O (make up to 50 µl)								

5.2.2 In vivo protection assay

For small scale induction, 1 ml of an overnight LB-amp broth culture (either pTOPO::*XvPrx2*, pTOPO::*XvV76C* or pTOPO) was inoculated in 100 ml LB-amp broth and incubated with vigorous shaking at 37°C until an OD_{600} of ca. 0.5 was obtained. The culture was induced by addition of IPTG (1 mM final concentration) and incubated for an additional 4 h with vigorous shaking at 37°C.

Hydrogen peroxide (0.5 M) was prepared fresh. Top agar (Appendix D) was prepared and incubated at 48°C. Following 4 h of induction, 100 µl of the induced culture was mixed in 5 ml of top agar (supplemented with 50 µg/ml of ampicillin) and poured over LB-amp agar

plates. The top agar was allowed to settle for 1 h at RT. Sterile filter discs were inoculated with H_2O_2 (either 2.5 µl or 5 µl of 0.5 M H_2O_2). These were placed gently on the top agar containing the induced bacteria. Plates were incubated for 16 h at 37°C.

5.2.3 Enzyme specificity assays

The lipid substrates, phosphatidylcholine dilinoleoyl hydroperoxide (POOH) and linoleic acid hydroperoxide (LOOH) were prepared as described by Maiorino et al. (1990). The POOH (3.5 mg; Sigma, Germany) and LOOH (3.5 mg; Sigma, Germany) were prepared separately by dissolving in 70 µl chloroform. The chloroform was allowed to evaporate for ca. 15 min at RT and thereafter 10.8 ml of 10 mM deoxycholate was added to each lipid and mixed for 5 min by gentle agitation. Sodium borate (25.2 ml; 0.142 M, pH 9) was added to each lipid-deoxycholate solution (labelled Solution A). Six hundred microlitres of Solution A was added to an Eppendorf tube containing 6.7 mg Type IV soybean lipoxidase (Sigma, Germany). Two hundred microlitre aliquots of the soybean lipoxidase-Solution A mix was added to the remaining Solution A. After addition of the first 2 aliquots, the mix was incubated for 5 min at RT with continuous stirring after each addition. After the final 200 µl addition, the mix was incubated for 20 min with stirring. The mixture was applied to a Sep-Pak C18 cartridge (Waters, Germany) that had been washed consecutively with 10 ml each of water, methanol and water. After loading the sample, the column was washed with ca. 100 ml sterile water. The peroxide was eluted in ca. 4 ml methanol. The solvent was allowed to evaporate and thereafter the peroxide was dissolved in 1 ml methanol. The peroxide concentration was determined spectrophotometrically (ε_{234} = 25 $mM^{-1}.cm^{-1}$). Hundred microlitre aliquots were prepared and stored at -20°C.

In vitro peroxidase activity assays were performed according to the protocol described by Finkemeier et al. (2005). For the xylenol orange assay, XvPrx2 protein (1-50 µM) was maintained in its reduced state by using 10 mM DTT or 1/10 mM GSH in either the presence or absence of 10 µM Grx-CxxS10. Assays were also performed using $Trx_{E.\ coli}$ in the presence of 10 mM DTT. The reduction of H_2O_2, t-BOOH, COOH, LOOH and POOH was determined in a time course over a period of 2 min at 20 s intervals. The remaining peroxides were detected by ferrous-dependent oxidation of xylenol orange (FOX). Twenty microlitres of the reaction mix was incubated with 1 ml FOX reagent (Appendix D) for ca. 15 min. The absorbance (560 nm) was determined and compared with standard curves established for each

substrate. Activity tests were repeated 6-10 times using purified protein from two separate preparations.

The kinetic parameters, K_m, V_{max} and K_{cat} were calculated with a XvPrx2 concentration of 0.75 μM and varying concentrations of H_2O_2. The remaining substrate was determined by the FOX method as described above.

5.2.4 Limited proteolysis of XvPrx2 and XvV76C

For the limited proteolysis assay, XvPrx2 and XvV76C purified protein were each diluted to 65 μM. All reaction mixes were made up to 30 μl with 50 mM Tris. The control reaction mixtures were heat denatured by incubation for 5 min at 100°C and thereafter for 2 min on ice. The mixture was thereafter incubated for 3 h at 37°C.

All reagents (except trypsin) were added to the reaction tube and heat denatured by incubation for 5 min at 100°C and thereafter on ice for 2 min (Table 5.2). The various trypsin concentrations were added to the appropriate tubes and incubated for 3 h at 37°C. Tracking dye was added to each tube, samples were heat denatured for 5 min and loaded onto a 12% SDS PAGE Gel (standard PAGE conditions, Appendix A).

Table 5.2 Trypsin digestion reaction of XvPrx2 and XvV76C to determine conformational change in either the reduced (B and C) or oxidised (D and E) state using DTT (B), H_2O_2 (C), DTT + GSH (D) and H_2O_2 + GSH (E). Volumes are displayed in microlitres unless otherwise stated. A control reaction (A) lacking trypsin was also included

Component	Volume (µl) 3 mg/ml of trypsin	Volume (µl) 6 mg/ml of trypsin	Volume (µl) 9 mg/ml of trypsin
A	Control 1	Control 2	
Trypsin	0	0	
Tris (50 mM, pH 7.5)	17	17	
XvPrx2	10	10	
DTT (100 mM)	3	0	
H_2O_2 (20 mM)	0	3	
B			
Trypsin	1.1	2.3	3.4
Tris (50 mM, pH 7.5)	15.9	14.7	13.6
XvPrx2	10	10	10
DTT (100 mM)	3	3	3
C			
Trypsin	1.1	2.3	3.4
Tris (50 mM, pH 7.5)	15.9	14.7	13.6
XvPrx2	10	10	10
H_2O_2 (20 mM)	3	3	3
D			
Trypsin	1.1	2.3	3.4
Tris (50 mM, pH 7.5)	12.9	11.7	10.6
XvPrx2	10	10	10
DTT (100 mM)	3	3	3
reduced GSH (100 mM)	3	3	3
E			
Trypsin	1.1	2.3	3.4
Tris (50 mM, pH 7.5)	12.9	11.7	10.6
XvPrx2	10	10	10
H_2O_2 (20 mM)	3	3	3
reduced GSH (100 mM)	3	3	3

5.2.5 Crystallisation trials

The XvPrx2 and XvV76C purified proteins were concentrated to 10-20 $mg.ml^{-1}$. A sparse matrix approach (Crystal Screen I and II; Hampton Research, USA) was used for both XvPrx2 and XvV76C protein solutions according to the protocol of Sayed (2001).

The crystallisation procedure involved 24-well tissue culture Linbro plates (ICN Biomedicals, Australia) that were used for vapour-diffusion crystallisation trials. Siliconised cover slips (Hampton Research, USA) were used. Typically, 1 ml of crystallisation solution containing a mixture of precipitant agents and buffer was pipetted into each well of a Linbro plate. The rim of the well was covered with a layer of vacuum grease. A drop of protein solution with a volume ranging from 2-4 µl was pipetted onto the prepared cover slip, and an equal volume of precipitant solution was added. Mechanical mixing of the drop was avoided. The cover slip was carefully inverted and placed on top of the well with gentle pressure applied along the rim to ensure good sealing. Observations were carried out using a stereo-microscope (Leica MZ12, Germany) with a fibre-optic light source to prevent overheating of the crystallisation trials. Sitting drops using microbridges (Hampton Research, USA) were prepared for some of the screens using 3 µl each of protein and precipitant solution. Sitting drops were used for screening the XvPrx2 and XvV76C proteins.

5.2.6 Structural bioinformatics

Comparative modelling of the XvPrx2 and XvV76C proteins were performed based on the known 3-D structure of the poplar type II Prx molecule (PtPrxII, pdb code = 1TP9). The 3-D models of the XvPrx2 and XvV76C proteins were generated by Sayed (University of Western Cape, RSA).

Sequences homologous to the query sequence were determined. Only those proteins that shared a high degree of similarity (> 30%) were used as templates for protein structure determination. The framework was constructed by aligning the query sequence against the best templates. Non-conserved loops and side chains were added and the backbone was completed. The model was refined by energy minimisation, which removes unfavourable non-bonded contacts and optimises bond geometry.

5.2.6 1 Modelling of XvPrx2 and XvV76C

The similarity of XvPrx2 and XvV76C protein sequences to other known Prx sequences were determined using FUGUE (Shi et al., 2001). Multiple 3-D models of both the XvPrx2 and XvV76C proteins were built using MODELLER (Sali & Blundell, 1993) using the X-ray structure of the PtPrxII molecule as template. The model with a combination of lowest energy and lowest number of restraint violations was selected for evaluation.

5.2.6 2 Acquisition and alignment of homologous sequences

Sequences of Prxs of known structure available in the Brookhaven protein data bank (Bernstein et al., 1977) were aligned on the basis of structural features such as solvent accessibility, secondary structure and side chain-main chain hydrogen bonding patterns using COMPARER (Sali & Blundell, 1990; Zhu et al., 1992). Sequences of XvPrx2 and XvV76C were aligned by matching structural templates derived from aligned Prx structures.

5.2.6.3 Energy minimisation and model validation

The models were energy minimised in SYBYL using the AMBER force-field (Weiner et al., 1984). During the initial cycles of energy minimisation the backbone was kept rigid and only side chains were moved. Subsequently, all atoms in the structure were allowed to move during minimisation. This approach kept disturbance of the backbone structure to a minimum. Energy minimisation was performed till all short contacts and inconsistencies in geometry were rectified. During the initial stages of minimisation, the electrostatic term was not included as the main objective was to relieve steric clashes and to rectify bad geometry. The electrostatic term was invoked only at an advanced stage of minimisation. Model evaluation was performed using ProsaII (Sippl, 1993), which uses Ca and Cb atom based potentials to calculate energy profiles for protein structures. The PROCHECK software (Laskowski et al., 1993) was used to evaluate stereo-chemical quality of the final models. Figures for visual analysis of the models were generated using PyMol (www.pymol.org).

5.3 RESULTS

5.3.1 In vitro DNA protection assay

The DNA protection assay using DTT and $FeCl_3$ displayed protection of plasmid DNA against cleavage in the presence of 20 μM purified XvPrx2 (Fig. 5.1A). In the absence of XvPrx2, supercoiled DNA was nicked as evidenced by the larger amounts of open circular DNA. For the negative control, XvPrx2 was replaced with BSA and nicking of supercoiled DNA was observed. In the presence of DTT or $FeCl_3$ only, no nicking of supercoiled DNA was observed.

The in vitro test was repeated using 20 μM XvPrx2 (second batch of purified protein) and XvV76C (Fig. 5.1B). Similarly, in the presence of DTT and $FeCl_3$ only, no nicking of the supercoiled plasmid DNA was observed. Using either XvPrx2 or XvV76C displayed protection to the plasmid DNA. Degraded plasmid DNA was observed in the control reaction in which no protein was added.

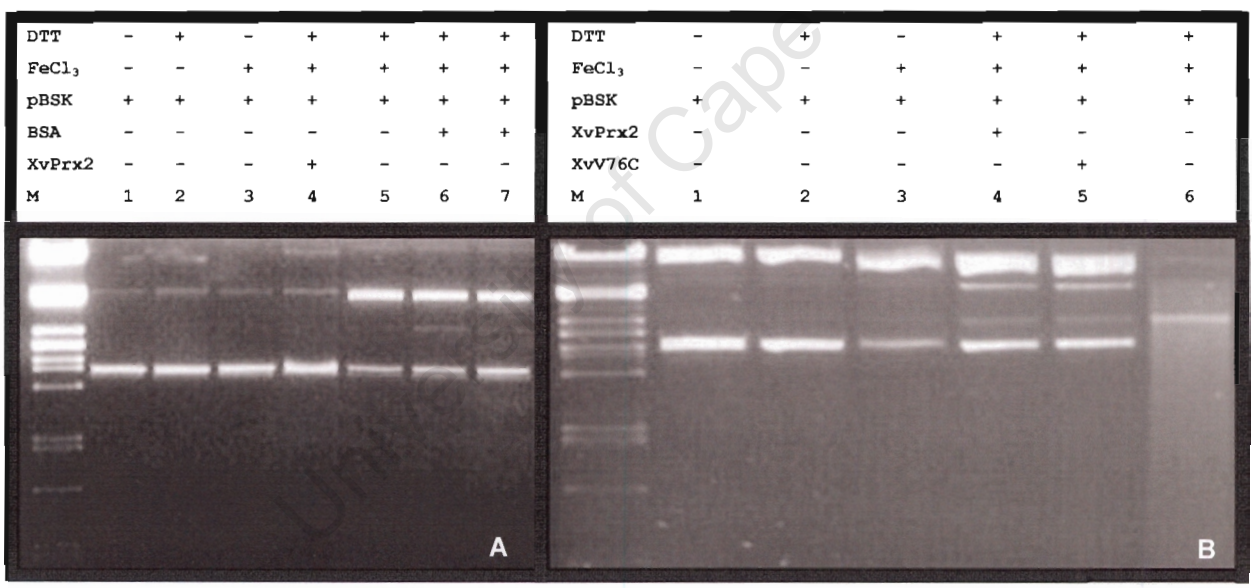

Figure 5.1 In vitro antioxidant activity of XvPrx2 and XvV76C using one microgram of pBluescript plasmid incubated with a mixture of DTT and $FeCl_3$. (A) Assay using XvPrx2, (B) assay using XvV76C and XvPrx2. Plasmid DNA was present in two forms, with the upper band corresponding to the open circular conformation and the lower band to the supercoiled conformation. The untreated pBSK DNA in the second assay (B) comprised a larger amount of open circular DNA. Each lane is annotated with either a "+" referring to presence of reagent or "-" referring to absence of reagent. (M) λ DNA digested with *Pst*I.

5.3.2 In vivo protection assay

For the in vivo assay, the size of the clear zone around the filter disc correlated with the level of sensitivity of cells to H_2O_2, with a smaller radius indicating decreased sensitivity. Bacterial cells expressing XvPrx2 (Fig. 5.2A) displayed marginally lower protection than cells expressing XvV76C (Fig. 5.2B). Wild type *E. coli* cells displayed the greatest sensitivity (Fig. 5.2C) to the peroxide when compared to the cells expressing either XvPrx2 or XvV76C.

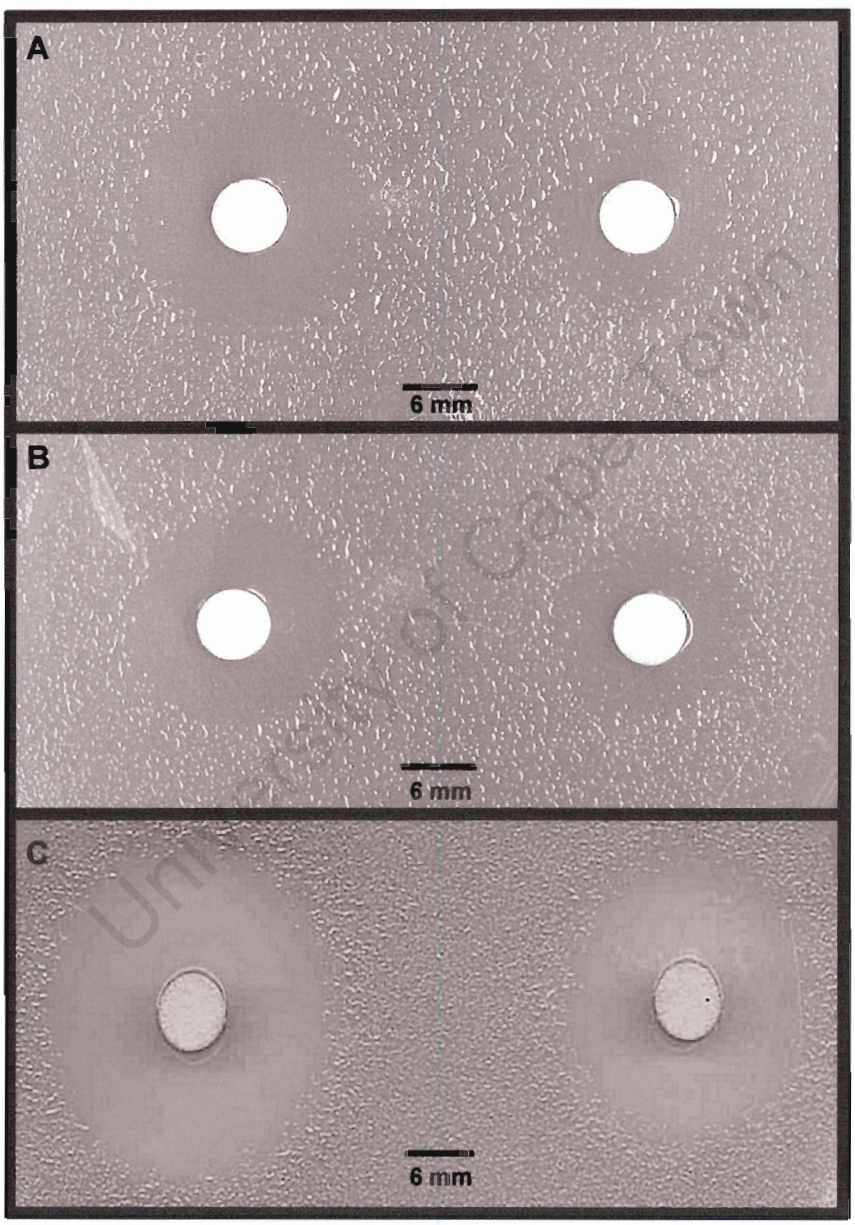

Figure 5.2 In vivo protection assay of *E. coli* cells expressing either (A) XvPrx2, (B) XvV76C or (C) no protein. Disks contained either 5 µl (left) or 2.5 µl (right) of 0.5 M H_2O_2.

5.3.3 Enzyme specificity assays

5.3.3.1 DTT dependent assay using various substrates

The XvPrx2 activity was observed to be maximal when DTT served as electron donor (Fig. 5.3). The highest level of XvPrx2 activity (295 µmol peroxide $min^{-1}.µmol^{-1}$) was observed using H_2O_2 as substrate. The next preferred substrate was t-BOOH with an enzyme activity of 247 µmol peroxide $min^{-1}.µmol^{-1}$. Enzyme activities of 26 and 25 µmol peroxide $min^{-1}.µmol^{-1}$ were observed for POOH and COOH, respectively. The lowest activity (9 µmol peroxide $min^{-1}.µmol^{-1}$) was observed with LOOH as substrate.

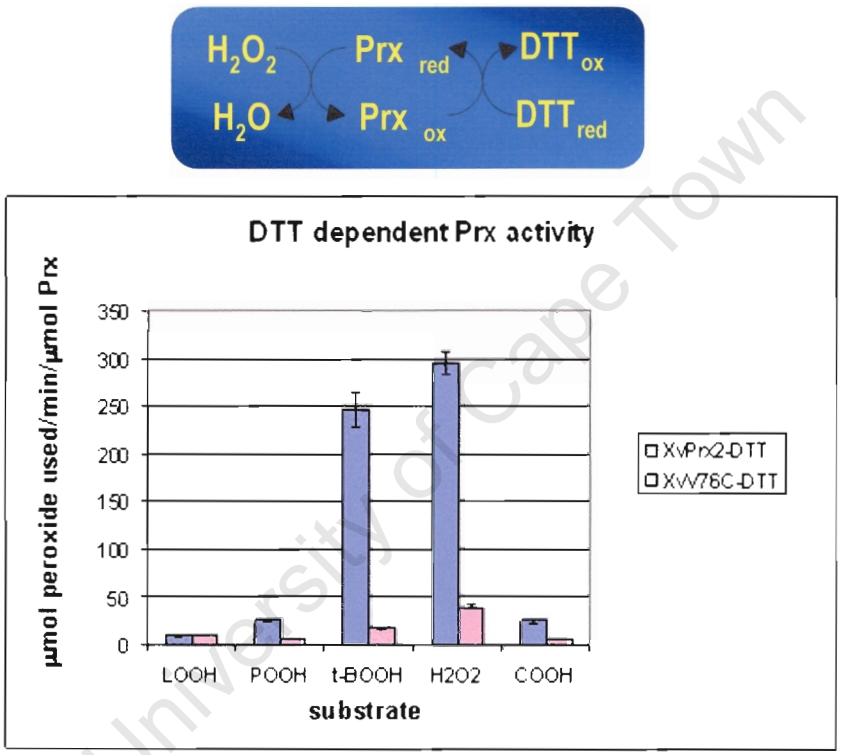

Figure 5.3 The XvPrx2 activity was assessed using various substrates in a non-enzymatic activity assay with 10 mM DTT as electron donor. The substrates included: 200 µM H_2O_2, 250 µM t-BOOH, 200 µM COOH, 400 µM LOOH and 300 µM POOH.

5.3.3.2 GSH dependent assay using H_2O_2 as substrate

The XvPrx2 activity using GSH as electron donor was observed to be low (Fig. 5.4). The Grx protein had no measurable effect on this reaction (data not shown). The XvV76C protein displayed significantly lower activity compared to XvPrx2 for both concentrations of GSH used. Using 10 mM reduced GSH, the XvPrx2 protein displayed an activity of 1.9 µmol peroxide $min^{-1}.\mu mol^{-1}$ as compared to XvV76C, which displayed an activity of 1.2 µmol peroxide $min^{-1}.\mu mol^{-1}$. There appeared to be no significant difference using either 10 mM or 1 mM GSH in combination with XvPrx2. The XvV76C protein had a slightly lower enzyme activity using 1 mM GSH as compared to the activity observed when using 10 mM GSH. This effect was not due to background activity of the DTT reacting with the peroxide as this was also determined (data not shown).

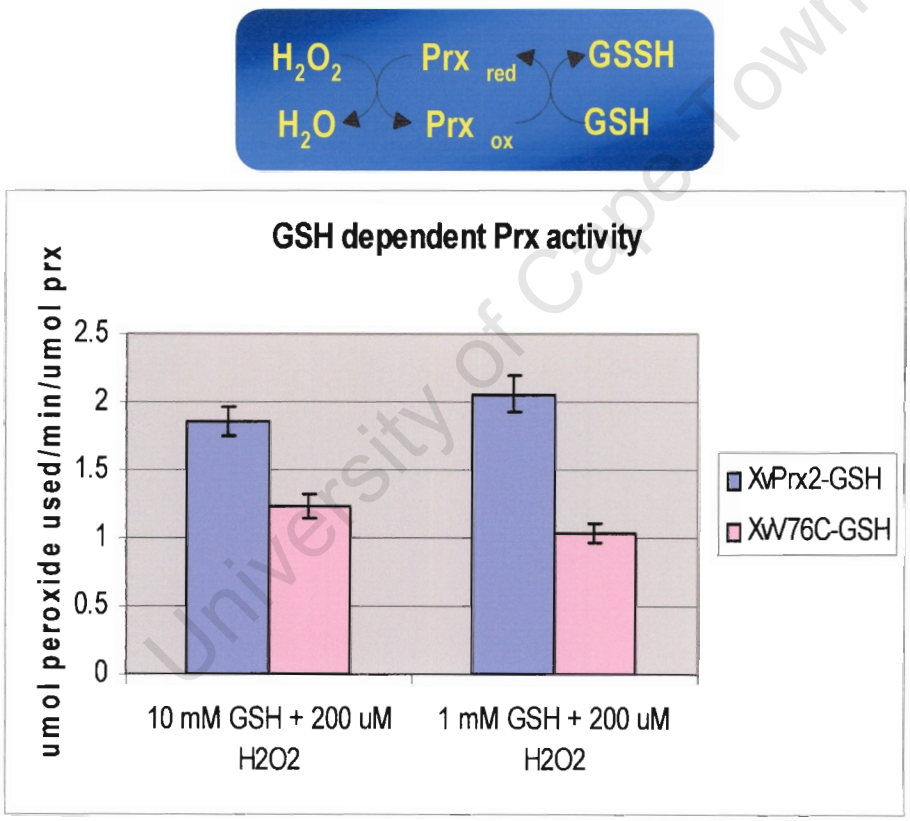

Figure 5.4 GSH dependent Prx activity using 200 µM H_2O_2 displaying reducing activity of 75 µM XvPrx2 and XvV76C in the presence of either 10 mM or 1 mM GSH.

5.3.3.3 Trx dependent assay using various substrates

A 2-15 fold lower enzyme activity was observed using XvPrx2 in combination with $Trx_{E.\ coli}$ as electron donor (Fig. 5.5) depending on substrate utilised (compared to XvPrx2 in combination with DTT; section 5.3.3.1). Highest activity was observed with H_2O_2 as substrate (130 µmol peroxide $min^{-1}.µmol^{-1}$) with t-BOOH (42 µmol peroxide $min^{-1}.µmol^{-1}$) being the next preferred. A low enzyme activity was observed using COOH as substrate (7 µmol peroxide $min^{-1}.µmol^{-1}$) when compared to H_2O_2 and t-BOOH. Using the larger alkyl hydroperoxides (LOOH and POOH), XvPrx2 displayed negligible levels of activity.

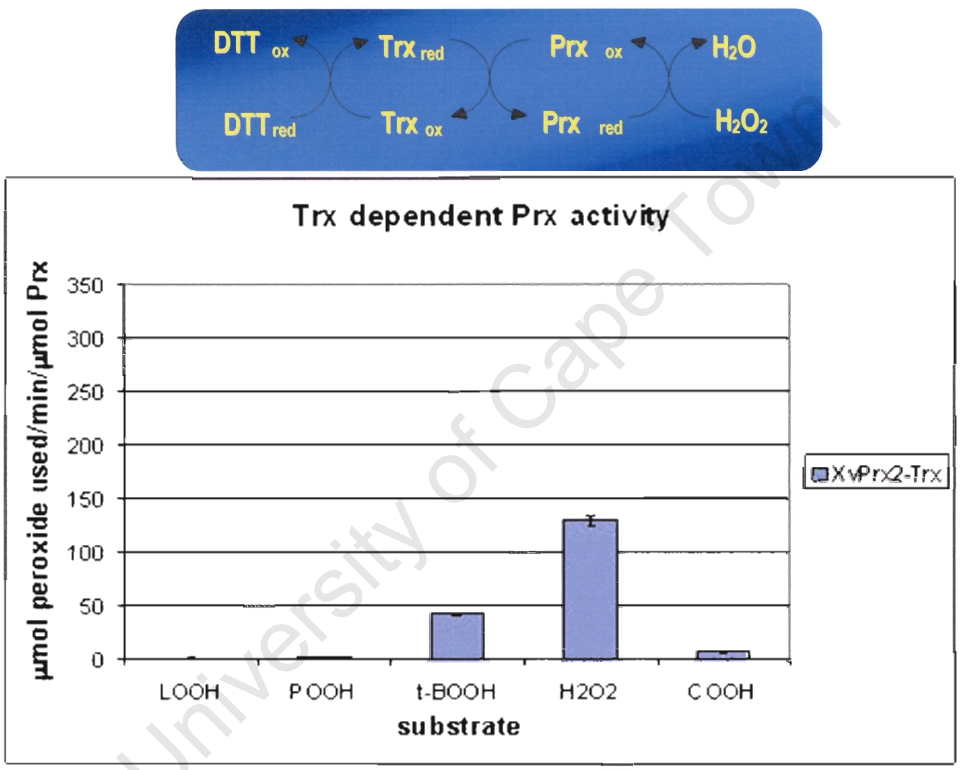

Figure 5.5 The XvPrx2 activity was assessed using various substrates in a non-enzymatic activity assay with 5 µM $Trx_{E.\ coli}$ as electron donor. The substrates included: 200 µM H_2O_2, 250 µM t-BOOH, 200 µM COOH, 400 µM LOOH and 300 µM POOH.

5.3.3.4 Determining the kinetic parameters of XvPrx2

The kinetic parameters of XvPrx2 using DTT as electron donor and varying H_2O_2 concentrations (50-600 μM) as substrate were determined at a constant concentration of XvPrx2 (0.75 μM) and DTT (10 mM). The enzymatic characteristics of XvPrx2 were as follows:

(i) $K_m = 45$ μM

(ii) $V_{max} = 278$ μmol.min^{-1}.mg^{-1}

(iii) $k_{cat} = 6.173 \times 10^3$ s^{-1}

(iv) $k_{cat}/K_m = 0.136 \times 10^3$ μM^{-1}.s^{-1}

5.3.4 Limited proteolysis

Limited proteolysis was used to determine conformational differences between the XvPrx2 and XvV76C proteins. For limited proteolysis, 2 mM and 25 mM final concentrations of H_2O_2 were evaluated. The 25 mM H_2O_2 over-oxidised both proteins and was consequently eliminated. Since, 2 mM H_2O_2 displayed good oxidation of the peroxiredoxin, it was used for all subsequent experiments performed.

Both proteins displayed differing proteolytic profiles (Fig. 5.6) in the presence of DTT (reductant) and H_2O_2 (oxidant). The XvPrx2 and XvV76C proteins were cleaved to 3 and 2 bands, respectively in the presence of DTT. In the presence of H_2O_2, XvPrx2 and XvV76C were observed as 4 and 3 compressed bands, respectively. In the presence of GSH, XvPrx2 retained the monomeric form and no dimer was observed in the presence of H_2O_2. However, for XvV76C the dimer was visible in the presence of H_2O_2.

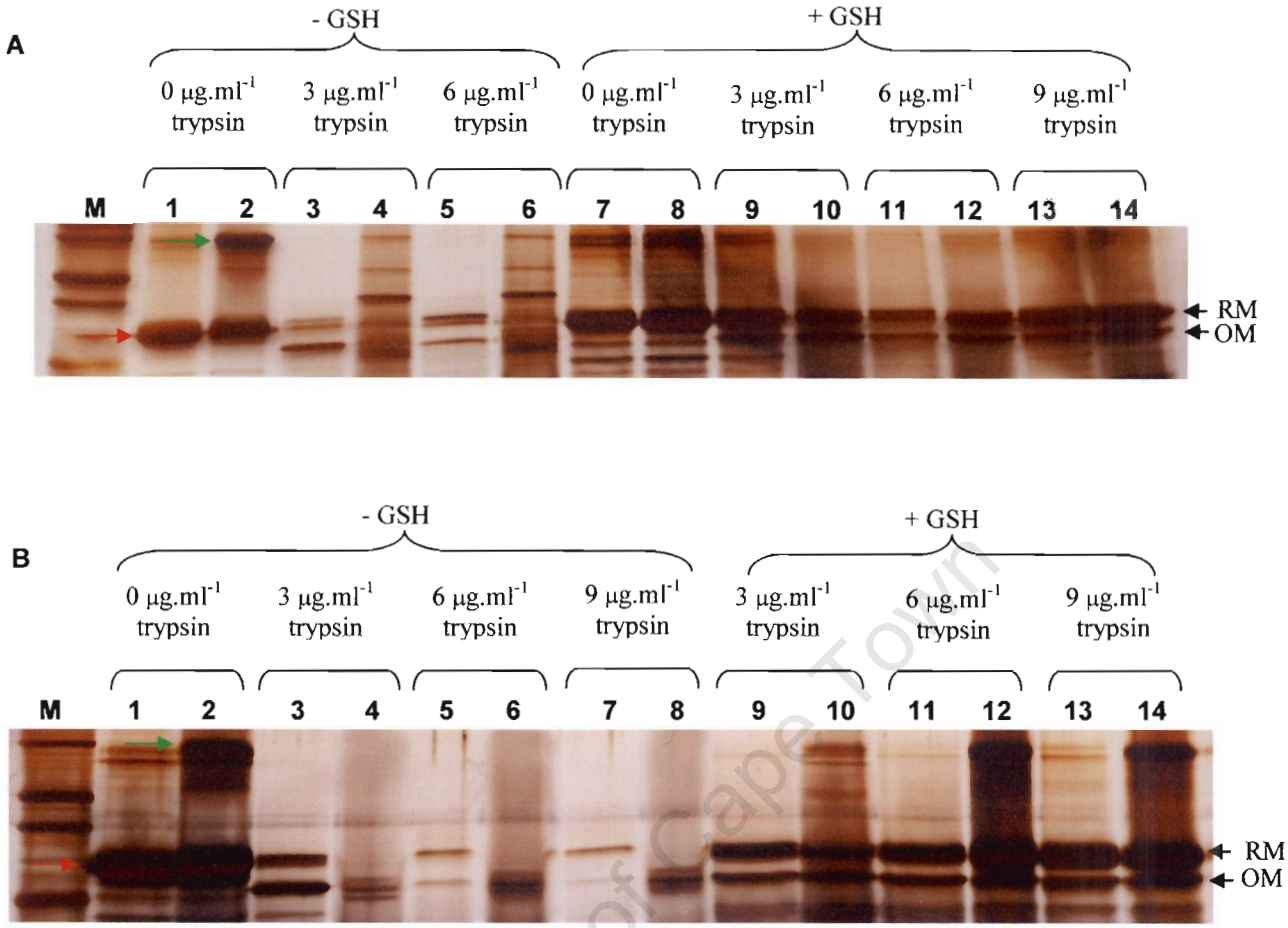

Figure 5.6 Proteolytic profiles of (A) XvPrx2 and (B) XvV76C. Lanes 1, 3, 5, 7, 9, 11, 13: reduced protein using 10 mM DTT. Lanes 2, 4, 6, 8, 10, 12, 14: oxidised protein using 2 mM H_2O_2. The monomer (22 kDa) is represented by a red arrow and the dimer (44 kDa) is represented by a green arrow. RM, reduced monomer; and OM, oxidised monomer.

5.3.5 Crystallisation trials

A sparse matrix strategy was applied for determination of initial crystallisation conditions. All solutions of crystal screen I and II were tested at two different temperatures (4°C and 22°C). A first examination of the drops was performed immediately after they had been set up. In approximately half the drops, the presence of precipitation, ranging from light and fluffy to heavy and dark, was observed. After approximately 24 h, the drops were examined again. Unfortunately, the screens were unsuccessful in yielding crystals for data collection possibly due to heterogeneity of the sample.

5.3.6 Structural bioinformatics

5.3.6 1 The XvPrx2 knowledge-based model

Of the known Prx structures, the poplar, PtPrxII sequence (Echalier et al., 2005) was determined to be the most homologous (ca. 75%) to XvPrx2. The 3-D XvPrx2 model was based on the reduced form of PtPrxII. The XvPrx2 structure created by MODELLER displays 9 β-sheets (purple) and 5 α-helices (blue, Fig. 5.7). The catalytic cysteine was positioned on an α-helice and was orientated towards the interior of the structure.

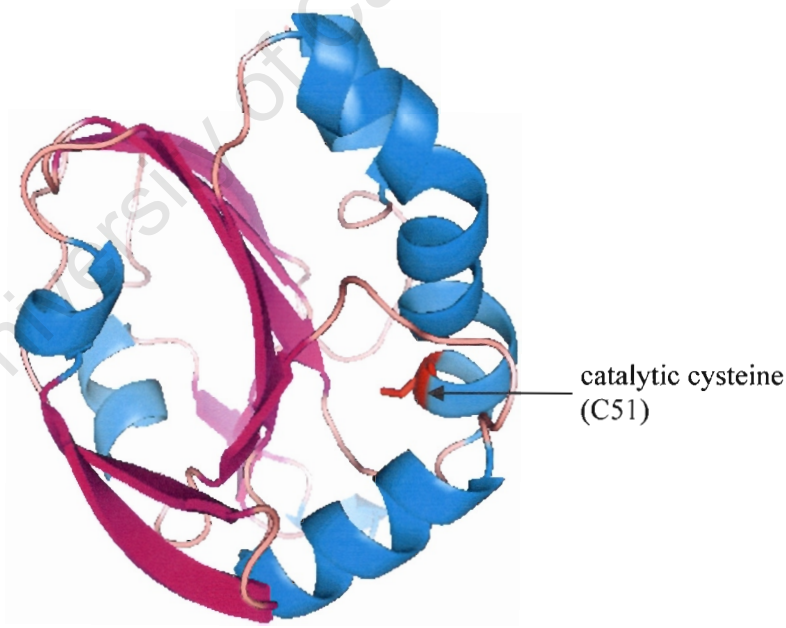

Figure 5.7 Structural model of XvPrx2 displayed as a ribbon. The α-helices are depicted in blue with the β-sheets in purple and loops in salmon. The catalytic cysteine residue is displayed in red.

When aligning the XvPrx2 sequence with homologous proteins from various sources (mammals, yeast, bacteria and trypanosome), three amino acid residues remained strictly conserved. These included the catalytic cysteine (C51), a threonine residue (T48) and a single arginine (R129). The threonine and arginine residues were observed to be in close proximity to the cysteine in the active site, and comprised the catalytic triad (Fig. 5.8).

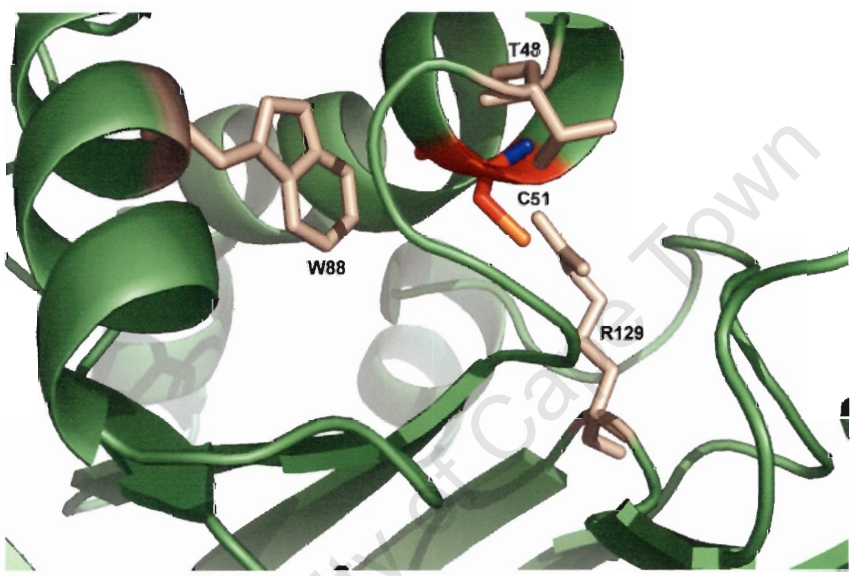

Figure 5.8 Magnified view of the catalytic region of XvPrx2 displaying the side chains of the catalytic triad, including T48, C51 and R129 (represented as sticks with a ribbon rendering of the nearby secondary structural units). The side chain residue W88 is also displayed.

5.3.6.2 The XvV76C knowledge-based model

The model generated for the mutant protein, XvV76C was almost identical to the XvPrx2 structure. Consequently, the properties noted for XvPrx2 were also true for XvV76C (Fig. 5.9). The only difference in the 2 structures involved the second introduced cysteine, which was positioned on a β-sheet towards the centre of the molecule.

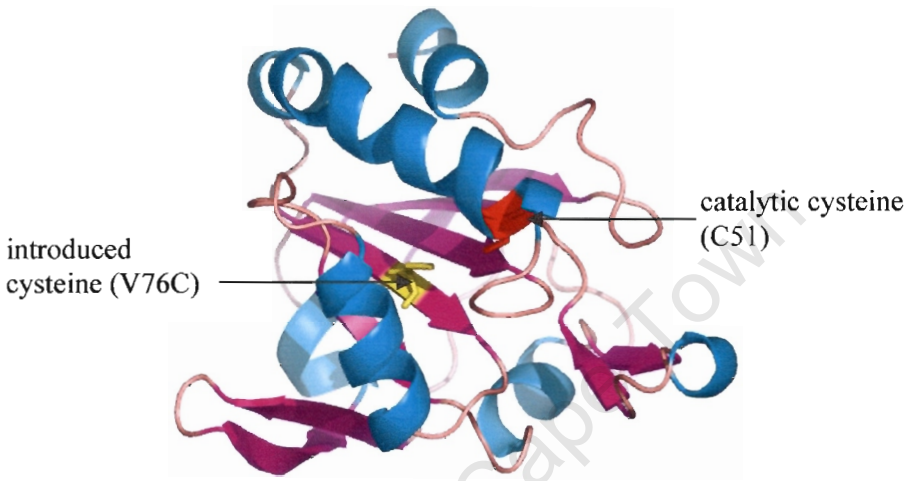

Figure 5.9 Structural model structure of XvV76C displayed as a ribbon. The α-helices are depicted in blue with the β-sheets in purple and the loops in salmon. The catalytic cysteine is displayed in red and the introduced cysteine is displayed in yellow.

The catalytic triad obtained for XvV76C was similar to that obtained for XvPrx2 (Fig. 5.10). The generated structure shows that the threonine and arginine (T48 and R129) residues are in close proximity to the cysteine of the active site. In addition, the introduced cysteine (C76) and tryptophan (W88) were observed to be more distant from the active site. The distance between the two cysteine residues within XvV76C was observed to be 5.41 Å (Fig. 5.11). It was noted that this distance was too large to form a disulphide bond between the two cysteine residues.

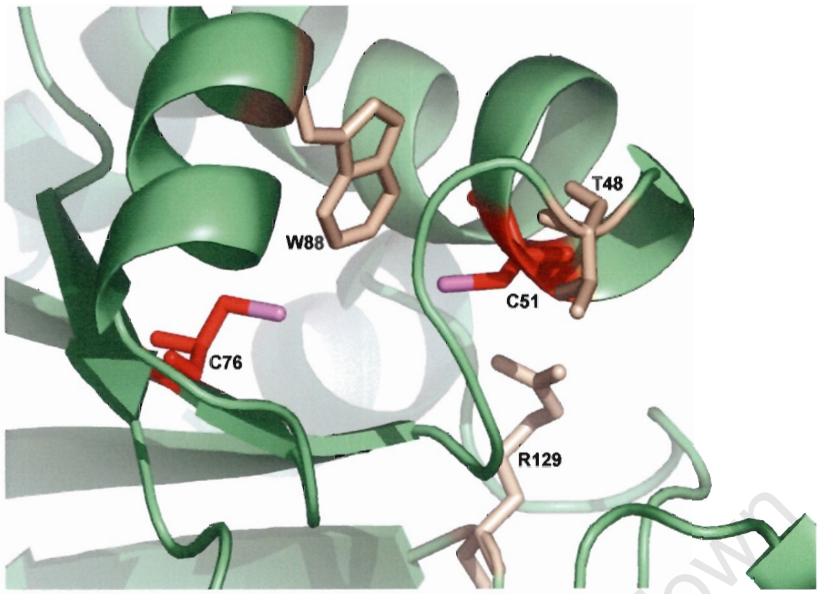

Figure 5.10 Magnified view of the catalytic region of XvV76C displaying the side chains of the catalytic triad, including T48, C51 and R129 (represented as sticks with a ribbon rendering of the nearby secondary structural units). The side chain residues of C76 and W88 are also displayed.

Figure 5.11 Magnified view of the XvV76C structure showing the distance between the two cysteine residues within the molecule.

5.3.7 Structure validation of XvPrx2 and XvV76C

The structure of XvPrx2 was validated using a Ramachandran plot (Figure 5.12). Based on this plot the model appeared to be good fit as 96.9% of the residues were observed to lie within the most favoured regions of the Ramachandran plot, with 3.1% of the residues in the allowed region and 0% of the residues in the outlier region. The XvV76C model displayed a similar result (data not shown).

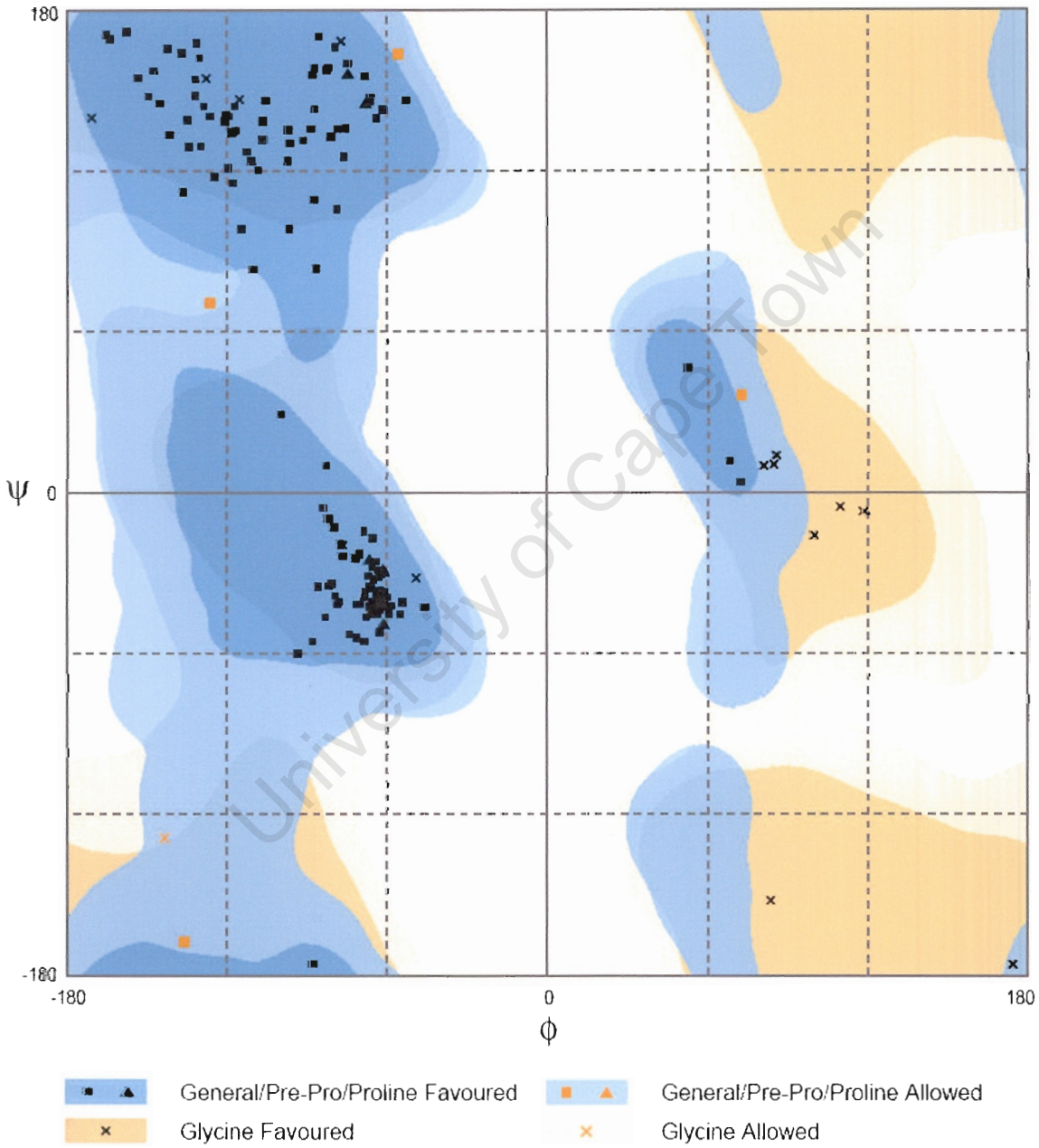

Figure 5.12 Ramachandran plot of XvPrx2 (PROCHECK) showing the favoured and allowed regions of the protein. The most favoured regions are coloured in a dark blue and orange, allowed regions are in light blue and orange, and unfavoured regions in white. Non glycine residues are represented by blocks (■) and triangles (▲) and glycines by crosses (x).

5.4 DISCUSSION

The classical assay of plasmid DNA protection against ROS generated by the Fenton reaction induced by a metal catalysed system is frequently used to test the protection of DNA in the presence of Prx. The first Prx was isolated from yeast by identifying a protein fraction that protected DNA from oxidative breakage and sensitive enzymes from oxidative inactivation in vitro (Kim et al., 1988; Chae et al., 1994a). Supplementation of the assay with a Prx suppressed damage development (Kim et al., 1988). Similarly, XvPrx2 was shown to protect the nicking of plasmid DNA from the harmful generation of ROS in vitro. Interestingly, both XvPrx2 and XvV76C displayed equal levels of protection. This implies that mutating the valine into a cysteine residue does not affect the enzyme at a functional level. Rouhier et al. (2001) showed that although the strong oxidising agents generated by the same in vitro system are able to destroy the plasmid, the addition of recombinant Prx clearly has a protective effect that cannot be reproduced by the addition of similar amounts of an unrelated protein. This lack of protection by an unrelated protein (BSA) was also observed in this study. The authors also showed that when DTT was replaced by reduced ascorbate, the plasmid was not protected and hence degraded. This therefore confirmed the requirement for a thiol as a reductant of Prx. Similarly, the type II Prx from *C. boidinii* (CbPmp20) prevented the O_2 consumption using a thiol metal catalysed oxidation system (DTT/Fe^{3+}/O_2) but did not prevent the O_2 consumption in a non-thiol metal catalysed oxidation system (ascorbate/ Fe^{3+}/O_2). This in turn indicates that type II Prxs may carry a thiol specific peroxidase activity.

Although protection was observed in vitro, it was not certain that this protection would be observed in vivo as well. It appears that native Prxs in *E. coli* were also expressed thus providing basal protection to the cells. Consequently, wild type *E. coli* cells exposed to the stress did show some tolerance. The *E. coli* cells expressing either XvPrx2 or XvV76C displayed increased tolerance in the presence of 0.5 M H_2O_2. However, *E. coli* cells over-expressing XvV76C displayed the highest level of tolerance. This could be due to the fact that more protein was observed to be from cell lines expressing XvV76C when compared to lines expressing XvPrx2 (Chapter 3). Consequently, it is postulated that the increased protection observed is due to increased protein being expressed rather than higher activity.

A very characteristic feature of all the Prx sequences is that one cysteine residue (cysteine 51 in the XvPrx2 enzyme) is strictly conserved. This residue has been shown to be the catalytic one in all Prxs characterised thus far through site-directed mutagenesis (Chae et al., 1994b). However, the other type II Prxs also possess a second cysteine residue at position 76 (XvPrx2 numbering).

Many in vitro studies have addressed the physiological substrate and electron donor specificities of the different Prx homologues. All plant Prxs except 1-Cys Prx have been shown to reduce a broad range of hydroperoxides, from the most simple compound (H_2O_2) to alkyl hydroperoxides such as t-BOOH or COOH, and to more complex phospholipid hydroperoxides such as LOOH and POOH (Brehelin et al., 2003; Rouhier et al., 2004a, b). The catalytic efficiency (k_{cat}/K_m) of the various Prxs is generally around 10^3-10^6 $M^{-1}.s^{-1}$, a value similar to plant Gpxs but low compared to ascorbate peroxidases, catalases or human Gpxs (10^7-10^8 $M^{-1}.s^{-1}$; Hofmann et al., 2002). This low efficiency provides more credence to the notion that Prxs are general acting oxidants rather than possessing specific functions. Furthermore, the low efficiency may also explain the abundance of homologues which would compensate for the reduced efficiency.

Since there are various homologues of Trxs and Grxs, which are located in various cell compartments in plants, the identification of the physiological electron donors of the various Prxs is complex. Considering the fact that the redox potential of the donors or of the Prxs could act as thermodynamic barrier, Trxs should be able to reduce all Prxs but Grxs should be poor reductants of 2-Cys Prx or PrxQ (Rouhier & Jacquot, 2005). In the case of type II Prxs, the SOH should be reduced directly either by Trxs or Grxs and only steric or electrostatic constraints could prevent such an interaction (Rouhier & Jacquot, 2005). In this study it appears that Grx has no effect, with reduced GSH being a poor reductant. The authors stated that in the case of type II Prx and 1-Cys Prx, the SOH should be reduced directly either by Trxs or Grxs and only steric or electrostatic constraints could prevent such an interaction. This is illustrated in vitro by the fact that poplar PtPrxII is able to use various cytosolic Trxs or Grxs as donors (Rouhier et al., 2002), whereas AtPrxIIB is only reduced by Grxs but not Trxs (Brehelin et al., 2003). In this study, however, XvPrx2 was reduced by Trx. The PtPrxII and AtPrxIIF seem to be the only two type II Prxs that accept both Trx as well as Grx as electron donors, whereas mammalian Prxs were shown only to use Trx or an unidentified donor as a proton source (Seo et al., 2000; Rouhier et al., 2001; Finkemeier et al., 2005). However, Rouhier et al. (2005) report that AtPrxIIF was not reduced whatever the Trx used while Finkemeier et al. (2005) show that both Grx and Trx can act as electron donors for AtPrxIIF. This could be due to the fact that a multitude of Trx homologues exist with each probably possessing a different affinity towards a particular Prx. Finkermeier et al. (2005) used AtTrx-o (an *Arabidopsis* thioredoxin) as opposed to Rouhier et al. (2005) whom tested Trxs from poplar, *C. reinhardtii* and *E. coli*.

Rouhier et al. (2001) reported that besides H_2O_2, PtPrxII can be reduced by COOH and t-BOOH with similar efficiencies. However, using both DTT and Trx as electron donors in this study showed that COOH was not a good substrate for XvPrx2. They reported that COOH is clearly detrimental to proteins of the Trx system because the activity recorded drops to about 35% of those obtained with either H_2O_2 or t-BOOH, whereas the activity remained nearly constant with the Grx system.

From the enzyme assays, it was evident that DTT is the best non-enzymatic electron donor with $Trx_{E.\ coli}$ (cytosolic) being the next preferred enzymatic electron donor. The XvPrx2 protein, however, was 1.9 times more active than AtPrxIIC (Horling et al., 2002) with DTT as an electron donor and reduced H_2O_2 at a rate of 295 µmol peroxide $min^{-1}.µmol^{-1}$. A 7.3 times increase in activity was observed when using XvPrx2 in the presence of DTT as electron donor and H_2O_2 as substrate when compared to AtPrxIIF (Finkemeier et al., 2005). Using t-BOOH, COOH, LOOH and POOH as substrates in the presence of DTT, XvPrx2 displayed very high activity rates with a 12 times increase in activity compared with AtPrxIIF.

When using reduced GSH in the presence of Grx negligible activity was recorded for XvPrx2. Interestingly, both XvPrx2 and XvV76C displayed some enzyme activity in the presence of reduced glutathione alone but no increase in activity was observed when Grx was added to the reaction. However, this activity did not change when Grx was removed and it was concluded that neither, XvPrx2 or XvV76C preferred *A. thaliana* chloroplastic Grx as an electron donor. It could be that Grxs are site specific and that a cytosolic Grx should have been used instead of a chloroplastic one. Future enzyme assays should include a cytosolic Grx to determine its efficiency as an electron donor.

Finkemeier et al. (2005) reported that both Trx and Grx could act as electron donors and that reduced GSH alone was capable of acting as an efficient electron donor for AtPrxIIF. Reduced GSH alone was also able to reduce XvPrx2 and Grx had no effect with or without reduced GSH. In contrast, Brehelin et al. (2003) characterised the cytosolic AtPrxIIB and the plastidic AtPrxIIE and reported that both function only in combination with Grx and GSH and 0.5 mM GSH alone had no effect on their activity. Even in the presence of Trx, the turnover number was low and estimated to be $2.9 \times 10^{-2}\ s^{-1}$. Interestingly, in that study, no peroxidase activity was detected when AtPrxIIB was coupled with Trxh2, whereas XvPrx2 was regenerated by the cytosolic $Trx_{E.\ coli}$.

The GSH mediated regeneration of oxidised Prx has been reported for the human 2-Cys Prx (Prdx4) and 1-Cys Prx (Prdx6), as well as for various yeast Prxs (Rhee et al., 2001;

Wood et al., 2003), but not for plant Prx. Two type II Prxs have now been found to be reduced by reduced GSH alone, namely AtPrxIIF (Finkemeier et al., 2005) and XvPrx2 (in this study). In contrast, Finkemeier also reported that the addition of mitochondrial Grx increased the rate of peroxide detoxification ca. 2 fold at 0.5 mM GSH and by 30% only at 5 mM GSH. In this study, the chloroplastic Grx used had no effect. Future studies should employ cytosolic Grxs as electron donors and assess their efficiency.

During both the non-enzymatic and enzymatic assays of XvPrx2 and XvV76C, H_2O_2 was the preferred substrate with t-BOOH being the next preferred and reducing activity decreased with the bulk size of the alkyl residue. Similarly, Finkemeier et al. (2005) reported that a truncated AtPrxIIF (in which the N-terminal targeting pre-sequence was removed) showed the highest rate of activity with H_2O_2. It was also reported that relative reduction rates of t-BOOH, COOH and lipid peroxides were 50, 40 and 2-14% respectively, proving a high preference of AtPrxIIF for H_2O_2 (set as 100%).

Since plants possess many cytosolic Trxs and Grxs, the appropriate method to determine the physiological proton donor for XvPrx2 would be to assess all possible cytosolic Trx and Grx donors present in *X. viscosa* and thereafter draw conclusions. This, however, is not feasible, so only a few selected donors were tested. Since different results were obtained for the orthologues of XvPrx2, it appears that these enzymes differ in their specificity to substrate and electron donors. In this study, the strongest non-enzymatic donor for XvPrx2 and XvV76C was DTT followed by a preference for the enzymatic donor $Trx_{E.\ coli}$, which is cytosolic but with a 2-15 fold lower activity depending on the substrate utilised when compared to DTT.

The kinetic parameters of XvPrx2 using a constant concentration of DTT and XvPrx2 with varying H_2O_2 concentrations were as follows: K_m = 45 µM, V_{max} = 278 µmol.min^{-1}.mg^{-1} protein for H_2O_2, k_{cat} = 6.173 x 10^3 s^{-1} and k_{cat}/K_m (ROOH) = 0.136 x 10^3 µM^{-1}.s^{-1}. Since previous studies used either Grx or Trx as their electron donor, these results could not be compared to data from the other studies (mentioned below). Rouhier et al. (2002) characterised the interactions between PtPrxII and Grx or Trx with a K_m of 2.5 and 3 µM respectively. Horiguchi et al. (2001) determined the Gpx activity of CbPmp20 at 1 mM substrate concentration and 0.1mM GSH. Although the V_{max} measured with each of the three peroxides was similar: 80; 75.8 and 71.4 µmol.min^{-1}mg^{-1} protein for COOH, t-BOOH and H_2O_2, respectively, the Km values for the alkyl hydroperoxides were lower than that for H_2O_2 being 0.562, 0.952 and 2.86 mM for COOH, t-BOOH and H_2O_2, respectively.

From the enzyme activity data it is evident that the addition of a second cysteine residue depressed the activity of XvV76C. This could possibly be due to a structural change that is preventing the accessibility of the active site. However, this possibility is eliminated as modelling data does not show a structural change. It could be that altering the amino acid identity somehow changed the binding efficiency of the active site. In the in vitro assay a similar protection was observed for both XvPrx2 and XvV76C proteins which can be attributed to the equal amounts of proteins used in the assay. However, in the in vivo assay the XvV76C protein displayed a slightly higher degree of protection than the XvPrx2 protein. This increased protection was attributed to an increased production of XvV76C protein as was determined by the increased production of XvV76C as opposed to XvPrx2 from the same culture volume and cell density.

Limited proteolysis displayed different banding profiles for XvPrx2 and XvV76C. In the presence of trypsin under reducing and oxidising conditions distinct banding patterns were observed, which differed between the two proteins. From the data it could be inferred that the two proteins differ in their conformation thus accounting for the differences in proteolytic profiles.

In the presence of trypsin and reduced GSH, XvPrx2 was observed as a monomer only. It could be postulated that GSH reduces XvPrx2 and thus more protein is available in the monomeric form. However, this postulate requires the XvPrx2 molecule to favour the monomeric form in the reduced state, which is not certain. It also appears that when GSH is incubated with XvPrx2 in the presence of trypsin, the susceptibility of the protein to proteolysis is reduced. The protection of XvPrx2 against cleavage might be due to interaction between the XvPrx2 and GSH, which may result in conformational changes thus preventing oxidation as well as cleavage of the protein.

For the XvV76C protein, in the presence of reduced GSH the homo-dimer was observed. It appears that a conformational change occurred as more dimer was visible. This form, although similar to Prxs from *Arabidopsis* in that it possesses 2 cysteines, does not appear to be effectively reduced by reductants such as GSH. This in turn may explain the reduced activity observed for XvV76C during enzyme activity assays. Consequently, ROS generated in the plant would be eliminated at a slower rate as it would not be scavenged as effectively by XvV76C. The loss of the second cysteine therefore possibly represents an evolutionary adaptation to increase the efficiency of the protein.

Structural data is scarce for type II Prxs. Currently, 12 crystal structures of Prxs have been solved in various redox and diverse oligomeric states (Echalier et al., 2005). The superimposition of the poplar PtPrxII with other Prx structures from different subfamilies shows a conserved fold of the protein core and more precisely of the Trx fold. The crystal structure of PtPrxII has been resolved at 1.6 Å resolution in the reduced state. Two similar structures of type II Prxs have been determined, including the human PrxV (Declercq et al., 2001; Evrard et al., 2004) and the Prx domain of hybrid PrxV (Kim et al., 2003) that share 42.4 and 36.5% sequence identity to PtPrxII, respectively. The crystal structures were reported by Echalier et al. (2005) to be very similar and superimposed with a root mean square deviation of 1.0 and 1.1 Å, respectively.

No X-ray crystallography data is currently available on a type II Prx possessing a single cyteine residue. Consequently, the elucidation of the crystal structure of XvPrx2 is vital in understanding the mechanism of action of type II Prxs containing a single cysteine residue. Since the XvPrx2 and XvV76C proteins failed to crystallise, knowledge-based modelling was employed to infer structure and possible function of the Prx. Knowledge-based models of XvPrx2 and XvV76C provide information regarding the catalytic function of XvPrx2 and show whether the XvPrx2 structure differs from that of XvV76C. It was thus important to compare the XvV76C mutant structure (which has 2 cysteine residues similar to most type II Prxs) with that of XvPrx2 to discern whether any structural differences may affect catalytic activity or dimerisation of the protein.

Echalier et al. (2005) report the following from crystallography results of PtPrxII:

(i) the reduced protein is a specific noncovalent homodimer;
(ii) the homodimer interface involves residues strongly conserved in the D type II Prxs, suggesting that all Prxs of this family can homo-dimerise; and
(iii) the two cysteines are too far apart to form an internal disulphide bridge unless considerable rearrangement occurs.

From the knowledge-based models, both XvPrx2 and XvV76C were observed to display a similar structure. Four assumptions were made based on the models:

(i) the XvPrx2 and XvV76C structures are very similar to PtPrxII;
(ii) both proteins display a catalytic triad similar to that in PtPrxII;
(iii) based on distances observed for intermolecular (using the PtPrxII structure) and intramolecular cysteines (using XvV76C), the formation of a disulphide bond was not supported; and

(iv) homo-dimers are due to tertiary interactions, excluding disulphide bonds, occurring between the two Prx molecules.

Since the PtPrxII structure was used as a template for deriving knowledge-based models of XvPrx2 and XvV76C certain implications apply:

(i) there is a bias to the PtPrxII structure and this includes the dimer as well;

(ii) due to model bias, the cysteines in XvPrx2 (intermolecular distance) and XvV76C (intramolecular distance) would be the same distance as PtPrxII; and

(iii) the same tertiary interactions would apply for homo-dimer formation due to model bias.

An important question relates to whether dimerisation is functionally relevant. This question cannot be answered using theoretical modelling alone. In hPrxVI (B Prx), the dimerisation has been proposed to play a role in shaping the active-site pocket (Echalier et al., 2005). Furthermore, the interactions between residues of one monomer and residues of the second monomer in the vicinity of the active site make the entrance narrower (Choi et al., 1998). If dimerisation is important for XvPrx2, then it could be that the mutation in XvV76C may be affecting the dimerisation in such a way that it affects substrate specificity and activity since reduced activity was observed for the mutated protein. However, models derived in this study would not be able to pick up these conformational changes if they are drastic due to model bias to the PtPrxII structure. Real atomic resolution structures (crystallography or NMR) are required to answer this question. Future work would thus involve determining the crystal structure of XvPrx2 and comparing this structure to the known crystal structures of plant type II Prxs containing two cysteine residues.

Chapter 6

General discussion

The Prxs are a family of multifunctional antioxidant thiol-dependent peroxidases that have been identified to be ubiquitous in most organisms. This diversity is reflected in slight evolutionary modifications in sequence and structure built around a common peroxidatic active site. The major functions of Prxs comprise cellular protection against oxidative stress, modulation of intracellular signalling cascades that apply H_2O_2 as a second messenger molecule and regulation of cell proliferation. The type II Prxs are the most abundant Prxs and are found in various cellular compartments. A stress inducible gene, designated *XvPrx2* was selected for analysis in this study due to its apparent role in oxidative stress as a type II Prx. The XvPrx2 protein was determined to be a cytosol localised, stress inducible antioxidant enzyme involved in the protection of nucleic acids by scavenging reactive oxygen species. Besides these characteristics, two further findings were of significance. The first involved the discovery that multiple *XvPrx2* homologues exist in *X. viscosa.* The second is that the XvPrx2 protein is atypical in that it possesses a single cysteine only.

Due to the various findings in this study, additional questions have been generated. These will be answered in future studies and include:

(i) characterising the various *X. viscosa* homologues;
(ii) determining the XvPrx2 crystal structure; and
(iii) evaluating the effect of XvPrx2 in transgenic plants.

The occurrence of multiple *X. viscosa* type II Prx homologues is not a unique scenario. The type II Prx family represents a large and diverse group of genes in the *A. thaliana* genome. These proteins are localised in various cellular compartments including the cytosol (three homologues), mitochondrion (one homologue) and chloroplast (one homologue) while the localisation of the sixth homologue is unknown. Due to their diverse localisation, it appears that these enzymes possess role-specific activities in the various cellular compartments. Three homologues (AtPrxIIB, C and D) are very similar (ca. 94%), differ in only a few amino acids and are all localised in the cytosol. The fact that half the number of type II homologues occur in the cytosol implies that either a larger amount of ROS is generated here or the macromolecules present here are more sensitive to ROS build-up.

It is interesting that plants produce a large number of type II Prxs rather than a single "super antioxidant" enzyme. This could possibly be explained by the incorporation of multiple copies of these genes into the plant genome. Over time these genes would have undergone recombination events eventually leading to divergence and the evolution of the current set of homologues. The fact that these genes occur in plants in abundant numbers points to their presence being advantageous to the cell. Based on the presence of these multiple homologues it is postulated that these enzymes possibly possess:

(i) a broad activity spectrum; or

(ii) similar activity but are merely localised in different cell compartments, with those in the same compartment either being expressed in concert or acting separately.

In addition, the expression of these enzymes may be regulated temporally or in response to specific conditions. The time of expression and the level at which expression of homologues occurs would thus be different.

Consequently, isolating the various type II Prx homologues from *X. viscosa* would allow for greater insight into their function and role. There are three potential options that can be pursued to identify the various homologues. These include:

(i) characterising genomic DNA fragments identified by Southern blot analyses;

(ii) screening the *X. viscosa* genome and transcriptome for homologues using PCR based approaches; and

(iii) isolating and analysing proteins identified by western blot analyses following proteome separation by 2-D gel electrophoresis.

Another more general explanation for the occurrence of multiple homologues would be differing substrate specificities for each enzyme. Thus, once the homologues have been isolated it would be essential to determine these. In the current study, XvPrx2 displayed optimal activity with H_2O_2 and t-BOOH. The other Prx homologues may display increased activity with the larger alkyl-hydroperoxides such as POOH and LOOH. Furthermore, electron donors such as Grx may be able to reduce the other homologues. In this study, it was demonstrated that the XvPrx2 protein displayed a preference for DTT and Trx as electron donors. It is possible that *X. viscosa* possesses multiple homologues of Trxs and Grxs and several antioxidant stress systems. Hence, it is worth investigating the expression levels of each protein and the efficiency of internal electron transfer to reveal the global redox network system in *X. viscosa*.

The absence of a second cysteine distinguishes XvPrx2 from common type II Prx orthologues and the question is why? Since crystal structure experiments were not successful in this study, only postulations can be put forward regarding this. The substrate (namely, ROS) with which the enzyme interacts is the same in both dicots and monocots, therefore this can be excluded. Consequently, the proteins it interacts with, specifically Trx, GSH and Grx, would be the obvious choice for this disparity. It could be that monocots possess a reducing enzyme, which is structurally different from that occurring in dicots thus requiring conformational differences in XvPrx2. However, *O. sativa*, a monocot, possesses type II Prxs with both one and two cysteines and it can be argued that these plants would therefore also possess a Trx that is similar to that occurring in dicots. This would therefore point to the inability or limited efficiency of XvPrx2 to being reduced by Grx and GSH as being central to this debate. Hence, it would be interesting to determine how many cysteines the other *X. viscosa* type II Prx homologues possess and whether they are efficiently reduced by Grx or GSH.

In this study, XvPrx2 displayed higher enzymatic activity with the various substrates when compared to XvV76C, the mutant with two cysteines. This is interesting as the addition of a second cysteine should have increased activity of the protein if it functions in a similar manner to previously characterised orthologues. This observation suggests that by altering the cysteine at position 76 a conformational change occurred, which decreased the protein's catalytic efficiency on various substrates. The absence of the second cysteine therefore appears to be beneficial to this enzyme. It is probable that through evolution it may have lost the second cysteine to better counteract oxidative stress as the enzyme has a marked increase in activity with H_2O_2 and t-BOOH. To understand the activity of XvPrx2, the activity of homologues need to be determined and comparisons can then be drawn.

All current models of activity describe type II Prxs possessing two cysteines. Since XvPrx2 possesses a single cysteine, the current models are not supported. Consequently, a mechanism of action is proposed (Fig. 6.1). The catalytic cysteine is first transformed into a sulphenic acid (SOH) intermediate during interaction with ROS. The SOH residue is reduced directly by bicysteinic Trx forming a transient intermolecular disulphide bridge between the two proteins. The disulphide is therefore reduced by the second cysteine of Trx with XvPrx2 reverting to the functional state. In the event that over-oxidised Prx is generated, it may be reduced by Srx or by other unknown electron donors.

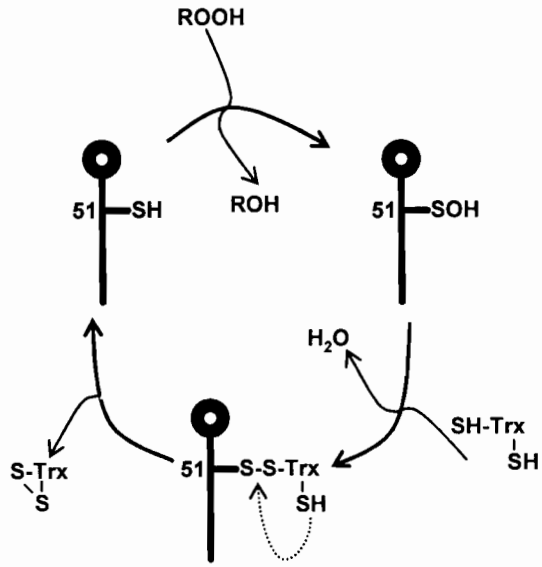

Figure 6.1 Schematic mechanism for XvPrx2 activation and catalytic activity. The catalytic cysteine is oxidised to a SOH intermediate during interaction with ROS. The SOH residue is reduced directly by Trx to form a transient intermolecular disulphide bridge between the two proteins. The disulphide bridge is then reduced by the second cysteine of Trx allowing XvPrx2 to revert to the functional state.

Based on the present study, it appears that generating a crystal structure of XvPrx2 is probably the most significant aspect for future study in order to deduce how this enzyme functions. It is envisaged that this information will provide insights into how the XvPrx2 protein forms oligomers and the actual mechanism of action. In addition to generating a crystal structure, it is necessary to use software based methods to simulate the protein in 3-D in the presence of various ions and substrates to show how the structure of the protein is altered in their presence. Furthermore, it would be possible to observe how the protein behaves in the presence of high and low temperatures and varying pHs.

Finally, molecular and biochemical analyses of maize plants over-expressing XvPrx2 in response to abiotic stress conditions are required. Currently, very little research has been performed on transgenic plants over expressing Prxs. The significance of these studies would be to determine whether over-expression of XvPrx2 in maize confers stress tolerance to these plants. Such transgenic studies would involve plants over-expressing the various Prxs and comparing these to antisense lines as well as control wild type plants.

The Prxs therefore appear to be important proteins for the generation of stress tolerant plants in the near future. However, these proteins should be used in conjunction with other protective proteins as a single protein acting alone may not confer significant stress tolerance. However, an ensemble of genes that function in a concerted fashion to allow the plant to overcome the various stresses would be more advantageous. Furthermore, the analyses of upstream stress inducible promoter regions and their utility to drive stress responsive genes may be an important tool for generating stress tolerant plants with no adverse phenotypic effects as occurs with constitutively expressed genes.

References

Abebe T, Guenzi AC, Martin B & Cushman JC. 2003. Tolerance of mannitol-accumulating transgenic wheat to water stress and salinity. Plant Physiol 131:1748-1755.

Allison SD, Chang B, Randolph TW & Carpenter JF. 1999. Hydrogen bonding between sugar and protein is responsible for inhibition of dehydration-induced protein unfolding. Arch Biochem Biophys 365:289-298.

Altman A. 2003. From plant tissue culture to biotechnology: scientific revolutions, abiotic stress tolerance, and forestry. In vitro Cell Dev Biol 39:75-84.

Altschul SF, Gish W, Miller W, Myers EW & Lipman DJ. 1990. Basic local alignment search tool. J Mol Biol 215:403-410.

Apel K & Hirt H. 2004. Reactive oxygen species: metabolism, oxidative stress, and signal transduction. Ann Rev Plant Biol 55:373-399.

Apse MP, Aharon GS, Snedden WA & Blumwald E. 1999 Salt tolerance conferred by over-expression of a vacuolar Na^+/H^+ antiport in *Arabidopsis*. Science 285:1256-1258.

Ashraf M & Harris PJC. 2004. Potential biochemical indicators of salinity tolerance in plants. Plant Sci 166:3-16.

Baier M & Dietz KJ. 1997. The plant 2-Cys peroxiredoxin BAS1 is a nuclear encoded chloroplast protein. Its expressional regulation, phylogenetic origin, and implications for its specific physiological function in plants. Plant J. 12:179-190.

Baier M & Dietz KJ. 1999. Protective function of chloroplast 2-cysteine peroxiredoxin in photosynthesis. Evidence from transgenic *Arabidopsis*. Plant Physiol 119:1407-1414.

Baier M, Noctor G, Foyer CH & Dietz KJ. 2000. Antisense suppression of 2-cysteine peroxiredoxin in *Arabidopsis* specifically enhances the activities and expression of enzymes associated with ascorbate metabolism but not glutathione metabolism. Plant Physiol 124:823-832.

Bartels D & Salamini F. 2001. Desiccation tolerance in the resurrection plant *Craterostigma plantagineum*. A contribution to the study of drought tolerance at the molecular level. Plant Physiol 127:1346-1353.

Bartels D, Schneider K, Terstappen G, Piatkowski D & Salamini F. 1990. Molecular cloning of abscisic acid modulated genes which are induced during desiccation of the resurrection plant *Craterostigma plantagineum*. Planta 181:27-34.

Bernstein, FC, Koetzle TF, Williams G.J, Meyer EF, Jr. Brice MD, Rodgers JR, Kennard O, Shimanouchi T & Tasumi M. 1977. The Protein Data Bank. A computer-based archival file for macromolecular structures. Eur J Biochem, 80:319-24.

Bewley JD & Black M. 1994. In: Seed physiology of development and germination (2nd ed.). Plenum Press, New York.

Biteau B, Labarre J & Toledano MB. 2003. ATP-dependent reduction of cysteine-sulphinic acid by *S. cerevisiae* sulphiredoxin. Nature 425:980-984.

Blomstedt CK, Gianello RD, Hamill JD, Neale AD & Gaff DF. 1998. Drought- stimulated genes correlated with desiccation tolerance of the resurrection grass *Sporobolus stapfianus*. Plant Growth Regul 24:210-228.

Bohnert HJ, Nelson DE & Jensen RG. 1995. Adaptations to environmental stresses. Plant Cell 7:1099-1111.

Bray EA. 1997. Plant responses to water deficit. Trends Plant Sci 2:48-54.

Brehelin C, Meyer EH, de Souris JP, Bonnard G & Meyer Y. 2003. Resemblance and dissemblance of *Arabidopsis* type II peroxiredoxins: similar sequences for divergent gene expression, protein localization, and activity. Plant Physiol 132:2045-2057.

Broin M & Rey P. 2003. Potato plants lacking the CDSP32 plastidic thioredoxin exhibit overoxidation of the BAS1 2-cysteine peroxiredoxin and increased lipid peroxidation in the thylakoids under photo-oxidative stress. Plant Physiol 132:1335-1343.

Broin M, Cuine S, Eymery F & Rey P. 2002. The plastidic 2-cysteine peroxiredoxin is a target for a thioredoxin involved in the protection of the photosynthetic apparatus against oxidative damage. Plant Cell 14:1417-1432.

Bryk R, Griffin P & Nathan C. 2000. Peroxynitrite reductase activity of bacterial peroxiredoxins. Nature 407:211-215.

Bryk R, Lima CD, Erdjument-Bromage H, Tempst P & Nathan C. 2002. Metabolic enzymes of mycobacteria linked to antioxidant defense by a thioredoxin-like protein. Science 295:1073-1077.

Bustos RO & Romo CR. 1996. Stabilisation of trypsin-like enzymes from Antarctic krill: effect of polyols, polysaccharides and proteins. J Chem Tech Biotech 65:193-199.

Chae HZ, Chung SJ & Rhee SG. 1994a. Thioredoxin-dependent peroxide reductase from yeast. J Biol Chem 269:27670-27678.

Chae HZ, Uhm TB & Rhee SG. 1994b. Dimerization of thiol-specific antioxidant and the essential role of cysteine 47. PNAS 91:7022-7026.

Chang TS, Jeong W, Choi SY, Yu S, Kang SW & Rhee SG. 2002. Regulation of peroxiredoxin I activity by Cdc2-mediated phosphorylation. J Biol Chem 277:25370-25376.

Chaves MM & Oliveira MM. 2004. Mechanisms underlying plant resilience to water deficits: prospects for water-saving agriculture. J Exp Bot 55:2365-2384.

Chen X, Kanokporn T, Zeng Q, Wilkins TA & Wood AJ. 2002. Characterisation of the V-type H((+))-ATPase in the resurrection plant *Tortula ruralis*: accumulation and polysomal recruitment of the proteolipid c subunit in response to salt-stress. J Exp Biol 53:225-232.

Cheong NE, Choi YO, Lee KO, Kim WY, Jung BG, Chi YH, Jeong JS, Kim K, Cho MJ & Lee SY. 1999. Molecular cloning, expression, and functional characterization of a 2Cys-peroxiredoxin in Chinese cabbage. Plant Mol Biol 40:825-834.

Choi HJ, Kang SW, Yang CH, Rhee SG & Rye SE. 1998. Crystal structure of a novel human peroxidase enzyme at 2 Å resolution. Nat Struc Biol 5:400-406.

Choi HYO, Cheong NE, Lee KO, Jung BG, Hong CH, Jeong JH, Chi YH, Kim K, Cho MJ & Lee SY. 1999. Cloning and expression of a new isotype of the peroxiredoxin gene of Chinese cabbage and its comparison to 2 Cys-peroxiredoxin isolated from the same plant. Biochem Biophys Res Comm 258:768-771.

Chopera DR. 2006. Molecular characterization of *XvINO1*, a myo-inositol 1-phosphate synthase from *Xerophyta viscosa*. MSc Thesis. University of Cape Town.

Claiborne A, Yeh JI, Mallett TC, Luba J, Crane EJ, Charrier V & Parsonage D. 1999. Protein-sulfenic acids: Diverse roles for an unlikely player in enzyme catalysis and redox regulation. Biochem 38:15407-15416.

Conrad N. 2005. Characterization of *XVEF* and *XvCaM*, two calcium-binding proteins isolated from the resurrection plant *Xerophyta viscosa*. MSc Thesis. University of Cape Town.

Crowe JH, Carpenter JF & Crowe LM. 1998. The role of vitrification in anhydrobiosis. Ann. Rev. Physiol. 60:73-103.

Crowe JH, Hoekstra FA, Nguyen KH & Crowe LM. 1996. Is vitrification involved in depression of the phase transition temperature in dry phospholipids? Biochim Biophys Acta. 1280:187-196.

Cushman JC & Bohnert HJ. 2000. Genomic approaches to plant stress tolerance. Curr Opin Plant Biol 3:117-124.

Declercq JP, Evrard C, Clippe A, Stricht DV, Bernard A & Knoops B. 2001. Crystal structure of human peroxiredoxin 5, a novel type of mammalian peroxiredoxin at 1.5 Å resolution. J Mol Biol 311:751-759.

Dellaporta SL, Wood J & Hicks JB. 1983. A plant DNA minipreparation: version II. Plant Mol Biol Report 1:19-21.

Denby K & Gehring C. 2005. Engineering drought and salinity tolerance in plants: lessons from genome-wide expression profiling in *Arabidopsis*. Trends Biotechnol 23:547-552.

Desikan R, Cheung M-K, Bright J, Henson D, Hancock J & Neill S. 2004. ABA, hydrogen peroxide and nitric oxide signalling in stomatal guard cells. J Exp Bot 55:205-212.

Devon RS, Porteous DJ & Brokkes AJ. 1995. Splinkerettes- improved vectorettes or greater efficiency in PCR walking. Nucleic Acids Res 23:1644-1645.

Dietz KJ. 2003. Plant Peroxiredoxins. Ann Rev Plant Biol 54:93-107.

Dietz KJ, Horling F, König J & Baier M. 2002. The function of the chloroplast 2-cysteine peroxiredoxin in peroxide detoxification and its regulation. J Exp Bot 53:1321-1329.

Dunwell JM. 2000. Transgenic approaches to crop improvement. J Exp Bot 51:487-496.

Echalier A, Trivelli X, Corbier C, Rouhier N, Walker O, Tsan P, Jacquot JP, Aubry A, Krimm I & Lancelin JM. 2005. Crystal structure and solution NMR dynamics of a D (type II) peroxiredoxin glutaredoxin and thioredoxin dependent: a new insight into the peroxiredoxin oligomerism. Biochem 44:1755-1767.

Ekmekci Y, Bohms A, Thomson JA & Mundree SG. 2005. Photochemical and antioxidant responses in the leaves of *Xerophyta viscosa* Baker and *Digitaria sanguinalis* L. under water deficit. Z Naturforsch [C].60:435-443.

Evrard C, Capron A, Marchand C, Clippe A, Wattiez R, Soumillion P, Knoops B & Declercq JP. 2004. Crystal structure of a dimeric oxidized form of human peroxiredoxin 5. J Mol Biol 337:1079-1090.

Farrant JM. 2000. A Comparison of Mechanisms of Desiccation Tolerance Among Three Angiosperm Resurrection Plant Species. Plant Ecol 151:29-39.

Farrant JM & Sherwin HW. 1997. Mechanisms of desiccation tolerance in seeds and resurrection plants. In: Progress in seed research (Taylor AG, Roos E & Huang XLK, eds.). Cornell University Press, New York, pp 109-120.

Farrant JM, Berjak P, Walters C & Pammenter NW. 1997. Subcellular organisation and metabolic activity in seeds which develop different degrees of tolerance to water loss. Seed Sci Res 7:135-144.

Farrant JM, Cooper K, Kruger LA & Sherwin HW. 1999. The effect of drying rate on the survival of three desiccation tolerant angiosperm species. Ann Bot 84:371-379.

Felsenstein J. 1985. Confidence limits on phylogenies: An approach using the bootstrap. Evolution 39:783-791.

Finkemeier I, Goodman M, Lamkemeyer P, Kandlbinder A, Sweetlove LJ & Dietz KJ. 2005. The mitochondrial type II peroxiredoxin F is essential for redox homeostasis and root growth of *Arabidopsis thaliana* under stress. J Biol Chem 280:12168-12180.

Fisher AB, Dodia C, Manevich Y, Chen JW & Feinstein SI. 1999. Phospholipid hydroperoxides are substrates for non-selenium glutathione peroxidase. J Biol Chem 274:21326-21334.

Flowers T. 2004. Improving crop salt tolerance. J Exp Bot 55:307-319.

Foyer CH & Noctor G. 2000. Oxygen processing in photosynthesis: regulation and signalling. New Phytol 146:359-388.

Foyer CH & Noctor G. 2003. Redox sensing and signalling associated with reactive oxygen in chloroplasts, peroxisomes and mitochondria. Physiol Plantarum 119:355-364.

Furini A, Koncz C, Salamini F & Bartels D. 1997. High level transcription of a member of a repeated gene family confers dehydration tolerance to callus tissue. Eur Mol Biol Org J 16:3599-3608.

Gaff DF. 1971. Desiccation tolerant plants in Southern Africa. Science 174:1033-1034.

Gaff DF. 1977. Desiccation tolerant vascular plants in southern Africa. Oecologia 31:95-104.

Gaff DF. 1987. Desiccation tolerant plants in South America. Oecologia 74:133-136.

Garg AK, Kim J-K, Owens TG, Ranwala AP, Choi YD, Kochian LV & Wu RJ. 2002. Trehalose accumulation in rice plants confers high tolerance levels to different abiotic stresses. PNAS 99:15898-15903.

Garwe D, Thomson JA & Mundree SG. 2003. Molecular characterization of *XVSAP1*, a stress responsive gene from the resurrection plant *Xerophyta viscosa* Baker. J Exp Bot 54:191-201.

Goyer A, Haslekas C, Miginiac-Maslow M, Klein U, Le Marechal P, Jacquot JP & Decottignies P. 2002. Isolation and characterization of a thioredoxin-dependent peroxidase from *Chlamydomonas reinhardtii*. Eur. J. Biochem. 269:272-282.

Hamann M, Zhang T, Hendrich S & Thomas JA. 2002. Quantitation of protein sulfinic and sulfonic acid, irreversibly oxidised protein cysteine sites in cellular proteins. Methods Enzymol 348:146-156.

Hartung W, Schiller P & Dietz KJ. 1998. Physiology of poikilohydric plants. Cell Biol and Physiology. Progress in Bot 59:299-327.

Hasegawa PM, Bressan RA, Zhu JK & Bonhert HJ. 2000. Plant cellular and molecular responses to high salinity. Ann Rev Plant Physiol Plant Mol Biol 51:463-499.

Haseloff J, Dormand E-L & Brand AH. 1999. Methods in molecular biology. In: Confocal Microscopy Methods and Protocols (Paddock S ed.) Humana Press, Totowa.

Haslekas C, Stacy RAP, Nygarrd V, Culianez-Macia FA & Aalen RB. 1998. The expression of a peroxiredoxin antioxidant gene *AtPer1* in *Arabidopsis thaliana* is seed-specific and related to dormancy. Plant Mol Biol 36:833-845.

Haslekas C, Grini PE, Nordgard SH, Thorstensen T, Viken MK, Nygaard V & Aalen RB. 2003b. *ABI3* mediates expression of the peroxiredoxin antioxidant *AtPER1* gene and induction by oxidative stress. Plant Mol Biol 53:313-326.

Haslekas C, Viken MK, Grini PE, Nygaard V, Nordgard SH, Meza TJ & Aalen RB. 2003a. Seed 1-cys Peroxiredoxin Antioxidants Are Not involved in Dormancy, But contribute to Inhibition of Germination during stress. Plant Physiol 133:1148-1157.

Hetherington AM. 2001. Guard cell signalling. Cell 107:711-714.

Hirotsu S, Abe Y, Okada K, Nagahara N, Hori H, Nishino T & Hakoshima T. 1999. Crystal structure of a multifunctional 2-Cys peroxiredoxin heme-binding protein 23 kDa/proliferation-associated gene product. PNAS 96:12333-12338.

Hofmann B, Hetcht H-J & Flohé L. 2002. Peroxiredoxins. Biol Chem 383:347-364.

Hoisington D, Khairallah M, Reeves T, Ribaut J-M, Skovmand B, Taba S & Warburton M. 1999. Plant genetic resources: What can they contribute toward increased crop productivity? PNAS 96:5937-5943.

Holmberg N & Bülow L. 1998. Improving stress tolerance in plants by gene transfer. Trends in Plant Sci 3:61-66.

Horiguchi H, Yurimoto H, Kato N & Sakai Y. 2001. Antioxidant system within yeast peroxisome. Biochemical and physiological characterization of CbPmp20 in the methylotrophic yeast *Candida boidinii*. J Biol Chem 276:14279-14288.

Horling F, Baier M & Dietz KJ. 2001. Redox-regulation of the expression of the peroxide-detoxifying chloroplast 2-cys peroxiredoxin in the liverwort *Riccia fluitans*. Planta 214:304-313.

Horling F, König J & Dietz KJ. 2002. Type II C, a member of the peroxiredoxin family of *Arabidopsis thaliana*: its expression and activity in comparison with other peroxiredoxins. Plant Physiol Biochem 40:491-499.

Horling F, Lamkemeyer P, König J, Finkemeier I, Kandlbinder A, Baier M & Dietz KJ. 2003. Divergent light-, ascorbate, and oxidative stress dependent regulation of expression of the peroxiredoxin gene family in *Arabidopsis*. Plant Physiol 131:317-325.

Hsieh TH, Lee JT, Yang PT, Chiu LH, Charng YY, Wang YC & Chan MT. 2002. Heterology expression of the *Arabidopsis* C-Repeat/Dehydration Response Element Binding Factor 1 gene confers elevated tolerance to chilling and oxidative stress in transgenic tomato. Plant Physiol 129:2086-2094.

Iljin WS. 1957. Drought resistance in plants and physiological processes. Ann Rev Plant Physiol 3:341-363.

Immenschuh S & Baumgart-Vogt E. 2005. Peroxiredoxins, oxidative stress, and cell proliferation. Antioxid Redox Sign 7:768-777.

Ingram J & Bartels D. 1996. The molecular basis of dehydration tolerance in plants. Ann Rev Plant Physiol Mol Biol 47:377-403.

Ishitani M, Liu J, Halfter U, Kim CS, Shi W & Zhu JK. 2000. SOS3 Function in Plant Salt Tolerance Requires N-Myristoylation and Calcium Binding. Plant Cell 12:1667-1677.

Iturriaga G, Schneider K, Salamini F & Bartels D. 1992. Expression of desiccation-related proteins from the resurrection plant *Craterostigma plantagineum* in transgenic tobacco. Plant Mol Biol 20:555-558.

Jacobson FS, Morgan RW, Christman MF & Ames BN. 1989. An alkyl hydroperoxide reductase from *Salmonella typhimurium* involved in the defence of DNA against oxidative damage. Purification and properties. J Biol Chem 264:1488-1496.

Jain RK & Selvaraj G. 1997. Molecular genetic improvement of salt tolerance in plants. Biotechnol Ann Rev 3:245-267.

Jiang L, Downing WL, Bazzczynski CL & Kermode AR. 1995. The 5' flanking regions of vicilin and napin storage protein genes are down-regulated by desiccation in transgenic tobacco. Plant Physiol 107:1439-1449.

Jin S, Chen CCS & Plant AL. 2000. Regulation by ABA of osmotic stress-induced changes in protein synthesis in tomato root. Plant Cell Environ 23:51-60.

Johnson DR, Bhatnagar RS, Knoll LJ & Gordon JI. 1994. Genetic and biochemical studies of protein N-myristoylation. Ann Rev of Biochem 63:869-914.

Jönsson TJ, Murray MS, Johnson LC, Poole LB & Lowther TW. 2005. Structural basis for the retroreduction of inactivated peroxiredoxins by human sulfiredoxin. Biochem 44:8634-8642.

Kampranis SC, Bates AD & Maxwell A. 1999 A model for the mechanism of strand passage by DNA gyrase. PNAS 96:8414-8419.

Kampranis SC & Maxwell A. 1998. Hydrolysis of ATP at only one GyrB subunit is sufficient to promote supercoiling by DNA gyrase. J Biol Chem 273:26305-26309.

Kandlbinder A, Finkemeier I, Wormuth D, Hanitzsch M & Dietz KJ. 2004. The antioxidant status of photosynthesizing leaves under nutrient deficiency: redox regulation, gene expression and antioxidant activity in *Arabidopsis thaliana*. Plant Physiol 120:63-73.

Kang SW, Baines IC & Rhee SG. 1998a. Characterisation of a mammalian peroxiredoxin that contains one conserved cysteine. J Biol Chem 273:6303-6311.

Kang SW, Chae HZ, Seo MS, Kim K, Ivan CB & Rhee SG. 1998b. Mammalian peroxiredoxin isoforms can reduce hydrogen peroxide generated in response to growth factors and tumour necrosis factor-alpha. J Biol Chem 273:6297-6302.

Karpinska B, Wingsle G & Karpinski S. 2000. Antagonistic effects of hydrogen peroxide and glutathione on acclimation to excess excitation energy in *Arabidopsis*. IUBMB 50:21-26.

Kasuga M, Liu Q, Setsuko M, Yamaguchi-Shinozaki K & Shinozaki K. 1999. Improving plant drought, salt, and freezing tolerance by gene transfer of a single stress-inducible transcription factor. Nat Biotechnol 17:287-291.

Kim K, Kim IH, Lee KY, Rhee SG & Stadtman ER. 1988. The isolation and purification of a specific protector protein which inhibits enzyme inactivation by a thiol/Fe(III)/O_2 mixed-function oxidation system. J Biol Chem 263:4704-4711.

Kim SJ, Woo JR, Hwang YS, Jeong DG, Shin DH, Kim K & Ryu SE. 2003. The tetrameric structure of *Haemophilus influenza* hybrid Prx5 reveals interactions between electron donor and acceptor proteins. J Biol Chem 278:10790-10800.

Kiyosue T, Yamaguchi-Shinozaki K & Shinozaki K. 1994. ERD15, a cDNA for a Dehydration-Induced Gene from *Arabidopsis thaliana*. Plant Physiol 106:1707.

Klimowski L, Chandrashekar R & Tripp CA. 1997. Molecular cloning, expression and enzymatic activity of a thioredoxin peroxidase from *Dirofilaria immitis*. Mol Biochem Parasitol 90:297-306.

Kluge C, Seidel T, Bolte S, Sharma SS, Hanitzsch M, Satiat-Jeunemaitre B, Ross J, Sauer M, Golldack D & Dietz KJ. 2004. Subcellular distribution of the V-ATPase complex in plant cells, and in vivo localisation of the 100 kDa subunit VHA-a within the complex. BMC Cell Biol 13:5-29.

Kong W, Shiota S, Shi YX, Nakayama H & Nakayama K. 2000. A novel peroxiredoxin of the plant *Sedum lineare* is a homologue of *Escherichia coli* bacterioferritin co-migratory protein (Bcp). Biochem J 351:107-114.

König J, Baier M, Horling F, Kahmann U, Harris G, Schurmann P & Dietz KJ. 2002. The plant-specific function of 2-Cys peroxiredoxin-mediated detoxification of peroxides in the redox hierarchy of photosynthetic electron flux. PNAS 99:5738-5743.

König J, Lotte K, Plessow R, Brockhinke A, Baier M & Dietz KJ. 2003. Reaction mechanism of plant 2-Cys peroxiredoxin. Role of the C terminus and the quaternary structure. J Biol Chem 278:24409-4420.

Kruft V, Eubel H, Jansch L, Werhahn W & Braun HP. 2001. Proteomic approach to identify novel mitochondrial proteins in *Arabidopsis*. Plant Physiol 127:1694-1710.

Kumar S, Tamura K & Nei M. 2004. MEGA3: Integrated software for molecular Evolutionary Genetics Analysis and sequence alignment. Brief Bioinform 5:150-163.

Kyte J & Doolittle RF. 1982. A simple method for displaying the hydropathic character of a protein. J Mol Biol 157:105-132.

Laporte MM, Shen B & Tarczynski MC. 2002. Engineering for drought avoidance: expression of maize NADP-malic enzyme in tobacco results in altered stomatal function. J Exp Bot 53:699-705.

Laskowski RA, Moss DS & Thornton JM. 1993. Main-chain bond lengths and bond angles in protein structures. J Mol Biol 231:1049-1067.

Lee M-Y. 2005. *XvERD15*, an early-responsive gene to stress from *Xerophyta viscosa*. MSc Thesis. University of Cape Town.

Lee SP, Hwang YS, Kim YJ, Kwon KS, Kim HJ, Kim K & Chae HZ. 2001. Cyclophilin a binds to peroxiredoxins and activates its peroxidase activity. J Biol Chem 276:29826-29832.

Lee KO, Jang HH, Jung BG, Chi YH, Lee JY, Choi YO, Lee JR, Lim CO, Cho MJ & Lee SY. 2000. Rice 1-Cys-peroxiredoxin over-expressed in transgenic tobacco does not maintain dormancy but enhances antioxidant activity. FEBS Lett 486:103-106.

Levine A, Tenhaken R, Dixon R, Lamb C. 1994. H_2O_2 from the oxidative burst orchestrates the plant hypersensitive disease resistance response. Cell 79:583-593.

Loggini B, Scartazza A, Brugnoli E & Navari-Izzo F. 1999. Antioxidative defence system, pigment composition and photosynthetic efficiency in two wheat cultivars subjected to drought. Plant Physiol 119:1091-1099.

Lopez-Molina L, Mongrand S, Kinoshita N & Chua NH. 2003. AFP is a novel negative regulator of ABA signalling that promotes ABI5 protein degradation. Gene Dev 17:410-418.

Maiorino M, Gregolin C & Ursini F. 1990. Phospholipid hydroperoxide glutathione peroxidase. Methods Enzymol 186:448-457.

Marais S, Thomson JA, Farrant JM, Mundree SG. 2004. *XvVHA-c''1*- a novel stress-responsive V-ATPase subunit c'' homologue isolated from the resurrection plant *Xerophyta viscosa*. Physiol Plantarum 122:54-61.

McAinsh MR, Clayton H, Mansfield TA & Hetherington AM. 1996. Changes in stomatal behaviour and guard cell cytosolic free calcium in response to oxidative stress. Plant Physiol 111:1031-1042.

McKersie BD, Bowley SR, Harjanto E & Leprince O. 1996. Water-deficit tolerance and field performance of transgenic alfalfa overexpressing superoxide dismutase. Plant Physiol 111:1177-1181.

Meyer Y, Vignols F & Reichheld JP. 2002. Classification of plant thioredoxins by sequence similarity an intron position. Methods Enzymol 347:394-402.

Mitra J. 2001. Genetics and genetic improvement of drought resistance in crop plants. Curr Sci 80:758-763.

Mowla SB. 2005. Molecular characterization of *XvPer1*, a novel antioxidant enzyme from the resurrection plant *Xerophyta viscosa*, and AC3, a LEA-like protein from *Arabidopsis thaliana*. PhD Thesis. University of Cape Town.

Mowla SB, Thomson JA, Farrant JM & Mundree SG. 2002. A novel stress-inducible antioxidant enzyme identified from the resurrection plant *Xerophyta viscosa* Baker. Planta 215:716-726.

Mundree SG & Farrant JA. 2000. Some physiological and molecular insights into the mechanisms of desiccation tolerance in the resurrection plant *Xerophyta viscosa* Baker. In Plant Tolerance to Abiotic Stress in Agriculture: Role of Genetic Engineering (Cherry JH, Locy RD & Rychter A, eds.). Kluwer Academic Publishers, The Hague, pp. 201-222.

Mundree SG, Whittaker A, Thomson JA & Farrant JM. 2000. An aldolase reductase homolog from the resurrection plant *Xerophyta viscosa* Baker. Planta 211:693-700.

Mundree SG, Iyer R, Baker B, Conrad N, Davis EJ, Govender K, Maredza AT & Thomson JA. 2006. Prospects for using genetic modification to engineer drought tolerance in crops. In: Plant Biotechnology: Current and future applications of genetically modified crops (Halford N, ed.). John Wiley and Sons, Chichester, pp. 193-205.

Mundree SG, Baker B, Mowla S, Peters S, Marais S, Vander Willigin C, Govender K, Maredza A, Muyanga S, Farrant JM & Thomson JA. 2002. Physiological and molecular insights into drought tolerance. Afr J Biotechnol 1:28-38.

Munns R. 2002. Comparative physiology of salt and water stress. Plant Cell Environ 25:239-250.

Munro S & Pelham H. 1985. What turns on heat shock genes? Nature 317:47747-47748.

Neill SJ, Desikan R & Hancock JT. 2003. Nitric oxide signalling in plants. New Phytol 159:11-35.

Neumann PM. 1995. The role of cell wall adjustment in plant resistance to water deficits. Crop Sci 35:1258-1266

Oberschall A, Deak M, Torok K, Sass L, Vass I, Kovacs I, Feher A, Dudits D & Horvath GV. 2000. A novel aldose/aldehyde reductase protects transgenic plants against lipid peroxidation under chemical and drought stresses. Plant J 24:437-446.

Oliver MJ, Wood AJ & O'Mahony P. 1998. "To dryness and beyond" – preparation for the dried state and rehydration in vegetative desiccation-tolerant plants. Plant Growth Regul 24:193-201.

Overington J, Johnson MS, Sali A &d Blundell TL. 1990 Tertiary structural constraints on protein evolutionary diversity: templates, key residues and structure prediction. Proc R Soc Lond B Biol Sci 241:132-145.

Pastori GM & Foyer CH. 2002. Common components, networks, and pathways of cross-tolerance to stress. The central role of 'redox' and abscisic acid-mediated controls. Plant Physiol 129:460-468.

Pei ZM, Murata Y, Benning G, Thomine S, Klusener B, Allen GJ, Grill E & Schroeder JI. 2000. Calcium channels activated by hydrogen peroxide mediate abscisic acid signalling in guard cells. Nature 406:731-734.

Peng Y, Yang PH, Guo Y, Ng SS, Liu J, Fung PC, Tay D, Ge J, He ML, Kung HF & Lin MC. 2004. Catalase and peroxiredoxin 5 protect *Xenopus* embryos against alcohol-induced ocular anomalies. Invest Ophtalmol Vis Sci 45:23-29.

Peshenko IV, Novoselov VI, Evdokimov VA, Nikolaev YV, Kamzalov SS, Shuvaeva TM, Lipkin VM & Fesenko EE. 1998. Identification of a 28 kDa secretory protein from rat olfactory epithelium as a thiol-specific antioxidant. Free Radical Biol Med 25:654-659.

Peters, S. 2005. *XvGolS*, a galactinol synthase is transcriptionally upregulated under water deficit: The role of raffinosaccharides in abiotic stress tolerance in the resurrection plant *Xerophyta viscosa* (Baker). MSc Thesis. University of Cape Town.

Pignocchi C & Foyer C. 2003. Apoplastic ascorbate metabolism and its role in the regulation of cell signalling. Curr Opin Plant Biol 6:379-389.

Pilon-Smits EAH, Terry N, Sears T, Kim H, Zayed A, Hwang S, van Dun K, Voogd E, Verwoerd TC, Krutwagen RWHH & Gooddijn OJM. 1998. Trehalose-producing transgenic tobacco plants show improved growth performance under drought stress. J Plant Physiol 152:525-532.

Qin J, Yang Y, Velyvis A & Gronenborn A. 2000. Molecular views of redox regulation: three-dimensional structures of redox regulatory proteins and protein complexes. Antioxid Redox Sign 2:827-840.

Ramanjulu S & Bartels D. 2002. Drought- and desiccation-induced modulation of gene expression in plants. Plant Cell Environ 25:141-151.

Rhee SG, Chae HZ & Kim K. 2005. Peroxiredoxins: a historical overview and speculative preview of novel mechanisms and emerging concepts in cell signalling. Free Radical Biol Med 38:1543-1552.

Rhee SG, Kang SW, Chang TS, Jeong W & Kim K. 2001. Peroxiredoxin, a novel family of peroxidases. IUBMB Life 52:35-41.

Rouhier N & Jacquot JP. 2002. Plant peroxiredoxins: alternative hydroperoxide scavenging enzymes. Photosynth Res 74:259-268.

Rouhier N & Jacquot JP. 2005. The plant multigenic family of thiol peroxidases. Free Radical Biol Med 38:1413-1421.

Rouhier N, Gelhaye E & Jacquot JP. 2002. Glutaredoxin-dependent peroxiredoxin from poplar. Protein-protein interaction and catalytic mechanism. J Biol Chem 277:13609-13614.

Rouhier N, Gelhaye E & Jacquot JP. 2004c. Plant glutaredoxins: still mysterious reducing systems. Cell Mol Life Sci 61:1266-1277.

Rouhier N, Gelhaye E, Corbier C & Jacquot JP. 2004b. Active site mutagenesis and phospholipid hydroperoxide reductase activity of poplar type II peroxiredoxin. Physiol Plant 120:57-62.

Rouhier N, Gelhaye E, Sautiere PE, Brun A, Laurent P, Tagu D, de Fay E & Meyer Y. 2001. Isolation and characterization of a new peroxiredoxin from poplar sieve tubes that uses either glutaredoxin or thioredoxin as a proton donor. Plant Physiol 127:1299-1309.

Rouhier N, Villarejo A, Srivastava M, Gelhaye E, Keech O, Droux M, Finkemeier I, Samuelsson G, Dietz KJ, Jacquot JP & Wingsle G. 2005. Identification of plant glutaredoxin targets. Antioxid Redox Sign 7:919-929.

Rouhier N, Gelhaye E, Gualberto JM, Jordy MN, de Fay E, Hirasawa M, Duplessis S, Lemaire SD, Frey P, Martin F, Manieri W, Knaff DB & Jacquot JP. 2004a. Poplar peroxiredoxin Q. A thioredoxin-linked chloroplast antioxidant functional in pathogen defence. Plant Physiol 134:1027-1038.

Saijo Y, Hata S, Kyozuka J, Shimamoto K & Izui K. 2000. Over-expression of a single Ca^{2+}-dependent protein kinase confers both cold and salt/drought tolerance on rice plants. Plant J 23:319-327.

Sali A & Blundell TL. 1990. Definition of general topological equivalence in protein structures. A procedure involving comparison of properties and relationships through simulated annealing and dynamic programming. J Mol Biol 212:403-428.

Sali A & Blundell TL. 1993. Comparative protein modelling by satisfaction of spatial restraints. J Mol Biol 234:779-815.

Sambrook J, Fritsch EF & Maniatis T. 1989. Molecular cloning: a laboratory manual (2^{nd} ed.). Cold Spring Harbor Laboratory Press, Cold Spring Harbor.

Sayed M. 2001 Structural studies of protein kinases: CK2 and DYRK1A. PhD Thesis. University of Cambridge.

Schroder G, Beck M, Eichel J, Vetter H-P & Schroder J. 1993. Hsp90 homologue from Madagascar periwinkle (*Catharanthus roseus*): cDNA sequence, regulation of protein expression and location in the endoplasmic reticulum. Plant Mol Biol 23:583-594.

Schröder E, Littlechild JA, Lebedev AA, Errington N, Vagin AA & Isupov MN. 2000. Crystal structure of decameric 2-Cys peroxiredoxin from human erythrocytes at 1.7 Å resolution. Struct Fold Des 8:605-615.

Schürmann P & Jacquot JP. 2001. Plant thioredoxin systems revisited. Ann Rev Plant Physiol Plant Mol Biol 51:371-400.

Scott P. 2000. Resurrection plants and the secrets of eternal leaf. Ann Bot 85:159-166.

Seo MS, Kang SW, Kim K, Baines IC, Lee TH & Rhee SG. 2000. Identification of a new type of mammalian peroxiredoxin that forms an intramolecular disulfide as a reaction intermediate. J Biol Chem 275:20346-20354.

Sgherri CLM, Loggini B, Bochicchio A & Navai-Izzo F. 1994b. Antioxidant systemin *Boea hygroscopica*: changes in response to desiccation and rehydration. Phytochem 35:377-381.

Sgherri CLM, Loggini B, Puliga S & Navai-Izzo F. 1994a. Antioxidant systemin *Sporobolus stapfianus*: changes in response to desiccation and rehydration. Phytochem 35:561-565.

Sherwin HW & Farrant JM. 1995. Surviving desiccation. Veld & Flora 119-121.

Sherwin HW & Farrant JM. 1996. Differences in rehydration of three desiccation-tolerant angiosperm species. Ann Bot 78:703-710.

Sherwin HW & Farrant JM. 1997. Protection mechanism against excess light in the resurrection plants *Craterostigma wilmsii* and *Xerophyta viscosa*. Plant Growth Regul 24:203-210.

Sherwin HW & Farrant JM. 1998. Protection mechanisms against excess light in the resurrection plants *Craterostigma wilmsii* and *Xerophyta viscosa*. Plant Growth Regul 24:203-210.

Sheveleva E, Chmara W. Bohnert HJ & Jensen RG. 1997. Increased salt and drought tolerance by D-Ononitol production in transgenic *Nicotiana tabacum* L. Plant Physiol 115:1211-1219.

Shi J, Blundell TL & Mizuguchi K. 2001. FUGUE: sequence structure homology recognition using environment-specific substitution tables and structure-dependent gap penalties. J Mol Biol 310:243-257.

Shi H, Lee BH, Wu SJ, Zhu JK.. 2003. Overexpression of a plasma membrane Na^+/H^+ antiporter gene improves salt tolerance in *Arabidopsis thaliana*. Nat Biotechnol 21:81-85.

Shinozaki K & Yamaguchi-Shinozaki K. 1996. Molecular responses to drought and cold stress. Curr Opin Biotechnol 7:161-167.

Shinozaki K & Yamaguchi-Shinozaki K. 1997. Gene expression and signal transduction in water-stress response. Plant Physiol 115:327-334.

Simon EW. 1974. Phospholipids and plant membrane permeability. New Phytol 73:377-420.

Sippl MJ. 1993. Recognition of errors in three-dimensional structures of proteins. Proteins 17:355-362.

Sivamani E, Bahieldin1 A, Wraith JM, Al-Niemi T, Dyer WE, Ho TD & Qu R. 2000. Improved biomass productivity and water use efficiency under water deficit conditions in transgenic wheat constitutively expressing the barley *HVA1* gene. Plant Sci 155:1-9.

Smith JAC & Bryce JH. 1992. Metabolite compartmentation and transport in CAM plants. In: Plant organelles (Tobin AK, ed.). Cambridge University Press, Cambridge, pp. 141-167.

Sneath PHA & Sokal RR. 1973. Numerical taxonomy. W. H. Freeman, San Francisco.

Sonnewald U. 2003. Plant biotechnology: from basic science to industrial applications. J Plant Physiol 160:723-725.

Stacy RAP, Nordeng TW, Culianez-Macia FA & Aalen RB. 1999. The dormancy-related peroxiredoxin anti-oxidant, PER1, is localized to the nucleus of barley embryo and aleurone cells. Plant J 19:1-8.

Stacy RAP, Munthe E, Steinum T, Sharma B & Aalen RB. 1996. A peroxiredoxin antioxidant is encoded by a dormancy-related gene, *Per1*, expressed during late development in the aleurone and embryo of barley grains. Plant Mol Biol 31:1205-1216.

Starke DW, Chock PB & Mieyal JJ. 2003. Glutathione-thiyl radical scavenging and transferase properties of human glutaredoxin (thioltransferase). Potential role in redox signal transduction. J Biol Chem 278:14607-14613.

Strid A, Chow WS & Anderson JM. 1994. UV-B damage and protection at the molecular level in plants. Photosynth Res 39:475-489.

Suzuki T, Imamura K, Yamamoto K, Satoh T & Okazaki M. 1997. Thermal stabilisation of freeze-dried enzymes by sugars. J Chem Eng Jpn 30:609-613.

Swidzinski JA, Leaver CJ & Sweetlove LJ. 2004. A Proteomic Analysis of Plant Programmed Cell Death. Phytochem 65:1829-1838

Tan NS, Ho B & Ding JL. 2002. Engineering a novel secretion signal for cross-host recombinant protein expression. Protein Eng 15:337-345.

Tuba Z, Lichtenthaler HK, Csintalan Z, Nagy Z & Szente K. 1996. Loss of chlorophylls, cessation of photosynthetic CO_2 assimilation and respiration in the poikilochlorophyllous plant *Xerophyta scabrida* during desiccation. Physiol Plantarum 96:383-388.

Turner SR, Senaratna T, Touchell DH, Bunn E, Dixon KW & Tan B. 2001. Stereochemical arrangement of hydroxyl groups in sugar and polyalcohol molecules as an important factor in effective cryopreservation. Plant Sci 160:489-497

Uehlein L, Lovisolo C, Siefritz F & Kadenhoff R. 2003. The tobacco aquaporin NtAQP1 is a membrane CO_2 pore with physiological functions. Nature 425:734-737.

Verdoucq L, Vignols F, Jacquot JP, Chartier Y & Meyer Y. 1999. In vivo characterization of a thioredoxin h target protein defines a new peroxiredoxin family. J Biol Chem 274:19714-19722.

von Arnim AG, Deng XW & Stacey MG. 1998. Cloning vectors for the expression of green fluorescent protein fusion proteins in transgenic plants. Gene 221:35-43.

Walford SA, Thomson JA, Farrant JM & Mundree SG. 2004. Isolation and characterization of a novel dehydration-induced Grp94 homologue from the resurrection plant *Xerophyta viscosa*. S Afr J Bot 70:741-750.

Wang W, Vinocur B & Altman A. 2003. Plant responses to drought, salinity and extreme temperatures: towards genetic engineering for stress tolerance. Planta 218:1-14.

Weiner SJ, Kollman PA, Case DA, Singh UC, Ghio C, Alagona G, Profeta S & Weiner P. 1984. A new force field for molecular mechanical simulation of nucleic acids and proteins. J Am Chem Soc 106:765-784.

Woo HA, Chae HZ, Hwang SC, Yang KS, Kang SW, Kim K & Rhee SG. 2003. Reversing the inactivation of peroxiredoxins caused by cysteine sulfinic acid formation. Science 300:653-656.

Wood ZA, Schroder E, Robin Harris J & Poole LB. 2003. Structure, mechanism and regulation of peroxiredoxins. Trends Biochem Sci 28:32-40.

Xiong L & Zhu JK. 2002. Molecular and genetic aspects of plant responses to osmotic stress. Plant Cell Environ 25:131-140.

Xiong L, Schumaker KS & Zhu JK. 2002. Cell signalling during cold, drought and salt stress. Plant Cell 14:S165-S183.

Xu D, Duan X, Wang B, Hong B, Ho THD & Wu R. 1996. Expression of a late embryogenesis abundant protein gene, HVA1, from barley confers tolerance to water deficit and salt stress in transgenic rice. Plant Physiol 110:249-257.

Ye X, Al-Babili S, Kloti a, Zhang J, Lucca P, Beyer P & Potrykus I. 2000. Engineering the provitamin A (β-carotene) biosynthetic pathway into (carotenoid-free) rice endosperm. Science 287:303-305.

Zentella R, Mascorro-Gallardo JO, Van Dijck P, Folch-Mallol J, Bonini B, Van Vaeck C, Gaxiola R, Covarrubias AA, Nieto-Sotelo J & Thevelein JM. 1999. A *Selaginella lepidophylla* trehalose-6-phosphate synthase complements growth and stress-tolerance defects in a yeast tps1 mutant. Plant Physiol 119:1473-1482.

Zhu ZY, Sali A & Blundell TL. 1992. A variable gap penalty function and feature weights for protein 3-D structure comparisons. Protein Eng 5:43-51.

Appendices

Appendix A

General protocols

A1 Standard PCR reaction

The PCR reaction was performed using a GeneAmp 9700 thermal cycler (Applied Biosystems, Singapore). For each amplification, 50 µl reactions were set up using component concentrations summarised in Table A1. Supertherm *Taq* DNA polymerase, PCR buffer and $MgCl_2$ used for the amplification process were supplied by SR Products.

Table A1 PCR reagents and final concentrations used in a standard PCR protocol

Component	Final concentration
Primer concentration	200 pM
dNTP mixture (Roche, Germany)	40 µM
$MgCl_2$	1 mM
Taq polymerase buffer	1X
Template DNA	2 ng/µl
Supertherm *Taq* polymerase	0.02 U/µl

A2 Standard ligation protocol

Purified DNA fragments (insert DNA) were ligated to the respective linearised vectors in a reaction comprising 1 µg of insert DNA, 400 ng vector, 2 U of T4 DNA ligase (Roche) and 1X ligation buffer. The reaction volume was made up to 10 µl, mixed well and incubated for 20 h at 16°C.

A3 Standard transformation protocol

Competent *E. coli* cells were allowed to thaw on ice. Ten microlitres of ligation mix or pure plasmid DNA (ca. 10 ng) was added to the competent *E. coli* cells and mixed gently. The transformation mix was incubated for 10 min on ice. The cells were heat shocked by incubation for 5 min at 37°C and immediately thereafter on ice for 2 min. Nine hundred microlitres of LB broth was added to the transformed cells and incubated for 45 min at 37°C with vigorous shaking. Fifty microlitres of the transformation mix was plated on LB agar plates (supplemented with the appropriate antibiotic) and incubated for 16 h at 37°C.

A4 Plasmid extraction

Plasmid DNA was isolated using the High Pure Plasmid Extraction Kit (Roche). Bacterial cells (ca. 1.5 ml) were centrifuged for 60 s at 6000 x g at RT. The supernatant was discarded and 250 µl of Suspension Buffer added to the pellet. The contents were mixed well and 250 µl of Lysis Buffer was added. The contents were mixed well and thereafter incubated for 5 min at RT. Three hundred and fifty microlitres of chilled Binding Buffer was added to the tube and the contents mixed gently. The tube was incubated for 5 min on ice and thereafter centrifuged for 10 min at 14000 x g at RT. A High Pure filter tube was inserted into one collection tube. The sample was transferred using a pipette to the upper reservoir of the filter tube. The sample was centrifuged for 60 s at 14000 x g in a microcentrifuge. The flow through was discarded and the filter tube combined again with the same collection tube. Five hundred microlitres Wash Buffer I was added to the upper reservoir and centrifuged for 60 s. The flow through was discarded and the filter tube again combined with the collection tube. Seven hundred microlitres of Wash Buffer II was added and the sample centrifuged and recovered as described above. An additional centrifugation step for 60 s at 14000 x g was performed. The flow through solution and collection tube was discarded and the filter tube inserted into a clean 1.5 ml reaction tube. The DNA was eluted using 50 µl elution buffer, which was pipetted onto the filter tube and centrifuged for 60 s at 14000 x g. The purified DNA was stored at 4°C.

A5 PCR Product purification

Amplified DNA was purified using the High Pure PCR Product Purification Kit (Roche). Two hundred and fifty microlitres Binding Buffer was added to a 50 µl PCR reaction and mixed well. The High Pure filter and collection tubes were combined and the sample pipetted into the upper reservoir. The sample was centrifuged for 60 s at 14000 x g in a microcentrifuge. The flow through was discarded and the filter tube combined again with the same collection tube. Five hundred microlitres Wash Buffer was added to the upper reservoir and centrifuged for 60 s. The flow through was discarded and the filter tube again combined with the collection tube. Two hundred microlitres of Wash Buffer was added and the sample centrifuged and recovered as described above. The collection tube was discarded and the filter tube inserted into a clean 1.5 ml reaction tube. The DNA was eluted using 50 µl elution buffer, which was pipetted onto the filter tube and centrifuged for 60 s at 14000 x g. The purified DNA was stored at 4°C.

A6 Purification of DNA from agarose gels

The DNA fragments excised from agarose gels were purified using the High Pure PCR Product Purification Kit (Roche). The excised agarose gel slice was placed in a sterile 1.5 ml Eppendorf tube and the mass was estimated. For every 100 mg of excised agarose 300 µl of Binding Buffer was added to the Eppendorf tube. The tube was vortexed for 60 s to resuspend the gel slice in Binding Buffer. The suspension was incubated for 10 min at 56°C and vortexed briefly every 2-3 min during this period. For every 100 mg of agarose gel slice in the tube 150 µl of isopropanol was added and vortexed thoroughly. The High Pure filter and collection tubes were combined and the sample pipetted into the upper reservoir. The sample was centrifuged for 60 s at 14000 x g in a microcentrifuge. The flow through was discarded and the filter tube combined again with the same collection tube. Five hundred microlitres Wash Buffer was added to the upper reservoir and centrifuged for 60 s. The flow through was discarded and the filter tube again combined with the collection tube. Two hundred microlitres of Wash Buffer was added and the sample centrifuged and recovered as described above. The collection tube was discarded and the filter tube inserted into a clean 1.5 ml reaction tube. The DNA was eluted using 50 µl elution buffer, which was pipetted onto the filter tube and centrifuged for 60 s at 14000 x g. The purified DNA was stored at 4°C.

A7 Standard PAGE conditions

To each sample, 5X SDS loading buffer (0.225 M Tris, pH 6.8; 50% glycerol; 5% SDS; 0.05% bromophenol blue; 0.25 M DTT) was added. Samples were incubated for 8 min in a boiling water bath and immediately thereafter placed on ice. Ten microlitres of the denatured sample was electrophoresed on a 12% polyacrylamide gel (40% BDH acrylamide mix; 1.5 M Tris, pH 8.8; 10% SDS; 10% ammonium persulphate; 10 µl TEMED; made up to 10 ml), which included a 5% stacking gel (40% BDH acrylamide mix; 0.5 M Tris, pH 6.8; 10% SDS; 10% ammonium persulphate; 5 µl TEMED; made up to 5 ml). The sample was electrophoresed for 3 h in 1X SDS PAGE running buffer (10 g SDS; 30.3 g Tris; 144.1 g glycine) at 30 mA. Gels were stained for 1 h with Coomassie staining solution (2.5 g Coomassie Brilliant Blue R-250; 450 ml methanol; 100 ml glacial acetic acid; made up to 1000 ml with sterile distilled water) and thereafter destained overnight in destaining solution (450 ml methanol; 100 ml glacial acetic acid; made up to 1000 ml with sterile distilled water).

Appendix B

Primer sequences and genbank accession numbers

Table B1 List of primers used in this study

Primer name	Primer sequence
F4 HisTOPO-S	5' gct ccg atc gca gtc g 3'
F4 HisTOPO-A	5' gcc aac aca aga cac cca ac 3'
F4 Point Mut-S	5' gcg ttg atg agt tcc ttt gta tta gtg 3'
F4 Point Mut-A	5' cac taa tac aaa gga act cat caa cgc 3'
Smart IV	5' aag cag tgg tat caa cgc aga gtg gcc att acg gcc ggg 3'
CDSIII/3'	5' aat cta gag gcc gag gcg gcc gac atg-d$(T)_{30}N_{-1}N$-3'
5' PCR primer	5' aag cag tgg tat caa cgc aga gt 3'
XvPrx2-F	5' ggg gag gga gag agt gtg g 3'
XvPrx2-R	5' cag gac gaa caa cgt cat agc 3'
splnktop	5' cga atc gta acc gtt cgt acg aga att cgt acg aga atc gct gtc ctc tcc aac gag cca aga 3'
splnkA	5' cga atc gta acc gtt cgt acg aga a 3'
splnkB	5' tcg tac gag aat cgc tgt cct ctc c 3'
splnkBamH1	5' gat ctc ttg gct cgt ttt ttt ttg caa aaa 3'
splnkDra1	5' aaa ttc ttg gct cgt ttt ttt ttg caa aaa 3'
splnkEcoR1	5' aat ttc ttg gct cgt ttt ttt ttg caa aaa 3'
splnkNde1	5' tat gtc ttg gct cgt ttt ttt ttg caa aaa 3'
Prom-R2	5' ccg ggg aaca ccg atg agc acg atc 3'
Prom-R1	5' ctc gtc ctt ctc gtc gaa cca tcc gag 3'
T7 TOPO-F	5' taa tac gac tca cta tag gg 3'
XvPrx2HindIIIXbaI-F	5' cca agc ttg tct aga atg gct ccg atc gca gtc 3'
XvPrx2NcoI-R	5' ctt caa gat ctc cat ggc acc tg 3'
p35SGFPNosTerm-F	5' aag cgg ccg ctc gaa ttt ccc cga tcg 3'
p35SGFPNosTerm-R	5' agt gaa ttc ccg atc tag taa cat aga tga c 3'
EcoR1CAT-F	5' agg aat tcc atg tct ggt tct c 3'
LoxPEcoR1-F	5' gat gct gaa ttc ata act tcg tat agc ata cat tat 3'
LoxPXbaI-R	5' agt ctt cta gaa cgt cag gtg gca ctt ttc g 3'

Table B2 Organisms, gene products and accession numbers of thioredoxin-dependent peroxidases analysed in this study

Organism	Gene Product	Accession number
Gpxs (in plants)		
Arabidopsis thaliana	AtGpx1	At2g25080
Arabidopsis thaliana	AtGpx2	At2g31570
Arabidopsis thaliana	AtGpx3	At2g43350
Arabidopsis thaliana	AtGpx4	At2g48150
Arabidopsis thaliana	AtGpx5	At3g63080
Arabidopsis thaliana	AtGpx6	At4g11600
Arabidopsis thaliana	AtGpx7	At4g31870
Arabidopsis thaliana	AtGpx8	At1g63460
Brassica napus	BnGpx	AAM12502
Oryza sativa	OsGpx	AAM47493
Pisum sativum	PsGpx	O24296
Populus trichocarpa	PtGpx2	AI166663
Populus trichocarpa	PtGpx3	BU883373
Populus trichocarpa	PtGpx4	BU895144
Populus trichocarpa	PtGpx5	CB239682
2 Cys Prxs (in plants)		
Arabidopsis thaliana	At2CysPrxA	At3g11630
Arabidopsis thaliana	At2CysPrxB	At5g06290
Brassica napus	Bn2CysPrx	AAG30570
Nicotiana tabacum	Nt2CysPrx	CAC84143
Spinacia oleracea	So2CysPrx	CAA63910
Type II Prxs (in plants)		
Arabidopsis thaliana	AtPrxIIA	At1g65990
Arabidopsis thaliana	AtPrxIIB	At1g65980
Arabidopsis thaliana	AtPrxIIC	At1g65970
Arabidopsis thaliana	AtPrxIID	At1g60740
Arabidopsis thaliana	AtPrxIIE	At3g52960
Arabidopsis thaliana	AtPrxIIF	At3g06050
Brassica rapa	BrPrxII	AAD33602
Capsicum annuum	CaPrxII	AAL35363
Hyacinthus orientalis	HoPrxII	AAS21026
Ipomoea batatas	IbPrxII	AAP42502
Lycopersicon esculentum	LePrxII	AAP34571
Oryza sativa	aOsPrxII	BAD37738
Oryza sativa	bOsPrxII	NP_912904
Oryza sativa	cOsPrxII	NP_916886

Organism	Gene Product	Accession number
Oryza sativa	dOsPrxII	XP_464429
Plantago major	PmPrxII	CAH58634
Populus trichocarpa	PtPrxII	AAL90751
Xerophyta viscosa	XvPrx2	this study
Type II Prxs (in animals)		
Homosapiens	HsPrxV	NM_012094
Prototheca wickerhamii	PwPrxII	AAV65381
Xenopus laevis	XlPrxII	AAH72972
Type II Prxs (in bacteria)		
Agrobacterium tumefaciens	AtPrxII	NP_353803
Bordetella parapertussis	BpPrxII	NP_883436
Candida boidinii	CbPrxII	P14292
Haemophilus somnus	HsPrxII	ZP_00132875
Pseudomonas putida	PpPrxII	NP_744844
Rhodopseudomonas palustris	RpPrxII	NP_949604
Silicibacter sp.	SspPrxII	ZP_00336842
Vibrio cholerae	VcPrxII	AAF94508
Xanthomonas campestris	XcPrxII	NP_636421
Type II Prxs (in fungi)		
Debaryomyces hansenii	DhPrxII	CAG90822
Gibberella zeae	GzPrxII	EAA72267
Magnaporthe grisea	MgPrxII	EAA47467
Malassezia furfur	MfPrxII	BAA32435
Ustilago maydis	UmPrxII	EAK84119
Yarrowia lipolytica	YlPrxII	CAG79980
Type II Prxs (in insects)		
Anopheles gambiae	AgPrxII	XP_306217
Drosophila yakuba	DyPrxII	AAR10263
1 Cys Prxs (in plants)		
Arabidopsis thaliana	At1CysPrx	At1g48130
Brassica napus	Bn1CysPrx	AAF61460
Hordeum vulgare	Hv1CysPrx	P52572
Triticum aestivum	Ta1CysPrx	AAQ74769
Xerophyta viscosa	Xv1CysPrx	AAL88710
PrxQ (in plants)		
Arabidopsis thaliana	AtPrxQ	At3g26060
Gentiana triflora	GtPrxQ	BAD04985
Populus trichocarpa	PtPrxQ	AAS46230
Sedum lineare	SlPrxQ	BAA90524
Suaeda maritime subsp *salsa*	SmPrxQ	AAQ67661

[a] The accession numbers are from NCBI (National Center for Biotechnology Information) database

Appendix C

Vector maps

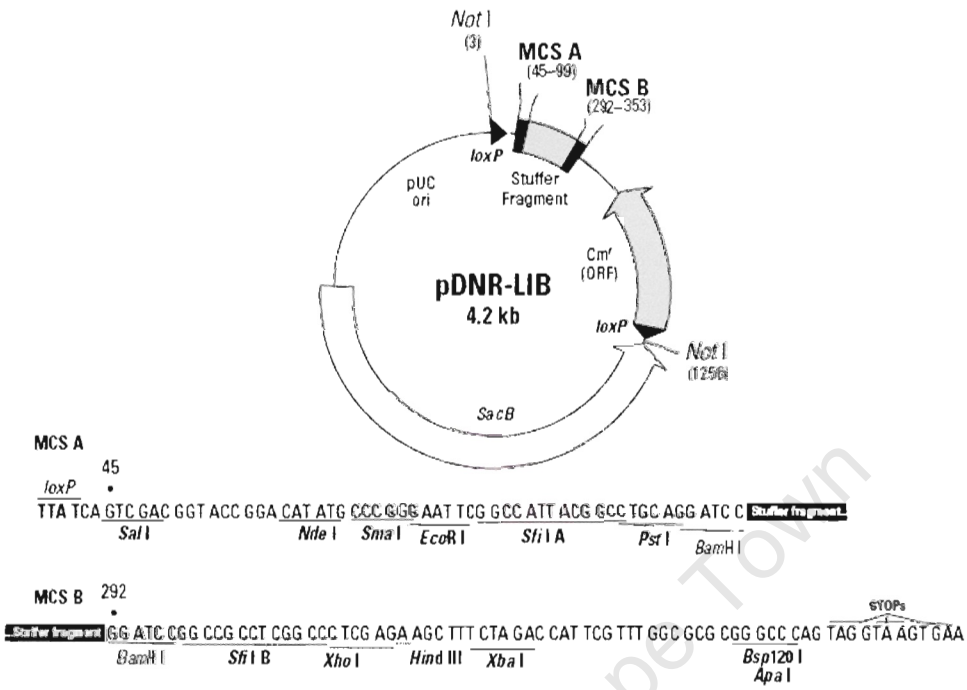

Figure C1 Restriction map and multiple cloning site of pDNR-Lib vector.

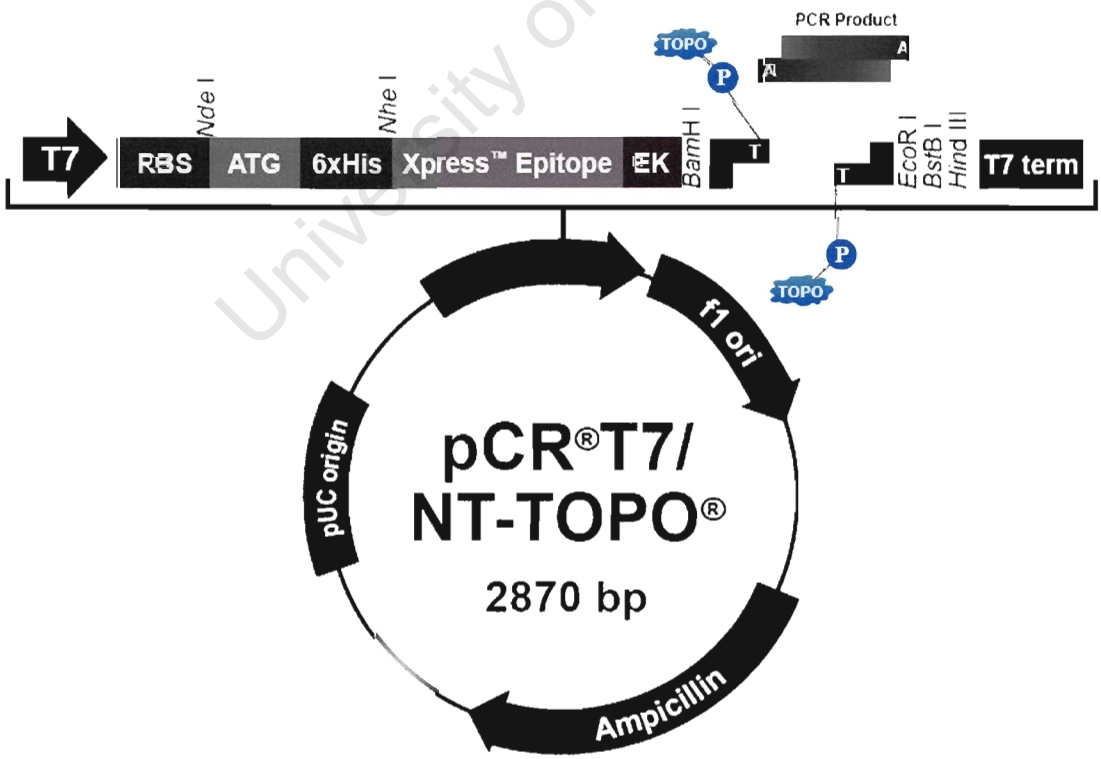

Figure C2 Map of pCR T7/NT TOPO displaying major features.

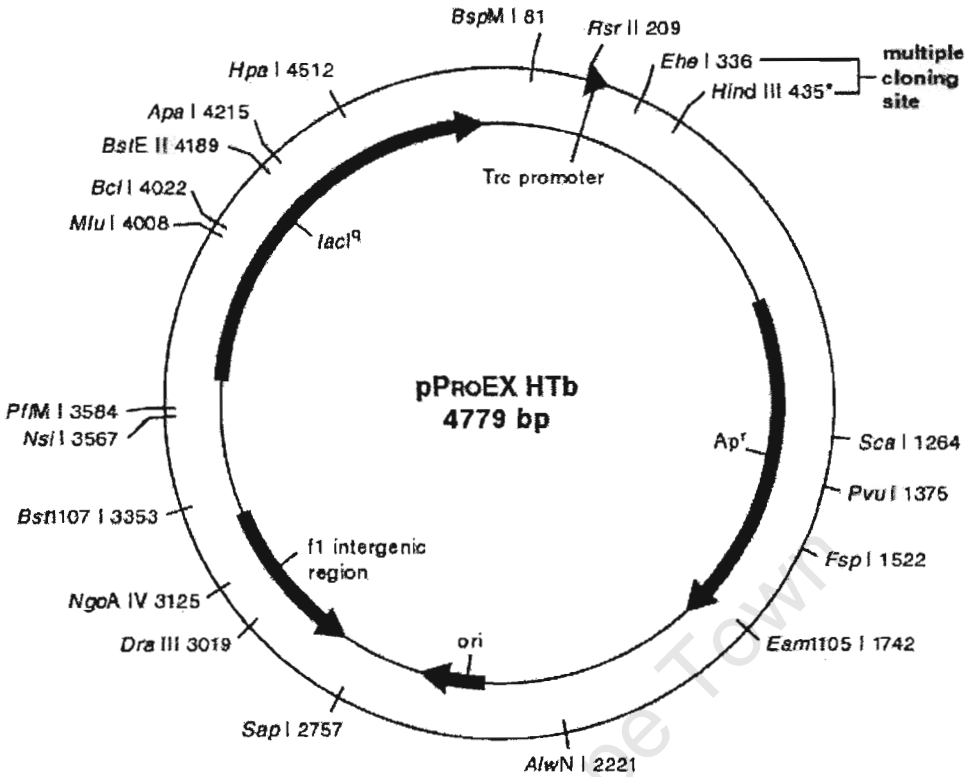

Figure C3 Restriction map of pProEx HTb vector.

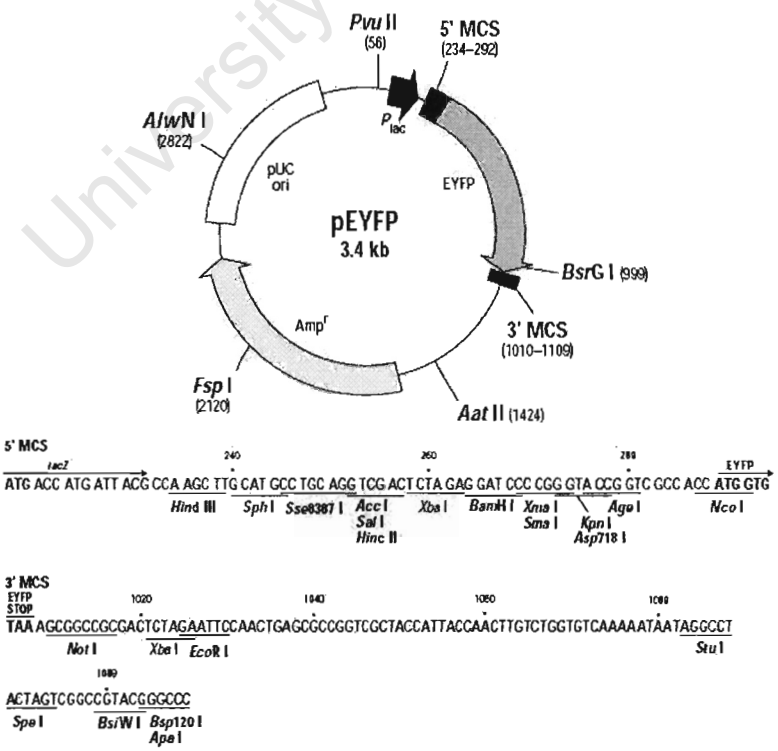

Figure C4 Restriction map and multiple cloning site of pEYFP vector.

Appendix D

Media and solutions

C1 KPi buffer

500 mM KH_2PO_4 (acidic)

500 mM $K_2HPO_4.3H_2O$ (alkaline)

Both solutions were mixed to obtain a single solution of pH 7.0. The resulting KPi buffer was autoclaved.

C2 SOC broth

20 g tryptone

5 g yeast extract

0.5 g NaCl

2.5 ml 1 M KCl

All components were combined. The broth was adjusted to pH 7.0, made up to 1000 ml and autoclaved. Sterile glucose (1 M; 20 ml) and $MgCl_2$ (1 M; 10 ml) was added prior to use.

C3 Top agar

1 g tryptone

0.5 g yeast extract

0.5 g NaCl

0.7% agar

All components were combined and the volume was adjusted to 100 ml. The solution was autoclaved and incubated at 42°C until required.

C4 FOX reagent

The FOX reagent contained 25 mM H_2SO_4, 100 mM sorbitol, 250 μM $Fe^{II}(NH4)_2(SO4)_2$ and 125 μM xylenol orange.